

Synthesis and Reactivity of Main Group Complexes for  
Applications in Small Molecule Activation

Minh Tho Nguyen

Chemistry

Submitted in partial fulfillment  
of the requirements for the degree of  
Doctor of Philosophy

Faculty of Mathematics and Science, Brock University

St. Catharines, Ontario

© 2019

## Abstract

The work described in this thesis is focused on the preparation of a series of novel main group complexes, featuring unusual structural and bonding situations, and the study of their reactivity toward small molecules.

The new zinc complexes dimphZnBu (**V-2**) and dimphZnCl<sub>2</sub>Li(THF)<sub>3</sub> (**V-3**), supported by a diiminophenyl (dimph) ligand were prepared. The reaction of complex **V-3** with LiHBEt<sub>3</sub> resulted in hydride transfer to the C=N imine group to give an unusual zinc dimer (**V-7**). The latter transformation occurs via formation of compound ( $\eta^1(\text{C}),\kappa^1(\text{N})$ -2,6-(2,6-<sup>i</sup>Pr<sub>2</sub>C<sub>6</sub>H<sub>3</sub>N=CH)<sub>2</sub>C<sub>6</sub>H<sub>3</sub>)<sub>2</sub>Zn (**V-5**) which can be also accessed by reduction of **V-7** with KC<sub>8</sub>.

Diiminophenyl (dimph) proved to be an excellent ligand platform to stabilise a low-valent phosphorus centre. The resultant compound dimphP (**VI-2**), which can be rationalised as an imino-stabilised phosphinidene or benzoazaphosphole, shows remarkable chemical stability toward water and oxygen. **VI-2** reacts with excess strong acid HCl to generate the P(III) chloride (dimHph)PCl (**VI-6**). Surprisingly, substitution of the chloride under some nucleophilic (KOBU<sup>t</sup>) and electrophilic conditions (Me<sub>3</sub>SiOTf) regenerates the parent compound **VI-2** by proton removal from the weakly acidic CH<sub>2</sub>N position. A related species (dimH<sub>2</sub>ph)P (**VI-10**) is produced upon thermal rearrangement of the hydride (dimHph)PH (**VI-9**). The molecular structure and reactivity of compounds **VI-2** and other related compounds are also discussed.

The reduction of the O,C,O-chelated phosphorus (III) chloride (**VI-16**) ( O,C,O = 2,6-bis[(2,6-diisopropyl)phenoxy]phenyl) with KC<sub>8</sub> or PMe<sub>3</sub> resulted in the formation of

a cyclic three-membered phosphorus compound (**VI-18**). The intermediacy of phosphinidene **VI-17** was confirmed by trapping experiments and a VT  $^{31}\text{P}\{^1\text{H}\}$  NMR study. The reaction of *in-situ* generated phosphinidene with either  $\text{PhSiH}_3$  or HBpin resulted in the formation of an unprecedented phosphine (**VI-23**). The treatment of **VI-16** with two equivalents of  $^{\text{Dipp}}\text{NHC}$  carbene led to  $\text{ArP}(\text{Cl})\text{NHC}$  product (**VI-24**).

The germylone  $\text{dimNHCGe}$  ( $\text{dimNHC} = \text{diimino } N\text{-Heterocyclic Carbene}$ , **VII-8**) was successfully prepared by the reduction of germanium cation (**VII-7**) with  $\text{KC}_8$ . The molecular structure of **VII-8** was unambiguously established, using NMR spectroscopy and single-crystal X-ray diffraction analysis. The reactivity of **VII-8** was investigated. **VII-8** is inactive towards butadiene but undergoes an oxidative cyclization with tetrachloro-*o*-benzoquinone to give a tetragermanium derivative. **VII-8** undergoes oxidation addition of  $\text{CH}_3\text{I}$  and  $\text{PhI}$ , followed by an unusual migration of the Me and Ph groups from germanium to the carbene ligand. Related chemistry takes place upon protonation with dry  $\text{HCl}$ , which results in the migration of the hydride to the carbene ligand.

## Acknowledgements

I would like to express my deepest and sincerest gratitude to my advisor Prof. Georgii I. Nikonov for offering me a valuable opportunity to join and work in his research group. His patient guidance, sustained encouragement, immense support, and unconditional belief throughout my Ph.D. gave me huge confidence and abilities and led me a great success in my research projects. Under his expertise supervision, my knowledge has been enriched, which allowing me to grow as a scientist.

I would also like to thank Prof. Jeffrey Atkinson and Prof. Feng Li for being as my committee members and for their valuable comments and constructive suggestions during my Ph.D. research process.

I would like to send a big thank to internal and external technicians including Mr. Razvan Simionescu for his assistance in NMR spectroscopy, Ms. Liqun Qui for her support in Mass Spectroscopy, Mark, and Nico for helping me in IR spectroscopy and UV-vis spectroscopy, Dr. Bulat Gabidullin in the University of Ottawa, Dr. James F. Britten in McMaster University, and Dr. Denis Spasyuk in Canadian Light Source Inc. for X-ray data collection and for their assistance in solving the molecular structures described in this thesis. I also wish to thank Prof. Dmitri G. Goussev (Gusev) from Wilfrid Laurier University for sharing his valuable insights into DFT methods and calculations.

I want to thank labmates, past and present: Dr. Terry Chu, Dr. Van Hung Mai, Iryna Alshakova, John Lortie, Anton Dmitrienko, Aishabibi Kassymbek, Joshua Clarke, Aliona Bazadsenka, Billy Petrushko, Jan-Willem Lamberink, Brandon Corbett for their friendship,

help and support all the time of my Ph.D. research, and for all the fun we had in the last four and half years at Brock.

Last but not the least, I would like to express special thanks to my family: my parents Mr.&Mrs. Nguyen, my eldest brother Thanh, and my little sister Thom, who have provided me with moral and emotional support throughout my life. Finally, I thank my beloved fiancée Phuoc-Sang for his unlimited sharing, support and encouragement through all the happiness and difficulties over the past years.

Thanks for all your encouragement!

# Table of Contents

<b>Abstract</b> .....	i
<b>Acknowledgements</b> .....	iv
<b>Table of Contents</b> .....	vi
<b>Abbreviations</b> .....	viii
<b>List of Scheme</b> .....	x
<b>List of Figures</b> .....	xvi
<b>List of Tables</b> .....	xx
<b>I. Introduction</b> .....	1
<b>Part A. Historical Background</b> .....	3
<b>II. Pincer complexes of main group elements</b> .....	4
II.1. Main Group Complexes Supported by Bis(imino)ary NCN Pincer Ligand .....	5
II.1.1. Group 13 .....	6
II.1.2. Group 14 .....	6
II.1.3. Group 15 .....	12
II.2. Main Group Complexes Supported by Bis(imino)aryl Pyridine Ligand .....	17
III.1.1. Group 1 .....	19
III.1.2. Group 2 .....	20
III.1.3. Group 13 .....	23
III.1.4. Group 14 .....	30
III.1.5. Group 15 .....	32
III.1.6. Group 16 .....	33
II.3. Main Group Complexes Supported by Bis(imino)aryl N-heterocyclic Carbene Platform.....	35
<b>III. Phosphinidene</b> .....	36
<b>IV. Zerovalent Heavier Group 14 Compound</b> .....	58
IV.1 Heavier Group 14 Compound in Zero Oxidation State.....	58
IV.2 The Reactivity of Zerovalent Heavy Group 14 Compounds.....	74
<b>Part B. Results and Discussion</b> .....	81

<b>V. Synthesis and Characterization of Zinc Complexes Stabilised by 2,6-bis[(2,6-diisopropyl)imino]phenyl Pincer Ligand</b> .....	82
V.1 Introduction .....	82
V.2 Synthesis, Characterization, and Reactivity of Zinc Complexes Stabilised by 2,6-bis[(2,6-Diisopropyl)imino]phenyl Pincer Ligand .....	83
<b>VI. Synthesis, Characterization, and Reactivity of Base-Stabilised-Phosphinidene</b> 94	
VI.1. Preparation, Characterization, and Reactivity of “Phosphinidene” Stabilised by 2,6-bis[(2,6-diisopropyl)imino]phenyl Pincer Ligand. ....	94
VI.2. Preparation, Characterization, and Reactivity of “Phosphinidene” Stabilised by 2,6-bis[(2,6-diisopropyl)phenoxy] Pincer Ligand. ....	109
<b>VII. Synthesis, Characterization, and Reactivity of Germanium Complexes in Low Oxidation State</b> .....	118
<b>VIII. Conclusion and Future Work</b> .....	131
<b>Part C. Experimental Section</b> .....	134
<b>IX. Experimental</b> .....	135
IX.1 General Methods and Solvents.....	135
IX.2 Instrumentation and Analysis.....	135
IX.3 Starting Materials .....	136
IX.4 Experimental Procedures for Chapter V .....	138
IX.5 Experimental Procedures for Chapter IV .....	144
IX.6 Experimental Procedures for Chapter VII.....	156
<b>X. Appendix</b> .....	163
<b>XI. References</b> .....	220

## Abbreviations

°	degree (angle)
Å	Angström
Ar	2,6-diisopropylphenyl
g	gram(s)
h	hour(s)
Hz	Hertz
K	Kelvin
°C	degrees Celsius
IR	infrared spectroscopy
DFT	density functional theory
LUMO	lowest unoccupied molecular orbital
HOMO	highest occupied molecular orbital
NHC	N-heterocyclic carbene
cAAC	cyclic alkyl amino carbene
<i>o</i>	<i>ortho</i>
<i>m</i>	<i>meta</i>
<i>p</i>	<i>para</i>
rt	room temperature
NMR	nuclear magnetic resonance
δ	chemical shift
MHz	megahertz



{ <sup>1</sup> H}	proton decoupled
m	multiplet (NMR)
s	singlet (NMR)
d	doublet (NMR)
t	triplet (NMR)
quint	quintet (NMR)
sept	septet (NMR)
<i>J</i>	coupling constant (NMR)
br	broad (NMR)
<sup>t</sup> Bu	tert-butyl
<i>n</i> Bu	n-butyl
<sup>i</sup> Pr	isopropyl
Tripp	2,4,6-triisopropylphenyl
Ph	phenyl
Me	methyl
Mes	mesityl
Dipp	2,6-diisopropylphenyl
Et	ethyl
THF	tetrahydrofuran
DCM	dichloromethane
ACN	Acetonitrile
VT	variable temperature
equiv	equivalent

## List of Scheme

<b>Scheme II-1.</b> Three classes of pincer ligands for main group elements discussed in this work. ....	5
<b>Scheme II-2.</b> General procedure for the preparation of bis(imino)aryl NCN pincer ligand ( <b>L<sub>2</sub></b> , <b>dimph</b> ).....	5
<b>Scheme II-3.</b> Synthetic method for the preparation of $\kappa^3$ N,C,N-NCN pincer aluminum compounds <b>II-1</b> .....	6
<b>Scheme II-4.</b> Preparation of compound <b>II-2</b> and <b>II-3</b> .....	7
<b>Scheme II-5.</b> Synthetic method for hydride compounds <b>II-6</b> and <b>II-7</b> .....	8
<b>Scheme II-6.</b> Synthetic method for preparation of compounds <b>II-8</b> and <b>II-9</b> .....	9
<b>Scheme II-7.</b> Synthetic methods for the preparation of Ge compounds. ....	11
<b>Scheme II-8.</b> Synthetic method for preparation of compounds <b>II-16</b> and <b>II-17</b> .....	12
<b>Scheme II-9.</b> Synthetic method for preparation of compounds <b>II-19</b> , <b>II-20</b> , and <b>II-21</b> . .	13
<b>Scheme II-10.</b> Reactivity of <b>II-22</b> and <b>II-25</b> .....	15
<b>Scheme II-11.</b> Synthetic method to trapping phosphinidene <b>II-29</b> and mechanism of P-N exchange by a “bell-clapper” pathway.....	16
<b>Scheme II-12.</b> Synthetic method to ligand bis(imino)aryl pyridine and electronic structures in various oxidation states.....	18
<b>Scheme II-13.</b> Synthetic route to <b>II-30</b> and <b>II-31</b> .....	20
<b>Scheme II-14.</b> Synthetic method to several complexes of group 2 elements supported by dimpyr ligand. ....	21
<b>Scheme II-15.</b> Magnesium alkyl react with dimpyr ligand affording <b>II-45</b> and <b>II-46</b> ....	22
<b>Scheme II-16.</b> Synthesis of compounds <b>II-47</b> and <b>II-48</b> . ....	23

<b>Scheme II-17.</b> Synthesis of <b>II-50</b> and <b>II-51</b> .....	24
<b>Scheme II-18.</b> Several isolated alkylated products reported by Budzelaar et al.....	24
<b>Scheme II-19.</b> The preparation of <b>II-56</b> and its reactivity .....	26
<b>Scheme II-20.</b> Insertion of CO <sub>2</sub> into the Al-H bond of <b>II-55</b> and proposed mechanism for HCOOH dehydrogenation by <b>II-55</b> .....	27
<b>Scheme II-21.</b> Preparation of Gallium compounds and Aluminum compound reported by Richeson et al.....	28
<b>Scheme II-22.</b> Preparation of In compounds <b>II-64</b> and <b>II-65</b> .....	29
<b>Scheme II-23.</b> Preparation of the heavier group 14 elements complexes of dimpyr, <b>II-66</b> and <b>II-67</b> .....	30
<b>Scheme II-24.</b> Preparation of Sn(0) compounds <b>II-68</b> and some Sn(II) compounds. ....	31
<b>Scheme II-25.</b> Preparation of germanium complex <b>II-73</b> .....	32
<b>Scheme II-26.</b> Synthetic methods for the preparation of dimpyr compounds of elements from group 15. ....	33
<b>Scheme II-27.</b> Synthetic method for the preparation of dimpyr compounds of elements from group 15. ....	34
<b>Scheme III-1.</b> Yoshifuji's dimeric phosphinidene.....	36
<b>Scheme III-2.</b> Generation of phosphaindane <b>III-5</b> by photolysis of <b>III-3</b> .....	38
<b>Scheme III-3.</b> Photolysis of <b>III-6</b> in the presence of 2,3-dimethyl-1,5-butadiene .....	38
<b>Scheme III-4.</b> Photolysis of <b>III-9</b> .....	39
<b>Scheme III-5.</b> Photolysis reactions reported by Protasiewicz et al.....	40
<b>Scheme III-6.</b> The reduction of 2,6-Trip <sub>2</sub> C <sub>6</sub> H <sub>3</sub> PCl <sub>2</sub> .....	41

<b>Scheme III-7.</b> The NHC- phosphinidene adduct reported by Cowley and Arduengo. ....	42
<b>Scheme III-8.</b> Phosphinidene stabilised by NHC reported by Robinson et al. ....	44
<b>Scheme III-9.</b> The procedure for the synthesis of parent NHC-phosphinidene adduct reported by Tamm et al. (top) and by Grützmacher et al. (bottom). ....	45
<b>Scheme III-10.</b> Preparation of carbene–phosphinidene adducts using dichlorophenylphosphine. ....	45
<b>Scheme III-11.</b> Synthesis of zwitterionic imidazolium phosphanide reported by Streubel and Nyalazsi. ....	47
<b>Scheme III-12.</b> Cleavage of the P=P double bond in a diphosphene reported by Hatanaka and Matsuo. ....	48
<b>Scheme III-13.</b> Carbene stabilised P(I) cations reported by Macdonald et al. ....	49
<b>Scheme III-14.</b> Carbene stabilised P(I) cations reported by Weigand et al. ....	50
<b>Scheme III-15.</b> The preparation and reactivity of <b>III-58</b> . ....	51
<b>Scheme III-16.</b> Preparation of reactivity of phosphinidene stabilised by a perisubstituted acenaphthyl backbone. ....	53
<b>Scheme III-17.</b> Zwitterionic P(I) compound reported by Macdonald and Ragona. ....	54
<b>Scheme III-18.</b> Zwitterionic species reported by Stalke et al. ....	54
<b>Scheme III-19.</b> P(I) compound reported by Xie et al. ....	55
<b>Scheme III-20.</b> Synthesis of Bertrand’s “bottle-able” phosphinidene and their reactivity. ....	57
<b>Scheme IV-1.</b> Description of the bonding situation in carbodiphosphorane in terms of donor–acceptor interactions .....	59

<b>Scheme IV-2.</b> Synthesis of tristannaallene <b>IV-4</b> and its resonance structures.....	60
<b>Scheme IV-3.</b> Synthesis of the trissilaallene <b>IV-6</b> .....	61
<b>Scheme IV-4.</b> Synthesis of disilagermaallene <b>IV-7</b> , trigermaallene <b>IV-8</b> , digermasilaallene <b>IV-9</b> .....	61
<b>Scheme IV-5.</b> Synthesis of <b>IV-11</b> reported by Robinson et al.....	62
<b>Scheme IV-6.</b> Synthesis of germanium(0) dimer <b>IV-12</b> and stannum(0) dimer <b>IV-13</b> ..	63
<b>Scheme IV-7.</b> Synthesis of siladibene <b>IV-16</b> .....	64
<b>Scheme IV-8.</b> Synthesis of silylone <b>IV-18</b> and germylone <b>IV-20</b> .....	65
<b>Scheme IV-9.</b> Synthesis of compound <b>IV-21</b> .....	67
<b>Scheme IV-10.</b> Synthesis of 1,3-digerma-2-silaallene <b>IV-24</b> .....	69
<b>Scheme IV-11.</b> Examples of dimpyr-stabilised stannylone <b>II-68</b> and dimpyr-stabilised germylone <b>II-73</b> .....	71
<b>Scheme IV-12.</b> Synthesis of stannylone <b>IV-26</b> .....	72
<b>Scheme IV-13.</b> Synthesis of germylone <b>IV-29</b> .....	73
<b>Scheme IV-14.</b> The reactivity of silylone <b>IV-18</b> and related compounds.....	75
<b>Scheme IV-15.</b> The reactivity of silylone <b>IV-18</b> toward CO <sub>2</sub> gas.....	77
<b>Scheme IV-16.</b> The reactivity of germylone <b>IV-20</b> .....	78
<b>Scheme IV-17.</b> The reactivity of germylone <b>IV-29</b> .....	79
<b>Scheme IV-18.</b> Synthesis of <b>IV-49</b> and its reactivity.....	80
<b>Scheme V-1.</b> Preparation of compounds <b>V-2</b> and <b>V-3</b> .....	83
<b>Scheme V-2.</b> Synthetic routes to the binuclear species <b>V-7</b> .....	87
<b>Scheme V-3.</b> An alternative method to prepare <b>V-5</b> .....	88

<b>Scheme V-4.</b> The first pathway to the zincate <b>V-8(Li)</b> .....	91
<b>Scheme V-5.</b> The second pathway to the zincate <b>V-8(K)</b> .....	92
<b>Scheme V-6.</b> Preparations of compound <b>V-11</b> .....	93
<b>Scheme VI-1.</b> Preparation of phosphinidene <b>VI-2</b> .....	95
<b>Scheme VI-2.</b> X-ray characterised azaphospholes.....	97
<b>Scheme VI-3.</b> Description of the bonding situation in <b>VI-2</b> in terms of resonance. The left form describes the N→P σ donations, the middle form accounts for P →N=C π back-donation, and the right form shows the contribution of an azaphosphole component. ....	97
<b>Scheme VI-4.</b> Stability of <b>VI-2</b> to water media.....	99
<b>Scheme VI-5.</b> Reactivity of compound <b>VI-2</b> .....	101
<b>Scheme VI-6.</b> Reactivity of chlorophosphine <b>VI-6</b> .....	103
<b>Scheme VI-7.</b> Reactivity of chlorophosphine <b>VI-6</b> .....	105
<b>Scheme VI-8.</b> Oxidation of chloride <b>VI-6</b> .....	107
<b>Scheme VI-9.</b> The preparation of the pincer ligand <b>VI-15</b> .....	109
<b>Scheme VI-10.</b> The preparation of phosphorus dichloride <b>VI-16</b> .....	110
<b>Scheme VI-11.</b> The reduction of phosphorus dichloride complex <b>VI-16</b> .....	112
<b>Scheme VI-12.</b> The second path to cyclic product <b>VI-18</b> .....	113
<b>Scheme VI-13.</b> <sup>31</sup> P{ <sup>1</sup> H} VT-NMR experiment (top) and possible mechanism of the reduction of <b>VI-16</b> by PMe <sub>3</sub> (bottom). .....	115
<b>Scheme VI-14</b> The reactivity of <b>VI-16</b> . .....	116
<b>Scheme VI-15.</b> The reactivity of <b>VI-16</b> toward NHC carbene. ....	117

<b>Scheme VII-1.</b> Preparation free diimino carbene ligand <sup>Me</sup> dimNHC ( <b>VII-3</b> ) and <sup>Ph</sup> dimNHC ( <b>VII-4</b> ).....	119
<b>Scheme VII-2.</b> Attempts in preparation of germanium cation from dimNHC carbene ligands. ....	120
<b>Scheme VII-3.</b> A novel approach to germanium cation <b>VII-7(ZnCl<sub>3</sub>)</b> .....	121
<b>Scheme VII-4.</b> The synthesis to germylone <b>VII-8</b> , its fluxionary, and description in terms of resonance. ....	124
<b>Scheme VII-5.</b> The reaction of germylone <b>VII-8</b> with Lewis acid GeCl <sub>3</sub> . ....	126
<b>Scheme VII-6.</b> The reactivity of germylone <b>VII-8</b> towards several substrates. ....	127
<b>Scheme VII-7.</b> Reactivity of germylone <b>VII-8</b> towards iodobenzene. The intermediate <b>VII-11</b> can be not observed in this reaction.....	128
<b>Scheme VII-8.</b> The reaction of <b>VII-8</b> with strong acid HCl. ....	129
<b>Scheme VII-9.</b> The oxidation of germylone <b>VII-8</b> . ....	130

## List of Figures

- Figure V-1.** Molecular structure of complex **V-2.** Hydrogen atoms are omitted for clarity. Displacement ellipsoids are shown at the 30% probability level..... 84
- Figure V-2.** Molecular structures of complex **V-3.** The molecule is disordered in the location and ligation pattern for the lithium ion. Only one part of the disordered structure is shown. Hydrogen atoms and a THF molecule symmetrically related to the O3' ligand are omitted for clarity. Displacement ellipsoids are shown at the 30% probability level. 86
- Figure V-3.** Molecular structure of complex **V-5** Hydrogen atoms are omitted for clarity. Displacement ellipsoids are shown at the 30% probability level..... 88
- Figure V-4.** Molecular structure of complex **V-7.** Displacement ellipsoids are shown at the 30% probability level. Hydrogen atoms and the <sup>i</sup>Pr groups are omitted for clarity..... 90
- 
- Figure VI-1.** Molecular structure of compound **VI-2.** Thermal ellipsoids are shown at the 30% probability level. Hydrogen atoms are omitted for clarity. The molecule is bisected by a crystallographically imposed mirror plane running through the C(1)-C(4) vector... 96
- Figure VI-2.** Molecular structure of compound **VI-10.** Thermal ellipsoids are shown at the 30% probability level. Hydrogen atoms, except the protons on amine, N=CH and in the NCH<sub>2</sub> moieties, are omitted for clarity. .... 103
- Figure VI-3.** Molecular structure of compound **VI-13.** Thermal ellipsoids are shown at the 30% probability level. Hydrogen atoms, except the hydrogen atom in the formate and in the CH<sub>2</sub>N moiety, are omitted for clarity..... 106
- Figure VI-4.** Molecular structure of compound **VI-14.** Thermal ellipsoids are shown at the 30% probability level. Hydrogen atoms are omitted for clarity. .... 107



<b>Figure VII- 1.</b> Molecular structure of compound <b>VII-8</b> Thermal ellipsoids are shown at the 30% probability level. Hydrogen atoms are omitted for clarity.....	124
<b>Figure X-1.</b> $^1\text{H}$ and $^{13}\text{C}\{^1\text{H}\}$ NMR spectra of <b>V-2</b> .....	163
<b>Figure X-2.</b> $^1\text{H}$ and $^{13}\text{C}\{^1\text{H}\}$ NMR spectra of <b>V-3</b> .....	164
<b>Figure X-3.</b> $^1\text{H}$ and $^{13}\text{C}\{^1\text{H}\}$ NMR spectra of <b>V-5</b> .....	165
<b>Figure X-4.</b> $^1\text{H}$ and $^{13}\text{C}\{^1\text{H}\}$ NMR spectra of <b>V-7</b> .....	166
<b>Figure X-5.</b> $^1\text{H}$ and $^{13}\text{C}\{^1\text{H}\}$ NMR spectra of <b>V-8(Li)</b> or <b>V-8(K)</b> .....	167
<b>Figure X-6.</b> $^1\text{H}$ and $^{13}\text{C}\{^1\text{H}\}$ NMR spectra of <b>V-9</b> .....	168
<b>Figure X-7.</b> $^1\text{H}$ spectrum of <b>V-10</b> .....	169
<b>Figure X-8.</b> $^1\text{H}$ and $^{13}\text{C}\{^1\text{H}\}$ NMR spectra of <b>V-9</b> + $\text{PhSiH}_3$ .....	169
<b>Figure X-9.</b> $^1\text{H}$ NMR spectrum of the reaction between <b>V-3</b> + (superhydride) $\text{LiBHEt}_3$ at various time (yellow diamond corresponding to compound <b>V-7</b> , purple cycle corresponding to compound <b>V-5</b> ). .....	170
<b>Figure X-10.</b> $^1\text{H}$ , $^{13}\text{C}\{^1\text{H}\}$ , and $^{31}\text{P}\{^1\text{H}\}$ NMR spectra of <b>VI-2</b> in $\text{C}_6\text{D}_6$ .....	172
<b>Figure X-11.</b> $^1\text{H}$ , $^1\text{H}\{^{31}\text{P}\}$ , $^{13}\text{C}\{^1\text{H}\}$ , and $^{31}\text{P}\{^1\text{H}\}$ NMR spectra of <b>VI-6</b> in $\text{C}_6\text{D}_6$ .....	174
<b>Figure X-12.</b> $^1\text{H}$ , $^1\text{H}\{^{31}\text{P}\}$ , $^{13}\text{C}\{^1\text{H}\}$ , and $^{31}\text{P}\{^1\text{H}\}$ NMR spectra of <b>V-7</b> in $\text{CD}_2\text{Cl}_2$ .....	176
<b>Figure X-13.</b> $^1\text{H}$ , $^1\text{H}\{^{31}\text{P}\}$ , $^{13}\text{C}\{^1\text{H}\}$ , and $^{31}\text{P}\{^1\text{H}\}$ NMR spectra of <b>VI-8</b> in $\text{CD}_2\text{Cl}_2$ .....	178
<b>Figure X-14.</b> $^1\text{H}$ , $^1\text{H}\{^{31}\text{P}\}$ , $^{13}\text{C}\{^1\text{H}\}$ , $^{31}\text{P}\{^1\text{H}\}$ , and $^{31}\text{P}$ NMR spectra of <b>VI-9</b> in $\text{C}_6\text{D}_6$ ...	180
<b>Figure X-15.</b> $^1\text{H}$ , $^1\text{H}\{^{31}\text{P}\}$ , $^{13}\text{C}\{^1\text{H}\}$ , and $^{31}\text{P}\{^1\text{H}\}$ , $^1\text{H}$ - $^1\text{H}$ COSY NMR spectra of <b>VI-10</b> in $\text{C}_6\text{D}_6$ .....	183
<b>Figure X-16.</b> $^1\text{H}$ , $^1\text{H}\{^{31}\text{P}\}$ , $^{13}\text{C}\{^1\text{H}\}$ , and $^{31}\text{P}\{^1\text{H}\}$ NMR spectra of <b>V-11</b> in $\text{C}_6\text{D}_6$ .....	185

<b>Figure X-17.</b> $^1\text{H}$ , $^1\text{H}\{^{31}\text{P}\}$ , $^{13}\text{C}\{^1\text{H}\}$ , and $^{31}\text{P}\{^1\text{H}\}$ NMR spectra of <b>VI-12</b> in $\text{C}_6\text{D}_6$ .....	187
<b>Figure X-18.</b> $^1\text{H}$ , $^1\text{H}\{^{31}\text{P}\}$ , $^{13}\text{C}\{^1\text{H}\}$ , and $^{31}\text{P}\{^1\text{H}\}$ NMR spectra of <b>VI-13</b> in $\text{C}_6\text{D}_6$ .....	189
<b>Figure X-19.</b> $^1\text{H}$ , $^1\text{H}\{^{31}\text{P}\}$ , $^{13}\text{C}\{^1\text{H}\}$ , and $^{31}\text{P}\{^1\text{H}\}$ NMR spectra of <b>VI-14</b> in $\text{C}_6\text{D}_6$ .....	191
<b>Figure X-20.</b> $^1\text{H}$ , $^{13}\text{C}\{^1\text{H}\}$ , $^{31}\text{P}\{^1\text{H}\}$ NMR spectra of <b>VI-16</b> in $\text{C}_6\text{D}_6$ .....	193
<b>Figure X-21.</b> $^1\text{H}$ , $^{13}\text{C}\{^1\text{H}\}$ , $^{31}\text{P}\{^1\text{H}\}$ NMR spectra of <b>VI-18</b> in $\text{C}_6\text{D}_6$ .....	194
<b>Figure X-22.</b> $^1\text{H}$ , $^1\text{H}\{^{31}\text{P}\}$ , $^{13}\text{C}\{^1\text{H}\}$ , $^{31}\text{P}\{^1\text{H}\}$ , $^{31}\text{P}$ NMR spectra of <b>VI-23</b> in $\text{C}_6\text{D}_6$ .....	197
<b>Figure X-23.</b> $^1\text{H}$ , $^{13}\text{C}\{^1\text{H}\}$ , $^{31}\text{P}\{^1\text{H}\}$ NMR spectra of <b>VI-24</b> in $\text{C}_6\text{D}_6$ .....	198
<b>Figure X-24.</b> $^1\text{H}$ NMR spectrum of $^{\text{Me}}\text{dimNHC}$ ligand <b>VII-3</b> in $\text{C}_6\text{D}_6$ .....	199
<b>Figure X-25.</b> $^1\text{H}$ , $^{13}\text{C}\{^1\text{H}\}$ NMR spectrum of <b>VII-4</b> in $\text{C}_6\text{D}_6$ .....	200
<b>Figure X-26.</b> $^1\text{H}$ NMR spectrum of <b>VII-5</b> in $\text{C}_6\text{D}_6$ .....	200
<b>Figure X-27.</b> $^1\text{H}$ , $^{13}\text{C}\{^1\text{H}\}$ NMR spectra of zinc compound <b>VII-6</b> in $\text{CDCl}_3$ .....	201
<b>Figure X-28.</b> $^1\text{H}$ , $^{13}\text{C}\{^1\text{H}\}$ NMR spectra of germanium cation <b>VII-7</b> ( $\text{ZnCl}_3$ ) in $\text{CDCl}_3$ . .....	202
<b>Figure X-29.</b> $^1\text{H}$ , $^{13}\text{C}\{^1\text{H}\}$ NMR spectra of germylone <b>VII-8</b> in $\text{C}_6\text{D}_6$ and $^1\text{H}$ NMR spectra of <b>VII-8</b> at various temperature ( $22^\circ\text{C}$ (red), $-70^\circ\text{C}$ (blue)) in toluene- $d_8$ . .....	204
<b>Figure X-30.</b> $^1\text{H}$ , $^{13}\text{C}\{^1\text{H}\}$ NMR spectra of <b>VII-9</b> in $\text{C}_6\text{D}_5\text{CD}_3$ . .....	205
<b>Figure X-31.</b> $^1\text{H}$ , $^{13}\text{C}\{^1\text{H}\}$ , 2D-HMBC NMR spectra of <b>VII-12</b> in $\text{C}_6\text{D}_6$ . .....	207
<b>Figure X-32.</b> $^1\text{H}$ , $^{13}\text{C}\{^1\text{H}\}$ NMR spectra of mixture <b>VII-13</b> + <b>VII-14</b> in $\text{C}_6\text{D}_6$ . .....	208
<b>Figure X-33.</b> $^1\text{H}$ , $^{13}\text{C}\{^1\text{H}\}$ NMR spectra of <b>VII-15</b> in $\text{CDCl}_3$ .....	209
<b>Figure X-35.</b> ESI $^+$ mass spectrum (MeOH/DCM) of <b>VI-2</b> .....	210
<b>Figure X-36.</b> ESI $^+$ mass spectrum (MeOH/DCM) of <b>VI-7</b> (a and b, top) and theoretical modes with $\text{OH}^-$ (b, middle) and $\text{H}_2\text{O}$ (b, bottom). The MS data is consistent with theoretical modes of $[(\text{dimph})\text{PBr}]^+$ cation with two $[\text{OH}]^-$ moiety. It's approximately 1.5	

mins from when sample vial was open to when sample got into the MS analyzer. Two [OH]<sup>-</sup> moiety are presented due to exposing the sample to air during the process of preparation. .... 211

**Figure X-37.** ESI<sup>-</sup> mass spectrum (MeOH/DCM) of **VI-8** ..... 210

**Figure X-37.** ESI mass spectrum (DCM/ACN) of **VII-15** ..... 212

**Figure X-38.** IR spectrum of **VI-10** ..... 213

**Figure X-38.** IR spectrum of **VII-7(ZnCl<sub>3</sub>)**..... 213

**Figure X-38.** IR spectrum of **VII-8**..... 214

## List of Tables

<b>Table III-1:</b> $^{31}\text{P}$ NMR for the adducts <b>III-34.PPh</b> – <b>III-45.PPh</b> reported by Bertrand et al. .....	46
<b>Table V-1.</b> Selected bond lengths and angles for compound <b>V-2</b> .....	85
<b>Table V-2.</b> Selected bond lengths and angles for compound <b>V-3</b> .....	86
<b>Table V-3.</b> Selected bond lengths and angles for compound <b>V-7</b> .....	90
<b>Table VI-1.</b> Selected bond lengths and angles for compound <b>VI-2</b> .....	96
<b>Table VI-2.</b> Selected bond lengths and angles for compound <b>VI-10</b> .....	103
<b>Table VI-3.</b> Selected bond lengths and angles for compound <b>VI-13</b> .....	106
<b>Table VI-4.</b> Selected bond lengths and angles for compound <b>VI-14</b> .....	108
<b>Table VII-1.</b> Selected bond lengths and angles for compound <b>VII-8</b> .....	125
<b>Table X-1.</b> Crystal and structure refinement data for compound <b>V-2, V-5, V-7</b> .....	215
<b>Table X-2.</b> Crystal and structure refinement data for <b>VI-2, VI-10, VI-13, VI-14</b> .....	217

## I. Introduction

The development of metal-based catalysts for applications in organic chemistry has been an important area of research.<sup>[1-4]</sup> The presence of partially occupied d valence orbitals, which are relatively close in energy, allow transition metals complexes to interact with small molecules, such as CO, C<sub>2</sub>H<sub>4</sub> or H<sub>2</sub>. Because of the ability to change the oxidation state or participate in small molecule activation, the majority of catalysts reported in both the academic and industrial fields were prepared based on transition metals.<sup>[5]</sup> However, most of transition metals are known to be expensive and often toxic. Main group elements, in contrast, are usually cheap, less toxic, and abundant, and are promising alternatives to transition metal-based catalysts.<sup>[5-8]</sup> Main group compounds, however, are less prone to interact with small molecules due to the large energy gap between the s or p valence orbitals. However, some impressive advances that have been made in recent years show that several types of main-group compounds can behave like transition-metal complexes. They include the systems containing multiple bonds between heavier main-group elements, low-valent main group compounds with open coordination sites, stable radicals with unpaired electrons centred on heavier main-group elements, frustrated Lewis pairs, and compounds with stable singlet diradicaloid electronic configurations. My research is focus on bond activation by main group compounds in low oxidation states. Such systems are often formed in unusual structural and bonding situations, with vacant coordination sites and frontier orbitals separated by relatively small energy gaps, which enables bond activation.<sup>[9]</sup> Activation of strong bonds is the key step in many catalytic

transformations. Thus, exploring the use of low-valent main group compounds in molecule activation has been of great interest in the last decades, leading to several breakthroughs.

The goal of this Thesis is to design and synthesize new low-valent main group compounds, as well as to study their reactivity. In this work, I classify the content by three major parts:

Part **A** of this Thesis will focus on the historical background, including the pincer chemistry of main group elements (chapter II), the chemistry of phosphinidenes (chapter III), the chemistry of group 14 elements in zero oxidation state (chapter IV).

Part **B** of this Thesis will focus on the results and discussion, including the synthesis, characterization, and reactivity of zinc complexes stabilised by a dimph ligand (chapter V), the preparation, characterization, and reactivity of a novel “phosphinidene” (chapter VI), and the preparation, characterization, and reactivity of germanium compounds in low oxidation states (chapter VII).

Part **C** contains the conclusion (chapter VIII), the experimental section, and the supporting information (Chapter IV, Chapter X)

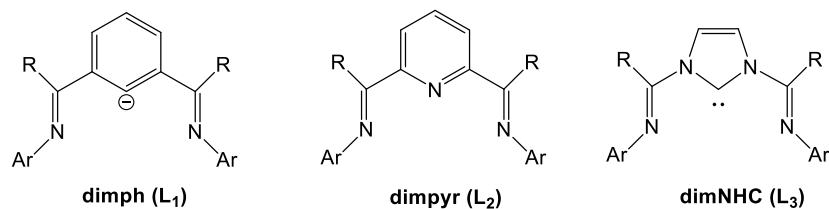
# **Part A. Historical Background**

## II. Pincer complexes of main group elements

A pincer ligand consists of a central aromatic or heteroaromatic ring that is ortho-disubstituted with heteroatom substituents, which generally coordinate to the metal centre in the tridentate fashion. The chemistry of pincer ligands and their organometallic derivatives has been of interests for many years.<sup>[10-15]</sup> In 1976, the first pincer ligand was synthesised by Mouton and Shaw.<sup>[16]</sup> Then, the examination of properties of these complexes revealed their potential for applications in homogenous catalysis, leading to a significant number of publications on pincer chemistry later on. Modifications of the central ring, the donor atoms and their substituents allow for fine tuning of the steric and electronic properties of metal complexes, which finds multiple applications in catalysis as well as in material science, chemical sensors, physical science, etc.<sup>[14]</sup> Over the past decades, the majority of studies have been performed, using transition metals, rare earth metals and main group elements. Compared to the remarkable progress of the pincer chemistry of transition metal complexes, the corresponding chemistry of main group elements remains relatively undeveloped.<sup>[10,17]</sup> Although the first pincer derivative of a main group element was studied by Spek et. al in 1978,<sup>[18]</sup> the actual development of this field started only very recently. A new chapter in the chemistry main group pincers was opened when Jrukschat et al. synthesised the first COC pincer ligand and utilised it to stabilize tin and silicon compounds in 2001.<sup>[19]</sup> Since that time, the pincer chemistry of main group elements has been enriched significantly and several very interesting results have been discovered. Due to the limited space, this chapter is focused on the recent progress in the chemistry of main group compounds supported by three different classes of pincer ligands: the bis(imino)aryl NCN pincer ligand (**L**<sub>1</sub>, dimph), the bis(imino)NNN



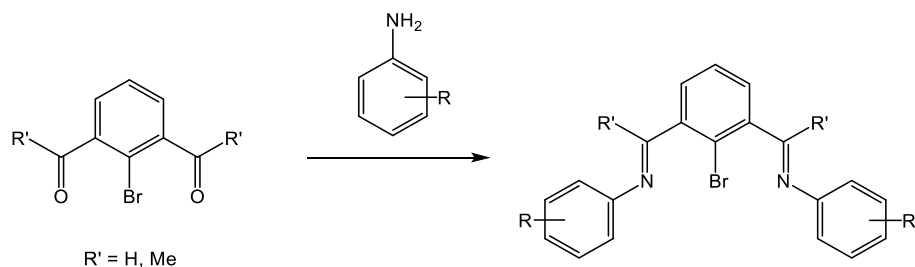
pincer ligand (**L**<sub>2</sub>, dimpyr), and the bis(imino)aryl NHC pincer (**L**<sub>3</sub>, dimNHC) (Scheme II-1).



**Scheme II-1.** Three classes of pincer ligands for main group elements discussed in this work.

### II.1. Main Group Complexes Supported by Bis(imino)aryl NCN Pincer Ligand

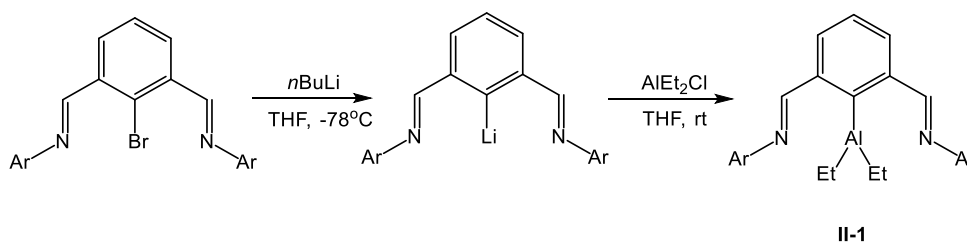
The organometallic chemistry of bis(imino)aryl NCN pincer ligand complexes has been of interests for many years.<sup>[20,20,21]</sup> Bis(imino)aryl NCN pincer are easily available from a condensation reaction between the commercially available 2-bromoisophthalaldehyde (or 2-bromo-1,3-phenylene)bis-ethenone) and anilines bearing different substituents (Scheme II-2). The compounds of such ligand are stabilised by the formation of the C-M  $\sigma$ -bond supported by two ortho,ortho-chelated heteroatom groups. Despite the significant development of transition metal complexes supported by such ligands,<sup>[22–28]</sup> much fewer examples are reported for main group elements.



**Scheme II-2.** General procedure for the preparation of bis(imino)aryl NCN pincer ligand (**L**<sub>2</sub>, dimph)

### II.1.1. Group 13

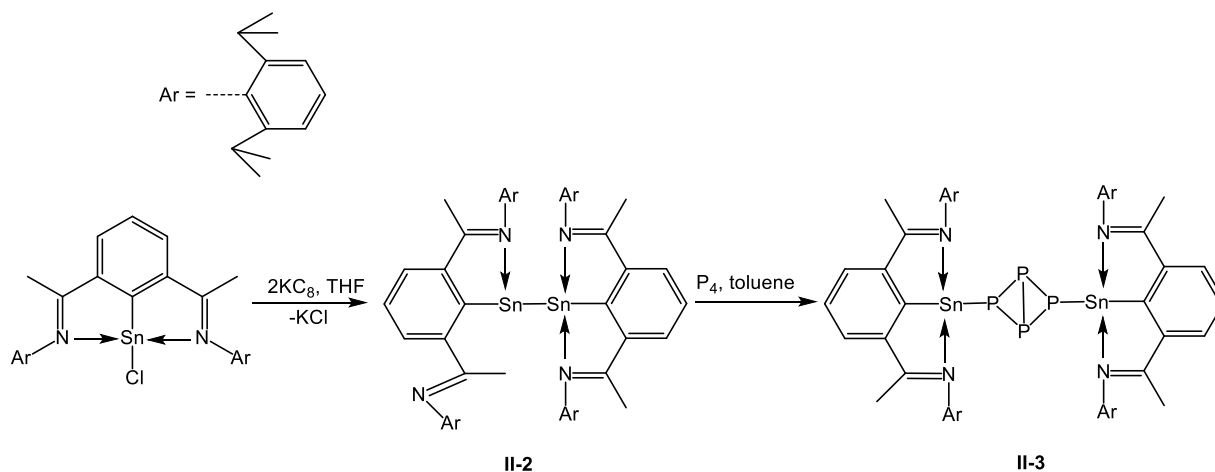
The chemistry of NCN pincers of group 13 elements is still limited. In 2010, Mu et al. reported reactions of 2,6-(ArN=CH)<sub>2</sub>C<sub>6</sub>H<sub>3</sub>Li with AlEt<sub>2</sub>Cl to afford a series of NCN pincer aluminum complexes (2,6-(ArN=CH)<sub>2</sub>C<sub>6</sub>H<sub>3</sub>)AlEt<sub>2</sub> **II-1**, where Ar =Ph, 2,6-Me<sub>2</sub>C<sub>6</sub>H<sub>3</sub>, 2,6-Et<sub>2</sub>C<sub>6</sub>H<sub>3</sub>, 2,6-<sup>i</sup>Pr<sub>2</sub>-C<sub>6</sub>H<sub>3</sub>.<sup>[29]</sup> All aluminum complexes were obtained in the monomeric form in which the Al atom is chelated by a κ<sup>3</sup>N,C,N-NCN pincer ligand, being one of a few examples of group 13 compounds supported by this ligand. These aluminum compounds **II-1** were also shown to be efficient initiators for L-lactide ring-opening polymerization in the presence of benzyl alcohol.



**Scheme II-3.** Synthetic method for the preparation of κ<sup>3</sup>N,C,N-NCN pincer aluminum compounds **II-1**.

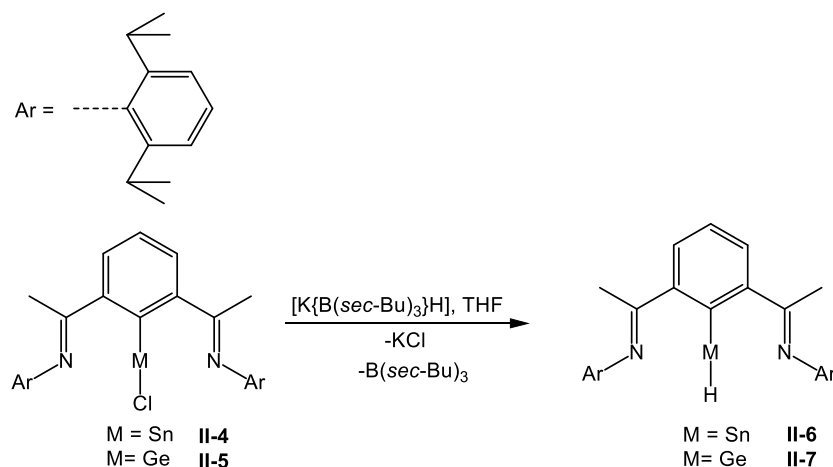
### II.1.2. Group 14

In 2010, Stalke et al. reported the reduction of [dimph]SnCl precursor with potassium graphite KC<sub>8</sub> at room temperature to generate a novel interesting bis(stannyne) [{2,6-<sup>i</sup>Pr<sub>2</sub>C<sub>6</sub>H<sub>3</sub>NC(CH<sub>3</sub>)<sub>2</sub>}]<sub>2</sub>C<sub>6</sub>H<sub>3</sub>Sn]<sub>2</sub> **II-2** containing a single Sn-Sn bond, which was shown by X-ray diffraction to have two unsymmetrically coordinated Sn(I) atoms.<sup>[30]</sup> Finally, this compound was demonstrated to activate P<sub>4</sub> under ambient conditions, which presents the first example of phosphorus activation by a Sn(I) compound.



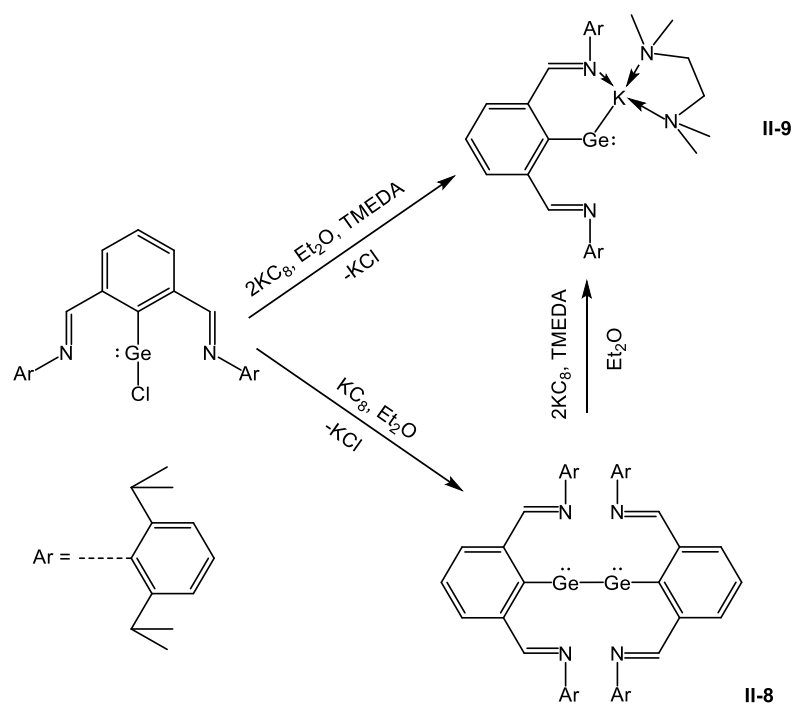
**Scheme II-4.** Preparation of compound **II-2** and **II-3**.

Later, the same group also showed that such a ligand is also useful to support monomeric Sn(II) and Ge(II) hydrides.<sup>[31]</sup> Treatment of precursors [ $\{2,6\text{-}^i\text{Pr}_2\text{C}_6\text{H}_3\text{NCMe}\}_2\text{C}_6\text{H}_3\text{MCl}$ ] (M = Sn (**II-4**), Ge (**II-5**)) with  $[\text{K}\{\text{B}(\text{sec-Bu})_3\}\text{H}]$  as a hydrogenating agent at 0°C afforded the hydride compound **II-6** and **II-7**, respectively. The compound **II-6** was considered as the first example of a Sn(II) hydride without a Sn-H intermolecular interaction.  $^1\text{H}$  NMR study shows sharp signals at  $\delta$  10.59 ppm for **II-6** and 6.69 ppm for **II-7**, assigned to Sn-H and Ge-H, respectively. The theoretical calculations revealed that these monomeric structures are stabilised by a significant donation from each N lone pair to the empty p orbital of the central metal atoms. Metal hydride bonds were built from a metal hybrid orbital with 89.3% *p*-character for Sn-H and 85.8% *p*-character for Ge-H. The lone pair of Sn and Ge had predominantly  $\sigma$ -character (79.4% (Sn); 70.9% (Ge)) supported by NBO analysis.



**Scheme II-5.** Synthetic method for hydride compounds **II-6** and **II-7**.

In 2011, the So group introduced digermynes [LGe–GeL] **II-8** supported by a 2,6-diiminophenyl ligand, which was prepared by the reaction of chlorogermynes [LGeCl] with 1 equiv of  $\text{KC}_8$ .<sup>[32]</sup> Ge atom in **II-8** adopts a distorted trigonal-pyramidal geometry supported by X-ray crystallography, which indicates that there is a lone pair of electrons on each Ge atom. The bond length of Ge–Ge (2.5059(5) Å) implies the absence of multiple bond character in this structure. The digermynes **II-8** further reacted with 2 equiv of  $\text{KC}_8$  and excess TMEDA to afford the gerylidenide anion **II-9**. The combination of X-ray crystallographic and spectroscopic data features that the K atoms are  $\eta^1$ -coordinated with the low-valent Ge atoms and negative charges at the Ge atoms are localised over the heterocycles.

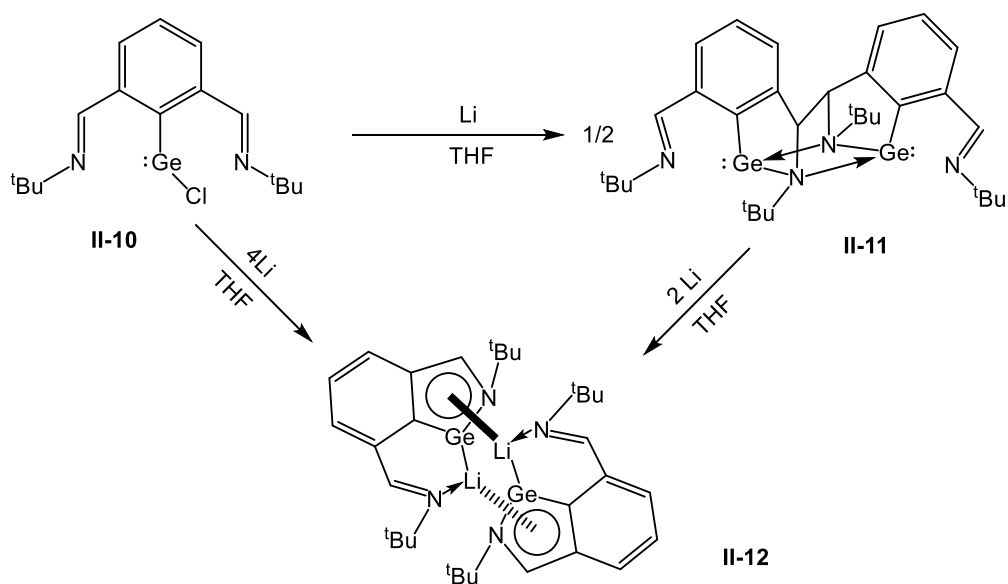


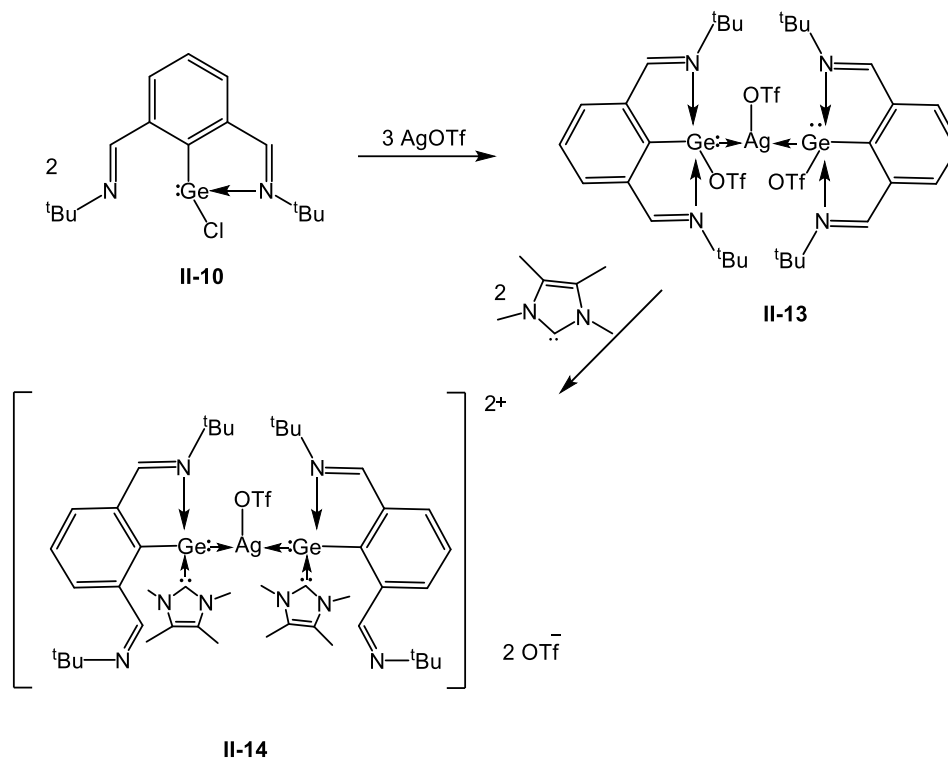
**Scheme II-6.** Synthetic method for preparation of compounds **II-8** and **II-9**.

Bis(germylene) [2-(HC-N<sup>t</sup>Bu)-6-(HC=N<sup>t</sup>Bu)C<sub>6</sub>H<sub>3</sub>Ge:]<sub>2</sub> **II-11**, which was synthesised by a reaction of the precursor **II-10** with 1 equiv of lithium in THF at room temperature, was introduced by So et al. in 2016.<sup>[33]</sup> The reaction was proposed to proceed via the reduction of the imine moiety to form an imine radical anion intermediate, followed by a C-C coupling reaction and salt elimination of LiCl to generate the compound **II-11**. The quantum chemical calculations revealed that the HOMO has a lone pair character of Ge atoms and whereas the LUMO illustrates the  $\pi^*$  orbitals on the ligand backbone and the C-Ge bonds. Further reduction of **II-11** by 2 equivalents of lithium in THF afforded the lithium gemyldenide [LGeLi]<sub>2</sub> **II-12**. It is proposed that the reaction proceeds through the reduction of Ge(II) centre in **II-11**, along with the homolytic cleavage of the C-C bond to form **II-12**. X-ray crystallography showed that each Li atom in **II-12** is  $\eta^1$ -coordinated to

the imine N atom,  $\eta^1$ -coordinated to the Ge centre atom, and  $\eta^5$ -coordinated to the GeCCCN ring of another molecule.

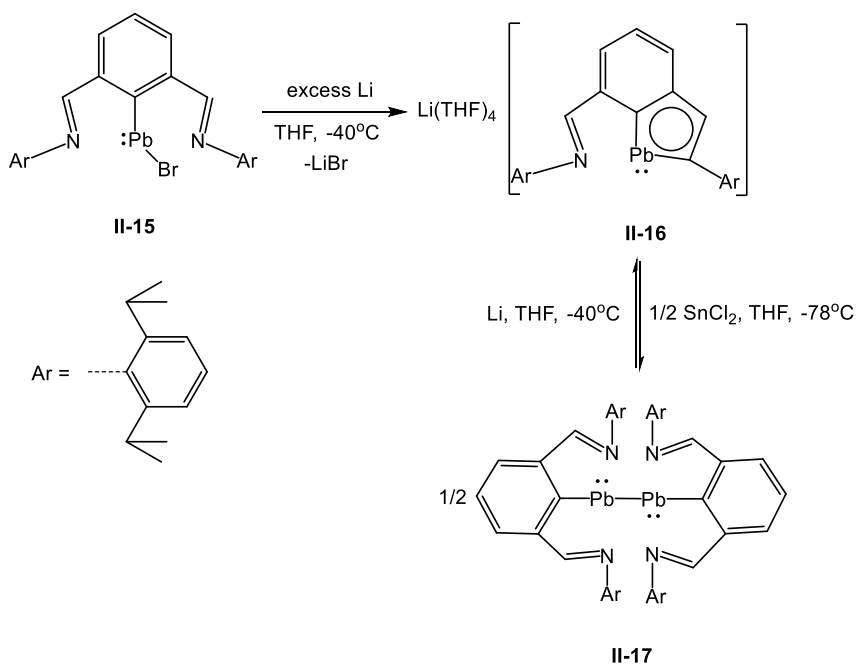
In a very recent paper published in 2018, <sup>[34]</sup> the same group reported the first example of a bis(germyliumylidene)silver(I) complex dication **II-14**. The combination of X-ray crystallography and DFT calculation showed that the Ge atoms in **II-14** bear positive charges (0.93, 0.92 e) and form donor–acceptor interaction with both C<sub>IME</sub> and Ag centres.





**Scheme II-7.** Synthetic methods for the preparation of Ge compounds.

The 2,6-diiminophenyl ligand was also found to be useful to stabilize a lead(I) radical and its dimeric derivative. The reaction of the Pb(II) compound **II-15** with excess Li in THF at  $-40^{\circ}\text{C}$  afforded the plumblydenide anion  $[\text{LPb}]^-\text{Li}(\text{THF})_4$  (**II-16**)<sup>[35]</sup> DFT calculation illustrated that the negative charge is aromatically delocalised over the  $\text{PbC}_3\text{N}$  five-membered ring in which 2p orbitals of C/N atoms and a 6p orbital of the low valent Pb atom can sufficiently overlap to form an aromatic compound. Compound **II-16** is the first aromatic low-valent lead analogue of an indenyl anion. The preparation of a 2,6-diiminophenyllead(I) dimer  $[\{2,6\text{-}i\text{Pr}_2\text{C}_6\text{H}_3\text{NC}(\text{CH}_3)\}_2\text{C}_6\text{H}_3\text{Pb}]_2$  (**II-17**) was carried out via oxidation of the plumblydenide anion  $[\text{LPb}]^-\text{Li}(\text{THF})_4$  (**II-16**) by  $\text{SnCl}_2$ . Reversibly, the reduction of lead (I) dimer **II-17** with lithium was able to regenerate anionic compound  $[\text{LPb}]^-$  **II-16**.



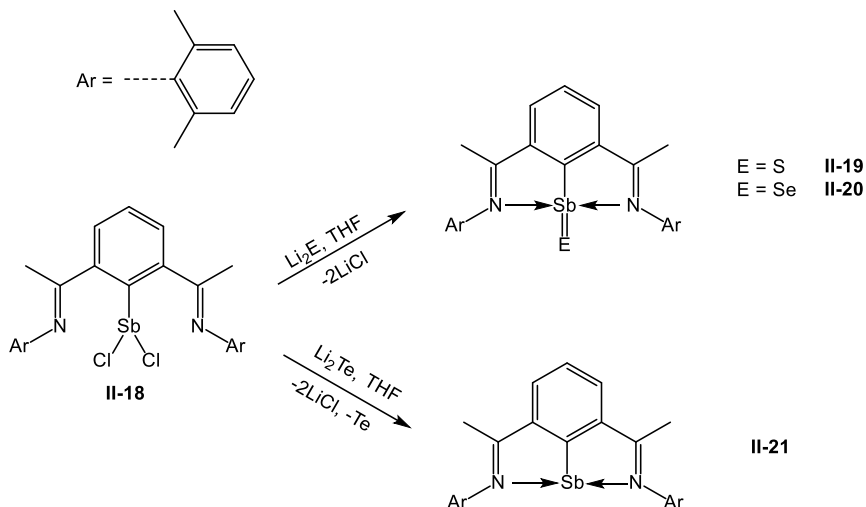
**Scheme II-8.** Synthetic method for preparation of compounds **II-16** and **II-17**.

### II.1.3. Group 15

The chemistry of group 15 elements supported by the dimph (**L<sub>1</sub>**) ligand has received significant attention. Dostal et al. reported a series of dimph-based antimony and bismuth compounds. The monomeric organoantimony sulphide and selenide LSbE (E=S (**II-19**), Se (**II-20**), L = 2,6-bis[(2,6-dimethylphenyl)ketimino]phenyl) were prepared by the reaction of the precursor LSbCl<sub>2</sub> **II-18** with the *in situ* prepared Li<sub>2</sub>S or Li<sub>2</sub>Se.<sup>[36]</sup> The antimony centres in these compounds adopt a distorted trigonal bipyramid geometry. The combination of X-ray crystallography and computational studies indicate the double bond character of S-Se and Se-Sb. Compound **II-19** is the first organometallic compound with a terminal double bond S=Sb. The strong interaction N→Sb was detected, with the bond length Sb(1)–N(1) of 2.415(5) Å and Sb(1)–N(2) of 2.416(4) Å in **II-19**, Sb(1)–N(1) of 2.395(2) Å and Sb(1)–N(2) of 2.393(2) Å in **II-20**, indicating strong Lewis acidity of Sb



atoms. Similarly, a reaction of  $\text{LSbCl}_2$  **II-18** with  $\text{Li}_2\text{Te}$  generated the organoantimony(I) compound **II-21** as the result of fast decomposition of  $\text{LSbTe}$  compound.

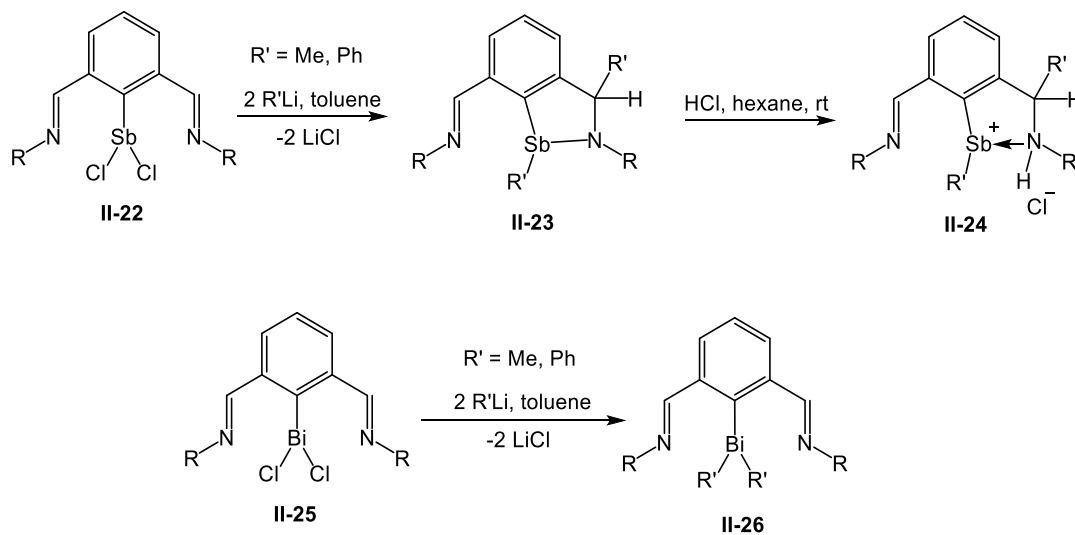


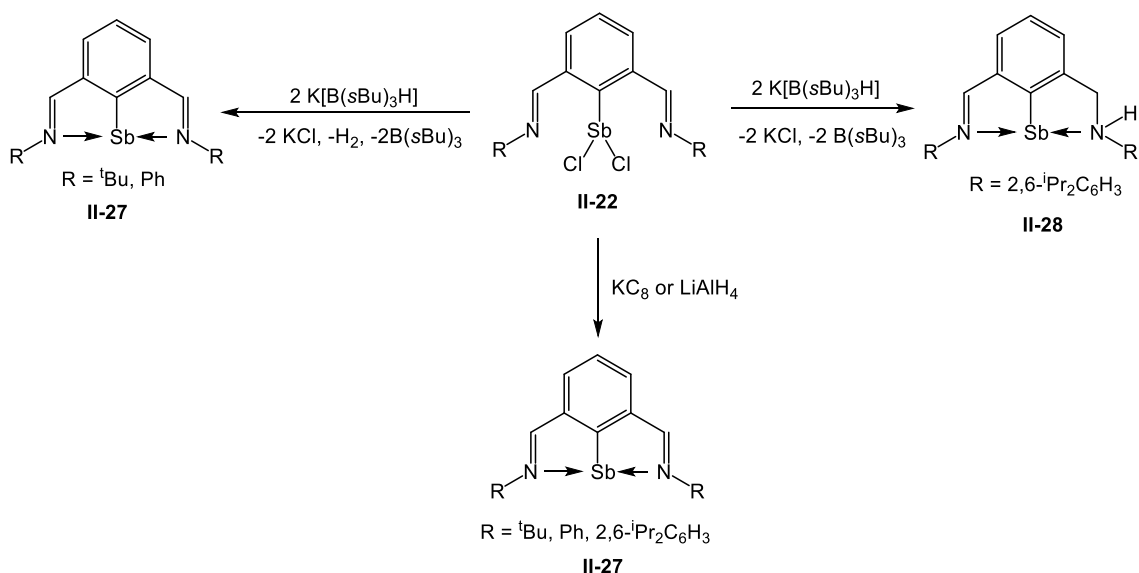
**Scheme II-9.** Synthetic method for preparation of compounds **II-19**, **II-20**, and **II-21**.

The reactivity of N,C,N-chelated antimony(III) compound **II-22** and bismuth(III) compound **II-25**, containing pincer type ligands, with organolithium reagents were investigated by Dostal et al.  $\text{LiMe}$  and  $\text{LiPh}$  add to the  $\text{C}=\text{N}$  bond in **II-22** to give the amido products **II-23**.<sup>[37]</sup> The compound **II-23** was further treated with 1 molar equiv. of  $\text{HCl}$ , which resulted in the cleavage of the  $\text{Sb}-\text{N}$  bond to form a cationic species **II-24**. In contrast, adding organolithium reagents to the bismuth(III) compound **II-25** afforded the dialkyl species **II-26** by chloride substitution, whereas the reduction of the  $\text{C}=\text{N}$  bond was not observed.<sup>[37]</sup> The central Bi atom adopts a trigonal-pyramidal geometry, with the sum of  $\text{C}-\text{Bi}-\text{C}$  bonding angles of  $279.69^\circ$ . This was considered as the first example of a structurally characterised aryl(dimethyl)bismuth(III) compound.

Later on, the same group reported that the symmetrical  $\text{Sb(I)}$  compound **II-27** can be prepared by the reduction of precursor **II-22** by using different reducing reagents, such

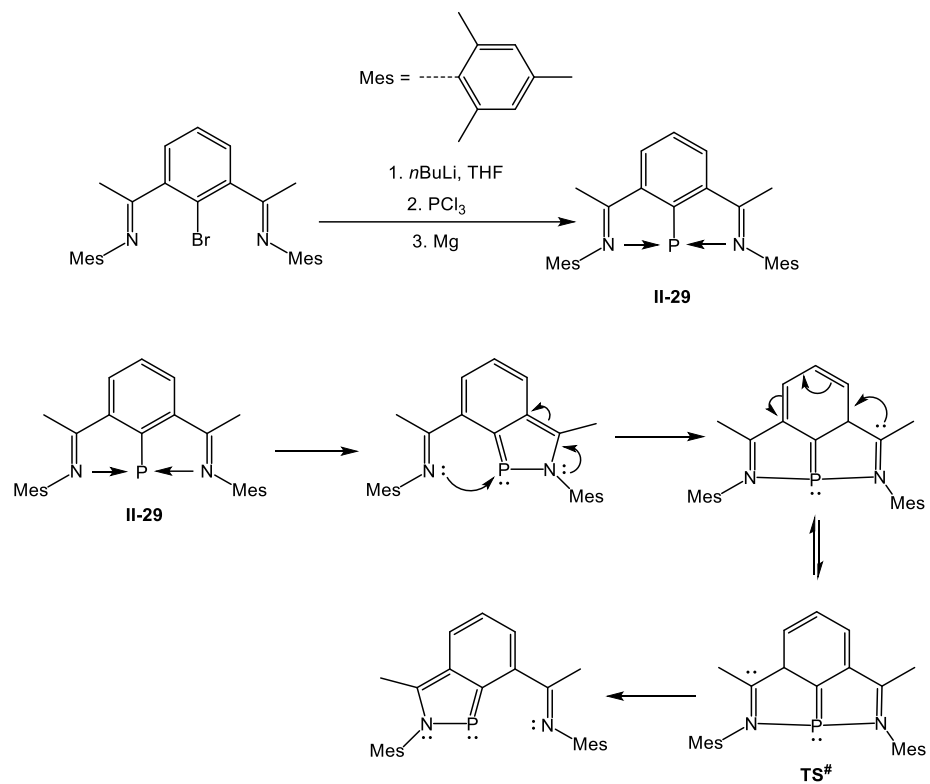
as  $\text{KC}_8$ ,  $\text{LiAlH}_4$ .<sup>[38]</sup> Interestingly, the selection of the reducing agent and the ligand was shown to be crucial for determining the outcome of the reaction. By using a bulky borohydride  $\text{K}[\text{B}(\text{sBu})_3\text{H}]$ , the reduction of compounds **II-22** bearing less sterically encumbered substituents led to the formation of compounds **II-27** as the major products. However, the analogous reaction of Sb compound bearing the bulky substituents ( $\text{R} = 2,6\text{-}^i\text{PrC}_6\text{H}_3$ ) proceeded via the reduction of the imino functionality, which led to the formation of an unsymmetrically substituted stibinidene [ $\text{C}_6\text{H}_3\text{-}2\text{-(CH=NDipp)-}6\text{-(CH}_2\text{NHDipp)]Sb$  (Dipp =  $2,6\text{-}^i\text{Pr}_2\text{C}_6\text{H}_3$ , **II-28**). Moreover, the experimental and theoretical data for **II-28** indicate a significant aromatic character of the  $\text{SbC}_3\text{N}$  ring with a very strong intramolecular  $\text{N} \rightarrow \text{Sb}$  interaction, contributing to the stabilization of the discussed compound.





**Scheme II-10.** Reactivity of **II-22** and **II-25**.

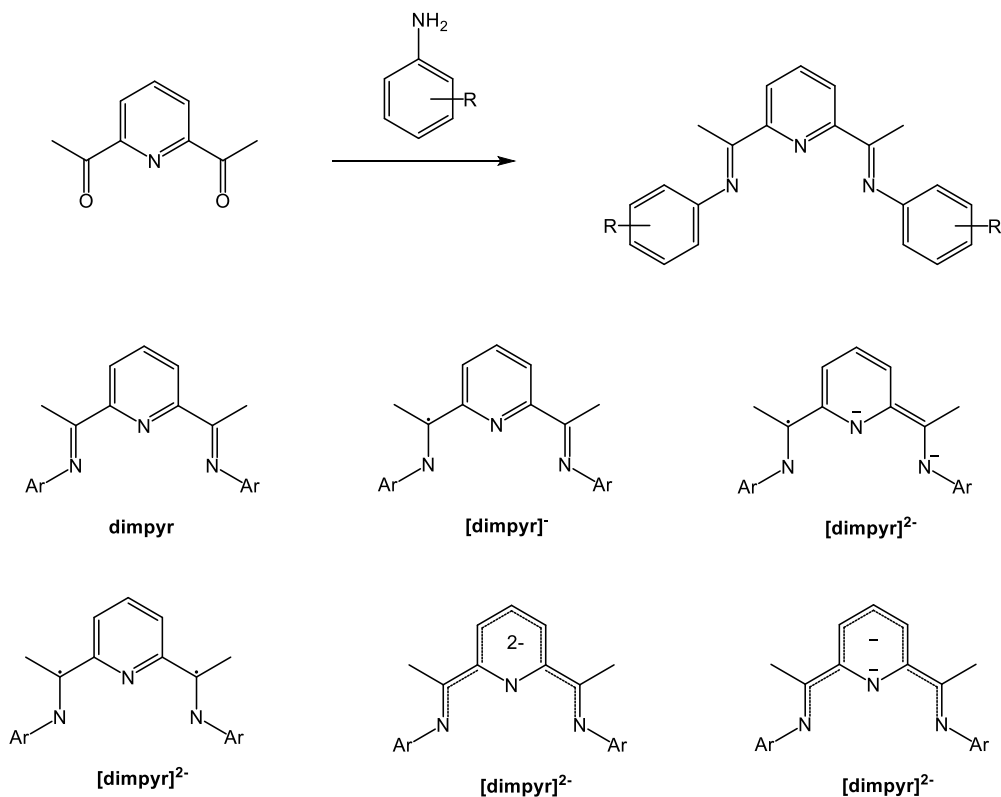
Inspired by the Dostal's work, Cain et al.<sup>[39]</sup> attempted to use an NCN ligand to trap phosphinidene by forming an analogue of the symmetrical Sb(I) compound. The compound **II-29** was obtained by the treatment of ligand with *n*BuLi and PCl<sub>3</sub>, followed by reduction with magnesium. An NMR study indicated the presence of a C<sub>2v</sub> symmetrical species in solution between -60°C and 60°C. However, X-ray crystallography revealed an unsymmetrical compound in which the phosphorus centre is coordinated by only one adjacent N atom with the P-N bond length of 1.757(2) Å. The stronger P-N interaction (vs. Bi/Sb-N interaction)<sup>[37,38]</sup> was explained by the closer size and matching orbital energy between nitrogen and phosphorus, which can enhance the donating ability of the nitrogen lone pair into the empty p orbital of the P centre, with a possible back-bonding from the filled p orbital of P into the π\*(C=N) orbital. DFT calculations showed that an equilibration between two N ligands occurs rapidly in solution via a “bell-clapper” mechanism through a symmetric transition state calculated to lie only 4.0 kcalmol<sup>-1</sup> above the ground state.



**Scheme II-11.** Synthetic method to trapping phosphinidene **II-29** and mechanism of P-N exchange by a “bell-clapper” pathway.

## II.2. Main Group Complexes Supported by Bis(imino)aryl Pyridine Ligand

Bis(imino) pyridine (dimpyr) has been found as a powerful ligand for both transition metal and main group elements.<sup>[40-42]</sup> It grew to prominence with the discovery of very active Fe and Co catalysts for ethylene polymerization by the groups of Brookhart and Gibson in mid 90s,<sup>[43,44]</sup> and by later manifestation by Chirik and co-workers that bis(imino) pyridine-supported complexes of iron are effective catalysts for the hydrosilylation of olefins and alkynes.<sup>[45]</sup> It was also demonstrated that transition metals complexes of bis(imino) pyridine are able to catalyze C–C bond-forming processes including the cycloaddition of dienes and the Suzuki-Miyaura reaction.<sup>[46,47]</sup> Aryl substituted dimpyr ligands can be conveniently synthesised by Schiff base condensation of the commercially available 2,6-diacetylpyridine with two equivalents of substituted anilines. The steric environments of the ligand can be easily modified by using various substituted anilines (Scheme II-12). The dimpyr ligand can exist in the mono-anionic radical form and di-anionic form, with the radical character distributed over the ligand framework (Scheme II-12).



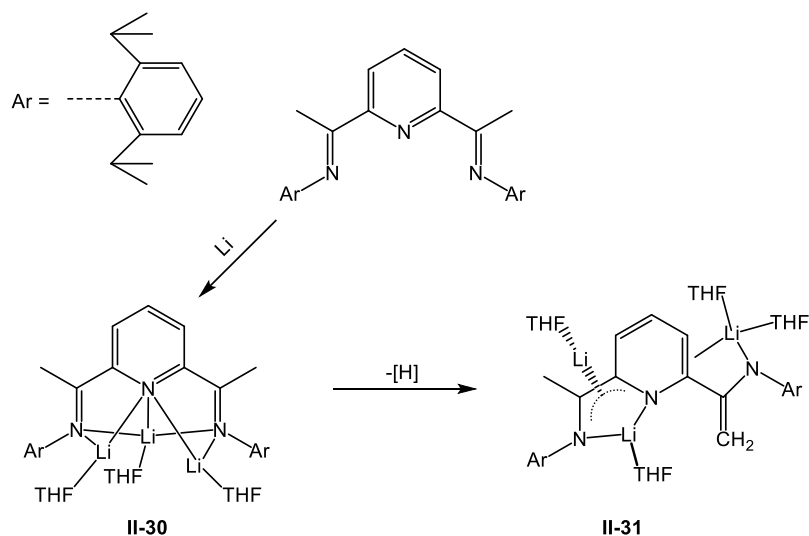
**Scheme II-12.** Synthetic method to ligand bis(imino)aryl pyridine and electronic structures in various oxidation states.

Since the initially published study by Alyea and Merrel,<sup>[48]</sup> numerous reports have appeared in the literature, dealing with the effects of ligand modification and the relationship between the structure and activity.<sup>[40,42,49,50]</sup> The bis(imino)aryl pyridine ligand has been demonstrated to accommodate up to three electrons in the antibonding orbitals of the imino unit and the pyridine ring.<sup>[51]</sup> Furthermore, the ability of the large  $\pi$ -system to accommodate the negative charge may increase the Lewis acidity of the metal centre and may help in stabilization of electron-rich, low-valent metals. Recently, such a ligand has been utilised to design main group complexes which can be applied in catalysis and

molecular activation.<sup>[41,51–54]</sup> This part will focus on the main group complexes of this ligand reported up to date.

### *III.1.1. Group 1*

To study the ability of the dimpyr ligand to accept negative charge, Gambarotta et al. in 2002 reported the reduction of [2,6-{2,6-(<sup>i</sup>Pr)<sub>2</sub>PhN=C(Me)}<sub>2</sub>(C<sub>5</sub>H<sub>3</sub>N)] with strong reductants, such as Li and [Li(naphthalenide)] in the absence of transition metals.<sup>[55]</sup> The reaction with Li resulted in the formation of a mixture of **II-30** and **II-31**. The structure of **II-31** is remarkably different as the result of the loss of one hydrogen atom, which corresponds to the formal one-electron oxidation. The reaction with [Li(naphthalenide)] at low temperature afforded only one product **II-31**. Compound **II-30** is a rare example of a paramagnetic organolithium complex with  $\mu_{\text{eff}} = 1.30 \mu_{\text{B}}$  with the presence of antiferromagnetic exchange between the radical anions. The ESR spectrum shows a single resonance peak at  $g = 2.001$  with a hyperfine pattern appearing as a complex 25 lines spectrum. A SOMO-LUMO gap is approximately 2.3 eV as revealed by a computational study. The LUMO and LUMO+1 are antibonding orbitals with respect to the pyridine ring and within the C=N bond of the imine moiety. The bis(imino)aryl pyridine ligand has been demonstrated to accommodate up to three electrons in the antibonding orbitals of the imino unit and the pyridine ring in a low-spin configuration.

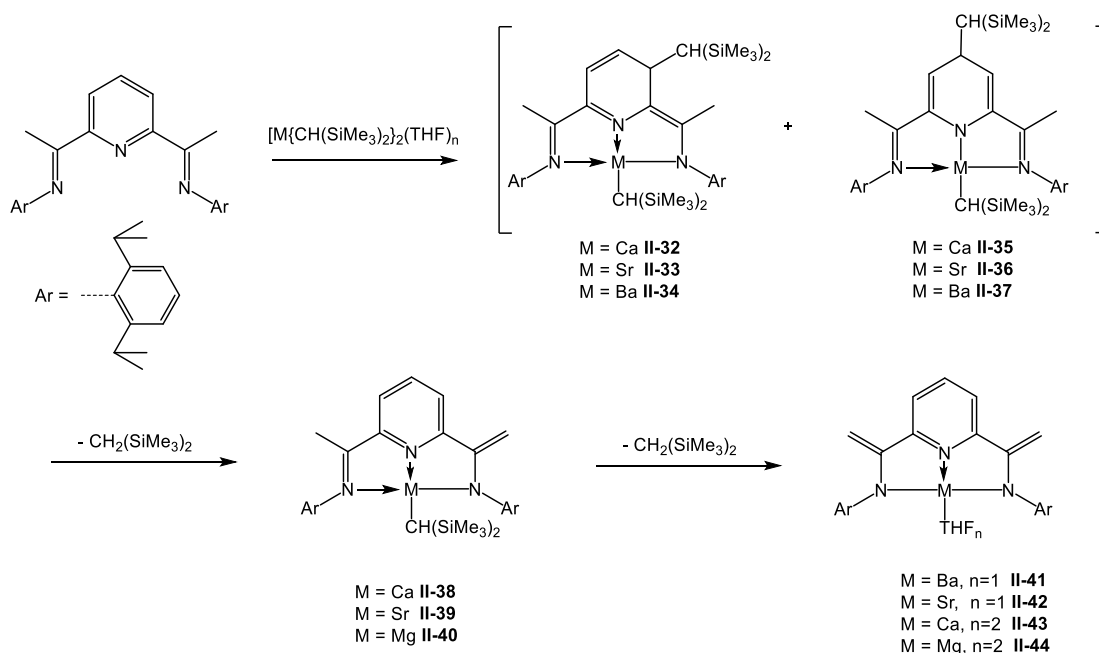


**Scheme II-13.** Synthetic route to **II-30** and **II-31**.

### III.1.2. Group 2

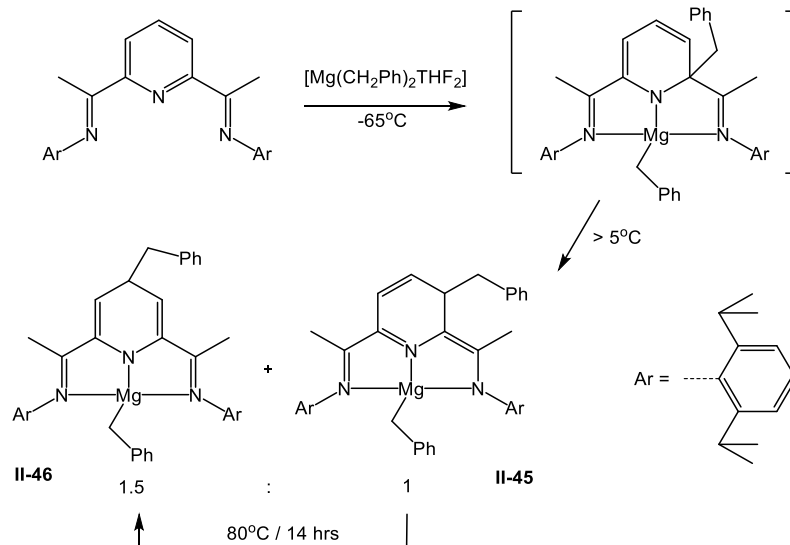
Hill et al. reported in 2010 a series of reactions of the heavier group 2 dialkyl derivatives and the analogous magnesium species with the dimpyr ligand.<sup>[56]</sup> The reaction of the magnesium dialkyl compound with ligand solution in benzene resulted in the formation of a  $C_2$  symmetric species **II-40** as a mono-deprotonated product. Heating this solution at 60°C for 24 h resulted in the conversion of this species to the product **II-44** as the result of deprotonation of both methyl groups attached to the imine unit. In contrast, analysis by NMR spectroscopy of the calcium- and strontium-based analogues indicated the presence of a singly deprotonated ligand in compounds **II-38** and **II-39** which appeared alongside two isomeric species **II-32**, **II-35** (Ca) and **II-33**, **II-36** (Sr) formed by the migration of alkyl groups to either the C<sub>3</sub> or C<sub>4</sub> position of the pyridine ring. In the case of the reaction with the barium dialkyl, no evidence for any singly deprotonated species was formed during the reaction. The reactivity of metal dialkyl with ligand occurred in the order Ba > Sr > Ca, supported by a kinetic study.





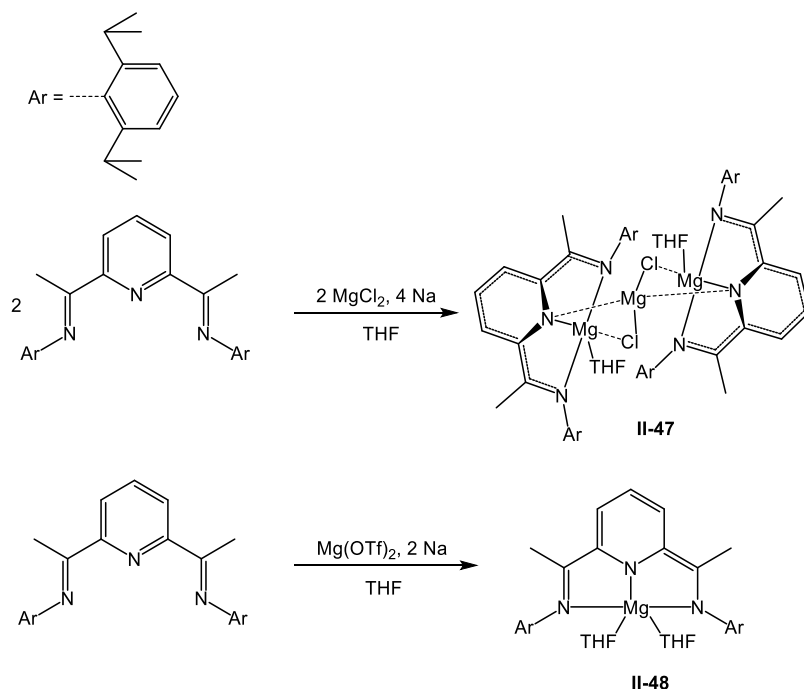
**Scheme II-14.** Synthetic method to several complexes of group 2 elements supported by dimpyr ligand.

In order to study further the reactivity of alkali-earth alkyls with dimpyr ligands, Rodríguez-Delgado et al. investigated the reaction of dimpyr ligands with  $Mg(Bn)_2(THF)_2$  (Bn = benzyl).<sup>[57]</sup> NMR studies showed that the reaction of  $[Mg(Bn)_2THF_2]$  with dimpyr at  $-65\text{ }^\circ\text{C}$  afforded a thermally unstable product as the result of migration of the benzyl unit to the C<sub>2</sub> position in the pyridine ring. A rearrangement of this compound was observed at above  $+5\text{ }^\circ\text{C}$ , yielding a mixture of two isomeric complexes **II-45** and **II-46**, in which the benzyl group has migrated to positions C<sub>3</sub> or C<sub>4</sub> of the central ring, respectively. Likewise, the reaction of dimpyr with  $[Mg(Bn)_2THF_2]$  at room temperature generated a similar isomeric mixture. Heating the mixture at  $80\text{ }^\circ\text{C}$  for 14h resulted in the rearrangement of the 3-benzyl isomer (**II-45**) into a stable 4-benzyl product (**II-46**). No further shift was observed when the heating continued for 24 h.



**Scheme II-15.** Magnesium alkyl react with dimpyr ligand affording **II-45** and **II-46**

Meanwhile, a successful attempt by Berden et al. in 2016 in developing the reduced chemistry of the dimpyr ligand with Mg(II) was focused on the methyl-substituted derivative.<sup>[51]</sup> Reaction of a dimpyr precursor with 2 equivs of sodium followed by salt metathesis with MgCl<sub>2</sub> resulted in the formation of a red powder of compound **II-47**. <sup>1</sup>H-NMR study of **II-47** showed a C<sub>2v</sub> symmetric species with two pyridine resonances at 6.42 and 5.28 ppm. Using Mg(OTf)<sub>2</sub> as a salt reagent, the reaction afforded a different compound **II-48**. The <sup>1</sup>H-NMR spectrum of **II-48** suggests an asymmetric geometry, with three distinct pyridine resonances at 6.98, 6.69 and 5.21 ppm. X-ray characterization of **II-47** showed the formation of five-coordinate Mg centres that can be described as distorted trigonal-bipyramidal, on the basis of the τ<sub>5</sub> value of 0.660. In contrast, the Mg centre in **II-48** adapted a distorted square pyramidal with the τ<sub>5</sub> value of 0.308.

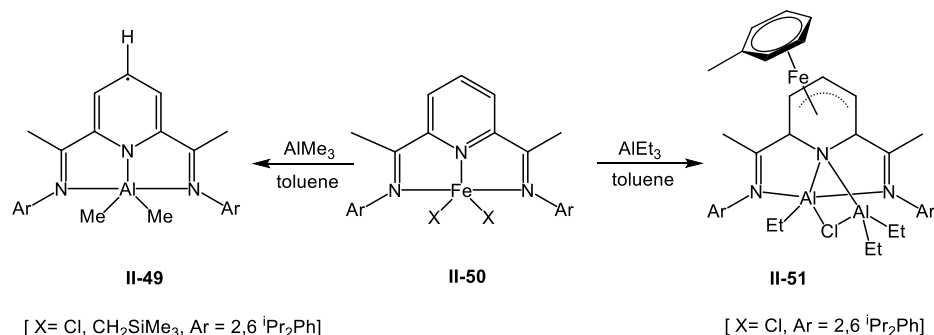


**Scheme II-16.** Synthesis of compounds **II-47** and **II-48**.

### III.1.3. Group 13

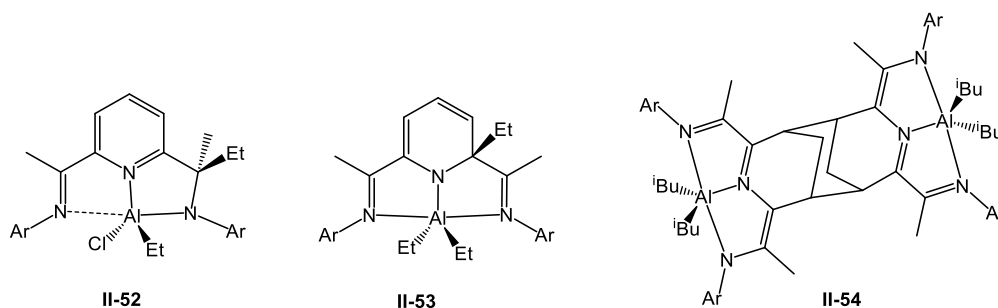
This first study of dimpyr compounds of elements from group 13 was reported by Gambarotta et al. in 2005.<sup>[58]</sup> Reactions of  $\text{LFeCl}_2$  ( $\text{L} = \{2,6\text{-}[2,6\text{-}(\text{iPr})_2\text{PhN}=\text{C}(\text{CH}_3)]_2(\text{C}_5\text{H}_3\text{N})\}$ ) with the alkylating reagents  $\text{R}_3\text{Al}$  [ $\text{R} = \text{Me}, \text{Et}$ ] were carried out in toluene at  $-35^\circ\text{C}$ , resulting in transmetalation and formation of aluminum compounds **II-50** and **II-51**, respectively. The crystal structure of **II-50** shows a distorted trigonal bipyramidal geometry at the Al centre with the  $\text{Me}_2\text{Al}$  unit bound to the apparently unperturbed ligand. EPR and DFT studies revealed that compound **II-50** is a paramagnetic divalent Al species, with  $\mu_{\text{eff}} = 1.73 \mu_{\text{B}}$  and the unpaired electron mainly centred on the one-electron reduced diiminepyridine radical. Similarly, **II-51** is paramagnetic with a lower value of the magnetic moment,  $\mu_{\text{eff}} = 1.48 \mu_{\text{B}}$ , in solution. An X-ray study shows a  $\text{Et}_2\text{Al}(\mu\text{-Cl})\text{AlEt}$  unit bound to the N atoms of the imine moiety. The Fe centre adapts the

$\eta^4$ -bonding mode to the distorted pyridine ring and is  $\eta^6$ -coordinated to a molecule of toluene.



**Scheme II-17.** Synthesis of **II-50** and **II-51**.

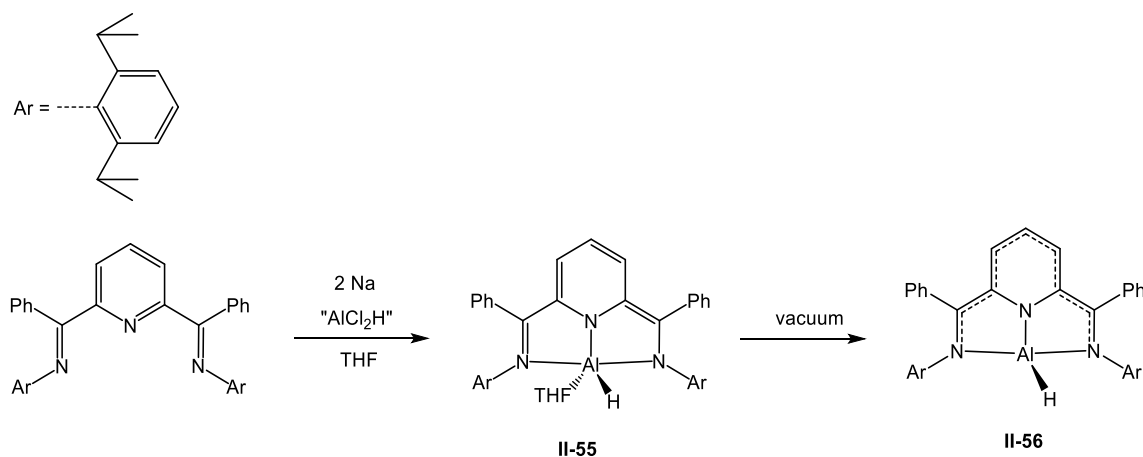
Similarly, Budzelaar et al.<sup>[52]</sup> observed ligand alkylation in a reaction of dimpyr ligand with a series of aluminum alkyls (Me<sub>3</sub>Al, Et<sub>3</sub>Al, <sup>i</sup>Bu<sub>3</sub>Al, <sup>i</sup>Bu<sub>2</sub>AlH, Et<sub>2</sub>AlCl). The addition of alkyls to the imine carbon and the pyridine C<sub>2</sub> and C<sub>4</sub> positions was observed, depending on the choice of aluminum alkyls reagents. Interestingly, C<sub>2</sub> alkylation is a reversible process, so that overtime the C<sub>2</sub> alkylation product converts to imine alkylation product. At this stage, the mechanism of ligand alkylation remains unclear.

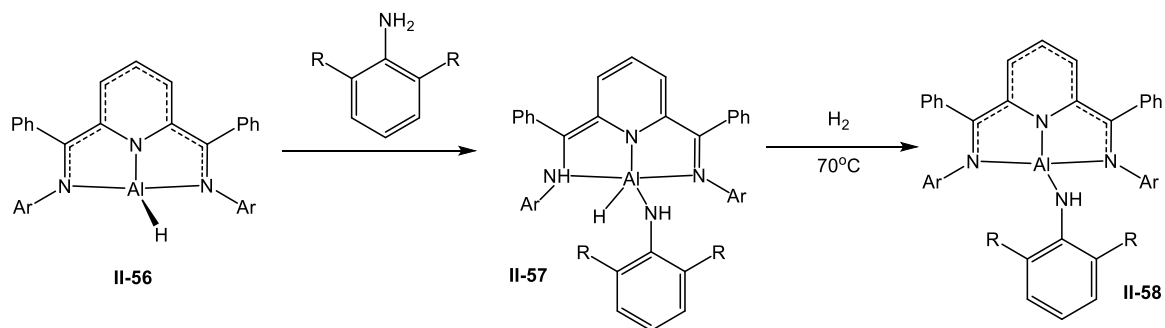


**Scheme II-18.** Several isolated alkylated products reported by Budzelaar et al.

In 2013, Berben et al. reported the preparation of aluminum complexes of a tridentate bis(imino)pyridine ligand, such as the tetrahydrofuran (THF)-adduct **II-55** and

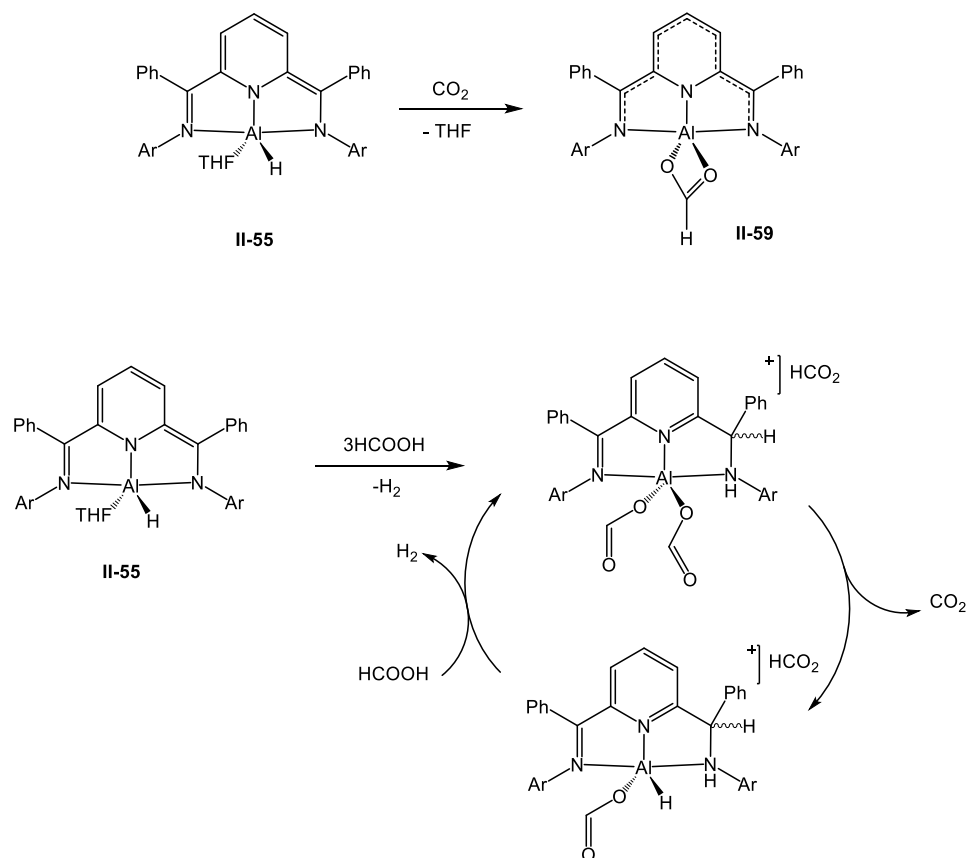
the base-free aluminum hydride complexes **II-56**.<sup>[59,60]</sup> <sup>1</sup>H NMR spectrum of **II-55** shows a broad peak at 4.60 ppm corresponding to the Al–H proton, and resonances for the coordinated THF ligand at 3.59 and 1.37 ppm. A stretching band at 1966 cm<sup>-1</sup> for Al–H was observed in the IR spectrum. X-ray crystallography shows that the geometry at the Al centre is close to square-pyramidal with  $\tau = 0.117$ . Moreover, the bond lengths in **II-55** indicate that the two electron reduction might localize at the pyridine nitrogen and one of the imine nitrogens, so that three N atoms consist of one formally imine N (Al–N<sub>im</sub> = 2.077(2) Å), an anionic pyridine (Al–N<sub>py</sub> = 1.851(2) Å), and one anionic amido N (Al–N<sub>am</sub> = 1.954(2) Å). The removal of THF from the Al coordination sphere under vacuum led to the formation of a four-coordinate complex **II-56** determined by NMR and IR studies. The hydride aluminum compound **II-56** was found to activate N–H bonds via a metal–ligand cooperative mechanism, making it a potential catalyst for amine dehydrogenation. Indeed, when 20 mol % of **II-56** was heated at reflux in a toluene solution of benzylamine at 70 °C for 24 h, 75% conversion to the product N-(phenylmethylene)benzenemethanamine was observed with 3.6 turnovers, as measured by GC–MS.





**Scheme II-19.** The preparation of **II-56** and its reactivity

Later on, aluminium complex **II-55** was demonstrated to promote selective dehydrogenation of formic acid to  $\text{H}_2$  and  $\text{CO}_2$  with the initial turnover frequency of 5200 turnovers per hour.<sup>[61]</sup> Berben and co-workers shown that the reaction of **II-55** with  $\text{HCOOH}$  at low-temperature results in a triple-protonation process: twice on the dimpyr ligand and once to liberate  $\text{H}_2$  from the Al-hydride. The exposure of **II-55** to  $\text{CO}_2$  atmosphere results in the insertion of  $\text{CO}_2$  into the Al-hydride bond, leading to formation of an Al-formate **II-59** in high yield. The reaction mechanism of dehydrogenation of formic acid by **II-55** includes two parts: O-H bond activation of  $\text{HCOOH}$  and the  $\text{HCOOH}$  dehydrogenation catalytic cycle. Such a reactivity of **II-55** is explained by the ability of aluminum hydride complex to affect  $\beta$ -hydride abstraction from the formate anion to generate an Al-hydride intermediate and liberate  $\text{CO}_2$ . DFT calculations of the reaction mechanism reported by Fu et al.<sup>[62]</sup> agree well with the Berden's proposal.

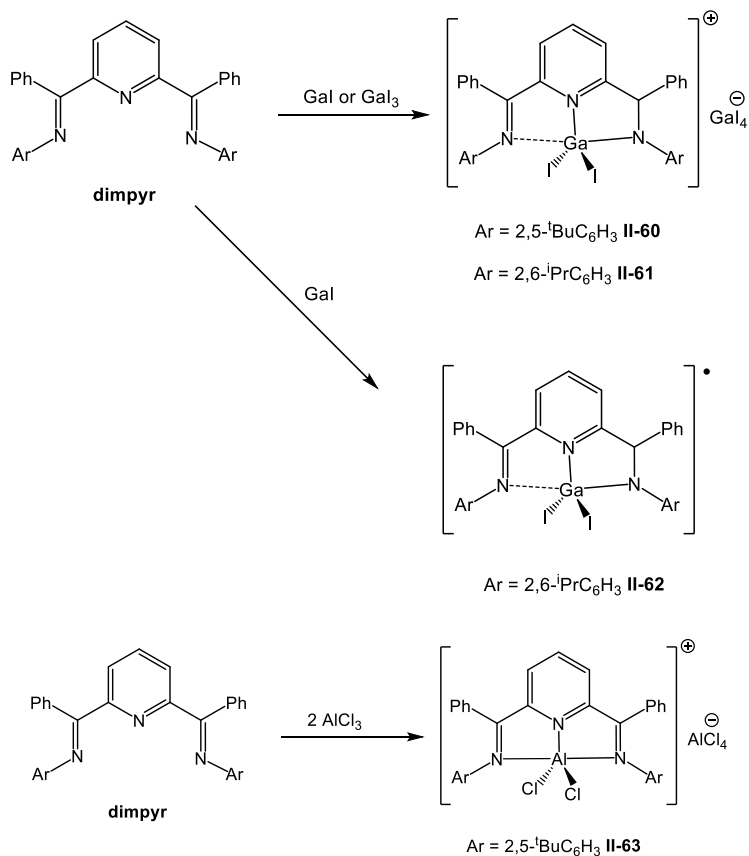


**Scheme II-20.** Insertion of  $\text{CO}_2$  into the  $\text{Al-H}$  bond of **II-55** and proposed mechanism for  $\text{HCOOH}$  dehydrogenation by **II-55**.

In 2010, Richeson et al.<sup>[63]</sup> introduced a series of Ga compounds supported by the bulky dimpyr ligands. The compound **II-60** and **II-61** were obtained from direct reactions of the ligand with either  $\text{GaI}_3$  or  $\text{GaI}$ . The molecular structure of **II-60** showed that the Ga atom adapts a distorted trigonal bipyramidal geometry and two five-membered rings  $\text{N}_2\text{C}_2\text{Ga}$  are planar. Moreover, the length of the  $\text{Ga-N}_{\text{py}}$  bond (2.017(5) Å) is shorter than those of  $\text{Ga-N}_{\text{imine}}$  (2.151(5) Å and 2.181(5) Å). Interestingly, an NMR experiment indicated the presence of second product **II-62** in the mixture from the reaction of dimpyr ligand with  $\text{GaI}$ . X-ray diffraction analysis of red crystals of **II-62** showed that this species is a neutral analogue of **II-61**. The coordination of ligand to the  $\text{GaI}_2$  unit in **II-61** and **II-**

**62** was found to be similar, suggesting that the neutral form **II-62** is a radical species. Additionally, an EPR spectrum of **II-62** revealed a signal with the g-value of 2.0029, which agrees well with the radical character of this compound.

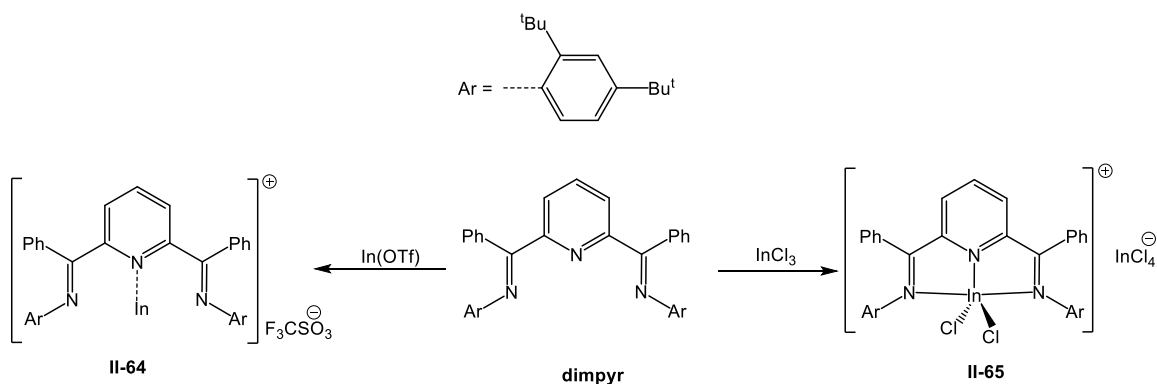
The same group reported an analogous reaction of dimpyr with  $\text{AlCl}_3$ , which furnished an Al(III) product **II-63**. The combination of NMR characterization and X-ray crystallography indicates the symmetrical arrangement in **II-63**, whereas the Al centre is in distorted trigonal pyramidal environment. Such an aluminum complex also consists of  $[\{2,5\text{-}^t\text{Bu}_2\text{C}_6\text{H}_3\text{N}=\text{CPh}\}_2(\text{NC}_5\text{H}_3)]\text{AlCl}_2^+/\text{AlCl}_4^-$  as a cation/anion pair, observed by X-ray crystallography.



**Scheme II-21.** Preparation of Gallium compounds and Aluminum compound reported by Richeson et al.



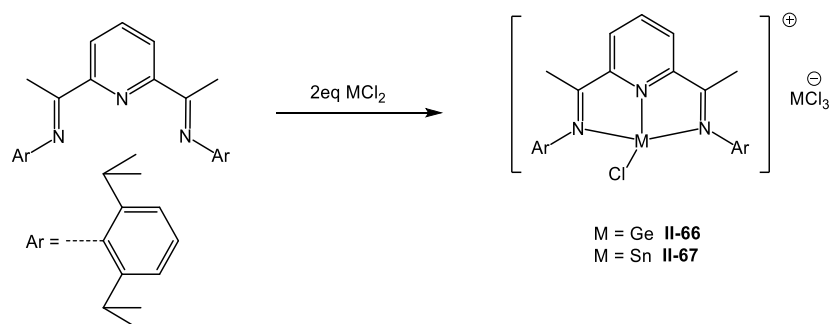
Similarly, Richeson et al. prepared a series of novel dimpyr-supported indium complexes. A symmetrical compound **II-64** was obtained from the reaction of dimpyr ligand with  $\text{In}(\text{OSO}_2\text{CF}_3)$ , which is the first low-valent main-group metal complex of the dimpyr scaffold.<sup>[64]</sup> The identity of this compound was established by a single-crystal X-ray diffraction analysis, where the In centre lies slightly out of the pyridine plane. The bond length  $\text{In-N}_{\text{pyridine}}$  (2.495(5) Å) is longer than that in the two-coordinate  $\beta$ -diketiminato complex  $[\text{In}\{(\text{NDippCMe})_2\text{CH}\}]$  (2.27 Å),<sup>[65]</sup> while the  $\text{In-N}_{\text{imine}}$  distances are weakly coordinating (2.748(6) Å and 2.689(6) Å). The distances of  $\text{In-O}_{\text{triflate}}$  [2.761(7) and 3.045(9) Å] are long, which are consistent with a well-separate triflate anion. The analysis of the electronic structure indicated that the  $\text{In}^+$  ion features little covalent donor-acceptor interaction from the ligand with very weak In-ligand interactions. In contrast, a 1:2 stoichiometric ratio reaction between dimpyr and  $\text{InCl}_3$  generated compound **II-65**, in which the indium centre adapts a distorted trigonal bipyramidal geometry supported by X-ray analysis.



**Scheme II-22.** Preparation of In compounds **II-64** and **II-65**

### III.1.4. Group 14

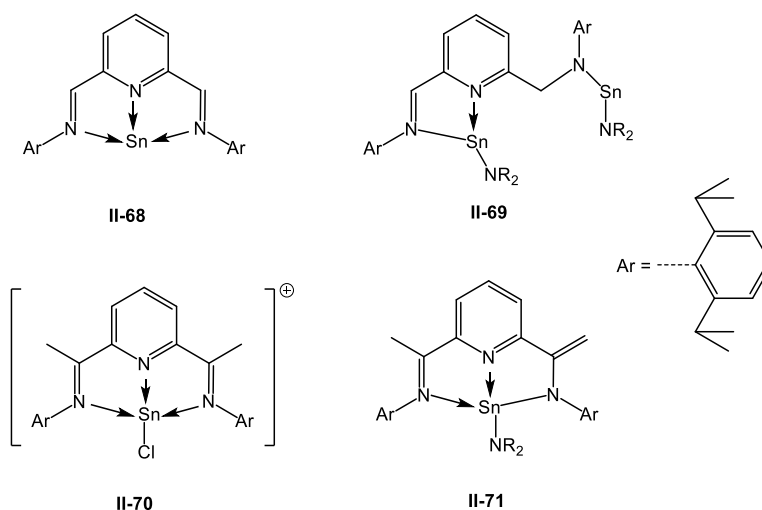
Stalke et al. introduced a new approach to the synthesis of compounds of heavier group 14 metals stabilised by a dimpyr ligand, i.e. [dimpyrGeCl]<sup>+</sup>[GeCl<sub>3</sub>]<sup>-</sup> **II-66** and [dimpyrSnCl]<sup>+</sup>[SnCl<sub>3</sub>]<sup>-</sup> **II-67**.<sup>[66]</sup> These authors observed self-ionisation of germanium and tin upon the reaction of dimpyr with GeCl<sub>2</sub>\*diox and SnCl<sub>2</sub>. The <sup>119</sup>Sn NMR spectrum of the Sn compound **II-67** consists of two singlets at -60.2 and -435.0 ppm corresponding to the SnCl<sub>3</sub><sup>-</sup> anion and the [dimpyrSnCl]<sup>+</sup> cation, respectively. X-ray analysis revealed that the metal centre is connected to three nitrogen atoms of the ligand and one chlorine atom. The metal centre in the cation [dimpyrMCl]<sup>+</sup> adopts a distorted square pyramidal geometry if the electron lone pair of the metal is considered as the fourth position of the basal plane, whereas the chlorine atom occupies the top of the square pyramid.



**Scheme II-23.** Preparation of the heavier group 14 elements complexes of dimpyr, **II-66** and **II-67**.

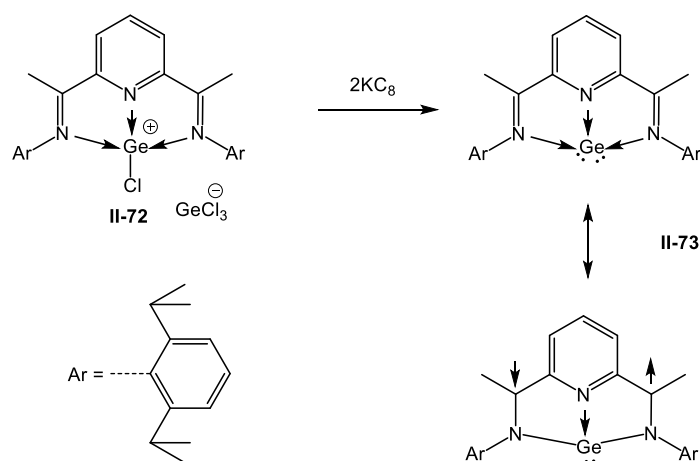
Following the Stalke's study,<sup>[66]</sup> Fischer et al. reported the first example of a Sn compound in the formal oxidation state of zero, stabilised by a dimpyr scaffold, **II-68**. The nitrogen atoms of the ligand coordinate to the Sn centre to form a planar complex with two five-membered chelating rings. The Sn-N<sub>imine</sub> bond lengths are 2.397(2) and 2.315(2) Å, and is consistent with those reported in the literature for the N→Sn bonds. However, such

distances in **II-68** are shorter than in the related dimer  $\text{RSn}^{\text{I}}\text{Sn}^{\text{I}}\text{R}$  ( $\text{R} = [\{2,6\text{-}^i\text{Pr}_2\text{C}_6\text{H}_3\text{NC}(\text{CH}_3)\}_2\text{C}_6\text{H}_3\text{Sn}]_2$ , 2.6879(17) and 2.4129(16) Å.<sup>[30]</sup> This is attributed to a significant degree of back bonding from the reduced tin to the dimpyr ligand. Such a complex can be viewed as a complex of Sn(0) interacting with a neutral dimpyr ligand, which was supported by DFT calculations. Alternatively, this compound can be rationalised as a Sn(II) centre coordinated by a doubly reduced, noninnocent dimpyr ligand. Furthermore, three related low-valent Sn(II) complexes were also prepared and isolated.



**Scheme II-24.** Preparation of Sn(0) compounds **II-68** and some Sn(II) compounds.

Previously, our group prepared the first example of a zero-valent Ge complex **II-68** of dimpyr by the reduction of the cationic Ge(II) complex **II-72** with potassium graphite in benzene.<sup>[53]</sup> Such a species has the singlet ground state. The combination of X-ray crystallography, IR spectroscopy data, and DFT calculations reveals a partial multiple-bond character between the Ge atom and imine nitrogen atoms and delocalization of the lone pair on Ge atom over the  $\pi^*(\text{C}=\text{N})$  orbitals of the imines.



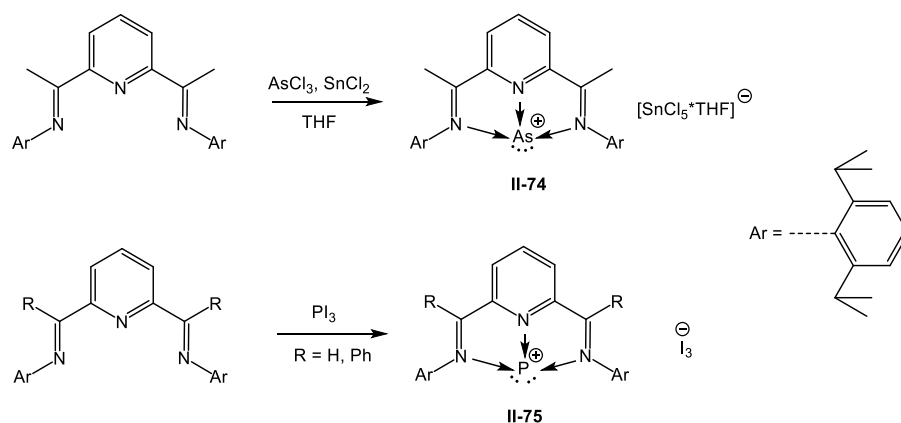
**Scheme II-25.** Preparation of germanium complex **II-73**

### III.1.5. Group 15

Cowley and co-workers prepared the arsenic(I) salt **II-74** by a reaction of AsCl, generated *in-situ* from a mixture of AsCl<sub>3</sub> and SnCl<sub>2</sub> in THF, with the dimpyr ligand.<sup>[67]</sup> The crystal structure of **II-74** determined by X-ray crystallography. The independent part of the unit cell contains one [SnCl<sub>5</sub>\*THF]<sup>-</sup> anion and two equivalent arsenic molecules which were reported as “two half [dimpyrAs]<sup>+</sup> cations”. Although no further explanation was provided, this unusual situation which can be interpreted as co-crystallization of one one cationic species [dimpyrAs]<sup>+</sup> and very unusual neutral dimpyrAs, thus providing an averaged “half-cation” geometry. This averaged geometry features an asymmetric unit with a planar AsN<sub>3</sub>C<sub>7</sub> skeleton. The arsenic centre is three-coordinate to the pyridine nitrogen and both imino centres, with bond lengths falling in the range of N→As dative bonds, indicating that electron transfer to the ligand does not occur and hence arsenic is in the +1 oxidation state.

In 2010, Ragogna et al. reported a series of P(I) cationic species **II-75** via the direct reactions of PI<sub>3</sub> with H- or C<sub>6</sub>H<sub>5</sub>-substituted dimpyr ligands.<sup>[68]</sup> The solid-state structures

of these species revealed a T-shaped phosphorus(I) cation consistent with the presence of two lone pairs and three bonds to nitrogen centres. The pyridine nitrogen occupies an equatorial site while the two imine nitrogen atoms reside in the axial positions. Especially, the two imine groups in **II-75**, bearing C<sub>6</sub>H<sub>5</sub>-substituents (R = Ph), are symmetrical. However, two imine groups in the phosphorus di(aldimino)pyridine compound, i.e. with R = H, are asymmetric, so that the P centre is closer to one of the imine nitrogen atoms. For all four compounds, the anions are distant from the cationic P(I) centres. These compounds represent the first isolated phosphorus based-dimpyr complexes.

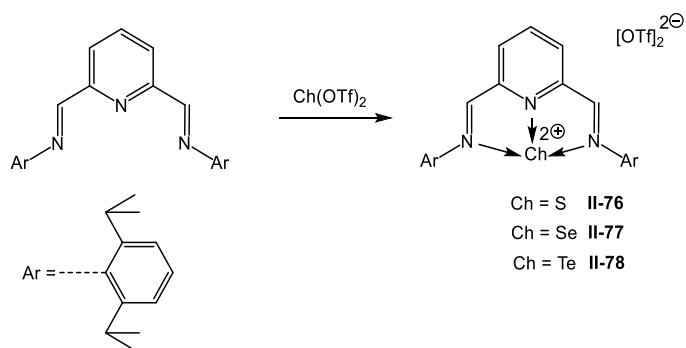


**Scheme II-26.** Synthetic methods for the preparation of dimpyr compounds of elements from group 15.

### III.1.6. Group 16

The 1:1 stoichiometric reaction of triflates Ch(OTf)<sub>2</sub> (Ch = S, Se, Te) with dimpyr at room temperature or at -78°C (Ch = S) resulted in the formation of salts **II-76**, **II-77**, **II-78**.<sup>[69]</sup> These compounds were characterised by NMR spectroscopy and X-ray diffraction analyses, which revealed a T-shaped geometry about the chalcogen centre. Both of the imine nitrogen atoms occupy the axial positions within the trigonal bipyramid, and the

pyridine nitrogen and the two lone pairs of the chalcogen occupy the equatorial positions. A positive correlation is observed between the increasing size of the central atom and increasing Ch-N bond lengths for **II-76** (S), **II-77** (Se), **II-78** (Te). In all of the compounds, the axial Ch-N bonds are longer than the equatorial Ch-N bonds. These compounds were found to be surprisingly stable to air, no signs of decomposition for a period of three weeks were observed. Especially, the addition of water to the sulfur complex **II-76** gave no decomposition.



**Scheme II-27.** Synthetic method for the preparation of dimpyr compounds of elements from group 15.

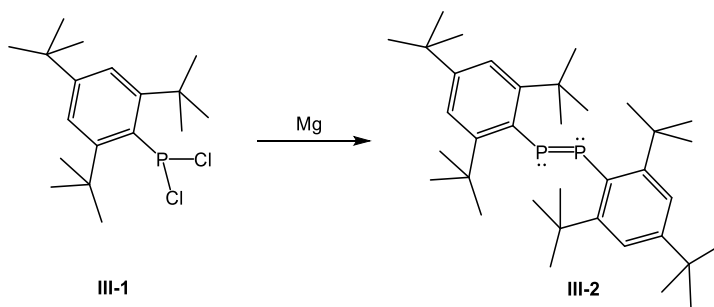
### II.3. Main Group Complexes Supported by Bis(imino)aryl N-heterocyclic Carbene Platform

In 1991, the first well-characterised and isolated N-heterocyclic carbene was reported by Arduengo and co-workers.<sup>[70]</sup> From the beginning, N-heterocyclic carbenes (NHCs) presented as excellent tools, which have found multiple applications in many fields, such as catalysis, small molecular activation, materials, sensors, etc.<sup>[71-74]</sup> In the organometallic chemistry, the NHCs have proven to be useful ligands for transition metals and main group elements because of their strong  $\sigma$ -donor and good  $\pi$ -acceptor properties.<sup>[75-80]</sup>

Taking the advantages of NHCs in coordination to either transition metals or p-block elements, Lavoie and co-workers developed the first generation of bis(imino)aryl N-heterocyclic carbenes (dimNHC) in 2010, which can be formally considered as modification of the dimpyr ligand by replacing the pyridine core with an NHC.<sup>[81]</sup> The modification of the ligand structure allow us to alter the electronic and steric properties of the corresponding metal complexes. Later on, several examples of transition metal complexes of dimNHC ligands have been reported. Thus, Lavoie et al. reported the preparation of Co(II), Fe(II) complexes stabilised by the dimNHC framework, which can be used as catalysts in ethylene polymerization.<sup>[81,82]</sup> Meanwhile, Byer et al. also introduced similar Fe(II) compounds, analogous to the well-known bis(imino)pyridine iron complexes developed by Brookhart, Gibson and Chirik.<sup>[83]</sup> However, there is still no literature example of a main group element complex supported by such ligands.

### III. Phosphinidene

Phosphinidenes of the general formula  $RP$  are 6 electron species that are considered as phosphorus analogues of carbenes, nitrene etc. Their triplet state is in lower energy than the corresponding singlet state. Thus, such species is a highly unstable molecule which may undergo oligomerization to cyclic polyphosphines  $(RP)_n$ ,<sup>[84,85]</sup> dimerization to diphosphenes  $RP=PR$  (for bulkier R),<sup>[86]</sup> or by C-H or C-C activation in the R substituent.<sup>[87]</sup> The species in the triplet state has only been detected in the gas phase by mass spectrometry or at low-temperatures by electron paramagnetic resonance, infrared, and UV-visible spectroscopy. In 1981, Yoshifuji et al. reported the first isolated compound containing a formal phosphorus-phosphorus double bond. The reduction of phosphorus dichloride **III-1** by Mg metal afforded a yellow solution, from which dimeric phosphinidene **III-2** was obtained by crystallization.<sup>[88]</sup> Since this initial report, this field is still being developed as one of the most exciting areas of main group chemistry. However, the isolation of singlet phosphinidenes is still a challenging task, which normally requires a careful choice of ligands.



**Scheme III-1.** Yoshifuji's dimeric phosphinidene.

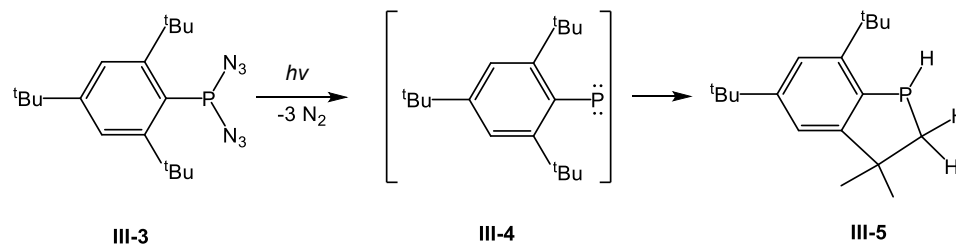
While unstable in the free state, phosphinidene fragments can be generated and stabilised in the coordination sphere of transition metals<sup>[89,90]</sup> by two different



approaches:<sup>[91]</sup> as electrophilic terminal-phosphinidene corresponding to Fischer carbene complexes<sup>[91,92]</sup> and as nucleophilic terminal-phosphinidene corresponding to Schrock alkydenes complexes.<sup>[93]</sup> In general, the electrophilic species can be seen as dative complexes between a singlet phosphinidene and a singlet transition metal moiety. A series of stable phosphinidene complexes of transition metals, such as molybdenum, tungsten, ruthenium, iron, cobalt, have been reported <sup>[94–98]</sup>. These species enter into the addition reactions with alkenes, leading to the formation of phosphiranes.<sup>[99]</sup> In contrast, the nucleophilic phosphinidene was considered as a combination of a triplet phosphinidene with a triplet of transition metal, forming the P=M double bond. These species show their characteristic reaction with ketones and aldehyde to form a phosphalkenes.<sup>[100,101]</sup> Their application to the synthesis organophosphorus compounds proved to be very beneficial.<sup>[89,90]</sup> A possibility of their transfer to organic substrates opens further investigation of novel reagents and new reactions.

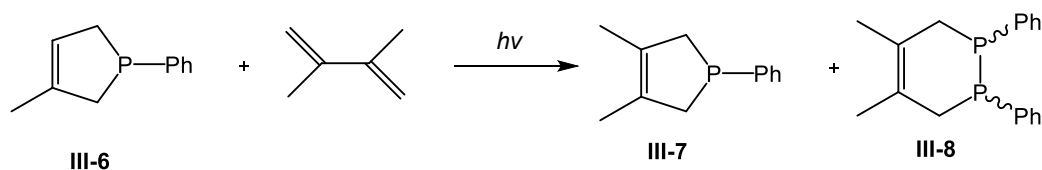
Despite many attempts to prepare free phosphinidene, this species still remains elusive. Many previous efforts in detecting a free phosphinidene from thermal-decomposition of cyclopolyphosphanes (R<sub>2</sub>P)<sub>n</sub> and the reduction of dihalophosphanes by alkali metals failed.<sup>[102]</sup> Alternatively, *in situ* generated phosphinidenes can be also trapped in the form of hetero-Diels-Alder products.<sup>[103,104]</sup> Cowley et al. proved the intermediacy of phosphinidenes obtained from a photochemical reaction. Thus, photolysis of Mes\*P(N<sub>3</sub>)<sub>2</sub> (Mes\* = 2,4,6-<sup>t</sup>Bu<sub>3</sub>C<sub>6</sub>H<sub>2</sub>) **III-3** with UV light (254 nm) afforded **III-5** as the result of insertion of the P atom into the C–H bond of one of the tert-butyl group in the ortho position of the arene ring. The photolysis was repeated in a deuterated solvent,

resulting in no deuterium incorporation, which indicated that the rearrangement from **III-3** to **III-5** occurred by an intramolecular process.<sup>[105]</sup>



**Scheme III-2.** Generation of phosphaindane **III-5** by photolysis of **III-3**

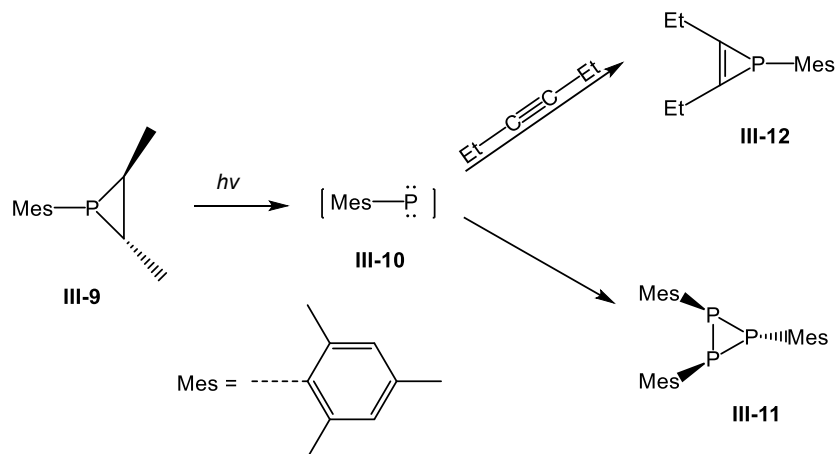
Later on Gaspar et al. also reported photolysis of 3-methyl-1-phenyl-3-phospholene **III-6** in the presence of 2,3-dimethyl-1,5-butadiene to generate phospholene **III-7** and a cis/trans mixture of 4,5-dimethyl-1,2-diphenyl-1,2-diphosphacyclohexenes **III-8**.<sup>[106]</sup> The phospholene **III-7** was generated from the reaction of phenylphosphinidene intermediate with diene via a [1+4] cycloaddition process. On the other hand, the phosphinidene dimerised to a diphosphene which underwent a Diels–Alder reaction to give **III-8**.



**Scheme III-3.** Photolysis of **III-6** in the presence of 2,3-dimethyl-1,5-butadiene

In 1994, Gaspar and Borden reported the first detection of a triplet phosphinidene by the ESR technique. The irradiation of a frozen solution of phosphirane **III-9** in methylcyclohexane at 77 K ( $\lambda = 254$  nm) was studied. In the absence of a trapping reagent, thawing the reaction solution afforded a cyclotriphosphane **III-11**. However, in the presence of a trapping reagent, the phosphirene **III-12** was formed, which is the product of

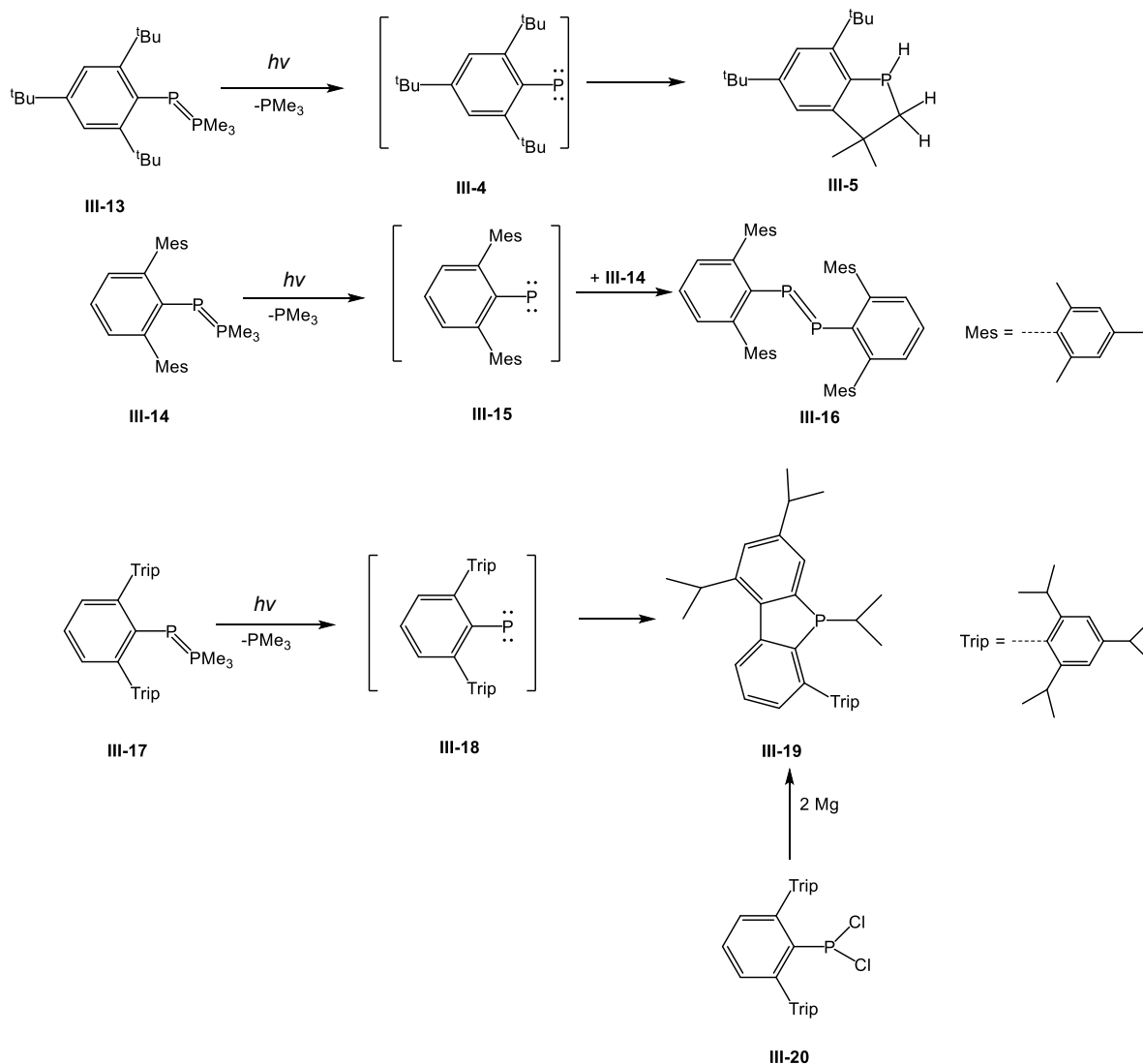
a reaction between the liberated mesitylphosphinidene and 3-hexyne. The intermediate **III-10** was detected by an ESR experiment at 4 K which displayed a strong signal at 11492 Gauss assigned to the free [Mes-P] in the triplet ground state.<sup>[107]</sup>



**Scheme III-4.** Photolysis of **III-9**

Protasiewicz et al. compared photolysis reactions of different phosphanylidene- $\sigma^4$ -phosphoranes  $\text{ArP}=\text{PMe}_3$  (scheme III-5). Treatment of  $\text{Mes}^*\text{P}=\text{PMe}_3$  ( $\text{Mes}^* = 2,4,6\text{-}^t\text{Bu}_3\text{C}_6\text{H}_2$ , **III-13**) under UV light gave the same C-H activated product **III-5** as observed in Cowley's system (scheme III-2). They suggested that irradiation of **III-14** afforded the diphosphene **III-16** as the result of an attack of phosphinidene at the precursor. This mechanism was confirmed by the photolysis of **III-14** in the presence of **III-13**, which yielded the asymmetric diphosphene  $\text{Mes}^*\text{P}=\text{PC}_6\text{H}_3\text{-2,6-Mes}_2$  as the major product. In contrast, UV irradiation of the bulkier substrate **III-17** gave the phosphafluorene **III-19**, the product of insertion of the P atom of intermediate into the carbon-carbon bond of an ortho-substituted isopropyl group.<sup>[108]</sup> The same product **III-19** was also obtained by the reduction  $\text{Mes}^*\text{PCl}_2$  by Mg powder.<sup>[109]</sup> Although these experiments do not provide

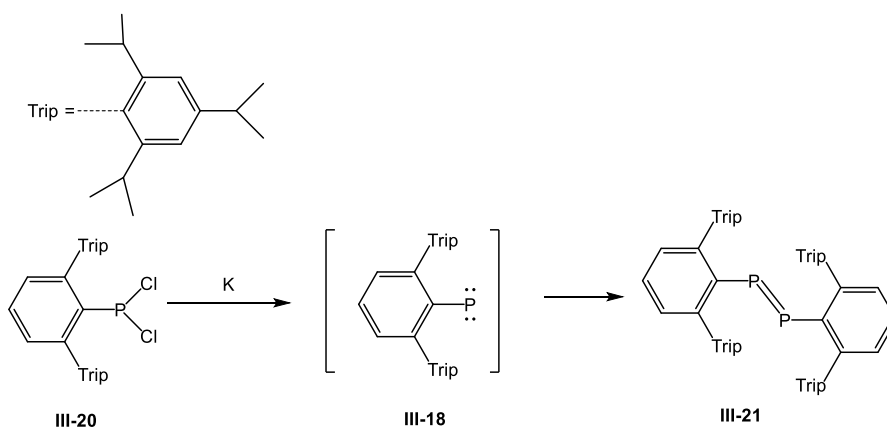
absolute proof for phosphinidenes, the formation of such various products can only be explained by assuming the intermediacy of a phosphinidene.



**Scheme III-5.** Photolysis reactions reported by Protasiewicz et al.

Similarly, phosphaphluorene **III-19** was also obtained by Power and co-workers via the reduction of 2,6-Trip<sub>2</sub>C<sub>6</sub>H<sub>3</sub>PCl<sub>2</sub> (**III-20**) with magnesium metal in 68% yield. In contrast, the reduction by potassium metal provided the diphosphene **III-21** as the main

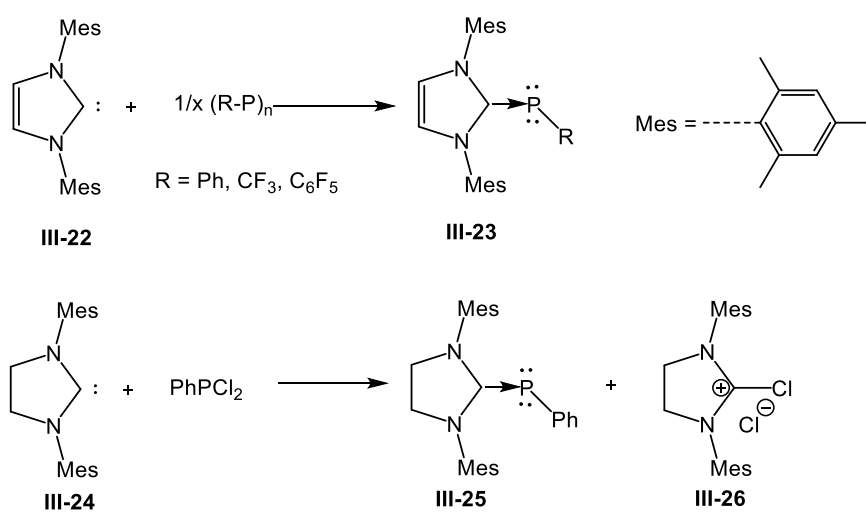
product. The formation of the phosphafluorene **III-21** suggests the intermediacy of the phosphinidene.<sup>[110]</sup>



**Scheme III-6.** The reduction of 2,6-Trip<sub>2</sub>C<sub>6</sub>H<sub>3</sub>PCl<sub>2</sub>.

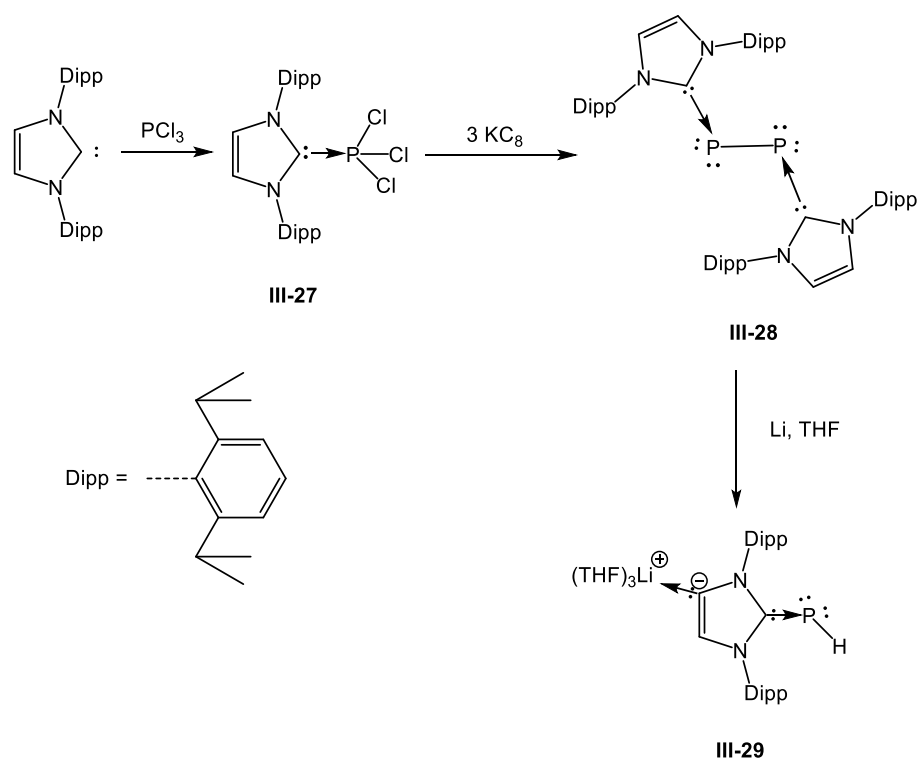
Many attempts to stabilise an electron-deficient phosphinidene centre were made by using strong donors, such as phosphines and *N*-heterocyclic Carbenes (NHCs). The chemistry of NHC-phosphinidene has been developed for many years with various type of NHC ligands. In a computational study reported by Frison et al.,<sup>[111]</sup> the carbene-phosphinidene adducts are considered as inversely polarised phosphaaenes, featuring a nucleophilic phosphorus centre rationalised by an effective  $\pi$ -electron delocalization into the P=C double bond ( $P^{\delta-}-C^{\delta+}$ ). In 1997, a landmark study in this field was reported by Cowley and Arduengo<sup>[112]</sup> who showed that the formation of a “phosphaalkene” **III-23** can be achieved from an attack of a nucleophilic carbene at P(III)-cyclic oligomers (Scheme III-7). On the other hand, a reaction between a nucleophilic carbene and phenyldichlorophosphine also led to the formation of a similar “phosphaalkene” **III-25**. In this case, the chlorine was consumed by the second equivalent of carbene forming a chloroimidazolium salt. The double-bond character between the C<sub>carbene</sub> and phosphorus

atoms is not well developed in these “phosphaalkenes”, as evinced by the NMR data and X-ray analysis. In particular, the C<sub>carbene</sub>-P bond in **III-23.Ph** is long for a typical phosphaalkene. The <sup>31</sup>P NMR spectra show the phosphorus chemical shift between at -10 and -25 ppm, which is in a higher field than the typical value for the 2-coordinate phosphorus centre of phosphaalkenes ( $\delta_{31\text{P}} = 240$  ppm).<sup>[113,114]</sup> A free rotation about the C<sub>carbene</sub>-P bond at room temperature was deduced from the proton and carbon NMR spectra of these NHC-phosphinidene adducts, indicating a weak (if any)  $\pi$ -bonding interaction between the imidazole C<sub>carbene</sub> centre and the phosphorus centre. Later on, a theoretical study on the effect of substituents in polarised phosphaalkenes, formed from aminocarbenes and phosphinidenes, was reported by Frison et al.<sup>[115]</sup> Electronic and steric effects were investigated by a combination of DFT, ELF and NICS calculations. They indicated that the more electronegative R group at the P centre increases the  $\sigma$ -donation from carbene. On the other hand, the  $\sigma$ -donating ability of R and steric interactions influence the  $\pi$ -back-donation from phosphinidene, which mainly governs the length of the P-C bond.



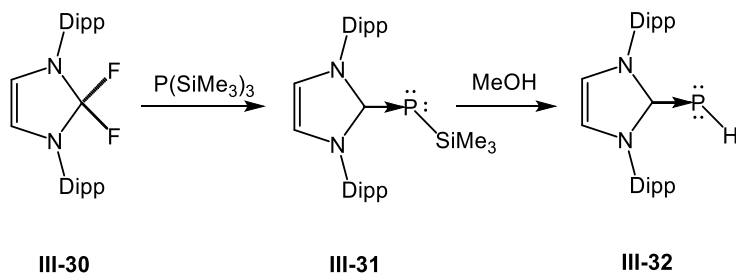
**Scheme III-7.** The NHC- phosphinidene adduct reported by Cowley and Arduengo.

The low triplet state of the parent phosphinidene (P-H) (it has the triplet-singlet energy gap of approximately 22 kcal/mole) makes such a species highly reactive and incapable of being isolated.<sup>[116]</sup> In 2010, Robinson et al.<sup>[117]</sup> succeeded in preparing the first carbene-stabilised parent phosphinidene **III-29** which was generated from the reaction of diphosphorus carbene **III-28** with lithium metal. It was suggested that the reaction involves both the cleavage of the P-P bond and the lithium-mediated C-H activation of the imidazole ring. The presence of the P-H fragment in **III-29** was also confirmed by <sup>1</sup>H NMR and <sup>31</sup>P NMR, showing the large coupling  $^1J_{\text{P-H}} = 167$  Hz and the <sup>31</sup>P doublet at  $\delta = -143.0$  ppm. The bond length of C<sub>carbene</sub>-P (1.763 Å) is slightly longer than the typical value for *P*-hydrogeno-C-phosphinophosphaalkenes (1.713(2) Å).<sup>[117]</sup> The computational results revealed that the  $\pi$ -bonding interaction between the C<sub>ipso</sub> of the lithiated NHC ligand and phosphorus atom was not strong. The two lone pairs localised on the P centre, of which one has mainly the s character (68.1% s, 31.9% p) and the other has essentially the pure p character (0.0% s, 99.8% p, 0.2% d).

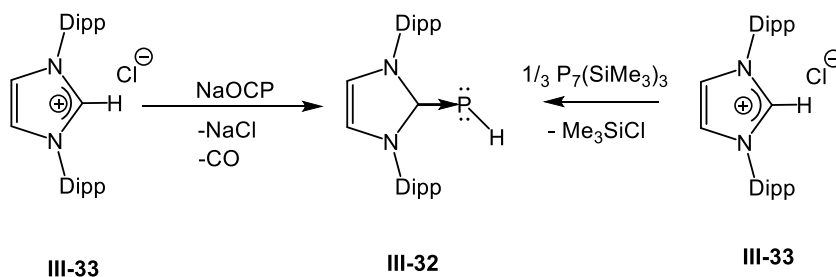


**Scheme III-8.** Phosphinidene stabilised by NHC reported by Robinson et al.

Tamm et al. reported that the reaction of N,N',3-bis(2,6-diisopropylphenyl)-2,2-difluoroimidazolidine **III-30** with  $\text{P}(\text{SiMe}_3)_3$  at 70 °C in toluene afforded the carbene– $\text{PSiMe}_3$  adduct **III-31**.<sup>[118]</sup> The  $^{31}\text{P}$  NMR signal was found at a higher field ( $\delta = -129.5$  ppm) and the  $^{29}\text{Si}$  NMR signal exhibited a doublet at  $\delta = -4.48$  ppm. Treatment of **III-31** with methanol afforded a (P-H) NHC-phosphinidene which is similar to the Robison's system.<sup>[119]</sup> Meanwhile, Grützmacher and coworkers disclosed a series of protocols to prepare the same (P-H) carbene adduct **III-32** by an improved procedure.<sup>[120–122]</sup>

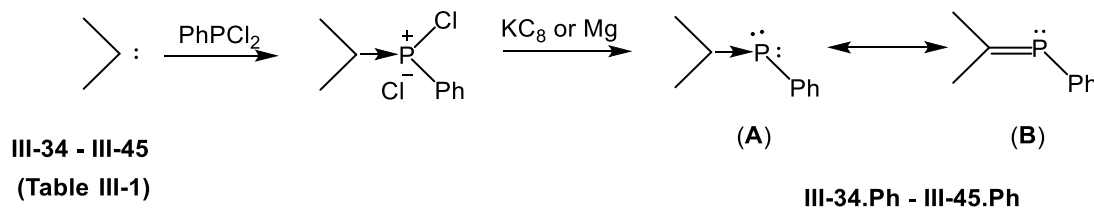






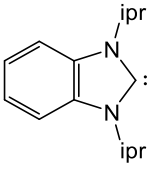
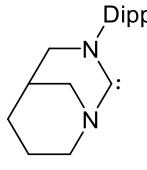
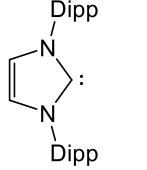
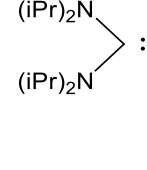
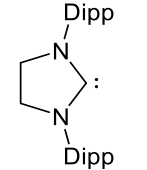
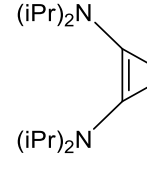
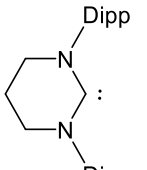
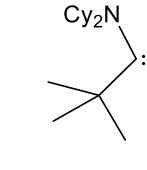
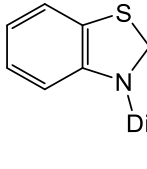
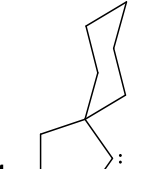
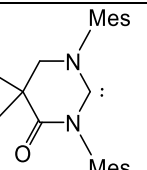
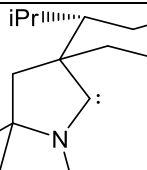
**Scheme III-9.** The procedure for the synthesis of parent NHC-phosphinidene adduct reported by Tamm et al. (top) and by Grützmacher et al. (bottom).

Bertrand et al.<sup>[123]</sup> reported a series of carbene-phosphinidene adducts (scheme III-10), which were obtained from two-step procedures: first, the reaction of carbene with  $\text{PhPCl}_2$  to form  $[\text{carbene-P}(\text{Ph})\text{Cl}]^+\text{Cl}^-$  salts, followed by reduction with either  $\text{Mg}$  or  $\text{KC}_8$ . The bonding situation for the  $\text{C}_{\text{carbene}}\text{-P}$  bond in these adducts can be rationalised as two canonical forms (A and B shown in scheme III-11). The  $^{31}\text{P}$  NMR chemical shifts of these compounds were studied (table III-1) to evaluate the relative  $\sigma$ -donating and  $\pi$ -accepting properties of carbenes. For instance, the (alkyl)(amino)carbenes **III-37–III-39** are much more  $\pi$ -accepting than diaminocarbenes **III-34–III-36**, leading to a lower field in  $^{31}\text{P}$  signal in the formers. Later on Hudnall et al. reported a similar approach using different carbonyl-substituted carbene.<sup>[124]</sup>

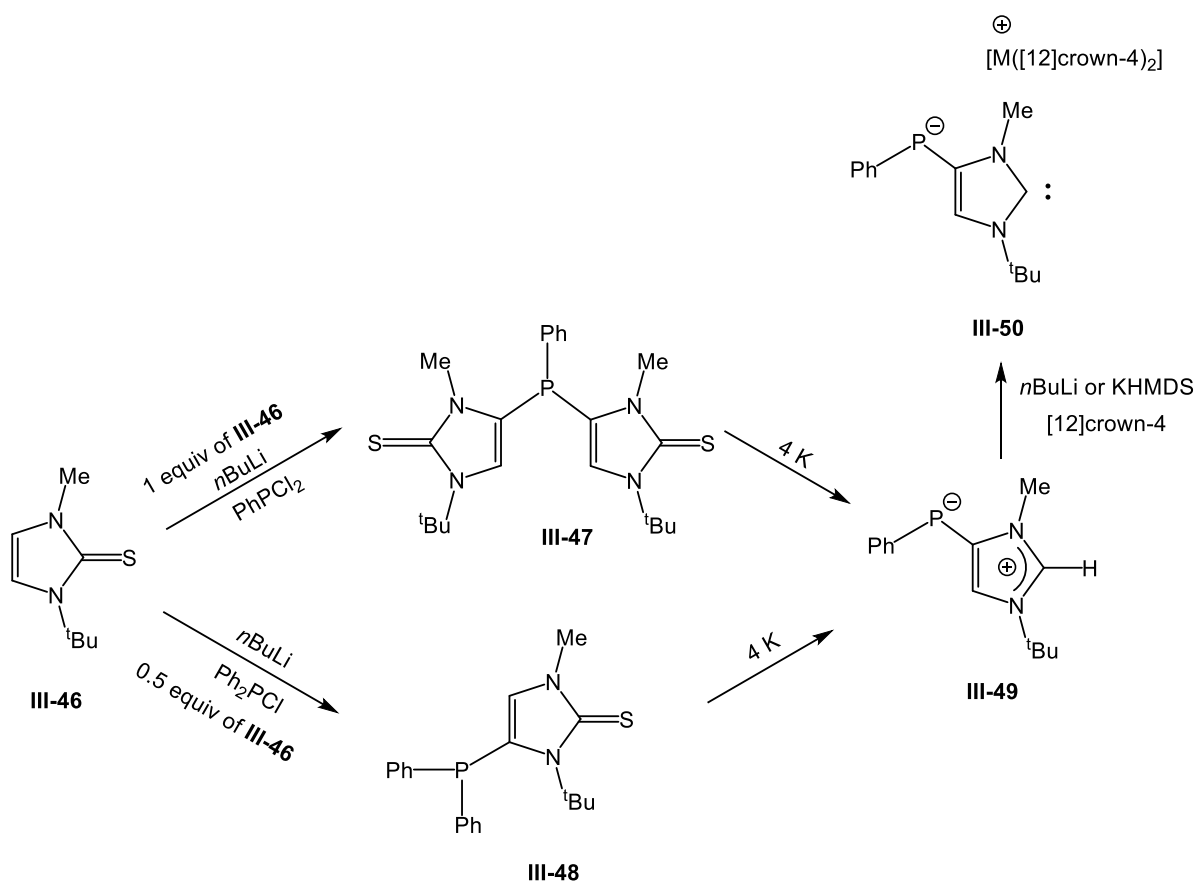


**Scheme III-10.** Preparation of carbene-phosphinidene adducts using dichlorophenylphosphine.

**Table III-1:**  $^{31}\text{P}$  NMR for the adducts **III-34.PPh** – **III-45.PPh** reported by Bertrand et al.<sup>[123]</sup>

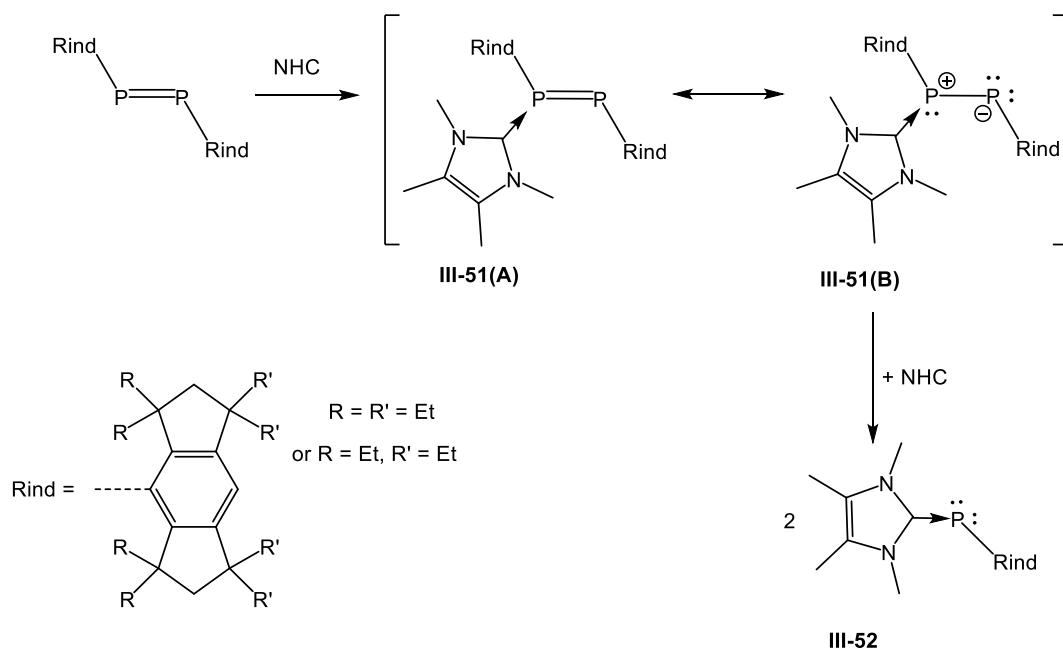
Carbenes	Carbene.PPh Adduct $\delta^{31}\text{P}(\text{ppm})$	Carbenes	Carbene.PPh Adduct $\delta^{31}\text{P}(\text{ppm})$
<b>III-34</b> 	-34.6	<b>III-40</b> 	34.9
<b>III-35</b> 	-18.9	<b>III-41</b> 	69.5
<b>III-36</b> 	-10.2	<b>III-42</b> 	-34.9
<b>III-37</b> 	14.8	<b>III-43</b> 	126.3
<b>III-38</b> 	57.0	<b>III-44</b> 	68.9
<b>III-39</b> 	39.7	<b>III-45</b> 	56.2

The chemistry of a NHC-phosphinidene adduct is still being developed by different groups. Streubel and Nyalazsi introduced the novel zwitterion **III-49** which can be described as an adduct of an abnormal NHC and a phosphinidene.<sup>[125]</sup> Two different methods to produce **III-49** were developed in which either the compound **III-47** or **III-48** was obtained by controlling the ratio of starting materials. Potassium metal was used as a reductant in the further step. Interestingly, the deprotonation of **III-49** by *n*BuLi or KHMDS converted it into the corresponding anion **III-50** which can be considered as a phosphinidene adduct of an anionic N-heterocyclic carbene.



**Scheme III-11.** Synthesis of zwitterionic imidazolium phosphanide reported by Streubel and Nyalazsi.

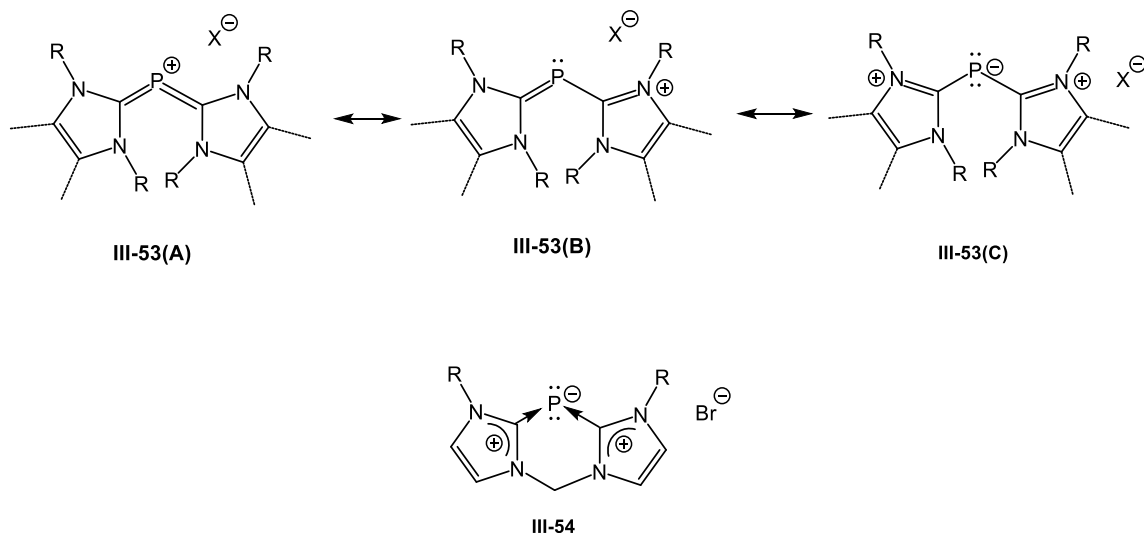
Hatanaka and Matsuo also contributed to the field by reporting the cleavage of the P=P double bond in diphosphenes, bearing bulky substituents, by two equivalents of NHC, resulting in the formation of the corresponding phosphinidene adduct **III-52** (Scheme III-12).<sup>[126]</sup> DFT calculations showed that the intermediate **III-51** was formed in the first step, followed by the cleavage of the P-P bond by the second NHC molecule to give the final product **III-52**. Such an interesting diphosphene/mono-NHC complex contains a highly polarised P-P bond supported by NMR study. The higher field <sup>31</sup>P NMR signals (-63.9 and -70.5) ppm compared to those of diphosphenes indicated an electron rich P centre in **III-52**.



**Scheme III-12.** Cleavage of the P=P double bond in a diphosphene reported by Hatanaka and Matsuo.

Macdonald et al. showed that NHCs can be used as effective ligands for the stabilization of P(I)cations. Compound **III-53** was prepared by using a variety of synthetic

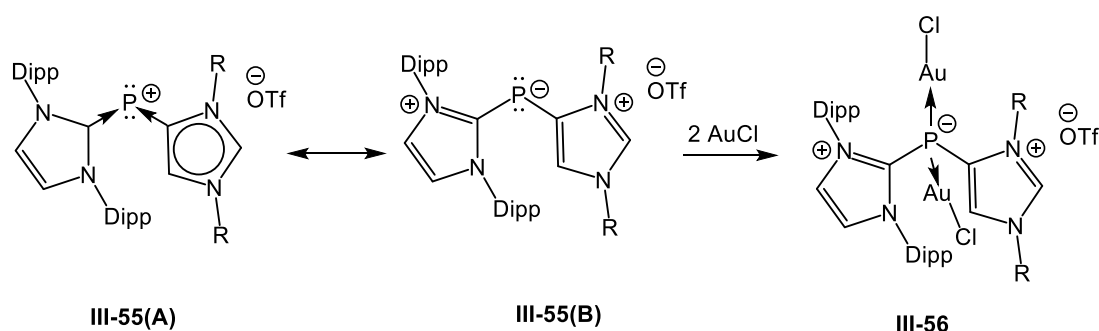
approaches. Such species can be represented as different canonical forms. The nature of bonding in this species was studied by the combination of X-ray crystallography and computational study, which indicated that the P centre contains two lone pairs being represented in the canonical form C. On the other hand, a weak  $\pi$ -interaction between the lone pair on P centre and the NHC system observed also agreed with the contribution of the resonance structure B to the overall structure.<sup>[127]</sup> A similar system **III-54**, stabilised by a chelating bis-NHC ligand, was also discussed by the same group.<sup>[128]</sup> The <sup>31</sup>P NMR spectrum of **III-54** features a singlet between -81 and -83 ppm, which is in a considerably weaker field than for **III-53** (-112 to -127 ppm).



**Scheme III-13.** Carbene stabilised P(I) cations reported by Macdonald et al.

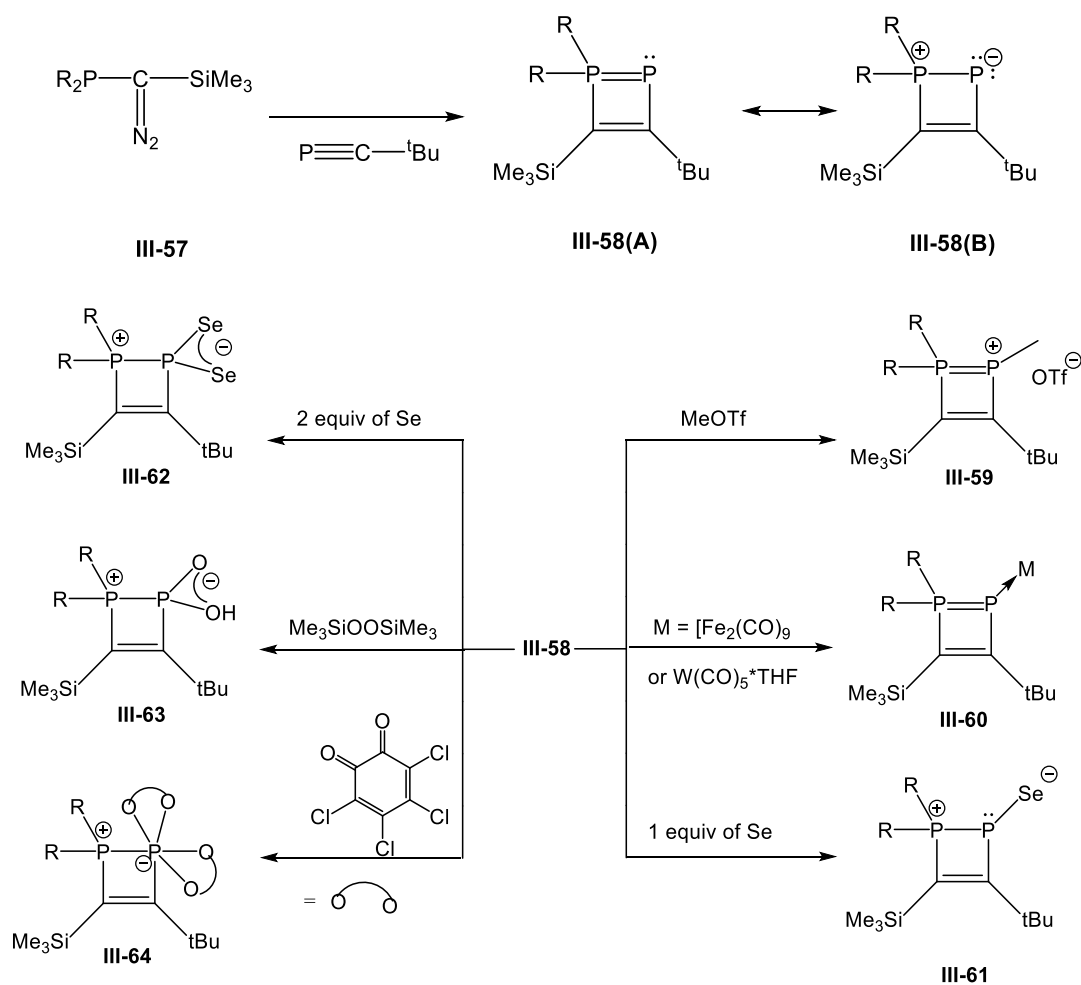
A related system was also reported by Weigand et al. in which the P centre was stabilised by one of NHC carbenes in the abnormal fashion (*a*NHC).<sup>[129]</sup> The reaction of these P cations with transition metals afforded the first example of transition metal

complexes of a cationic P(I) ligand. Such a reactivity of P cations to transition metals proved the presence of two lone pairs on the P centre.



**Scheme III-14.** Carbene stabilised P(I) cations reported by Weigand et al.

A phosphorus-base ligand is considered as a potential candidate to stabilise a phosphinidene P centre. In 1995, a phosphanylidene phosphorane **III-58** was successfully prepared by Regitz and Bertrand.<sup>[130]</sup> The photolysis of diazo compound **III-57** in the presence of tert-butylphosphaalkyne afforded the formation of phosphalkene **III-58**. The <sup>31</sup>P NMR spectrum showed a doublet of quintets at 49.2 ppm ( $J_{P-P} = 201.2$  Hz,  $J_{P-H} = 13.6$  Hz) and a doublet at 58.4 ( $J_{P-P} = 201.2$  Hz), which is consistent with the presence of two bonded phosphorus atoms. Later on such a species showed remarkable reactivity toward various substrates (scheme III-15).<sup>[131]</sup>

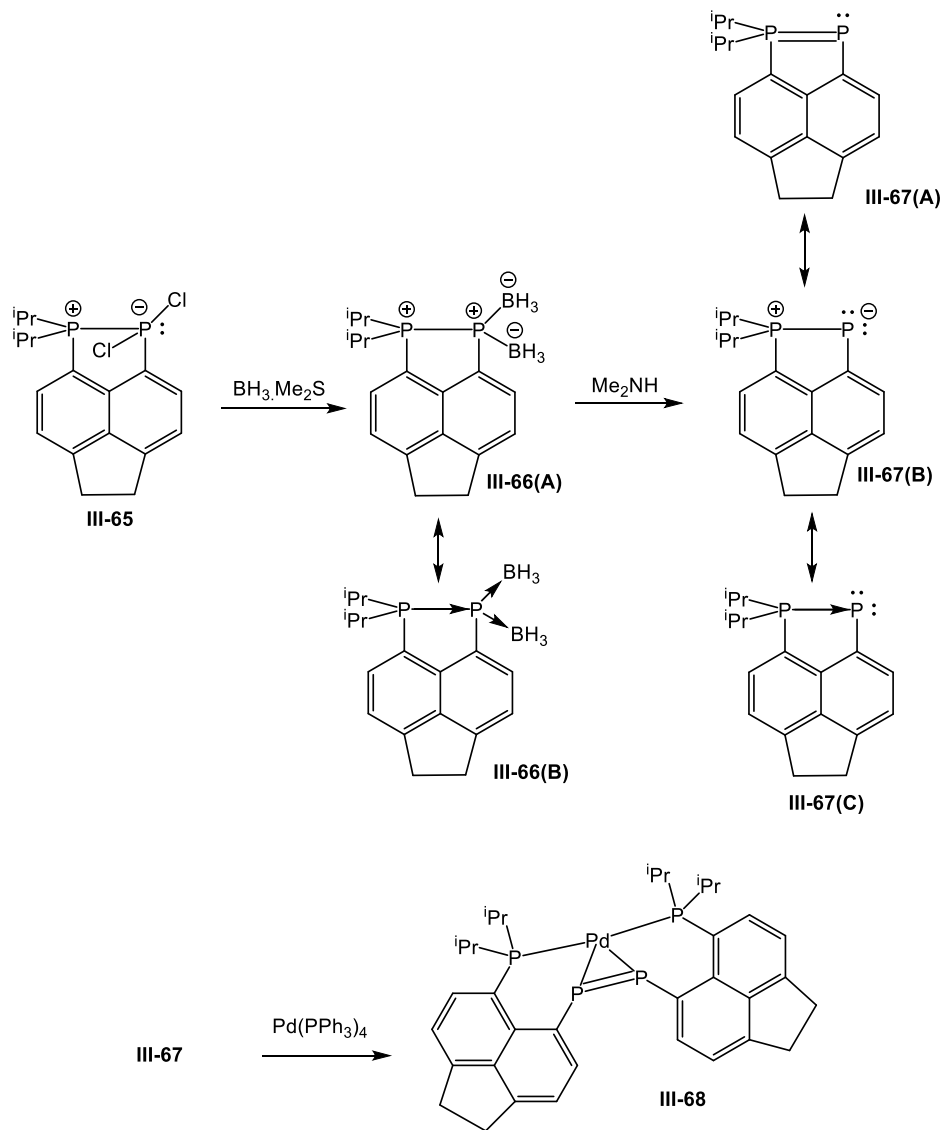


**Scheme III-15.** The preparation and reactivity of **III-58**

Following the work by Regitz and Bertrand, a closely related system was reported by Kilian et al. in which a rigid peri-substituted acenaphthyl backbone was utilised for the stabilization of low-valent phosphorus compounds.<sup>[132]</sup> Compound **III-67** was synthesised by the reduction of phosphorus chloride precursor with borane, followed by removal of the borane by dimethylamine. The X-ray study showed an interesting bonding situation in **III-66** in that a Lewis base-stabilised phosphinidene moiety acts as a double donor towards two Lewis acidic borane moieties, which can be represented as the resonance forms shown

in scheme III-17. The P-P bond length in **III-66** is consistent with a single bond. In contrast, the partial multiple P-P bond character in **III-67** was confirmed by a combination of X-ray crystallography and DFT calculations. The observation of  $^{31}\text{P}$  signals  $\delta = 76.7$  ( $\text{P}^i\text{Pr}_2$ ) and  $-157.7$  ppm (phosphanlydene), assigned to an AX system with a large coupling  $J_{\text{P-P}} = 480$  Hz, suggest the formation of product **III-67**. The  $^{31}\text{P}$  NMR chemical shift of such a phosphanlydene centre is at higher field than usually observed for a two-coordinate phosphorus, which suggests a high electron density of the phosphorus centre having two lone pairs. The free phosphanlydene- $\sigma^4$ -phosphorane showed reactivity towards  $[\text{Pd}(\text{PPh}_3)_4]$ , leading to the formation of diphosphene complex **III-68**. All four phosphorus atoms are coordinated to a  $\text{Pd}^0$  centre. The lengths of the P-P distance in each acenaphthene units (3.244 Å and 3.188 Å) indicate no bonding interaction across the peri gap, resulting in dimerization of the “deprotected” phosphinidene moiety to a diphosphene. These results agree with the presence of a phosphinidene centre in **III-67**.

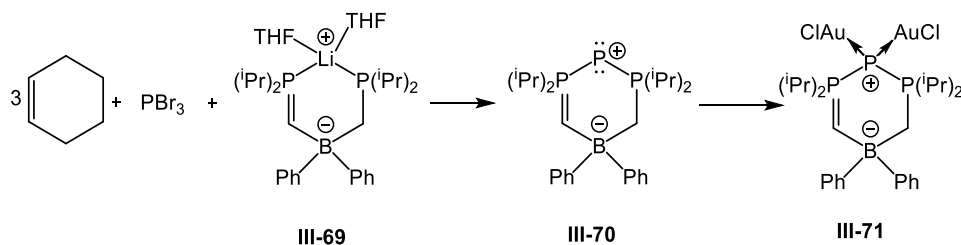




**Scheme III-16.** Preparation of reactivity of phosphinidene stabilised by a perisubstituted acenaphthyl backbone.

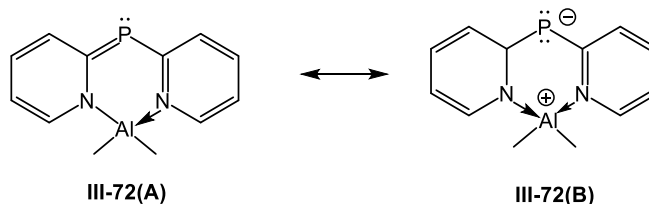
A new zwitterionic P(I) centre **III-70**, introduced by Macdonald and Ragona, was synthesised by the stoichiometric reaction of the bis(phosphino)borate  $[\text{Li}(\text{tmeda})_2][(\text{Ph}_2\text{PCH}_2)_2\text{BPh}_2]$  with  $\text{PBr}_3$  in the presence of 3 equivalents of cyclohexene.<sup>[133]</sup> A doublet at  $\delta = 32$  ppm and a triplet at  $\delta = -220$  ppm with a large coupling  $J_{\text{P-P}} = 414$  Hz were observed from the  $^{31}\text{P}$  NMR spectrum of **III-70**. Such a zwitterionic

phosphanide can coordinate to one or two {AuCl} fragments depending on the steric bulk of the ligand, which agrees well with the structure containing two lone pairs of the phosphinidene.



**Scheme III-17.** Zwitterionic P(I) compound reported by Macdonald and Ragogna.

Stalke et al. reported a related zwitterionic species [Me<sub>2</sub>Al(μ-Py)<sub>2</sub>P]. Theoretical calculations of charge density support the presence of two lone pairs at the central phosphorus atom.<sup>[134,135]</sup> A reaction of **III-72** with [W(CO)<sub>5</sub>(THF)] afforded a new product [{(OC)<sub>5</sub>W}<sub>2</sub>(μ-P)Py<sub>2</sub>(H)] with the phosphorus centre bridging two {W(CO)<sub>5</sub>} moieties. It indicated the ability of phosphorus to serve as a four-electron donor.

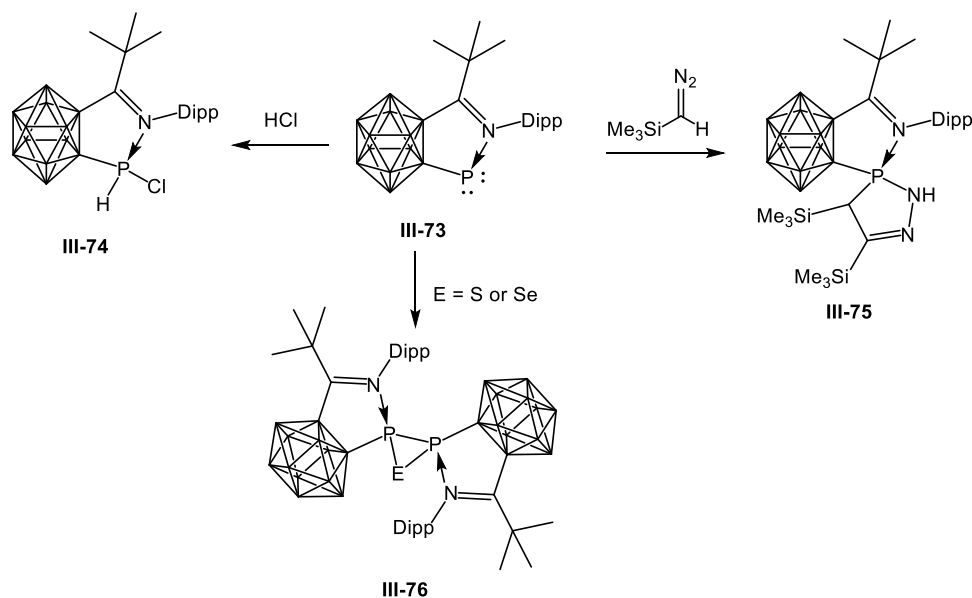


**Scheme III-18.** Zwitterionic species reported by Stalke et al.

The low-valent phosphorus atom can be also trapped by a pincer platform. As discussed in more detail in Chapter II.2, Cain et al. reported the synthesis of a P compound **II-29** stabilised by a (N,C,N) dimph ligand (Scheme II-11). Its <sup>31</sup>P NMR spectrum shows a signal at δ = 150.6 ppm, indicating a strong interaction between the P and N atoms of the

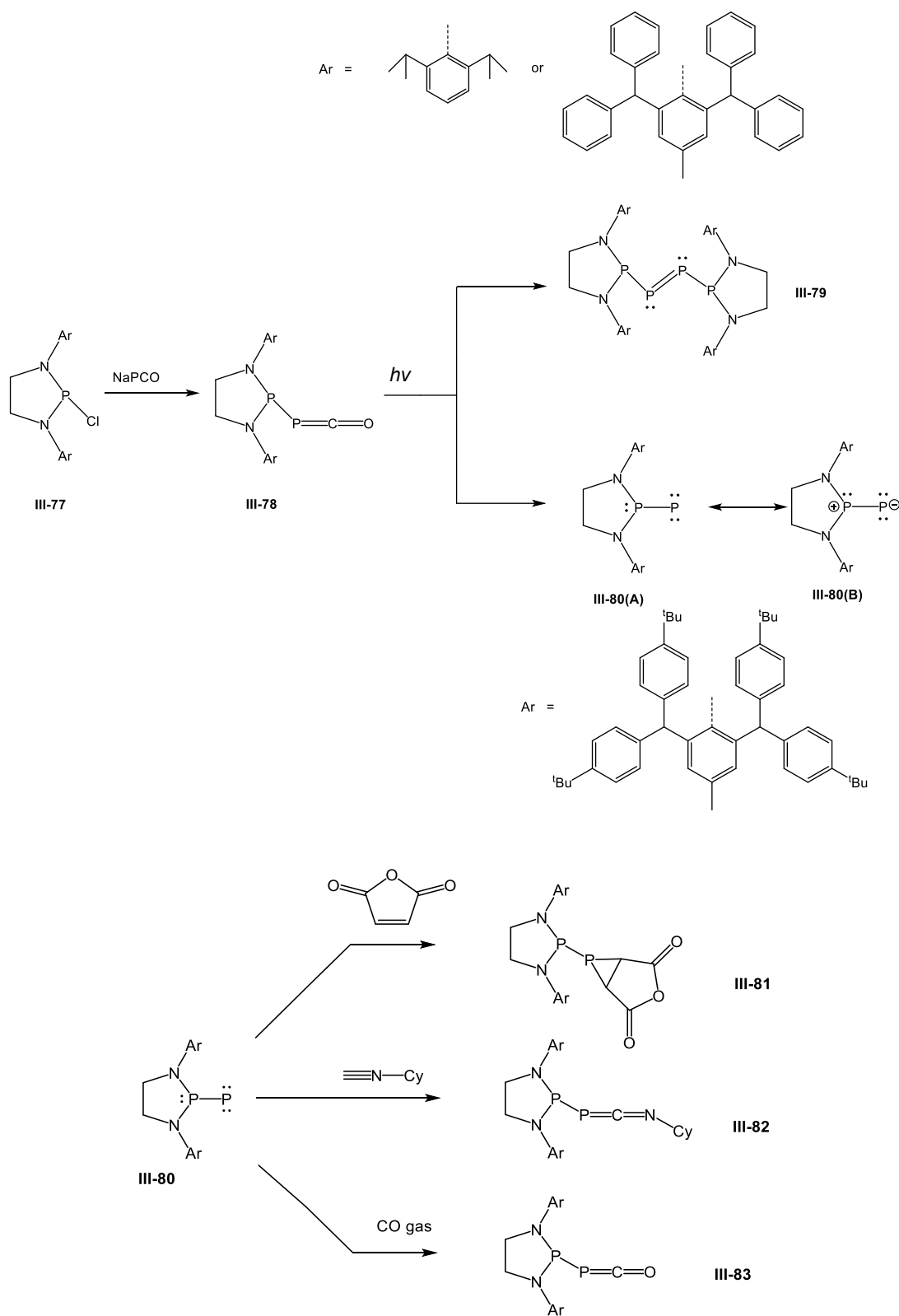
imine unit.<sup>[39]</sup> Similarly, Ragnona et al. succeeded in trapping a cationic P(I) centre by a N,N,N type pincer ligand by a reaction of dimpyr with phosphorus halides (PI<sub>3</sub>, PBr<sub>3</sub>). The solid state structures showed symmetrical coordination of N<sub>imine</sub> atoms to the P centre, whereas the <sup>31</sup>P signals were observed in the range from 154 ppm to 174 ppm.<sup>[68]</sup>

Xie et al. introduced a new imino-stabilised carboranyl-phosphenidene.<sup>[136]</sup> The phosphorus compound was obtained by deprotonation of ligand with *n*BuLi in ether followed by a reaction with PCl<sub>3</sub>. Further reduction by KC<sub>8</sub> afforded the target product **III-73**. The very bulky carboranyl ligand was used to prevent dimerization. The <sup>31</sup>P NMR spectrum of **III-73** showed a peak at  $\delta = 210.5$  ppm which is in lower field than that reported by Cain et al. The reactivity of this species was investigated, including the reactions with S, Se, (TMS)CHN<sub>2</sub> and HCl to give various phosphorus(III) species (Scheme III-19).



**Scheme III-19.** P(I) compound reported by Xie et al.

Due to the instability of phosphinidenes, the only monosubstituted, “bottle-able” phosphinidene prepared to date is the compound  $(-\text{H}_2\text{CNAr}^{**})_2\text{P-P}$  ( $\text{Ar}^{**} = 2,6\text{-bis}[(4\text{-tert-butylphenyl)methyl]-4\text{-methylphenyl}]$ ) **III-80** reported by Bertrand et al. in 2016.<sup>[137–139]</sup> The phosphinidene was generated by mixing the chlorodiazaphospholidine with the 2-phosphaethynolate anion, following by extrusion of CO gas under UV irradiation for 3 hours. A variety of substituents on the nitrogen atoms were investigated, but the phosphinidene centre was only protected by an extremely bulky substituent. For less bulky substituents, the dimerization to diphosphenes **III-79** occurred. While the  $^{31}\text{P}$  NMR spectrum of the dimer ( $\text{Ar} = \text{Dipp}$ ) showed two triplets at 675.0 and 137.4 ppm with  $J_{\text{PP}} = 75.1$  Hz, the signals for the monosubstituted phosphinidene showed an AX system at 80.2 and -200.4 ppm ( $J_{\text{PP}} = 883.7$  Hz). Although the X-ray characterization was missing, the presence of **III-80** was supported by a computational study which was also consistent with  $^{31}\text{P}$  NMR experiments. As expected for an analogue of nucleophilic carbenes, phosphinidene **III-80** shows similar reactivity. Thus, with isocyanides the expected product **III-82** was obtained. Furthermore, it reacts with an electron-poor maleic anhydride via [1+2] cycloaddition to give **III-81**, which agrees with the chemical behavior expected for a singlet phosphinidene.



**Scheme III-20.** Synthesis of Bertrand's "bottle-able" phosphinidene and their reactivity.

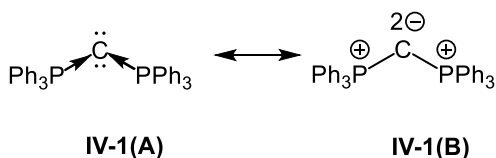
## IV. Zerovalent Heavier Group 14 Compound

### IV.1 Heavier Group 14 Compound in Zero Oxidation State

Main-group elements are those that use only their valence s- and p-orbitals for chemical bonding. This leads to a number of limitations in their chemical behaviours, given the fact that the chemistry of transition metals is richer than that of the main group elements. Since the last decade of the twentieth century, the chemistry of main group element complexes in low oxidation state has been extensively studied.<sup>[139–145]</sup> A number of studies revealed several types of low-valent complexes of main group elements that behave like transition metal complexes in that they feature unusual reactivity and, in particular, display ability to activate small molecular as well as to participate in multiple bonds.

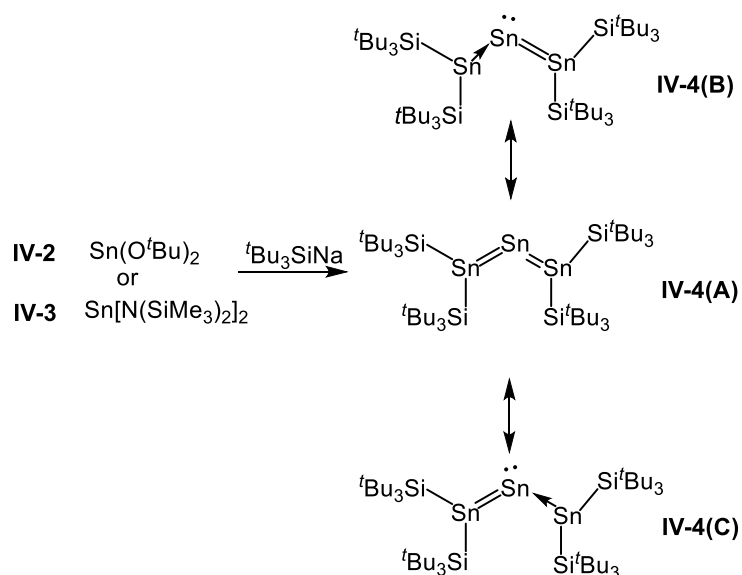
Zero-valent heavy group 14 compounds (ylidones) are the class of compounds in which four valence electrons are mainly localised on the tetrel centres (Ge, Si, Sn) as two electron lone pairs.<sup>[146,147]</sup> The central  $E^0$  atom in these species can be stabilised by various neutral donor ligands (L) by donor–acceptor interactions. This field started as long ago as 1961 when Ramirez and co-workers reported the first example of a carbodiphosphorane  $C(PPh_3)_2$  (**IV-1**), for which a very bent P-C-P angle ( $131.7^\circ$ ) was observed in the X-ray structure.<sup>[148,149]</sup> A combined experimental study and theoretical calculations indicated that  $C(PPh_3)_2$  is a divalent carbon(0) compound, where the valence electrons of carbon atom are not engaged in chemical bonds. There remain two electron lone pairs on the C centre, localised on a HOMO of the  $\pi$ -type orbital and HOMO-1, which is a  $\sigma$ -type lone pair.<sup>[150]</sup> The bonding situation for the carbon-phosphorus bond is described as donor–acceptor interactions. Since this first system was reported, the “ylidone” chemistry has continuously

developed as an interesting research field and many theoretical and experimental studies have been conducted.



**Scheme IV-1.** Description of the bonding situation in carbodiphosphorane in terms of donor–acceptor interactions

In 1999, Wiberg et al. reported the first example of a heavier stannylene. The compound **IV-4** was generated and crystallised from the mixture of  $\text{Sn}(\text{O}^t\text{Bu})_2$  or  $\text{Sn}[\text{N}(\text{SiMe}_3)_2]_2$  with  ${}^t\text{Bu}_3\text{SiNa}$  in *n*-pentane/benzene at low temperature,  $-25^\circ\text{C}$ .<sup>[151]</sup> The structure of the resulting tristannaallene **IV-4** was determined by  $^{119}\text{Sn}$  and  $^{29}\text{Si}$  NMR spectroscopy, as well as by an X-ray study. The  $^{29}\text{Si}\{^1\text{H}\}$  NMR spectrum of **IV-4** revealed one singlet peak at  $\delta = 77.3$  ppm, whereas the  $^{119}\text{Sn}\{^1\text{H}\}$  NMR spectrum showed two signals, at  $\delta = 503$  ppm and  $\delta = 2233$  ppm, with the intensity ratio 2:1, assigned to two terminal Sn atoms and one central Sn atom, respectively. The chemical shift of the terminal Sn atoms was close to those reported for distannene,<sup>[152]</sup> while the chemical shift of central Sn atom was compatible with a typical value for stannylenes.<sup>[153,154]</sup> The X-ray structure characterization revealed a bent angle of  $156^\circ$  for the  $\text{Sn}_3$  framework and the pyramidal geometry of the terminal Sn atoms. The length of the Sn-Sn bond ( $2.68 \text{ \AA}$ ) was shorter than those reported for distannenes ( $2.77\text{--}2.91 \text{ \AA}$ ).<sup>[152]</sup> These results indicated that the compound **IV-4** can be described as a stannylene adduct of a distannavinylidene, which is represented by two resonance structures shown in Scheme **IV-2**.

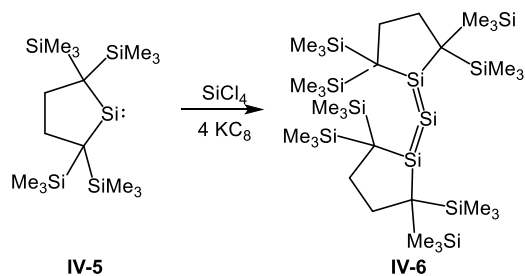


**Scheme IV-2.** Synthesis of trisilallene **IV-4** and its resonance structures.

Kabuto and Kira reported the formation of trisilallene **IV-6** via a two-step procedure from the silylene **IV-5**.<sup>[155]</sup> The structure of **IV-6** obtained from X-ray diffraction analysis is unusual in that the central Sn atom was disordered over four different position at temperatures higher than  $-100^\circ\text{C}$ . This indicates that at least four isomers of similar energy exist for **IV-4**. Furthermore, a bent Si-Si-Si arrangement ( $136.49(6)^\circ$ ) was also observed. The Si=Si bond length of  $2.177(1) \text{ \AA}$  is close to the typical values found for disilenes ( $2.14\text{--}2.29 \text{ \AA}$ ). The fluxional properties of **IV-6** were confirmed by the  $^{29}\text{Si}\{^1\text{H}\}$  NMR which showed one peak at  $\delta = 157$  ppm assigned to the central Si and only one peak at  $\delta = 197$  ppm assigned to two terminal Si atoms. Furthermore, an  $^1\text{H}$  NMR experiment at various temperatures showed a  $\text{C}_{2v}$  geometrical species even at  $-80^\circ\text{C}$ , indicating a very low energy barrier interconnecting four isomers. The bonding situation in **IV-6** was further studied by DFT calculation. The HOMO is a symmetrical  $\pi$ -orbital while the LUMO is an antisymmetrical  $\pi$ -orbital, and both are delocalised over the trisilallyl  $\pi$ -system.

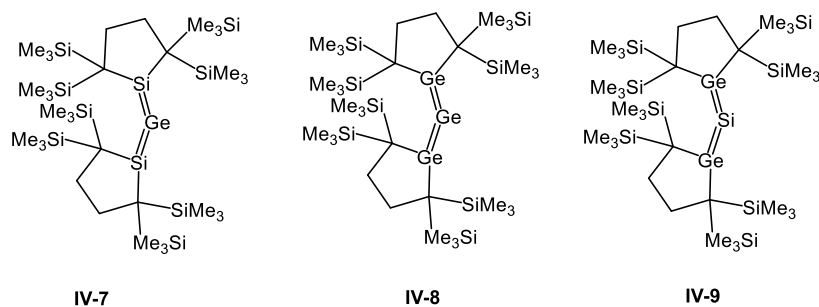


Following the Kira's report, Frenking et al. studied by quantum-chemical calculations the geometries and electronic structures of a series of di-coordinated silicon compounds of type  $\text{SiL}_2$ , in which L is a five-membered cyclic group based on group 14 element.<sup>[156]</sup> The calculations suggested that trissilaallene **IV-6** is best described as a divalent silicon(0) compound possessing two  $\text{L} \rightarrow \text{Si}$  donor-acceptor bonds and two lone-pairs with  $\pi$  and  $\sigma$  symmetry at silicon.



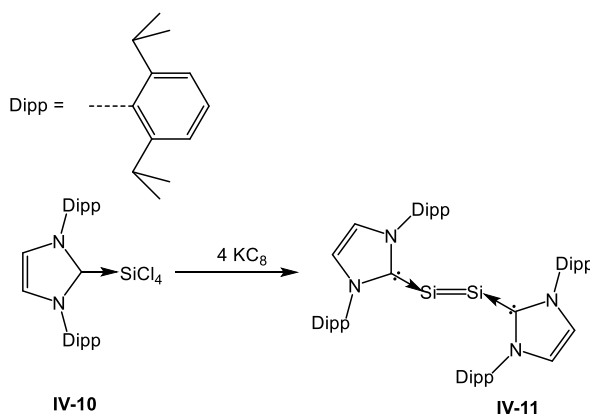
**Scheme IV-3.** Synthesis of the trissilaallene **IV-6**.

Similarly, Kira and co-workers reported a series of compounds **IV-7-9** shown in Scheme IV-4,<sup>[157,158]</sup> which are considered as analogues of the trissilaallene **IV-6**.



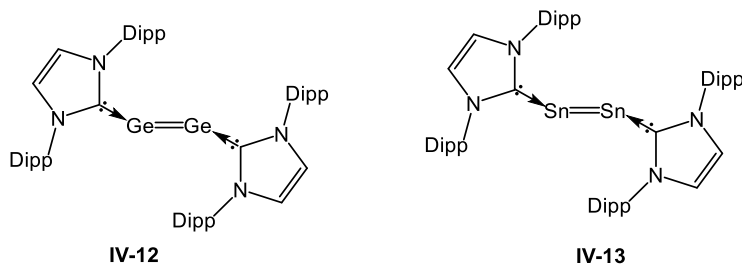
**Scheme IV-4.** Synthesis of disilagermaallene **IV-7**, trigermaallene **IV-8**, digermasilaallene **IV-9**.

In 2008, Robinson et al. reported a carbene-stabilised silicon compound in zero oxidation state containing the Si=Si double bond **IV-11**.<sup>[159]</sup> The target product was obtained from the reduction of L:SiCl<sub>4</sub> (L = C[N(2,6-*i*Pr<sub>2</sub>C<sub>6</sub>H<sub>3</sub>)CH]<sub>2</sub>) with 4 equivalents of KC<sub>8</sub> in THF. Both Si atoms in **IV-11** were found in the zero oxidation state supported by experimental data and calculations. Indeed, the <sup>29</sup>Si{<sup>1</sup>H} NMR spectrum of **IV-11** in C<sub>6</sub>D<sub>6</sub> reveals a peak at  $\delta = 224.5$  ppm which is in a lower field than typical disilene resonances (50 to 155 ppm). X-ray crystallographic analysis showed that the two-coordinate Si atoms in **IV-11** are in the trans-bent geometries formed by the C–Si–Si angles of 93.37°. The Si–Si bond length was measured as 2.2294(11), Å which falls in the reported range of disilene bond distances (2.14 to 2.29 Å),<sup>[160,161]</sup> indicating a double bond character. A UV-vis spectrum of this species in THF showed an absorption band at  $\lambda_{\text{max}} = 466$  nm corresponding to the  $\pi_{\text{Si}=\text{Si}}-\pi^*_{\text{Si}=\text{Si}}$  transition. The results obtained by DFT calculation are in good agreement with the experimental data for the Si=Si bond length and C–Si–Si angles. The HOMO is the  $\pi$ -orbital of the Si-Si bond and the HOMO-1 is dominated by the Si-Si  $\sigma$  bond, as well as the HOMO-2 is one of the two nonbonding lone-pair molecular orbitals.



**Scheme IV-5.** Synthesis of **IV-11** reported by Robinson et al.

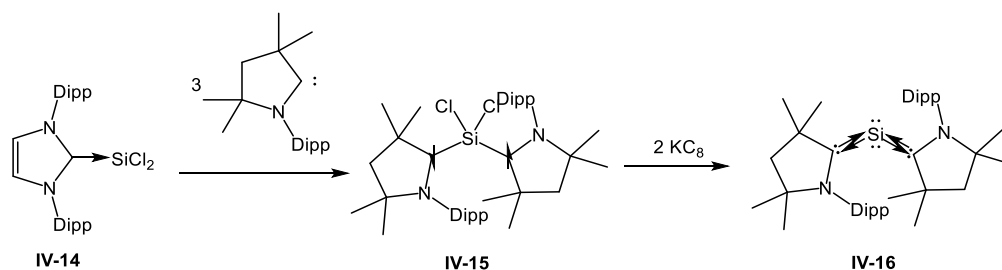
Similar to the structure discussed above, Jones, Frenking and co-workers studied two analogues of compound **IV-11**,<sup>[162,163]</sup> the germanium(0) dimer **IV-12** and the tin(0) dimer **IV-13** obtained by reduction of NHC-adducts of GeCl<sub>2</sub> and SnCl<sub>2</sub>, respectively, with magnesium(I) dimers.<sup>[164]</sup> The combination of spectroscopic, structural, and theoretical analyses suggest that the metal centre is best described as having zero oxidation state where M=M fragments (M = Ge, Sn) are datively coordinated by two NHC ligands.



**Scheme IV-6.** Synthesis of germanium(0) dimer **IV-12** and stannum(0) dimer **IV-13**

In 2013, Frenking and Stalke successfully isolated the first example of siladibene **IV-16** described as a low-valent silicon compound. **IV-16** was obtained from the reduction of a dichloride biradical precursor **IV-15** with KC<sub>8</sub>.<sup>[165]</sup> The <sup>29</sup>Si{<sup>1</sup>H} NMR spectrum of **IV-16** reveals a singlet at  $\delta = 66.71$  ppm which is in a higher field than that of the trissilaallene **IV-6** ( $\delta = 157$  ppm). The structure of such a siladibene was unambiguously determined by X-ray structural analysis which showed that the central Si atom is coordinated to the carbene carbon atoms of two cAAC ligands<sup>[166–168]</sup> and adopts a bent geometry with the C-Si-C bond angles around 117.18(8)°. The Si-C bond of 1.8411(18) Å in **IV-16** is shorter than the typical Si-C<sub>aryl</sub> single bond (average 1.879 Å),<sup>[169]</sup> but much longer than Si=C double bond (range 1.702–1.775 Å).<sup>[170]</sup> The bonding situation in **IV-16** was studied computationally, and the main findings support the formulation of

**IV-16** as a Si(0) species. Thus, the HOMO-1 is a  $\sigma$  lone-pair orbital of the Si atom whereas the HOMO is a  $\pi$ -type orbital that is mainly localised on Si but also exhibits a significant Si=C  $\pi$ -bonding. This analysis agrees well with the Si-C bond length found by X-ray analysis.

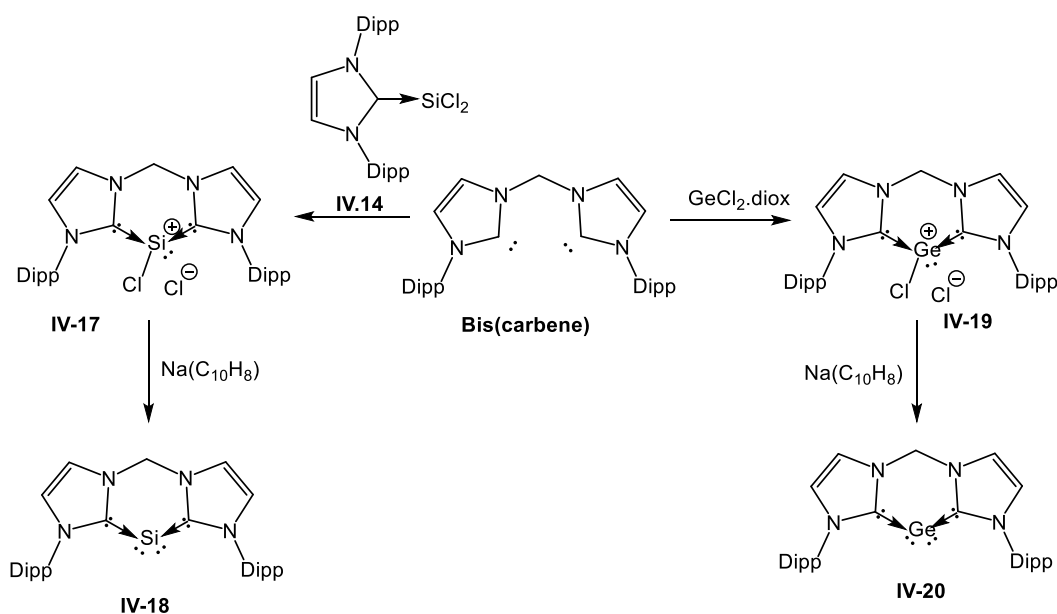


**Scheme IV-7.** Synthesis of siladibene **IV-16**

By adapting a similar approach, cyclic siladibene **IV-18** could be obtained by the reaction of bis(carbene) with NHC-SiCl<sub>2</sub> in THF, followed by reduction with sodium naphthalenide.<sup>[171]</sup> The <sup>29</sup>Si{<sup>1</sup>H} NMR chemical shift for **IV-18** was observed at  $\delta = -80.1$  ppm, which is in a higher field than that reported for the acyclic siladibene Si(cAAC)<sub>2</sub> ( $\delta = 66.7$  ppm) **IV-16**. It is reasonably explained by a stronger  $\sigma$ -donor but weaker  $\pi$ -acceptor ability of the two NHC moieties towards silicon. The Si atom is two-coordinate, with a C-Si-C angle of 89.1(1)<sup>o</sup> which is smaller than those reported for **IV-16**.<sup>[165]</sup> This value is consistent with the computational study. DFT calculations were performed to understand the electronic structure of **IV-18**, which showed the energy gap between the singlet ground state and triplet first excited state of approximately 33.0 kcalmol<sup>-1</sup>. The HOMO represents the silicon  $\pi$ -orbital, whereas the HOMO-1 is the  $\sigma$  lone-pair orbital localised on the Si atom. The observed Si-C bond distance of 1.869 Å in **IV-18** is in good

agreement with the DFT calculated values, supporting the partial multiple bond character of the Si-C bonds.

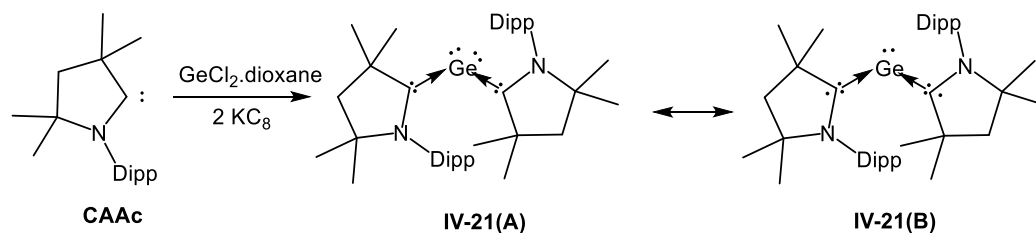
Driess et al. further contributed to this topic by using chelating bis(carbene) for stabilisation of a new germylone **IV-20**.<sup>[172]</sup> The first reaction involved the treatment of bis(carbene) with  $\text{GeCl}_2 \cdot \text{dioxane}$ , leading to the formation of a new germyliumylidene chloride **IV-19**. Using 2 equivalents of sodium naphthalene in the further step, the salt was reduced to the desired cyclic germadicarbene (germylone) **IV-20**. X-ray diffraction study showed a C-Ge-C bond angle of  $86.6(1)^\circ$ , which is much more acute than the Ge-Ge-Ge bond angle in **IV-8**.<sup>[158]</sup> The carbene carbon atoms adopt a trigonal-planar geometry with the bond angle sums equal to  $359.95^\circ$  and  $359.59^\circ$ . The energy gap between the singlet ground state and the first excited triplet state is approximately  $33.0 \text{ kcal mol}^{-1}$ , as revealed by DFT calculations. The HOMO is a  $\pi$ -type orbital localised on the Ge centre, whereas the HOMO-1 is a  $\sigma$  lone-pair orbital at Ge.



**Scheme IV-8.** Synthesis of silylone **IV-18** and germylone **IV-20**.

Meanwhile, Roesky, Stalke and Andrada reported a closely related germanium compound **IV-21** which was prepared by a one-pot reaction of  $\text{GeCl}_2$ -dioxane, cAAC ligand, and  $\text{KC}_8$  in the molar ratio: 1:2:2.1.<sup>[173]</sup> This germanium species is less stable than the silicon analogue **IV-16**, as decomposition to an unknown black powder occurred slowly during crystallization. The UV-vis spectrum showed bands at  $\lambda_{\text{max}} = 310, 410, 495,$  and  $653 \text{ nm}$ , which are comparable to the values found for the trigermaallene **IV-8** and germylone **IV-20**. However, the absorption band at  $653 \text{ nm}$  in **IV-21** was attributed to the diradicaloid character (form B) which was not observed in the Driess's cyclic germylone **IV-20**. The structural properties of **IV-21** were studied by X-ray diffraction to afford the  $\text{Ge}-\text{C}_{\text{carbene}}$  bond distances of  $1.9386(16)$  and  $1.9417(15) \text{ \AA}$  which are slightly shorter than those found in the germylone **IV-20**. ( $1.965(3), 1.961(3) \text{ \AA}$ ).<sup>[172]</sup> The C-Ge-C bond angles ( $114.71(6)^\circ$  and  $115.27(6)^\circ$ ) for two independent molecules are also significantly less acute than those in **IV-20**. Like in the silicon analogue, the HOMO-1 is a  $\sigma$  lone pair orbital at the Ge centre, whereas the HOMO is a  $\pi$  orbital with the largest contribution of the Ge atom, indicating a  $\pi$ -back donation from the Ge atom to the carbene moieties.

Summarising the electronic structures of Si and Ge species **IV-16**, **IV-18**, **IV-20** and **IV-21**, the relative order of the ylidone lone pairs is likely determined by the contribution of the more stable group 14 element s orbital to the  $\sigma$  lone pair, making it HOMO-1, whereas the HOMO has a pure  $\pi$ -character.

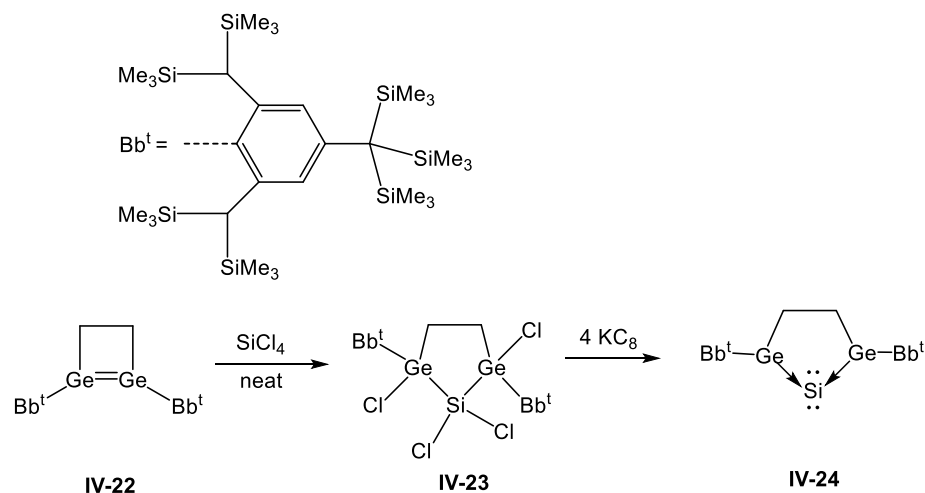


**Scheme IV-9.** Synthesis of compound **IV-21**.

In a recent publication, Sasamori and Tokitoh reported a 1,3-digerma-2-silaallene incorporated into a five-membered ring system, which was synthesised by heating 1,2-Bbt<sub>2</sub>-1,2 digermacyclobutene **IV-22** with SiCl<sub>4</sub> for 12 h to 55°C without a solvent, resulting in the formation of 1,1,2,5-tetrachloro-2,5-digerma-1-sila-cyclopentane **IV-23**.<sup>[174]</sup> The precursor **IV-23** was reduced by four molar equivalents of KC<sub>8</sub> in benzene to give the target 1,3-digerma-2-silaallene **IV-24**. The UV/vis absorption band at  $\lambda_{\text{max}} = 451 \text{ nm}$ , assigned to the HOMO-LUMO transition, was observed. The <sup>29</sup>Si{<sup>1</sup>H} NMR shift of **IV-24** at  $\delta = -16.5 \text{ ppm}$  is in a much higher field than that of the linear 1,3-digerma-2-silaallene **IV-9** ( $\delta = 236.6 \text{ ppm}$ ). Tokitoh et al. discussed the significant difference of <sup>29</sup>Si{<sup>1</sup>H} NMR chemical shift of Si(NHC)<sub>2</sub> **IV-18** ( $\delta = -80.1 \text{ ppm}$ ) and Si(CAAC)<sub>2</sub> **IV-16** ( $\delta = 66.7 \text{ ppm}$ ), and rationalized them by the the smaller C-Si-C bond angles in **IV-18** (89.1(1)°) as compared to those in **IV-16** (117.7(8)°) and stronger  $\sigma$ -donating properties of NHC vs CAAC. The latter argument, however, contradicts the experimental data by Bertrand and Driess who showed that CAAC are stronger  $\sigma$ -donors than phosphines and NHCs and are second only to abnormal NHCs.<sup>[167,171,172]</sup> Similarly, an upfield-shifted <sup>29</sup>Si{<sup>1</sup>H} NMR signal of **IV-24** might arise from the  $\sigma$ -donating properties of the germylene moieties and the acute Ge-Si-Ge angle due to the rigid cyclic skeleton. These results support the notion of a Si(0) character in **IV-24**. X-ray diffraction analysis reveals a two-coordinated silicon

atom surrounded by two germanium atoms and a planar five-membered SiGe<sub>2</sub>C<sub>2</sub> ring. The distance between Ge atoms (2.9325(4) Å) is longer than the sum of covalent radii of germanium (2.48 Å), indicating only weak if any interaction between the two germanium atoms. The Ge-Si bond lengths (2.2681(18) Å and 2.2900(18) Å) are shorter than the Si-Ge single bond in the precursor **IV-23** (2.410(4) Å and 2.433(3) Å), and close to the Si=Ge bond in **IV-9** (2.269(8) Å). The Ge-Si-Ge bond angle (80.08(4)°) is much more acute than the calculated angle in **IV-9**, which likely reflects the tethered nature of the ligand. The HOMO is a  $\pi$ -type lone pair delocalised over the Ge-Si-Ge fragment, likely stemming from the back donation from the 3p lone pair of the Si(0) moiety to the empty 4p orbitals of Ge atoms. The HOMO-1 and HOMO-2 are responsible for  $\sigma$ -donation from the lone pairs of the Ge atoms toward the vacant 3p orbitals of Si(0), whereas HOMO-5 is the  $\sigma$  lone pair of the Si(0) atom. The natural population analysis (NPA) charges of the silicon ( $q = +0.27$ ) and germanium atoms ( $q = +0.91, +0.90$ ) indicate the Si<sup>-</sup>-Ge<sup>+</sup> polarity of the bond, caused by the strong  $\sigma$ -donation from the Ge atoms towards the central Si atom. All together these results suggest that **IV-24** should be described as a dico-ordinate Si(0) species rather than a Ge=Si=Ge analogue of cumulene.



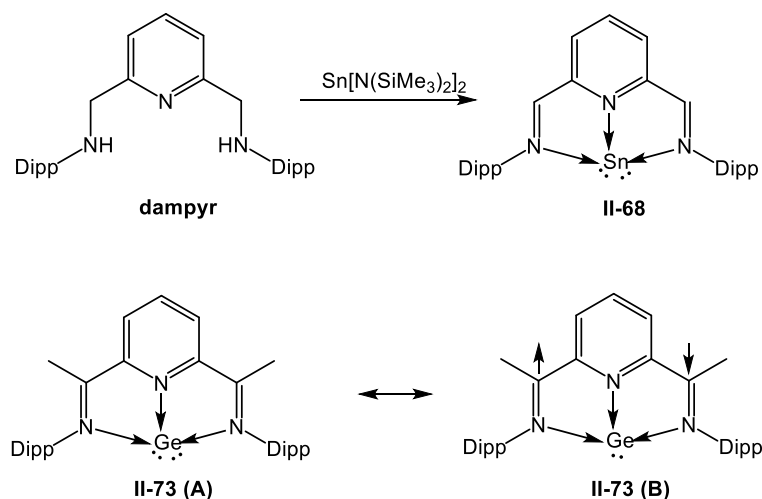


**Scheme IV-10.** Synthesis of 1,3-digerma-2-silaalene **IV-24**.

Fischer and Flock reported the first example of a mononuclear Sn compound in the oxidation state of zero.<sup>[54]</sup> A dimpyr-stabilised stannylene **II-68** was prepared by the reaction of (2,6-[ArNHCH<sub>2</sub>]<sub>2</sub>(NC<sub>5</sub>H<sub>3</sub>)) (dampyr) ligand with Sn[N(SiMe<sub>3</sub>)<sub>2</sub>]<sub>2</sub>. Such a species was stable in solid state but rapidly decomposed in solution (such as polar aprotic solvents). The <sup>119</sup>Sn{<sup>1</sup>H} NMR spectrum displayed a signal at  $\delta = 64$  ppm with the coupling constant of 236 Hz. The UV-vis spectrum revealed strong absorption bands at  $\lambda_{\text{max}} = 325$  and 510 nm which were assigned to weak n- $\pi^*$  transition (HOMO-1 to LUMO) and  $\pi$ - $\pi^*$  excitation (HOMO to LUMO-1), respectively. The other absorption band at 830 nm arises from a  $\pi$ - $\pi^*$  transition (HOMO to LUMO). The EPR spectrum of **II-68** was silent. The X-ray diffraction measurement showed that the Sn centre was coordinated to three nitrogen atoms of the dimpyr ligand which adopted a planar geometry with two five-membered chelating rings. The Sn-N(1) and Sn-N(2) bonds to imine centres, 2.397(2) Å and 2.315(2) Å, respectively, were comparable to those reported for N $\rightarrow$ Sn dative bonds, but longer than the Sn-N<sub>py</sub> bond length (2.122(2) Å).<sup>[30,66]</sup> Moreover, the bond length of N(1)=C(1) (1.308(3) Å) and N(2)=C(2) (1.321(3) Å) fall in the typical range of imine double bonds in

related compounds.<sup>[18,54,175]</sup> The HOMO is predominantly delocalised over the  $\pi$ -bonds between the Sn atom and three N atoms, as well as the  $\pi$ -system of the ligand. It indicates the back-bonding from Sn to the ligand which is crucial for the stabilization of **II-68**. HOMO-1 is a  $\sigma$ -type character at the Sn atom. The combination of these results confirms the structural features of **II-68** that is best rationalised in a closed-shell singlet species comprised of a neutral ligand and a Sn(0) atom.

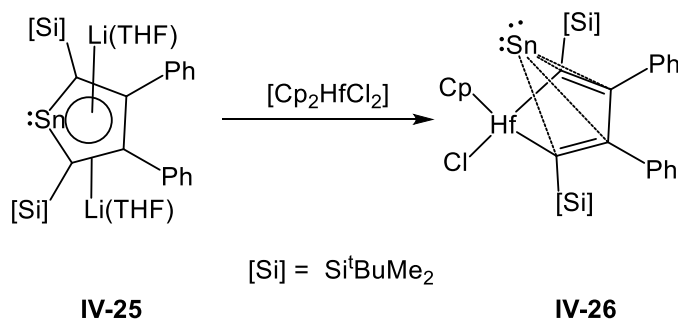
Similar to the structure just discussed, the Nikonov group reported the ability of dimpyr ligand to stabilize germanium(0). The compound **II-73** was obtained by the reduction of cationic germanium precursor with potassium graphite  $\text{KC}_8$ .<sup>[53]</sup> The HOMO of the singlet state corresponds to a  $\pi$ -type orbital at the Ge atom. DFT revealed partial delocalisation of the Ge lone pairs over the  $\pi^*(\text{C}=\text{N})$  orbitals of the imines, resulting in a partial multiple-bond character between the Ge atom and imine nitrogen atoms. These data agreed well with the X-ray diffraction analysis in which the Ge atom shifted closer to one of the imine nitrogen atoms, causing a shorter Ge1-N2 bond (2.047(7) Å) as compared to the Ge1-N2a bond (2.306(7) Å). Furthermore, the HOMO-1 is a  $\sigma$ -type lone pair at the Ge centre.



**Scheme IV-11.** Examples of dimpyr-stabilised stannylone **II-68** and dimpyr-stabilised germylone **II-73**.

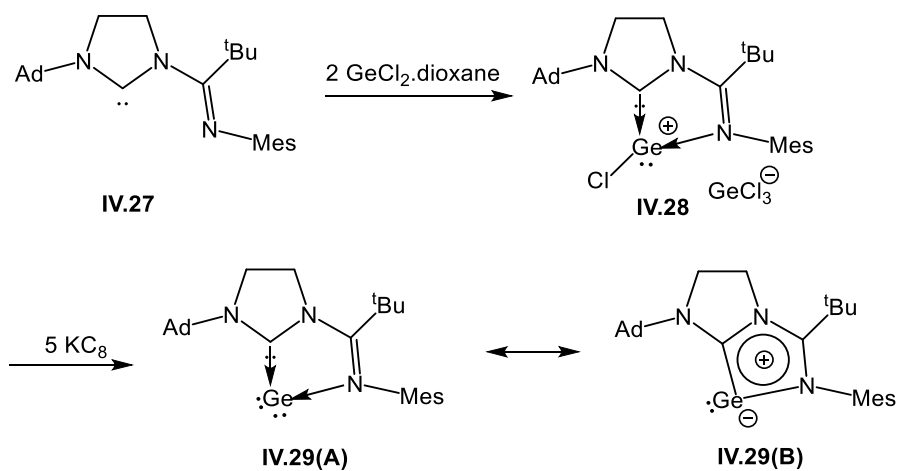
Saito and co-workers reported a unique approach to a novel Sn compound in the zero oxidation state. The stannylone **IV-26** was obtained from the reaction between dilithiostannole **IV-25** and hafnocene dichloride in THF.<sup>[176]</sup> A signal at  $\delta = -1020$  ppm was observed in the  $^{119}\text{Sn}\{^1\text{H}\}$  NMR spectrum. Such a compound is little stable and rapidly decomposes to a gray powder even when stored in inert atmosphere glovebox. The structural features of **IV-26** were studied by X-ray crystallography that showed the pyramidal coordination environment around the Sn atom as the result of a drastic deviation from the C4 plane of the butadiene moiety. Interactions between the Sn atom with both  $\text{C}_\alpha$  and  $\text{C}_\beta$  were observed, as evinced by the Sn- $\text{C}_\alpha$  and Sn- $\text{C}_\beta$  bond lengths of 2.314(4) Å and 2.451(4) Å, respectively. These values are longer than the Sn- $\text{C}_\alpha$  bond observed in the precursor **IV-25**, but compatible to those reported for the stannapyramidane  $\text{Sn}[\eta^4\text{-C}_4(\text{SiMe}_3)_4]$  (2.339–2.343 Å)<sup>[177]</sup> and  $(\eta^3\text{-allyl})\text{Sn}(\text{II})$  complexes (2.380–2.418 Å).<sup>[178]</sup> These results suggest that the Sn-C interaction in **IV-26** is best described as a  $\pi$ -bond rather than a  $\sigma$  bond, which confirms the presence of a Sn(0) atom in **IV-26**. The computational

study shows that the HOMO exhibits a lone pair in a  $\pi$ -orbital of the tin atom, which interacts with both  $\pi$ -orbitals of  $C_\alpha$  and  $C_\beta$ . The second lone pair having a high  $\sigma$ -character was reported to be spread over HOMO-3, HOMO-10, and HOMO-16. This allowed the authors to interpret **IV-26** as a  $(\eta^4\text{-butadiene})\text{Sn}(0)$  having the donor-acceptor interactions between 4  $\pi$ -electron donor of butadiene and the empty  $\pi$ -orbitals of the Sn centre.



**Scheme IV-12.** Synthesis of stannylone **IV-26**.

Kinjo and co-workers reported a reaction of  $\text{GeCl}_2^*$ dioxane with an imino-functionalised NHC to furnish the germyliumylidene **IV-28**.<sup>[179]</sup> A subsequent reduction of the salt precursor with  $\text{KC}_8$  affords the germylone **IV-29**. The UV/Vis spectrum exhibits a strong absorption band at  $\lambda_{\text{max}} = 415 \text{ nm}$  assigned to the  $\pi\text{-}\pi^*$  transition. The X-ray structure analysis reveals a C-Ge-N bond angle of  $80.59(6)^\circ$ , which is more acute than the corresponding C-Ge-C angle ( $86.6(1)^\circ$ ) of the cyclic germadicarbene **IV-20**.<sup>[172]</sup> The Ge-C<sub>carbene</sub> bond length of  $1.8870(15)\text{\AA}$  is the average distance between the typical Ge-C and Ge=C bonds.<sup>[180]</sup> The HOMO predominantly attributes to the 4p orbital of the Ge atom, whereas the HOMO-1 is a  $\sigma$ -type lone pair orbital on the Ge atom.



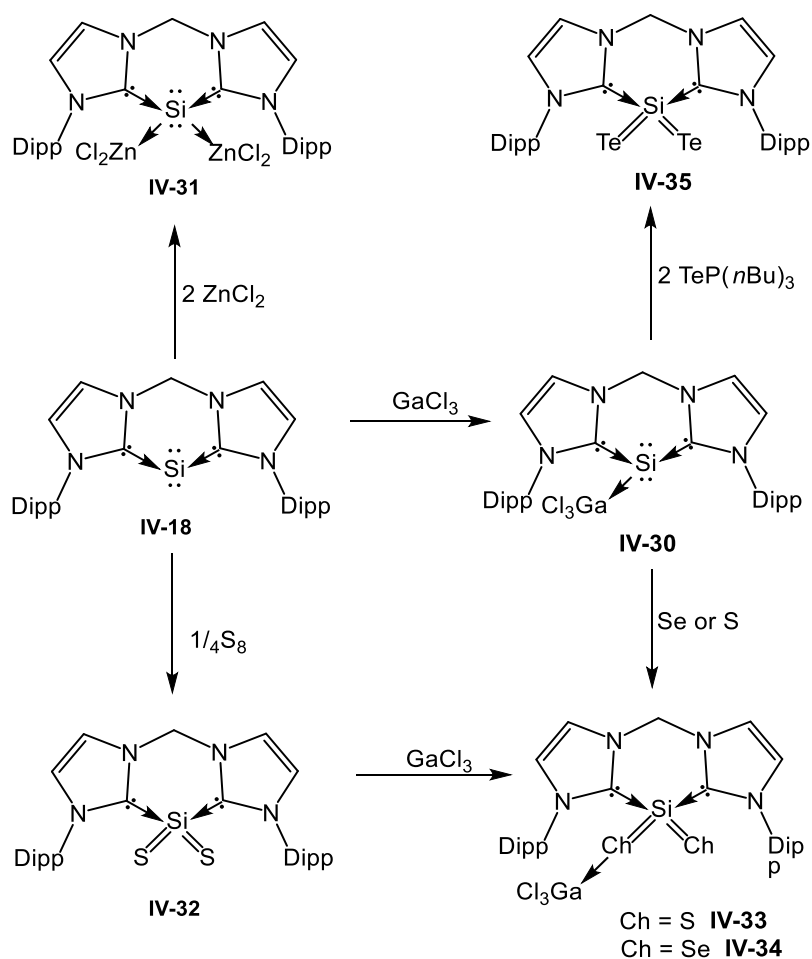
**Scheme IV-13.** Synthesis of germylone **IV-29**

## IV.2 The Reactivity of Zerovalent Heavy Group 14 Compounds

Remarkable progress has been achieved over the past decade in the isolation of heavier group 14 compounds in the zero oxidation state. However, only a few examples of reactivity studies have been reported. Thus, Driess and co-worker studied the reactivity of silylone **IV-18**. Firstly, an “ylidone” compound is expected to form adducts with Lewis acids due to the presence of two lone pairs of electrons on the group 14 centre. The reaction of silylone **IV-18** with GaCl<sub>3</sub> in THF produced the adduct LSi(0)→GaCl<sub>3</sub> (**IV-30**).<sup>[181]</sup> The molecular structure of **IV-30** shows a three-coordinate silicon atom that adopts a distorted pyramidal coordination geometry, with a lone pair on the Si centre. Furthermore, dimetallated compound **IV-31** was obtained by treatment of silylone **IV-18** with two molar equivalents of ZnCl<sub>2</sub> in THF.<sup>[182]</sup> X-ray analysis of **IV-31** reveals that two Zn atoms are in different coordination environments in which one Zn adopts a trigonal planar geometry, whereas the other Zn atom adopts a tetrahedral geometry with an additional coordinated THF molecule. The ability to be dimetallated is a characteristic property that distinguishes silylones from silylenes and silaallenes.

Meanwhile, the silylone **IV-18** was able to react with sulfur powder in THF to give a monomeric silicon disulfide complex **IV-32** from an oxidation reaction.<sup>[181]</sup> The NMR in solid state of this species showed an <sup>29</sup>Si{<sup>1</sup>H} NMR chemical shift at δ = -32.5 ppm, which is consistent with the theoretical value (δ = -29.8 ppm) obtained from DFT calculations. Attempt to grow single crystals for molecular structure analysis failed because of limited solubility of **IV-32** in most common organic solvents. A further reaction of **IV-32** with GaCl<sub>3</sub> in CH<sub>3</sub>CN produced the adduct **IV-33** in high yield.<sup>[181]</sup> The solid-state <sup>29</sup>Si{<sup>1</sup>H} NMR spectrum of **IV-33** exhibits a signal at δ = -40.0 ppm. X-ray diffraction study revealed

that one of the S atoms coordinates to GaCl<sub>3</sub> via a S→Ga bond. The length of the Si-S bond was 2.106(2) Å for Si-S(1) and 2.006(1) Å for Si-S(2). The strong polarity of Si-S bonds was confirmed by theoretical calculations that revealed a moderate π-bond character. The Si-S(1) bond in **IV-33** has a lower π-bond character than that of the Si-S(2) bond, so that the GaCl<sub>3</sub> moiety coordinates to the more negatively charged sulfur atom of the Si-S(1) bond. Compound **IV-33** can be independently prepared by direct oxidation of **IV-30** with elemental sulfur.



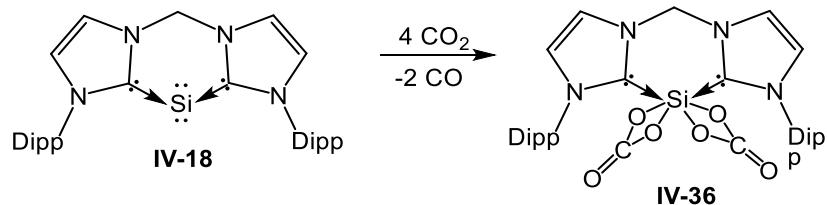
**Scheme IV-14.** The reactivity of silylone **IV-18** and related compounds.

Likewise, the monomeric bis(NHC)Si(Se)Se $\rightarrow$ GaCl<sub>3</sub> complex **IV-34** was achieved by the reaction of silylone $\rightarrow$ GaCl<sub>3</sub> adduct **IV-30** with Se in THF.<sup>[183]</sup> The <sup>29</sup>Si{<sup>1</sup>H} NMR chemical shift at  $\delta = -69.9$  ppm is in a higher field compared to the value reported for the complex bis(NHC)-Si(S)S $\rightarrow$ GaCl<sub>3</sub> (**IV-33**,  $\delta = -40.0$  ppm).<sup>[181]</sup> The <sup>77</sup>Se{<sup>1</sup>H} NMR spectrum revealed a single signal at  $\delta = -391$  ppm, indicating a rapid exchange of the GaCl<sub>3</sub> moiety between two selenium atoms. **IV-34** is isostructural with its sulfur analogue **IV-33**, as evinced by X-ray diffraction study.

Treatment of **IV-30** with Te=P(*n*Bu)<sub>3</sub> in THF afforded the monomeric compound bis(NHC)-SiTe<sub>2</sub> (**IV-35**) in 63% yield.<sup>[183]</sup> The <sup>29</sup>Si{<sup>1</sup>H} NMR spectrum shows a signal at  $\delta = -143.9$  ppm, and the <sup>125</sup>Te{<sup>1</sup>H} NMR spectrum displays a signal at  $\delta = -1120$  ppm. The silicon centre is coordinated by the bis(NHC) ligand and two terminal tellurium atoms, and thus adopts a distorted tetrahedral geometry.

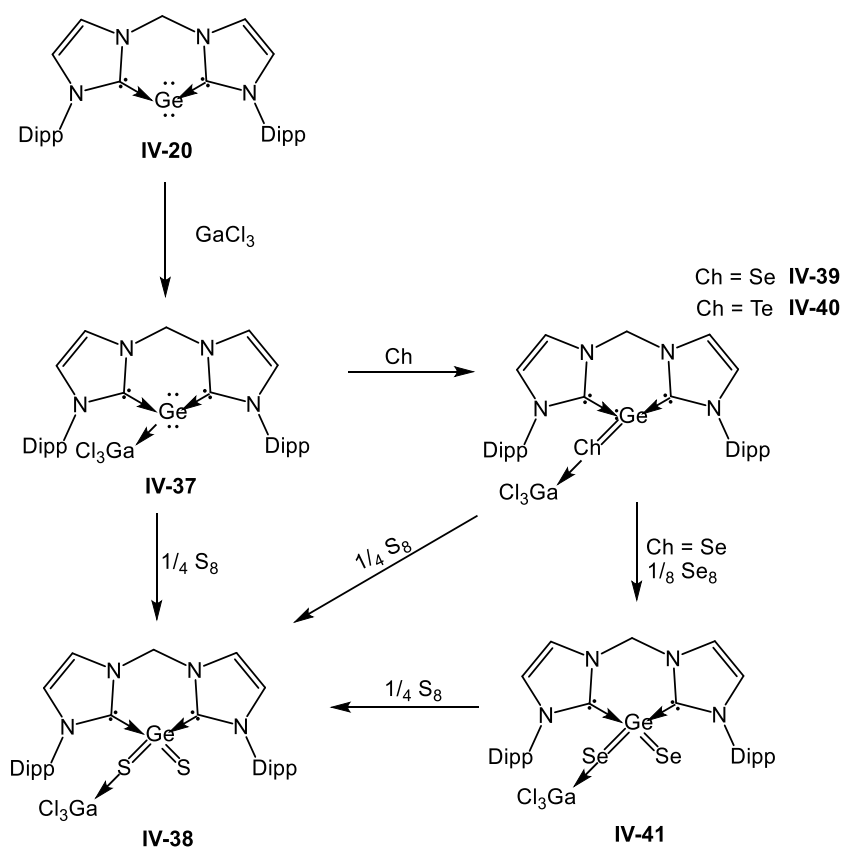
Interestingly, when a solution of **IV-18** was exposed to the atmosphere of CO<sub>2</sub>, the first bis(NHC)-silicon dicarbonate adduct **IV-35** was obtained.<sup>[184]</sup> The <sup>29</sup>Si{<sup>1</sup>H} NMR spectrum in THF displayed a singlet at  $\delta = -195.0$  ppm which is close to the observed signal in the solid state ( $\delta^{29}\text{Si} = -196.5$  ppm). The IR spectrum showed a band at  $\nu = 1746$  cm<sup>-1</sup> responding to the stretching vibration of the C=O group. The Si centre is coordinated by a chelating bis(NHC) ligand and two carbonate ligands to give a distorted octahedral geometry. The two planar carbonate ligands are twisted. Two key intermediates, bis(NHC)SiO and bis(NHC)SiO<sub>2</sub>, involved in the reaction were suggested by DFT calculation.





**Scheme IV-15.** The reactivity of silylone **IV-18** toward CO<sub>2</sub> gas.

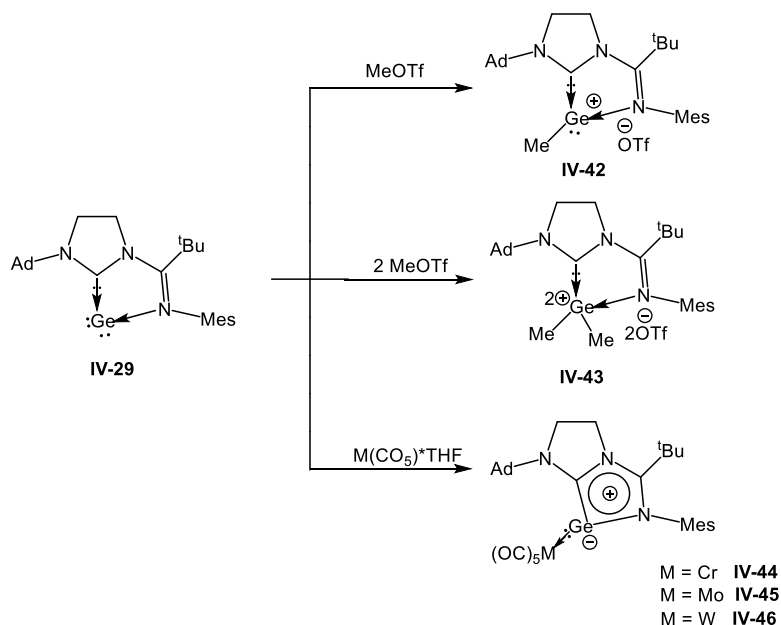
The reactivity of the germanium analogue of compound **IV-18** was also reported. Similarly to the silicon case, the reaction of germylone **IV-20** with Lewis acid GaCl<sub>3</sub> gave complex **IV-37**.<sup>[185]</sup> In the molecular structure, the three-coordinated Ge centre adopts a distorted pyramidal geometry. The reaction of germylone with elemental sulfur and elemental selenium yielded complexes **IV-38** and **IV-39**, respectively. The tellurium analogue **IV-40** was obtained by a similar approach. Furthermore, the selenium complex **IV-39** could react further with another equivalent of selenium to furnish the final product **IV-41**. Adding elemental sulfur into the solution of either **IV-39** or **IV-40** resulted in the displacement of heavier pnictogenes with the formation of sulfur compound **IV-38** and liberation of Se and Te, respectively. Finally, it was noted that a reaction of germylone **IV-20** with CO<sub>2</sub> leads to the formation of the Lewis adduct bis(NHC)(CO<sub>2</sub>) and the precipitation of GeO<sub>2</sub>.<sup>[182]</sup>



**Scheme IV-16.** The reactivity of germylone **IV-20**

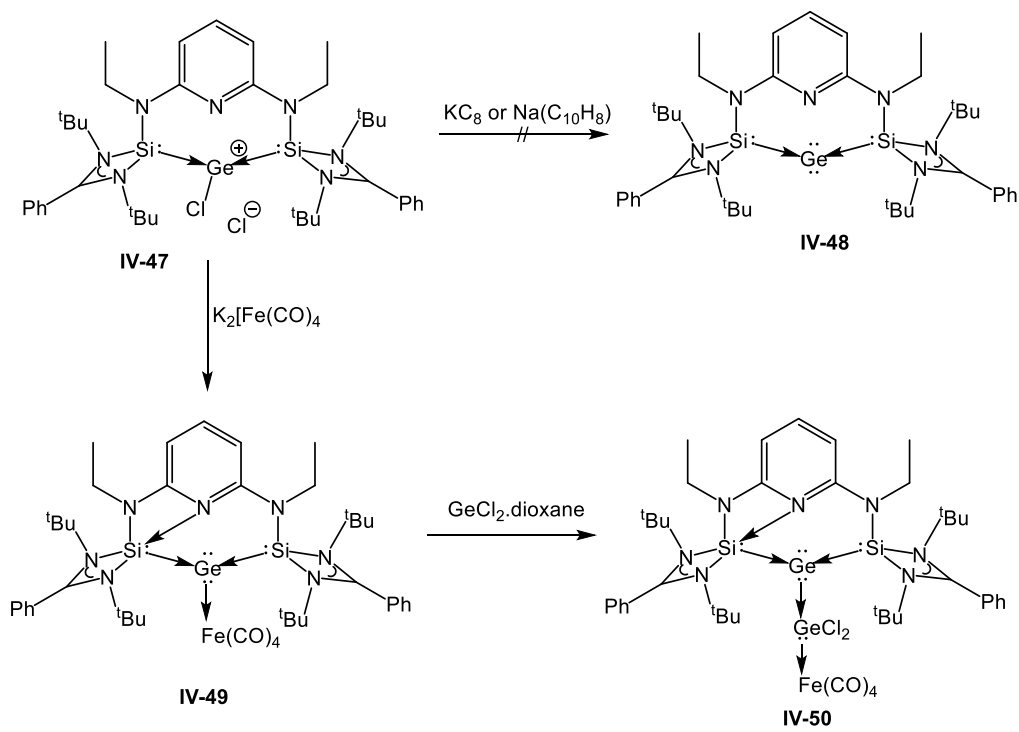
Kinjo et al. conducted the reaction of germylone **IV-29** with one equivalent of MeOTf, leading to the formation of germyliumylidene ion **IV-42**.<sup>[179]</sup> Further reaction with the second equivalent of MeOTf afforded the corresponding dicationic **IV-43**, which indicates the presence of two lone pairs in the germylone precursor. These results confirm the nucleophilic properties of germylone. Finally, the reactivity of germylone toward transition metals was investigated. Adding an equivalent of  $[\text{M}(\text{CO})_5 \cdot \text{THF}]$  ( $\text{M} = \text{Cr}, \text{Co}, \text{W}$ ) into a THF solution of **IV-29** furnished the germylone-metal(0) complexes.<sup>[186]</sup> The crystals of compounds **IV-42** – **IV-46** were suitable for X-ray diffraction analyses that showed the planar five-member  $[\text{C}_2\text{N}_2\text{Ge}]$  ring in these structures. The Ge atom in **IV-42**

adopts a pyramidal geometry, whereas the Ge atom in **IV-44** – **IV-46** adopts a trigonal planar geometry.



**Scheme IV-17.** The reactivity of germylone **IV-29**

Driess et al. also attempted to stabilize germylone by a bis(N-heterocyclic silylenyl)pyridine [SiNSi] pincer ligand. However, the reduction of germanium precursor **IV-47** by  $\text{KC}_8$  or sodium naphthalenide was unsuccessful. A novel germylone iron carbonyl complex  $[\text{SiNSi}]\text{Ge}0 \rightarrow \text{Fe}(\text{CO})_4$  **IV-49** was achieved by a reaction of the corresponding ligand with  $\text{GeCl}_2 \cdot \text{dioxane}$  and  $\text{K}_2[\text{Fe}(\text{CO})_4]$ .<sup>[187]</sup> X-ray diffraction analysis showed an interaction of the pyridine centre with one of the silylene moiety, leading to an unsymmetrical geometry of **IV-49**. The treatment of **IV-49** with  $\text{GeCl}_2 \cdot \text{dioxane}$  afforded the germylone–germylene–iron complex **IV-50**.



**Scheme IV-18.** Synthesis of **IV-49** and its reactivity.

## **Part B. Results and Discussion**

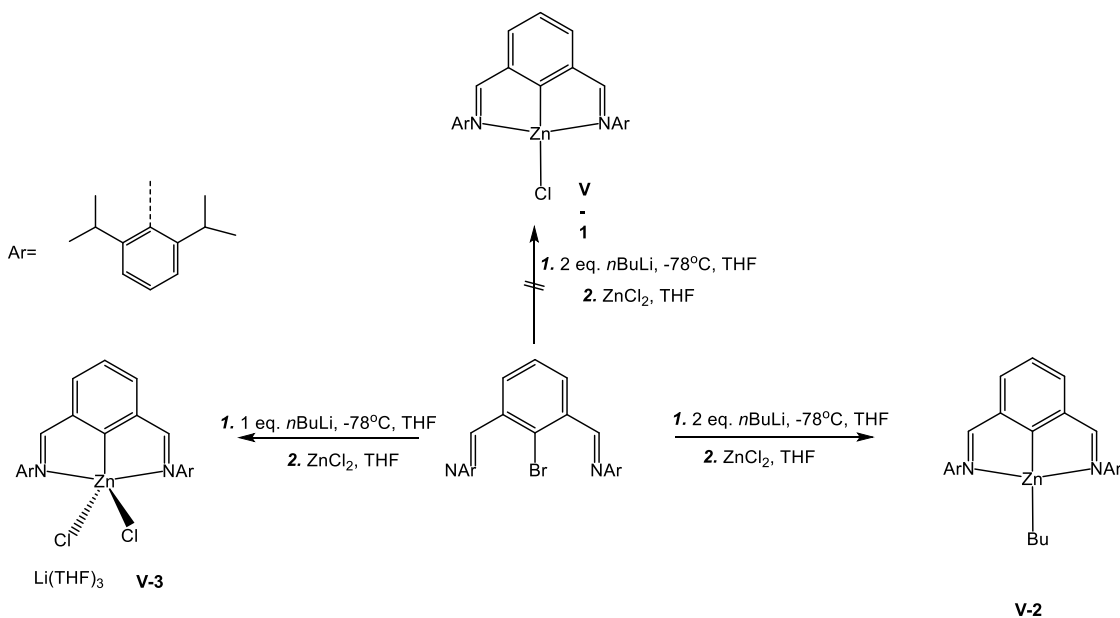
## V. Synthesis and Characterization of Zinc Complexes Stabilised by 2,6-bis[(2,6-diisopropyl)imino]phenyl Pincer Ligand

### V.1 Introduction

The application of pincer complexes has been very beneficial for the development of transition metal catalysis.<sup>[11,188–192]</sup> In contrast, main group compounds supported by pincer ligands have received much less attention. Main group catalysis is a highly promising research field due to the low cost and low toxicity of many s and p block elements.<sup>[193–196]</sup> Zinc, in particular, is a rising star in catalysis<sup>[197,198]</sup> because it is an earth abundant and biocompatible metal playing a vital role in >300 enzymes.<sup>[199]</sup> Thus, we have shown the potency of zinc hydrides to catalyze the hydrosilylation of very stable C≡N<sup>[200]</sup> bonds and aromatically stabilised C=N bonds.<sup>[201]</sup> Later on Parkin et al. reported the ability of the zinc hydride complex  $[\kappa^3\text{-Tp}^{\text{tm}}]\text{ZnH}$  to hydrosilylate carbonyl functionalities.<sup>[202]</sup> Very recently, Mosch-Zanetti and co-workers reported that the terminal zinc hydride complex  $[\text{Tntm}]\text{ZnH}$  (Tntm=tris(6-tert-butyl-3-thiopyridazinyl)methanide) is an efficient catalyst for the hydrosilylation of CO<sub>2</sub> at room temperature.<sup>[203]</sup> These reports show the promise of using zinc-based compounds as catalysis. However, the number of isolable zinc hydrides is rather limited.<sup>[204–206]</sup> In this Thesis, we report the preparation of a zinc analogue of germanium hydride **II-7** (Scheme II-5). The target compound was employed as a catalyst in the hydrosilylation of several substrates. Investigation of the reactivity of zinc compounds will be also discussed.

## V.2 Synthesis, Characterization, and Reactivity of Zinc Complexes Stabilised by 2,6-bis[(2,6-Diisopropyl)imino]phenyl Pincer Ligand

By adapting the synthetic procedure used by Driess et al. to prepare the chloride (NCN)GeCl **II-5** (Scheme II-5),<sup>[31]</sup> we reacted the 1,3 bis(aldimino)-2-bromobenzene with two equivalents of *n*BuLi, followed by addition of ZnCl<sub>2</sub> in THF. The bis(aldimine) system was chosen in this work instead of the previously used bis(ketamine) system because the parent 1,3-diacetyl-2-bromo-benzene is no longer commercially available. To our surprise, instead of obtaining the expected zinc chloride compound **V-1**, we isolated the butyl complex **V-2** (Scheme V-1).



**Scheme V-1.** Preparation of compounds **V-2** and **V-3**

Single crystals of compound **V-2** were obtained from a concentrated hexane solution at -30°C. The molecular structure of **V-2** is displayed in Figure V-1. Like the four-coordinate complex dimpyrZnCl supported by a related diimino-pyridine pincer platform, previously described by our group<sup>[207]</sup> and Berben et al.,<sup>[208]</sup> this compound has an unusual

square planar geometry, with the mean deviation from the N1-C1-N2-Zn1-C33 plane being 0.0271 Å. X-ray diffraction analysis showed the Zn-C bonds of 1.956(3) and 1.952(4) Å which are close to the average single Zn-C bond of 2.075 Å (which falls in the range 1.779 - 2.822 Å). In contrast, the Zn-N distances of 2.594 and 2.582 Å are longer than the Zn-imines bonds of 2.153(2) and 2.220(2) Å in the Zn(I) species dimpyrZnCl<sup>[207]</sup> and are much longer than the average crystallographically observed zinc-imine distance of 2.068 Å, which however belongs to a very broad range of values, 1.724 - 2.668 Å.<sup>[209]</sup> The essential molecular metrics of compound **V-2** can be compared to the related germanium(II) species **II-5** having a comparable Ge-C bond of 1.9483(18) Å but much shorter Ge-N coordination contacts of 2.2722(15) and 2.2746(15) Å. These data suggest that alternatively compound **V-2** can be described as a two-coordinate alkyl-aryl zinc having two additional weak zinc-imine contacts.

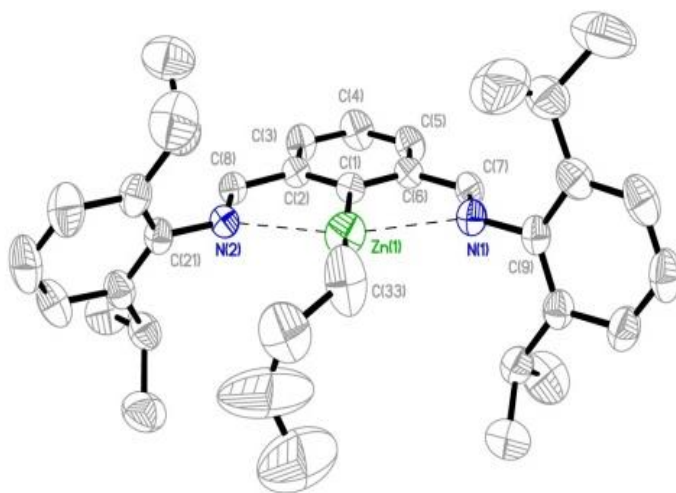


**Figure V-1.** Molecular structure of complex **V-2**. Hydrogen atoms are omitted for clarity. Displacement ellipsoids are shown at the 30% probability level.



**Table V-1.** Selected bond lengths and angles for compound **V-2**

Lengths, Å		Angles, °			
Zn1-C1	1.956(3)	Zn1-N1	2.594(1)	C33-Zn1-C1	175.70(16)
Zn1-C33	1.952(4)	Zn1-N2	2.582(3)	N1-Zn1-N2	149.50(10)

In contrast, by using only one equivalent of *n*BuLi in the lithiation step, we succeeded in preparing the ate-complex (NCN)ZnCl( $\mu$ -Cl)Li(THF)<sub>*n*</sub> (**V-3**, Scheme V-1). The compound **V-3** was crystallised as a mixture of two forms, (NCN<sub>2</sub>ZnCl<sub>2</sub>)Li(THF)<sub>3</sub> and (NCN<sub>2</sub>ZnCl<sub>2</sub>)Li(THF)<sub>4</sub>, different in the extent of ligation of the lithium cation by THF and its coordination to the zinc-bound chlorides. In the first form shown in Figure V-2, the lithium cation is weakly bound to the zincate via a chloride ligand (the Li-Cl distance is 2.294(15) Å), and is further ligated by three THF molecules. In the second form, the lithium cation is completely detached from the anion and is coordinated by four THF molecules. In the unit cell, two THF molecules of both forms are superimposed and disordered. Therefore, the observed geometry of the zincate part is an average of two closely related geometries. The zinc atom is bound to the NCN ligand and two chlorides. The complex is bisected by a crystallographically imposed mirror plane running through the zinc atom, both chlorides, and the carbon atom C3 directly bound to Zn1. Compared to compound **V-2**, complex **V-3** displays even longer zinc-imine distances of 2.613 Å, which suggests that its geometry should be better described as trigonal planar.

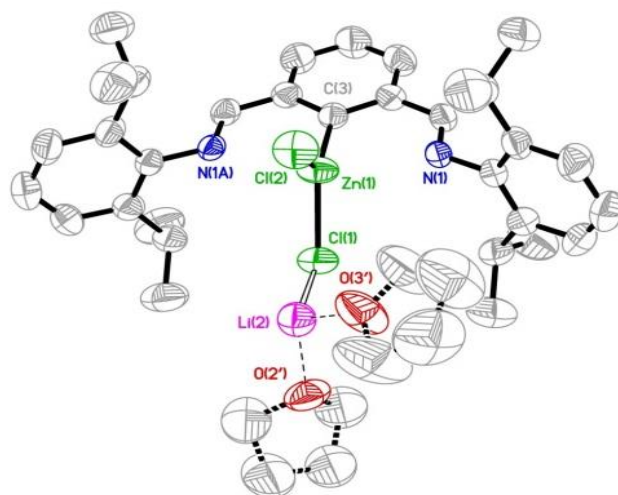


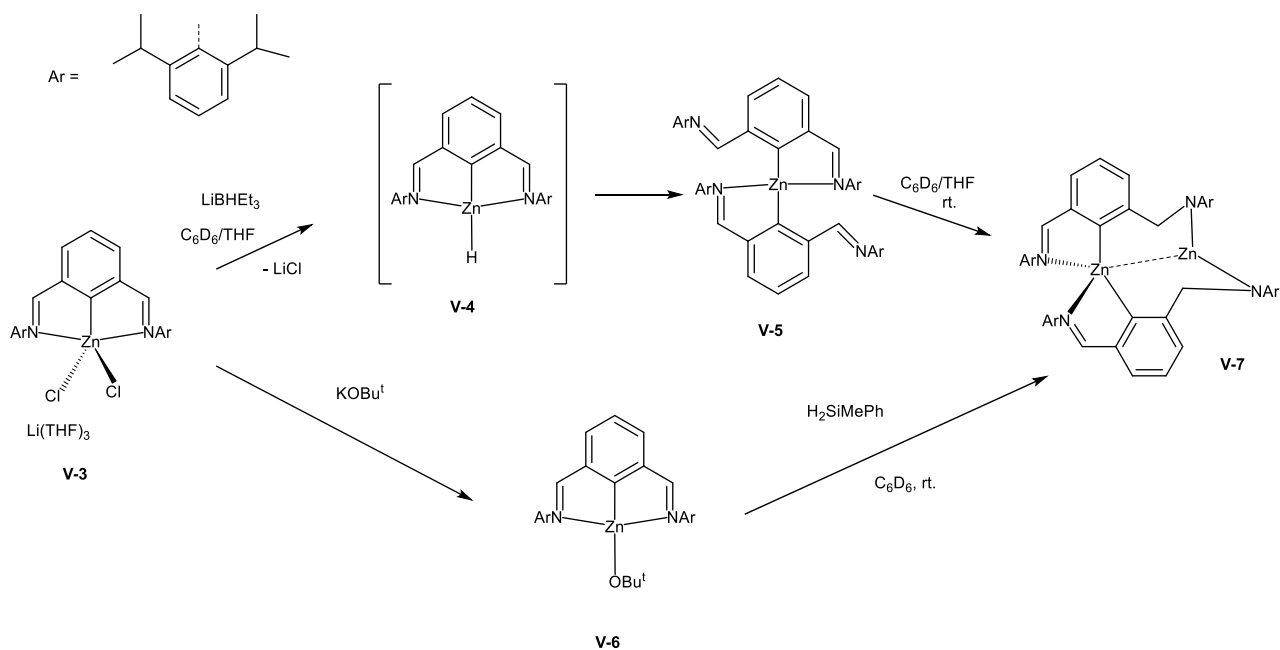
**Figure V-2.** Molecular structures of complex **V-3**. The molecule is disordered in the location and ligation pattern for the lithium ion. Only one part of the disordered structure is shown. Hydrogen atoms and a THF molecule symmetrically related to the O3' ligand are omitted for clarity. Displacement ellipsoids are shown at the 30% probability level.

**Table V-2.** Selected bond lengths and angles for compound **V-3**

Lengths, Å		Angles, °			
Zn1-C3	1.969(3)	O2'-Li2	1.919(16)	C3-Zn1-Cl2	124.71(10)
Zn1-Cl2	2.2480(11)	O3'-Li2	1.922(10)	C3-Zn1-Cl1	123.19(10)
Zn1-Cl1	2.2676(10)	Li2-Cl1	2.294(15)	Cl2-Zn1-Cl1	112.10(5)

The reaction of zincate **V-3** with one equivalent of Super Hydride (LiHBEt<sub>3</sub>) resulted in the unexpected formation the bis(aryl)-ligated compound **V-7**. The stoichiometry of this reaction and subsequent chemical events dictate that the zinc hydride ZnH<sub>2</sub> (**V-4**) should be also produced in the reaction mixture, but we were unable to determine a signal of this species by <sup>1</sup>H NMR. Having been formed, this mixture quickly

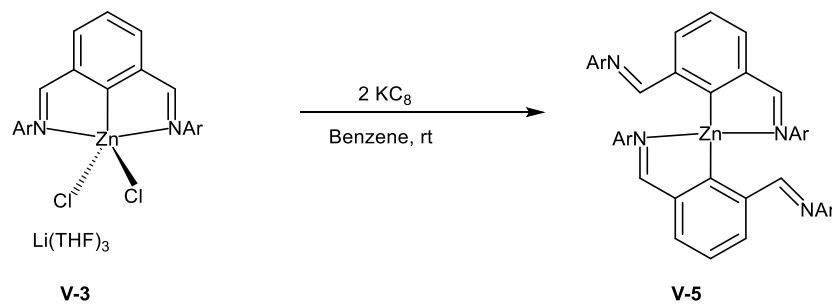
(~1.5 h) rearranges at room temperature into the binuclear species **V-5** (Scheme V-2). NMR data for the latter were consistent with the presence of a NCN'Zn species, where N' indicates an methyleneamido arm of the ligand (vide infra). We suggest that the intermediate **V-5** is quickly generated from the hydride compound **V-4**, which is too labile to be observed by NMR.



**Scheme V-2.** Synthetic routes to the binuclear species **V-7**.

Compound **V-5** was characterised by NMR spectroscopy. In the <sup>1</sup>H NMR spectrum, it gives rise to a C<sub>2v</sub> symmetric structure diagnosed by one singlet for the aldimine group at 8.17 ppm (2H) and one doublet at 0.95 ppm for the <sup>i</sup>Pr group of the Ar substituent. Compound **V-5** was also independently prepared by the reduction of **V-3** by 2 equivalents of KC<sub>8</sub> (scheme V-3). Its structure was confirmed by X-ray diffraction analysis which revealed a mononuclear zinc compound in the +2 oxidation state. The Zn atom is chelated by two NCN ligands, in which each NCN moiety coordinates to the zinc atom through the

$C_{ipso}$  atom and one of the two imine N atoms. The geometry around the metal centre in compound **V-5** can be described as distorted tetrahedral, with the geometry index  $\tau_4 = 0.71$  ( $\tau_4 = 1$  for tetrahedral structure and 0 for square planar).<sup>[210]</sup>



**Scheme V-3.** An alternative method to prepare **V-5**.

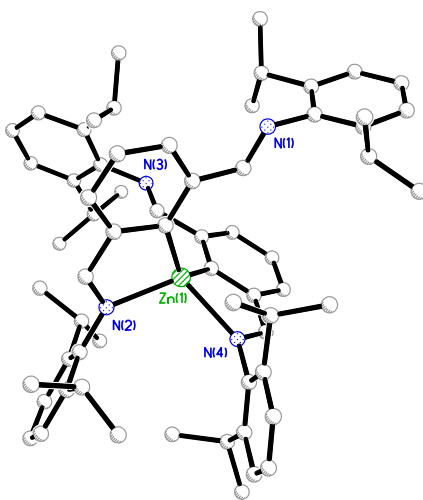


**Figure V-3.** Molecular structure of complex **V-5** Hydrogen atoms are omitted for clarity. Displacement ellipsoids are shown at the 30% probability level.

Compound **V-7** can be also accessed by reacting **V-3** with an equivalent of  $\text{KOBU}^t$  followed by a metathesis with  $\text{H}_2\text{SiMePh}$  (Scheme V-2). The latter reaction is believed to proceed via heterolysis of the H-Si bond on the Zn-O bond which is a standard method of

generating metal hydrides. We suggest that the same pathway as in the L-Selectride route occurred to generate the dimer **V-7**. Interestingly, we noticed that a quick removal of volatiles (benzene, THF, and excess silane) and re-dissolving the product in fresh C<sub>6</sub>D<sub>6</sub> results in fairly stable solutions of **V-4**, while keeping this compound in the original solution containing THF (from the starting compound **V-3**) results in decomposition into the dimer **V-7**, as was observed in the L-Selectride route. We, therefore, conclude that the formation of the amide **V-7** from **V-4** is promoted by THF, albeit the mechanism of this transformation is currently unknown.

The <sup>1</sup>H NMR spectrum of the hydride migration product **V-7** displays a singlet for the aldimino group at 8.03 ppm (1H) and two doublets with  $J_{H-H}=10.6$  Hz for two non-equivalent protons of the methylene CH<sub>2</sub>N group, at 3.85 and 4.97 ppm. The non-equivalent *meta* protons of the central phenyl ring come as doublets at 7.12 ppm and 7.47 ppm integrated as one proton each. X-ray quality crystals of **V-7** were grown from a toluene solution cooled to -30°C. X-ray diffraction analysis revealed an unusual dimeric structure (Figure V-3), with one zinc centre being coordinated to the phenyl/imino part of two NCN' ligands, thus having a four-coordinate environment, whereas the second zinc atom is only coordinated to the amido groups of the same ligand, thus forming a less common two-coordinate zinc species. The geometry of the Zn(1) centre can be described as a distorted tetrahedral, with the C1-Zn1-C33 angle being significantly increased (136.4°). In fact, the calculated geometry index  $\tau_4$  equals 0.39, which is more consistent with the presence of a see-saw geometry. For the two-coordinate zinc centre Zn(2), the bond angle comprised by the two amido ligand is obtuse (158.6°). Another interesting feature of this dimer is the presence of a fairly short Zn-Zn distance of 2.944 Å (*cf.* the sum of covalent radii 2.5 Å).

Since there are no available valence electrons on the zinc atoms to constitute a bond, this relatively short distance is either the consequence of the rigidity of the ligand framework or is a reflection of metallophilicity, well-documented for related closed-shell mercuriphilic and aurophilic interactions.<sup>[33,34]</sup>

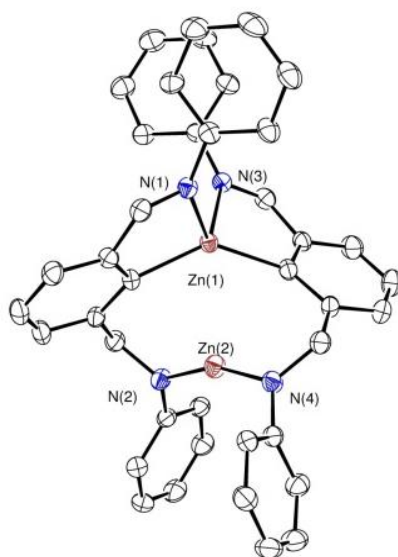
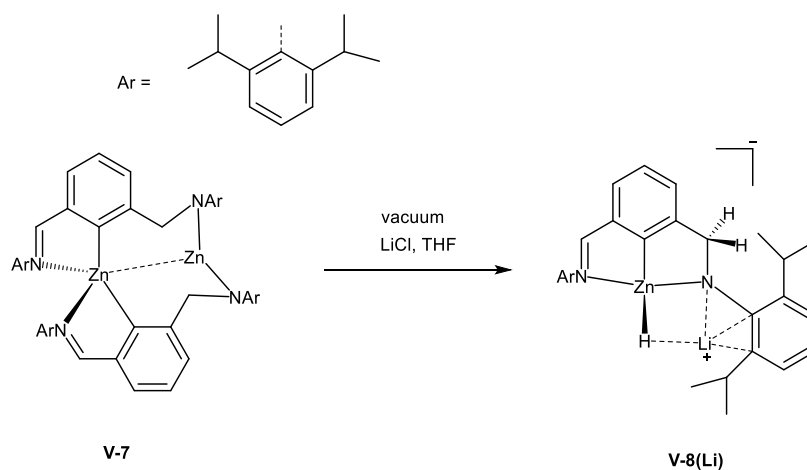


**Figure V-4.** Molecular structure of complex **V-7**. Displacement ellipsoids are shown at the 30% probability level. Hydrogen atoms and the <sup>i</sup>Pr groups are omitted for clarity.

**Table V-3.** Selected bond lengths and angles for compound **V-7**

Lengths, Å				Angles, °	
Zn1-C33	2.035(3)	Zn2-N2	1.810(3)	C1-Zn1-C33	136.48(13)
Zn1-C1	2.040(3)	Zn2-N4	1.819(3)	C1-Zn1-N1	83.86(11)
Zn1-N1	2.165(2)	N2-C7	1.456(4)	C33-Zn1-N3	84.28(11)
Zn1-N3	2.172(3)	N4-C39	1.447(4)	N1-Zn1-N3	101.93(10)
Zn1-Zn2	2.9437(6)			N2-Zn2-N4	158.54(13)

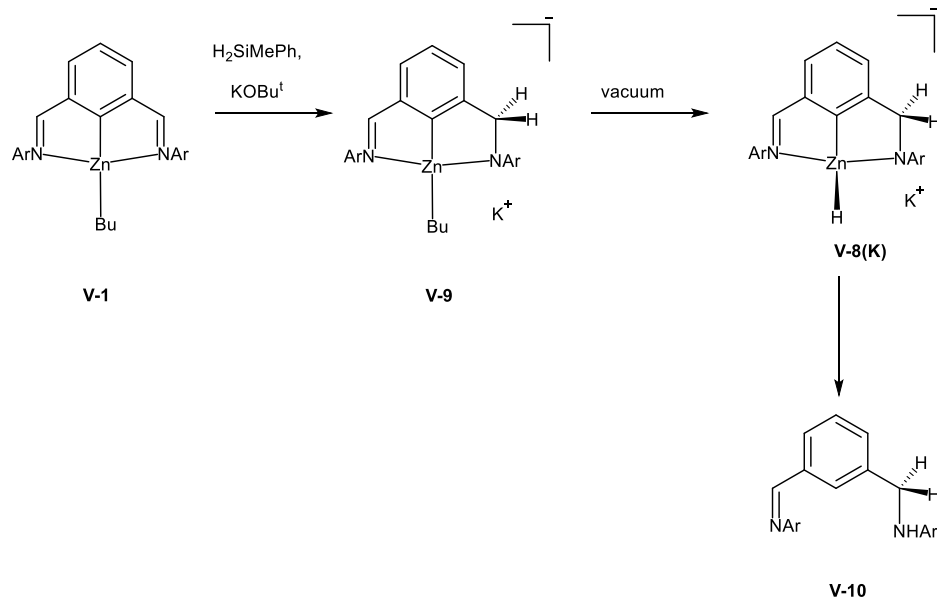
Even more surprisingly, removal of volatiles from an NMR sample of **V-7**, generated *in situ*, resulted in dissolution of the precipitate of LiCl and formation of the hydrido-zincate complex **V-8(Li)**, which according to  $^1\text{H}$  NMR is a  $C_1$  symmetric species. Thus, the protons of the methylene unit become diastereotopic, giving rise to two doublets of doublets at 4.45 and 4.26 ppm which are coupled to the zinc hydride at 3.56 ppm (t,  $J=7.8$  Hz, 1H). A NOESY experiment showed that the signal at 4.26 ppm is in proximity to the hydride indicating that the hydride lies outside of the plane of the central phenyl ring, resulting in a distorted tetrahedral geometry around zinc. The importance of LiCl re-coordination to the zinc atom to promote the rearrangement **V-7**→**V-8(Li)** was established by the following experiment: complex **V-7** was generated in  $\text{C}_6\text{D}_6$  and the precipitate was filtered prior to removal of volatiles. NMR study of thus obtained solid in fresh  $\text{C}_6\text{D}_6$  showed only negligible conversion of **V-7** to **V-8(Li)**. Addition of solid LiCl to this solution results in the formation of **V-8(Li)**, like in the *in-situ* experiment.



**Scheme V-4.** The first pathway to the zincate **V-8(Li)**

The ate-complex **V-8** was also generated by the two-step procedure outlined in Scheme V-5. First, complex **V-2** was treated by a mixture of  $\text{H}_2\text{SiMePh}$  and  $\text{KOBu}^t$  in  $\text{C}_6\text{D}_6$

or toluene to give the potassium butyl zincate **V-9**, different from **V-8** in the presence of a butyl group at zinc instead of hydride. Compound **V-9** can be isolated in the form of an orange toluene solvate, by crystallization at  $-30^{\circ}\text{C}$  from a toluene solution and after a quick drying is stable at room temperature for days. However, when placed under high vacuum for several hours, it decomposed to a mixture of **V-8(K)**, which likely forms by elimination of butene-1, and the amine imine compound **V-10**. This postulated olefin extrusion process from **V-9** is irreversible because addition of excess hexene-1 to a solution of **V-8(K)** does not lead to an insertion product. The exact way how **V-9** is formed and, in particular, what is the source of the additional proton and what is the scavenger for  $\text{K}^+$ , remains unknown. Exposing zincate **V-8** to air led to the decomposition and conversion to the protonated product **V-10**.

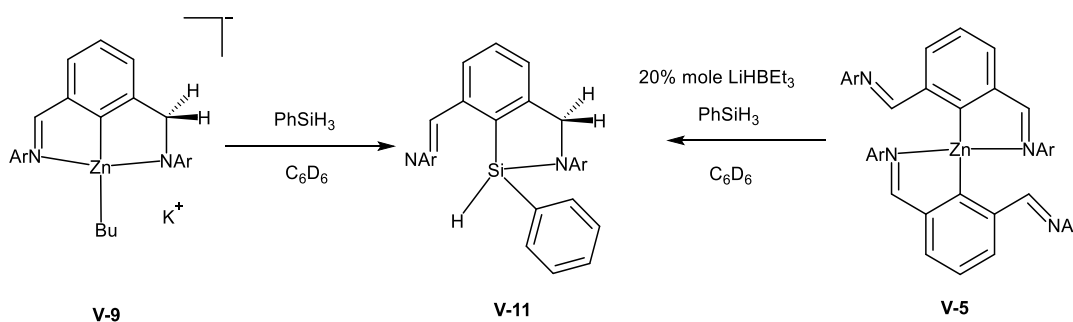


**Scheme V-5.** The second pathway to the zincate **V-8(K)**

In order to establish the potential for catalytic hydrosilylation, stoichiometric reactions were studied. Complex **V-9** does not react with acetophenone, benzonitrile, or



quinoline. However, addition of  $\text{PhSiH}_3$  does result in a noticeable reaction.  $^1\text{H}$  NMR data supported by  $^1\text{H}$ - $^{13}\text{C}$  HSQC,  $^1\text{H}$ - $^{13}\text{C}$  HMBC and  $^1\text{H}$ - $^{29}\text{Si}$  HSQC showed that the main product of this reaction is the silicon compound **V-11**. In particular, the unique Si-bonded proton gives rise to a doublet at 6.24 ppm coupled to one of two diastereotopic protons of the aminobenzyl group (4.75 ppm) with a coupling constant  $J_{\text{H-H}} = 4.2$  Hz. The stoichiometry of this reaction suggests the formation of zincate  $\text{KZnH}_2\text{Bu}$  or its derivatives. We indeed observed the Bu group pattern in the  $^1\text{H}$  NMR spectrum of the reaction mixture but could not assign the putative zinc-bound hydrides. Interestingly, the same silane **V-11** also forms upon treatment of compound **V-5** with  $\text{PhSiH}_3$  in the presence of 20% mole of Super Hydride ( $\text{LiHBEt}_3$ ), acting as a catalyst, after 20 hours at room temperature. Noticeably, this reaction occurred slowly when the catalyst load was reduced to 5% mole. The role of  $\text{LiHBEt}_3$  in this reaction is likely to reduce the bis(imino)phenyl ligand to afford a phenyl amido zincate which then undergoes double phenylamido/hydride metathesis with the  $\text{PhSiH}_3$  to give **V-11** and generate a new zincate.



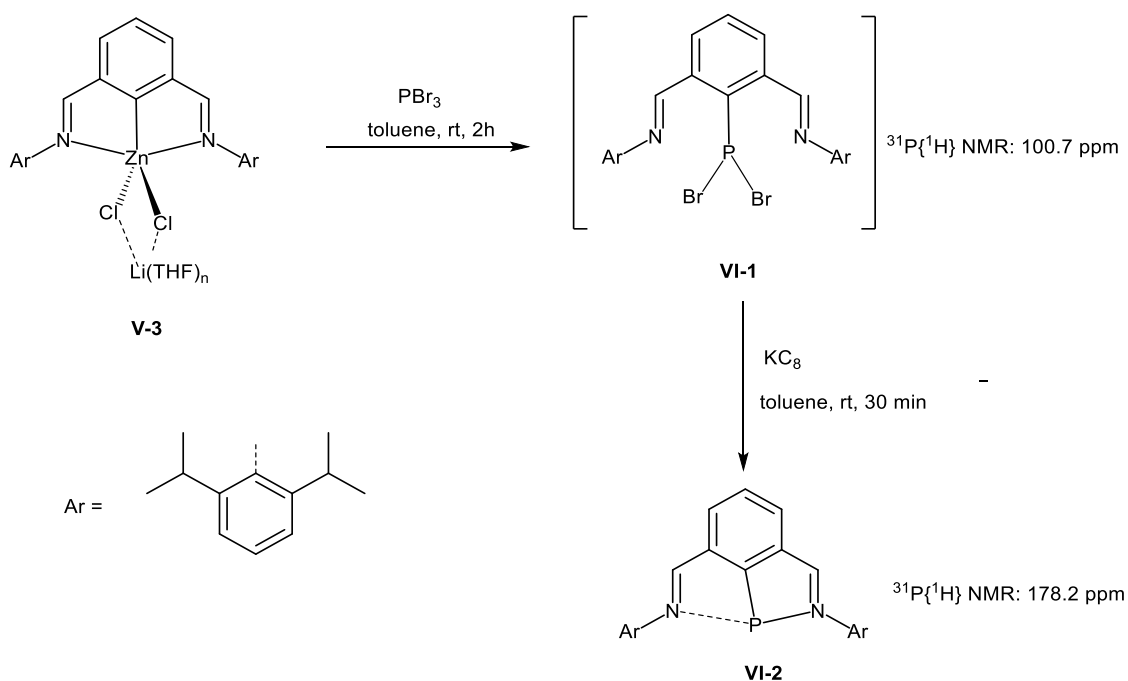
**Scheme V-6.** Preparations of compound **V-11**

## VI. Synthesis, Characterization, and Reactivity of Base-Stabilised-Phosphinidene

### VI.1. Preparation, Characterization, and Reactivity of “Phosphinidene” Stabilised by 2,6-bis[(2,6-diisopropyl)imino]phenyl Pincer Ligand.

To investigate further the potential of our NCN pincer ligand, we targeted the preparation of the P(I) compound dimphP (**VI-2**) which can be regarded as a phosphinidene stabilised intramolecularly by weakly  $\sigma$ -donating but  $\pi$ -accepting imino groups. The proposed compound **VI-2** can be obtained via a reaction of the zincate dimphZnCl<sub>2</sub>Li(THF)<sub>3</sub><sup>[213]</sup> with PBr<sub>3</sub> and that the resultant dibromide (**VI-1**) was reduced by potassium graphite (Scheme VI-1). Crystals of **VI-2** were grown from a solution of toluene at -30°C. **VI-2** was isolated in 80% yield and characterised by NMR spectroscopy and X-ray diffraction analysis. Thus, the molecular structure of **VI-2** (Figure VI-1) is asymmetric, which agrees well with the observations made by Cain et al. for a related Mes-substituted NCN compound of P(I) **II-29** (Scheme II-11).<sup>[39]</sup> However, the phosphorus atom in **VI-2** is shifted much closer to one of two imines groups (1.691(2) vs 2.681(2) Å). The former bond length is close to the average single P-N bond (1.70(4) Å).<sup>[214]</sup> Because of the crystallographically imposed mirror plane, the dimph ligand is disordered, so that the observed position of the nitrogen atoms is the superposition of two forms, i.e. the imine-bound-to-phosphorus and the distant imine. The averaged N=C bond is elongated to 1.307(3) Å, which lies between the values observed for the coordinated (1.350(4) Å) and uncoordinated (1.287(4) Å) C=N bonds in the Cain’s system **II-29** and is close to the values observed in the antimony(I) congener dimphSb (1.302(4) and 1.300(4) Å).<sup>[215]</sup> Analogous structural features were observed for the isolobal Ge(0) compound dimpyrGe **II-79** (Scheme IV-11) that showed a bit smaller asymmetry in the position of the germanium

atom (with the Ge-N distances of 2.047(7) and 2.306(7) Å) but a more significant charge transfer to the imine group, evidenced by the average N=C bond being elongated to 1.320(2) Å.<sup>[53]</sup> The latter effect is likely the consequence of the lower electronegativity of germanium relative to phosphorus (2.01 vs 2.19). It is also interesting to note that the P-N distance in **VI-2** is significantly shorter than the corresponding distance in the Cain compound **II-29**, 1.691(2) vs 1.757(2) Å, whereas the P-C distance is longer, 1.780(2) vs 1.744(3) Å.<sup>[39]</sup> These data likely indicate the stronger  $\pi$ -accepting ability of the aldimine vs ketimine groups.



**Scheme VI-1.** Preparation of phosphinidene **VI-2**.

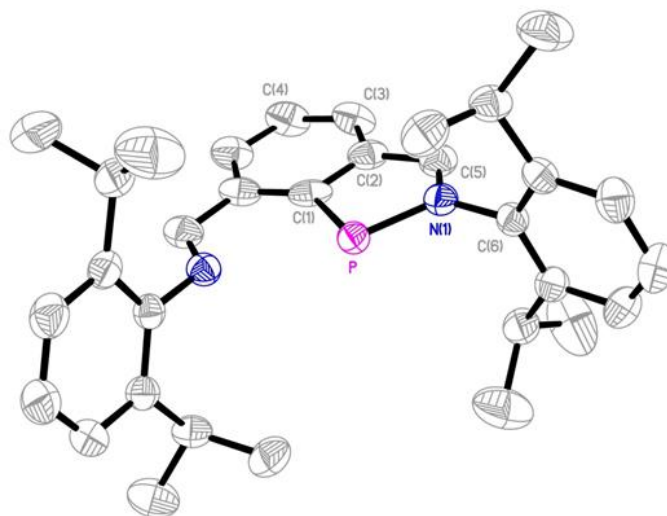


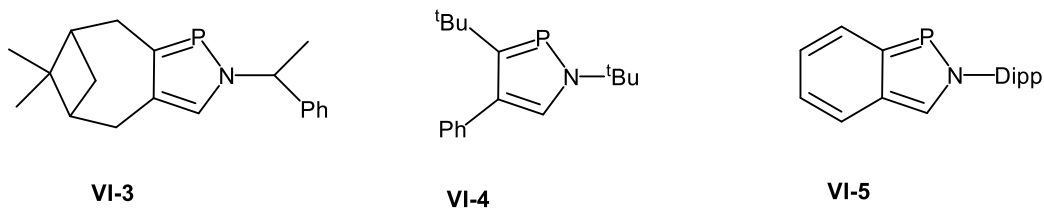
**Figure VI-1.** Molecular structure of compound **VI-2**. Thermal ellipsoids are shown at the 30% probability level. Hydrogen atoms are omitted for clarity. The molecule is bisected by a crystallographically imposed mirror plane running through the C(1)-C(4) vector.

**Table VI-1.** Selected bond lengths and angles for compound **VI-2**

Lengths, Å		Angles, °			
C1-P	1.780(2)	C5-N1	1.307(3)	C1-P-N1	95.66(9)
C2-C1	1.420(2)	P-N1	1.691(2)	P-C1-C2	103.88(13)
C2-C5	1.424(3)	N2-P	2.681(2)		

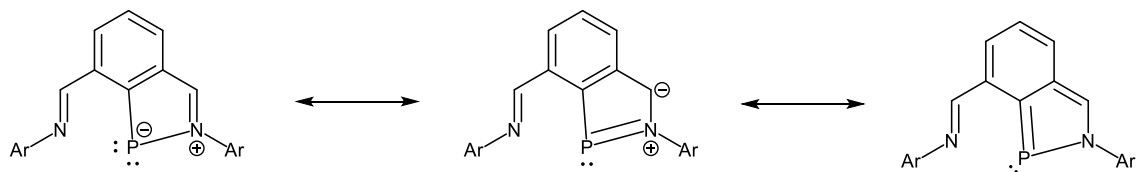
An alternative description of **VI-2** is that of a benzoazaphosphole. 1H-1,2-azaphospholes have been known since 1986,<sup>[216]</sup> but only three structurally characterised examples are known, two of them (**VI-3** and **VI-4**, Scheme IV-2) having an aliphatic backbone<sup>[217,218]</sup> and one being a benzophosphole **VI-5** (Scheme VI-2).<sup>[219,220]</sup> The P-N bonds in these species are 1.706(1) Å, 1.728(4) and 1.702(10) Å and are longer than the P-N bond in **VI-2** (1.691(2) Å). On contrary, the P=C bonds in 1H-1,2-azaphospholes (1.712(1), 1.713(5) and 1.744(4) Å) are close to the average P=C distance in

phosphaalkenes (1.70(4) Å) but are significantly shorter than the P(1)-C(1) bond in **VI-2** (1.780(2) Å). At the same time, the C-C bonds in azaphospholes are longer than C=C bonds (1.408(1) vs 1.377(1) Å, 1.395(6) vs 1.372(6) Å and 1.426(6) vs 1.416(7), whereas in **VI-2** the perceived “single” bond C(1)-C(2) of 1.420(2) Å is the same as the “double” bond C(2)-C(5) (1.423(3) Å). It is also noteworthy that the latter bond is more typical for a C<sub>sp2</sub>-C<sub>sp2</sub> single bond (1.46 Å)<sup>[221]</sup> than a double bond (1.34 Å).



**Scheme VI-2.** X-ray characterised azaphospholes.

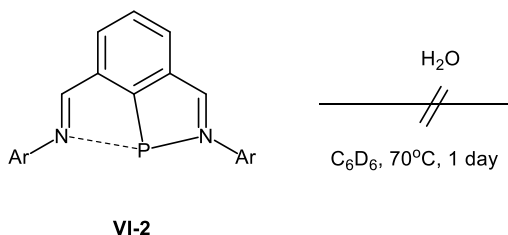
In other words, the compound **VI-2** has decreased multiple bond character in the P=C and C=C bonds but some increased bond character in the P-N bond in comparison to the known 1H-1,2-azaphospholes, which does not agree well with the rationalisation of this compound as an azaphosphole but complies well with the description in terms of a phosphinidene stabilised by dative interaction N→P and partial charge transfer from phosphorus to the π\*(N=C) of the imine group (Scheme VI-3).



**Scheme VI-3.** Description of the bonding situation in **VI-2** in terms of resonance. The left form describes the N→P σ donations, the middle form accounts for P →N=C π back-donation, and the right form shows the contribution of an azaphosphole component.

Another interesting feature of **VI-2** and Cain's compound **II-29**<sup>[39]</sup> that does not agree with the description of these compounds as azaphospholes only is fluxionality. Despite the asymmetric solid state geometry of **VI-2**, NMR data show an average  $C_{2v}$  symmetric pattern down to  $-70^{\circ}\text{C}$ , consistent with the observations made by the Cain group for the related diketimine system **II-29**. Cain et al. further calculated by DFT that the barrier for exchange in their system was only  $4.0\text{ kcal mol}^{-1}$ , which makes it impossible to decoalesce the spectrum. At room temperature, **VI-2** gives rise to one singlet for the aldimine group at 8.09 ppm, one septet at 2.89 ppm for the methine signal of the  $^i\text{Pr}$  groups of the Ar substituent, and one doublet at 1.15 ppm for the methyls of  $^i\text{Pr}$  groups. The  $^{31}\text{P}$  NMR signal in **VI-2** was observed at 178.2 ppm which is noticeably more downfield shifted relative to compound **II-29** (150.6 ppm) serving as additional indication of a stronger  $\pi$  back-donation in the former. It is also close to the value reported for compound **VI-5** (182.8 ppm).

With the reduced compound **VI-2** in hand, we decided to study its reactions with small molecules. To this end, a series of oxidative addition reactions were attempted. To our surprise, compound **VI-2** proved inactive upon addition of  $\text{PhSiH}_3$ , HBpin (pin = pinacolato), and  $\text{CH}_3\text{I}$ . Even more surprisingly, compound **VI-2** revealed remarkable stability towards oxygen both as solid and in solutions, suggesting that chemical robustness of **VI-2** was not provided by the bulkiness of the Ar groups at the flanking nitrogen atoms but by electronic factors. In line with this, there was no reaction observed between **VI-2** and water even upon heating to  $70^{\circ}\text{C}$  for one day.



**Scheme VI-4.** Stability of **VI-2** to water media.

The reactivity towards strong acids was studied then. An equimolar reaction between **VI-2** with HCl in dry Et<sub>2</sub>O/toluene mixture required a week to furnish the compound **VI-6** shown in Scheme IV-5, the product of formal 1,3 addition. Protonation of the usually electrophilic imine carbon instead of the reduced phosphorus centre or the basic imine group is quite remarkable and once again manifests the electron density transfer to the non-innocent dimph ligand. By using two equivalents of HCl, the reaction was complete after 2 days, likely because of homoconjugation of the incipient chloride anion in the form of [Cl-H-Cl]<sup>-</sup> prior to its transfer to the phosphorus atom. Increasing the acid content to three equivalents of HCl resulted in full conversion at room temperature in only 2 hours.

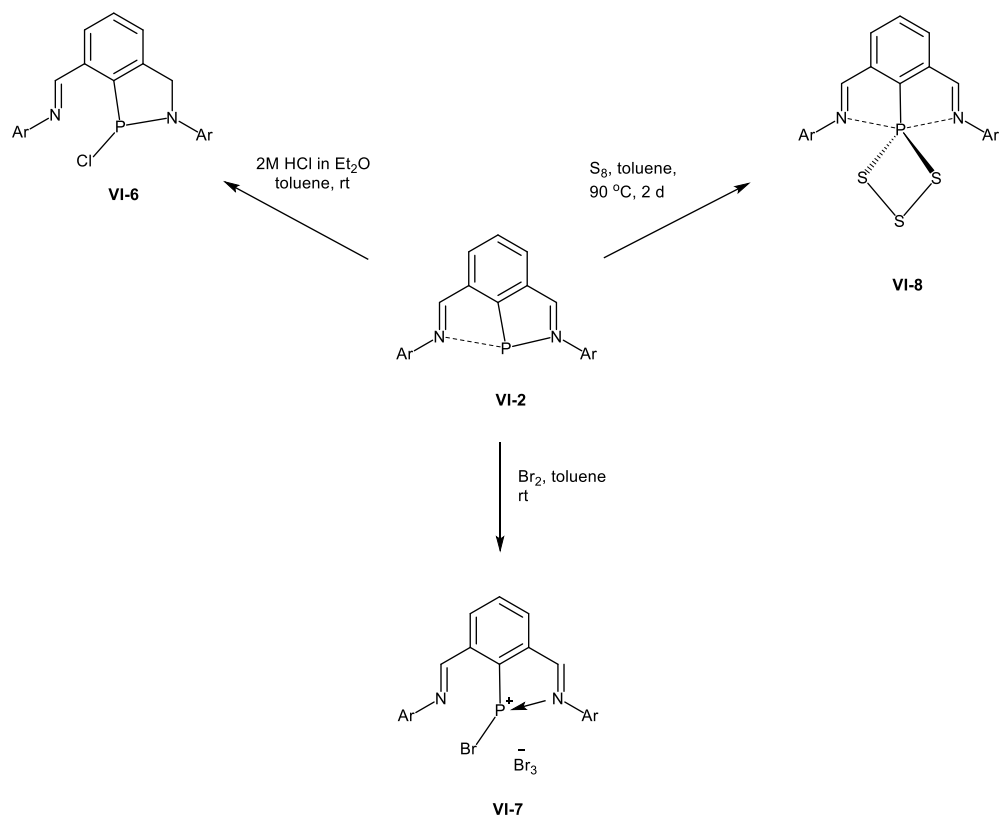
The compound **VI-6** was characterised by NMR spectroscopy. The unreacted aldimino group was evinced from a singlet at 8.23 ppm (1H), whereas the diastereotopic protons of the newly formed methylene group gave rise to two doublets of doublets at 4.09 and 4.97 ppm with  $J_{H-H} = 17.0$  Hz and  $J_{P-H} = 17.0$  Hz. The <sup>31</sup>P NMR spectrum displayed one singlet peak at 134.1 ppm.

Further attempts to oxidize **VI-2** with pyridine *N*-oxide failed, but a reaction with bromine led to the formation of a new product, which was insoluble in non-polar solvents, such as benzene and toluene. The chemical behaviour as well NMR features and elemental analysis prompts us to formulate this compound as the salt [dimph)PBr]<sup>+</sup>[Br<sub>3</sub>]<sup>-</sup> (**VI-7**). The

presence of [(dimph)PBr]<sup>+</sup> cation in **VI-7** was also supported by observation of the molecular peak in the ESI<sup>+</sup> mass-spectrum. In particular, the <sup>31</sup>P NMR signal of **VI-7** is very different from that of intermediate **VI-1**, 67.3 and 100.7 ppm, respectively. Attempts to crystallise this compound were unsuccessful.

Treatment of **VI-2** with sulfur powder under heating at 90°C in the course of two days gave a red precipitate, which was sparingly soluble in aromatic solvents and diethyl ether but moderately soluble in THF. <sup>1</sup>H NMR spectrum in the latter media revealed a C<sub>2v</sub> symmetric structure with one doublet peak at 1.20 ppm for the methyls of the <sup>i</sup>Pr group, one septet at 3.23 ppm for the methine proton, and the aldimine peak at 8.95 ppm, which comes as a doublet (*J*<sub>H-P</sub> = 1.7 Hz) due to coupling with phosphorus. Elemental analysis and MS data suggested the presence of three equivalent of sulfur per the dimph ligand. Taken together, these observations can be tentatively rationalised in terms of formation of polysulfide **VI-8** shown in Scheme VI-5. Unfortunately, multiple attempts at crystallising this compound failed because of the limited solubility of such species in most common organic solvents.

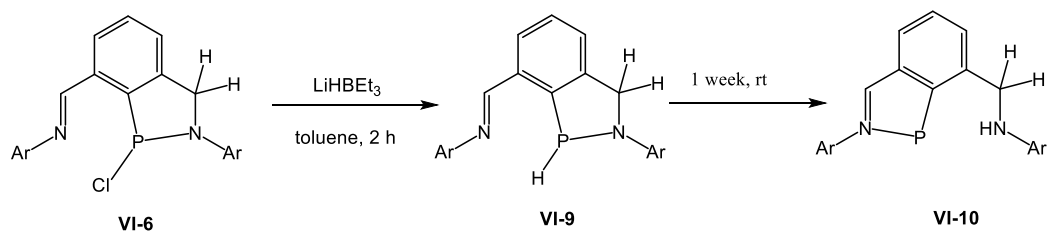




**Scheme VI-5.** Reactivity of compound **VI-2**

Puzzled by the chemical inertness of phosphinidene **VI-2** and by the serendipitous formation of chlorophosphine **VI-6**, we decided to study the reactivity of the latter. Addition of  $\text{KO}^t\text{Bu}$  to **VI-6** results in dehydrochlorination and regeneration of **VI-2** instead of the expected chloride substitution at phosphorus (Scheme VI-7). Noteworthy, in this reaction the proton is removed from the aminomethylene moiety, which is usually only weakly CH acidic. Reaction of **VI-6** with Superhydride ( $\text{LiHBEt}_3$ ) at ambient temperature led to chloride substitution and formation of phosphine **VI-9** in high yield (89%). In the  $^{31}\text{P}$  NMR spectrum taken in  $\text{C}_6\text{D}_6$ , the compound **VI-9** exhibits a resonance as a doublet of doublet at  $\delta = 19.9$  ppm with a large coupling  $^1J_{\text{P-H}} = 164.2$  Hz, indicating the presence of direct P–H bond as well as a weaker coupling to one of the methylene protons with  $J_{\text{P-H}} = 8.9$  Hz.

Compound **VI-9** is unstable in solution and in the course of one week transforms into a new species **VI-10**. The identity of the latter was established by  $^1\text{H}$ , COSY, and  $^1\text{H}$ - $^{13}\text{C}$  HSQC NMR experiments that showed the disappearance of the P-H peak in the  $^1\text{H}$  NMR spectrum and formation of a new peak at 3.56 ppm assigned to the N-H unit, based on the absence of correlation in the  $^1\text{H}$ - $^{13}\text{C}$  and  $^1\text{H}$ - $^{31}\text{P}$  HSQC spectra but observation of coupling to the  $\text{CH}_2\text{N}$  unit. Overall, this process can be classified as reductive N-H elimination from a P(III) centre to generate an imino-stabilised phosphinidene (or azaphosphole) via recoordination (or reoxidation) on the opposite side. The build-up of the aromatic character of the five-membered ring (CCCPN) is considered as a major driving force for such a reaction. Crystals of **V-10** suitable for single X-ray diffraction analysis were grown from a toluene solution at  $-30^\circ\text{C}$ . The molecular structure of **VI-10** is shown in Figure VI-2. The N-P distance of 1.729(5) Å is longer than in phosphinidene **VI-2** but still within the range of single N-P bonds.<sup>[222]</sup> The C=N bond is elongated to 1.359(6) Å which is close to the value observed in related P(I) compound **II-29** (1.350(4) Å). This fact and the short C(6)-C(7) bond to the phenyl ring (1.407(5) Å) shows enhanced charge delocalization from phosphorus on the single aldimine group. In contrast, the hydrogenated aldimine part is characterised by a single C(8)-N(1) bond of 1.472(6) Å and single C(2)-C(8) bond of 1.493(5) Å. IR spectrum of **VI-10** shows a band at  $3395\text{ cm}^{-1}$  assigned to the N-H stretch, supported the conclusion from NMR and X-ray data.



**Scheme VI-6.** Reactivity of chlorophosphine **VI-6**

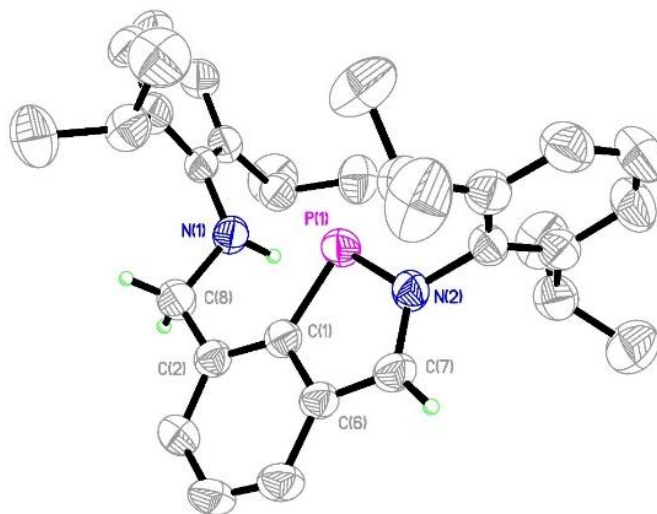


**Figure VI-2.** Molecular structure of compound **VI-10**. Thermal ellipsoids are shown at the 30% probability level. Hydrogen atoms, except the protons on amine, N=CH and in the NCH<sub>2</sub> moieties, are omitted for clarity.

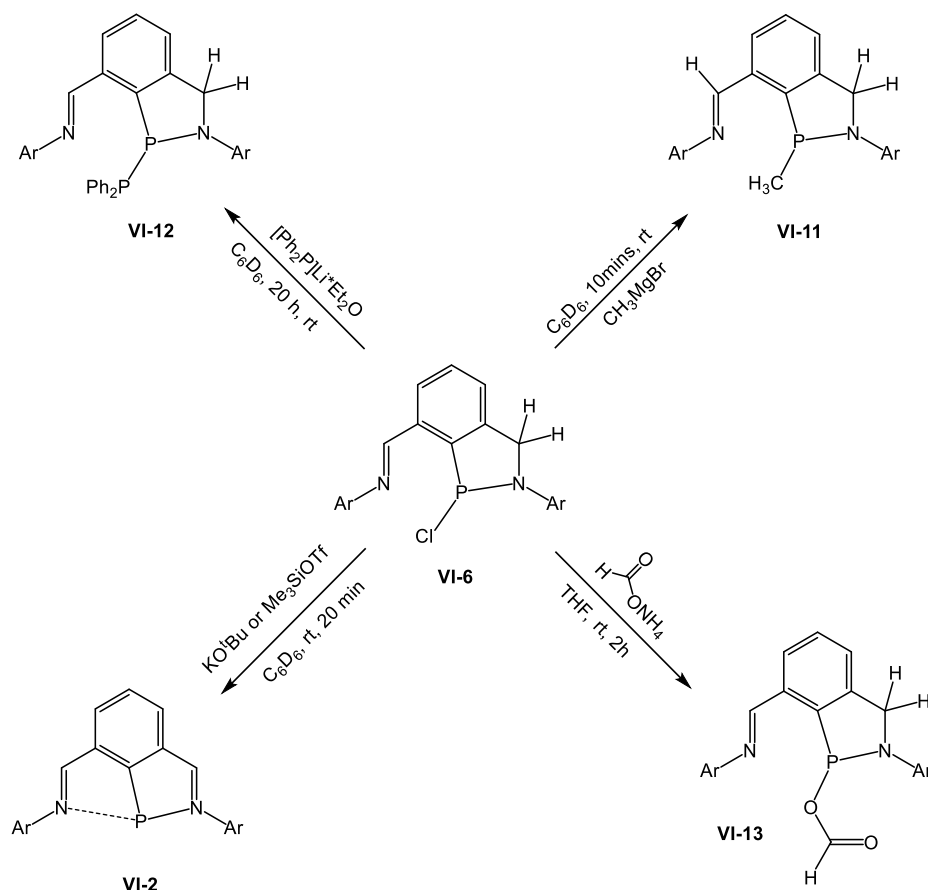
**Table VI-2.** Selected bond lengths and angles for compound **VI-10**

Lengths, Å		Angles, °			
N2-P1	1.729(5)	C8-N1	1.472(6) Å	C1-P1-N2	89.9(2)
C7-N1	1.359(6)	C2-C8	1.493(5) Å		
C6-C7	1.407(5)				

Reaction of compound **VI-6** with the Grignard reagent  $\text{CH}_3\text{MgBr}$  (3M in  $\text{Et}_2\text{O}$ ) in benzene results in chloride substitution to give the methyl derivative **VI-11**. Cain et al. have recently reported a similar Ph-for-Cl metathesis for an analogous oxazoline substituted species.<sup>[223]</sup> Compound **VI-11** was isolated by filtration, removal of volatiles and washing the crude product by hexane. The  $^{31}\text{P}\{^1\text{H}\}$  NMR spectrum of **VI-11** shows a single peak at 61.0 ppm. The coordination of the methyl group to the phosphorus centre was confirmed by the observation of a resonance at 1.50 ppm in the  $^1\text{H}$  NMR spectrum, which integrates as three protons and appears as a doublet as a result of  $^1\text{H}$ - $^{31}\text{P}$  coupling with  $^2J_{\text{P-H}} = 5.0$  Hz (confirmed by an  $^1\text{H}\{^{31}\text{P}\}$  experiment). Analogous reaction between **VI-6** with  $\text{Ph}_2\text{PLi}^*\text{OEt}_2$  led to diphosphine **VI-12** which was characterised by NMR spectroscopy. The formation of the P-P bond was asserted by  $^{31}\text{P}\{^1\text{H}\}$  NMR that showed two distinct doublets with a large coupling constant  $^1J_{\text{P-P}} = 324.3$  Hz. Unfortunately, all attempts to obtain X-ray quality crystals of this compound failed. It is interesting that neither the methyl derivative **VI-11** nor the phosphinyl-substituted compound **VI-12** undergo reductive elimination of the X-N (X= C or P) bond from the central phosphorus atom akin to that observed for phosphine **VI-9**.

Attempted substitution of chloride for triflate via addition of electrophilic reagent  $\text{Me}_3\text{SiOTf}$  unexpectedly resulted in regeneration of compound **VI-2**. We believe that the triflate anion does not recombine with the cationic intermediate  $[(\text{NCHN})\text{P}]^+$  (NCHN stands for the monohydrogenated dimph ligand) but rather deprotonates the methylene unit. Under the aprotic, low polarity conditions triflate is a strong base, which correlates well with the need of excess strong acid, such as HCl, for the protonation of **VI-2** under these conditions (vide supra). Interestingly, treatment of **VI-6** with a stoichiometric amount of

ammonium formate in THF at room temperature results in the formation of formate-substituted compound **VI-13** in excellent yield (90%, Scheme VI-7). When this reaction was attempted in benzene, only traces of **VI-13** were formed due to the low solubility of the salt. The  $^1\text{H}$  NMR spectrum of **VI-13** in  $\text{C}_6\text{D}_6$  shows a resonance at 8.48 ppm assigned (on the basis of an HMBC experiment) to the formate ligand  $\text{O}_2\text{CH}$  and a resonance at 8.10 ppm due to the imine group. The identity of **VI-13** was unambiguously confirmed by X-ray crystallography, which revealed the coordination of the formate unit to phosphorus (Figure VI-3). Compound **VI-13** adapts a distorted trigonal pyramidal geometry around the phosphorus centre, with the bond angles  $\text{N1-P1-C1}$ ,  $\text{N1-P1-O1}$ ,  $\text{O1-P1-C1}$  being  $89.30(9)^\circ$ ,  $103.32(8)^\circ$ ,  $95.31(8)^\circ$ , respectively.



**Scheme VI-7.** Reactivity of chlorophosphine **VI-6**

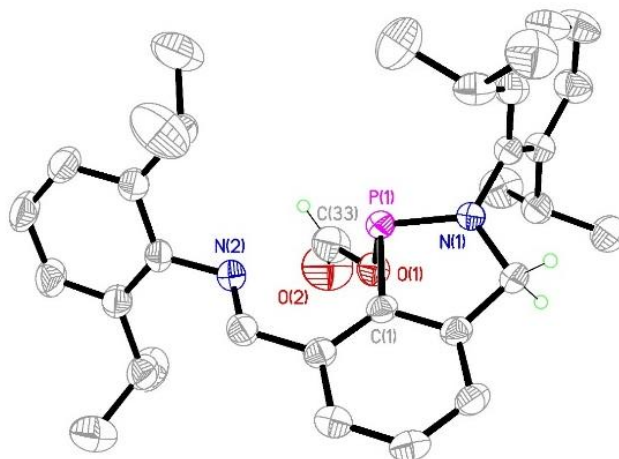


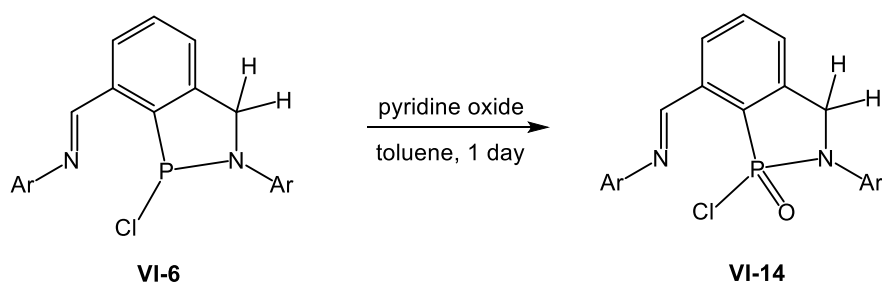
**Figure VI-3.** Molecular structure of compound **VI-13**. Thermal ellipsoids are shown at the 30% probability level. Hydrogen atoms, except the hydrogen atom in the formate and in the CH<sub>2</sub>N moiety, are omitted for clarity.

**Table VI-3.** Selected bond lengths and angles for compound **VI-13**

Lengths, Å				Angles, °	
P1-C1	1.817(2)	O1-C33	1.327(3)	N1-P1-C1	89.30(9)
P1-N1	1.664(16)	O2-C33	1.191(3)	N1-P1-O1	103.32(8)
P1-O1	1.731(15)			O1-P1-C1	95.31(8)

Unlike the parent phosphinidene **VI-2**, the chloride **VI-6** can be oxidised with pyridine oxide with the formation of the P(V) oxide **VI-14** (Scheme IV-8). The reaction was conducted at room temperature in toluene and monitored by NMR experiments until full conversion was reached. The <sup>31</sup>P NMR spectrum of **VI-14** shows a singlet peak at 29.1 ppm, which is in the typical range of phosphorus oxides, while the <sup>1</sup>H NMR exhibits a C<sub>1</sub> symmetric pattern consistent with the presence of a chiral phosphorus centre. X-ray quality crystals of **VI-14** were grown from a concentrated toluene solution at -30°C. The

molecular structure of **VI-14** is shown in Figure VI-4. The crystal was twinned which affected the accuracy of determining molecular metrics but the connectivity was established quite reliably. The phosphorus atom adapts the expected four-coordinate pseudo-tetrahedral geometry, with bond angles of C1-P1-O1, C1-P1-C11, C11-P1-O1 equal to 104.5(9)°, 110.7(3)°, 104.5(9)°, respectively. The P(1)-O(1) bond of 1.58(2) Å is slightly longer than the typical P=O double bond (1.50 Å), whereas the P(1)-N(1) bond of 1.630(10) Å is similar to the value reported for known cyclodiphosphazenes.<sup>[224]</sup> Attempts to dehydrochlorinate **VI-14** in a way similar to the transformation **VI-6**→**VI-2** by using strong bases, such as KO<sup>t</sup>Bu and LDA, resulted in mixtures of unknown composition.



**Scheme VI-8.** Oxidation of chloride **VI-6**

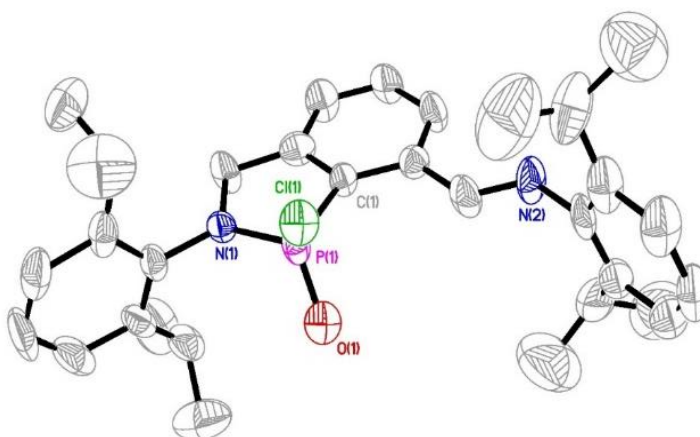


**Figure VI-4.** Molecular structure of compound **VI-14**. Thermal ellipsoids are shown at the 30% probability level. Hydrogen atoms are omitted for clarity.

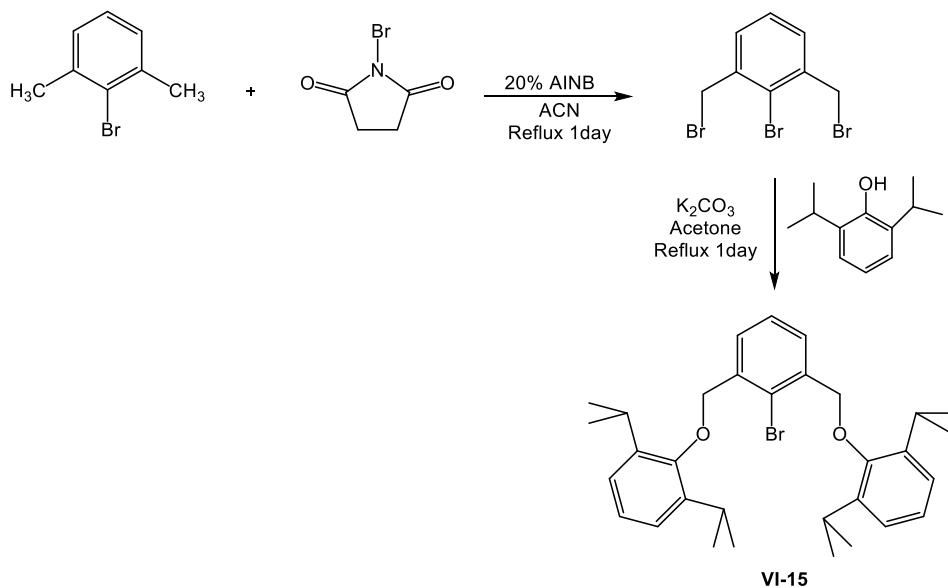
**Table VI-4.** Selected bond lengths and angles for compound **VI-14**

Lengths, Å		Angles, °			
P1-O1	1.58(2)	P1-C1	1.802(7)	C1-P1-O1	104.5(9)
P1-N1	1.630(10)			C1-P1-Cl1	110.7(3)
P1-Cl1	1.902(1)			Cl1-P1-O1	104.5(9)



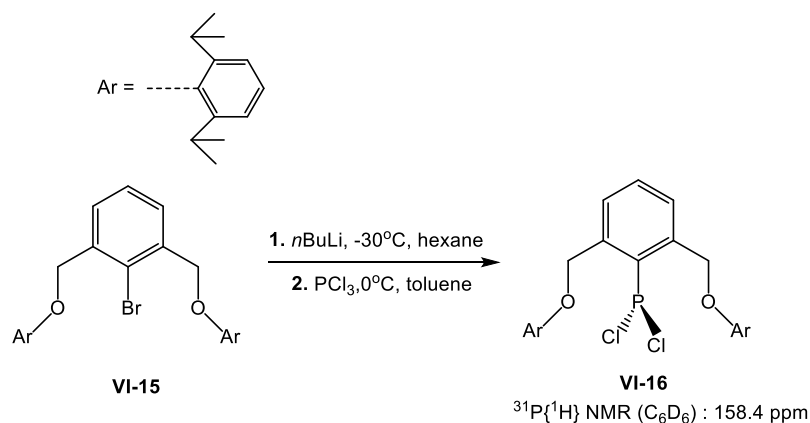
VI.2. Preparation, Characterization, and Reactivity of “Phosphinidene” Stabilised by 2,6-bis[(2,6-diisopropyl)phenoxy] Pincer Ligand.

While studying the structure and reactivity of compound **VI-2**, we realised that the strong  $\pi$ -accepting ability of the aldimine groups results in strong interaction between phosphorus and nitrogen atoms and strong charge transfer from the phosphinidene centre to the dimph ligand in **VI-2**. With the aim of preparing a more reactive phosphinidene-like compound, we attempted to synthesise a novel phosphorus (I) compound stabilised by the 2,6-bis[(2,6-diisopropyl)phenoxy] pincer (dioxyph) ligand **VI-15**. The target ligand **VI-15** can be prepared by a two-step procedure shown in Scheme VI-8. The first step involves the bromination of 2-bromo-*m*-xylene by N-bromosuccinimide with 20 mole % of azobis(isobutyronitrile) as catalyst, whereas the second step is the Williamson condensation with alcohol to give **VI-15** in high yield.



**Scheme VI-9.** The preparation of the pincer ligand **VI-15**

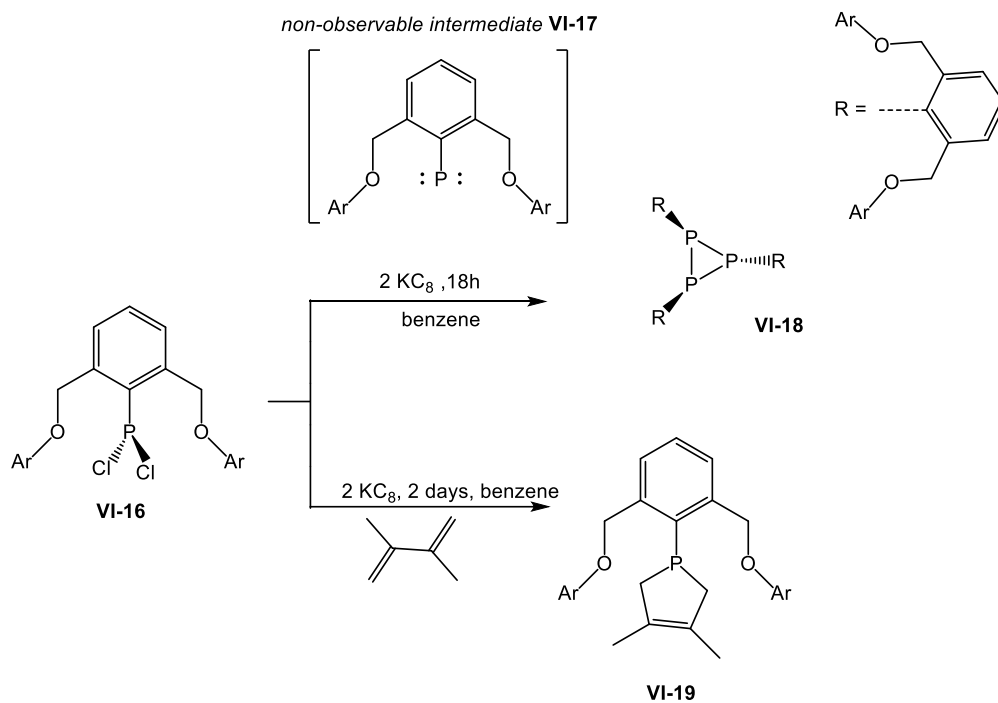
The phosphorus(III) compound **VI-16** was prepared by the following the procedure, first reported by the Jambor's group.<sup>[225]</sup> The lithiation of ligand **VI-15** by *n*BuLi in hexane at 0°C generates a white precipitate of the Li salt, which could react with PCl<sub>3</sub> in toluene to give the final product **VI-16**. Crystals of **VI-16** were grown from a hexane/toluene mixture at -30°C after one week. The <sup>1</sup>H NMR spectrum of **VI-16** showed a C<sub>2v</sub> symmetry, featuring a singlet at δ = 5.29 ppm for the OCH<sub>2</sub> groups, one septet at δ = 3.48 ppm for the methine groups, and one doublet for the <sup>i</sup>Pr groups with the 4 : 4 : 24 integral ratio. Interestingly, the <sup>31</sup>P{<sup>1</sup>H} spectrum of **VI-16** reveals a resonance at δ = 158.4 ppm which is close to the signal of the commercially available reagent PhPCl<sub>2</sub> (δ = 158.0 ppm). This result indicates that there is little or no interaction between the oxygen atoms and the phosphorus centre in **VI-16**. Jambor et al. also reported a similar compound LPCl<sub>2</sub> (L = 2,6-(MesOCH<sub>2</sub>)<sub>2</sub>C<sub>6</sub>H<sub>3</sub>, Mes = 2,4,6-Me<sub>3</sub>C<sub>6</sub>H<sub>2</sub>), which displayed a <sup>31</sup>P{<sup>1</sup>H} NMR signal at 157.9 ppm.<sup>[225]</sup> The similarity of <sup>31</sup>P{<sup>1</sup>H} NMR chemical shifts for these three compounds (158.4 ppm vs 158.0 ppm vs 159.7 ppm) indicates that the dioxyph moiety in **VI-16** does not act as a pincer ligand but as a sterically hindered ligand.



**Scheme VI-10.** The preparation of phosphorus dichloride **VI-16**.

As discussed above, the reduction of phosphorus (III) compound **VI-1** by  $\text{KC}_8$  affords the P(I) product **VI-2**. By applying this method, compound **VI-16** was reduced by  $\text{KC}_8$  in benzene. However, after 18 hours at room temperature the product was a cyclic three-membered compound **VI-18**, which can be rationalised as stemming from coupling of three phosphinidene units. Using magnesium instead of potassium graphite in the reduction of **VI-16** generated the same cyclic product.  $^1\text{H}$  NMR spectrum of **VI-16** revealed three set of signals corresponding to three [OCO] units, with two ligands being chemically equivalent. Furthermore, the  $^{31}\text{P}$  NMR spectrum showed one doublet at  $\delta = -114.6$  ppm and one triplet at  $\delta = -150.5$  ppm in the 2 : 1 ratio with a strong coupling constant  $J_{\text{P-P}} = 186$  Hz, indicating the presence of direct P-P bond.

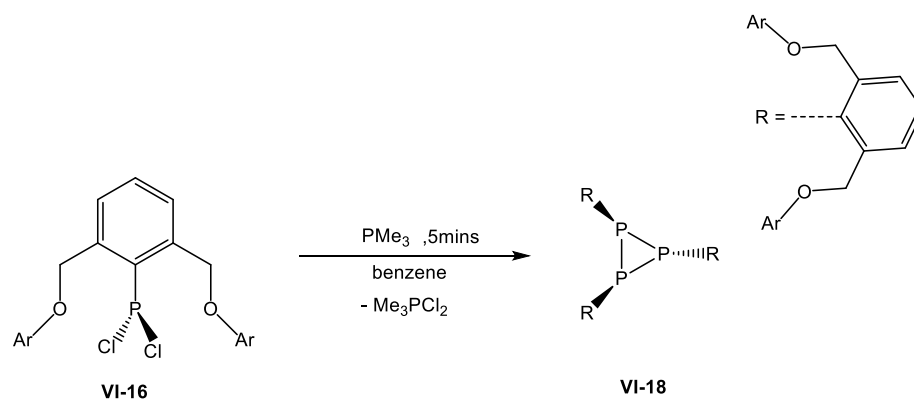
A simple explanation for the formation of compound **VI-18** is that it is formed via the cyclization of phosphinidene intermediate **VI-17**. To confirm the intermediacy of **VI-17** in the reaction, we conducted a trapping experiment: the reduction of **VI-16** by  $\text{KC}_8$  was carried in the presence of 2,3-dimethyl-1,3-butadiene, which furnished the cycloaddition product **VI-19**. The compound **VI-19** was characterised by NMR experiment that showed a  $\text{C}_{2v}$  symmetrical species in solution. The  $^{31}\text{P}\{^1\text{H}\}$  NMR signal was observed at  $\delta = 50.0$  ppm, whereas  $^1\text{H}$  NMR displayed one singlet peak at  $\delta = 5.29$  ppm for the  $-\text{CH}_2\text{O}-$  units, one septet peak at  $\delta = 3.54$  ppm for the methine groups, one doublet peak at  $\delta = 1.23$  ppm for  $^i\text{Pr}$  groups. For the butadiene moiety, we observed one singlet peak at  $\delta = 1.32$  ppm for  $\text{CH}_3$  and one peak at  $\delta = 2.70$  ppm for the  $\text{CH}=\text{CH}$  moiety.



**Scheme VI-11.** The reduction of phosphorus dichloride complex **VI-16**

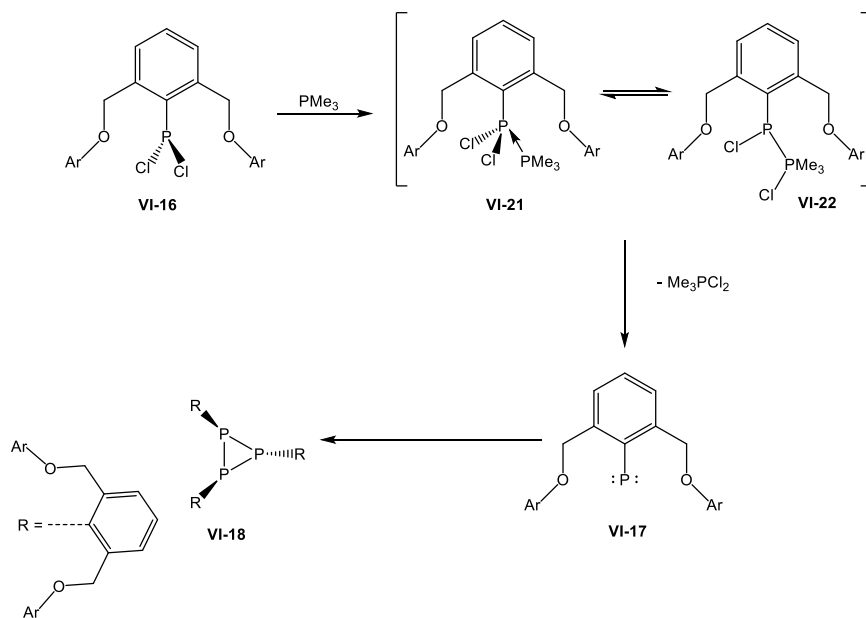
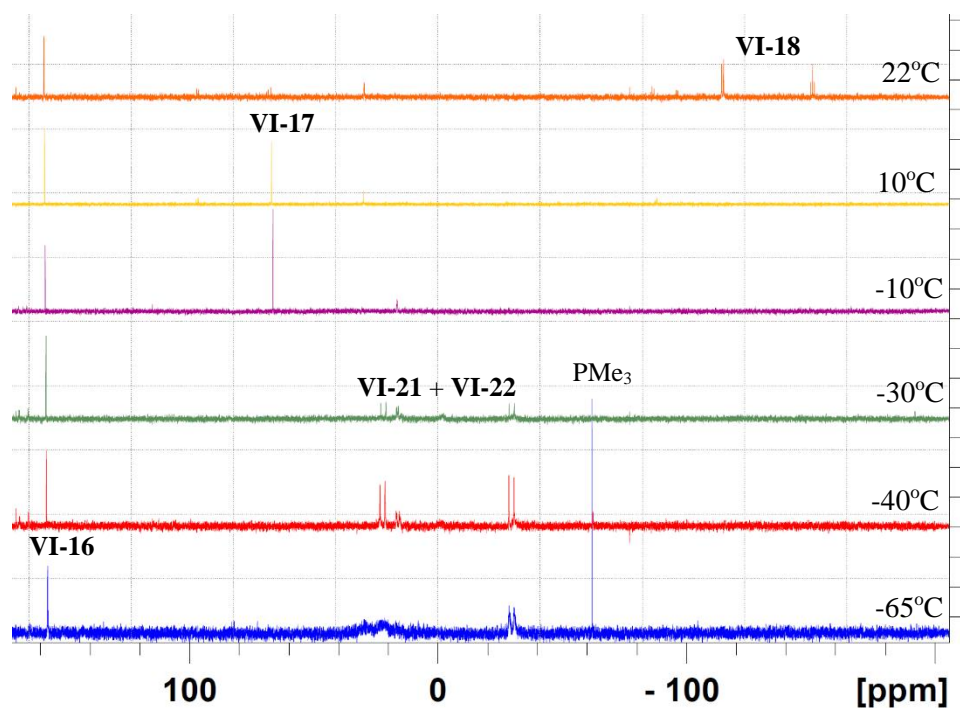
Addition of  $\text{PMe}_3$  into a benzene solution of **VI-16** provided the same product **VI-18**. The reaction occurred very fast (in 5 minutes) at room temperature with the formation of a white precipitate, presumably of  $[\text{Me}_3\text{PCl}]^+\text{Cl}^-$ . The  $^{31}\text{P}\{^1\text{H}\}$  NMR spectrum of this precipitate in DMSO showed a singlet at  $\delta = 61.7$  ppm assigned to  $[\text{Me}_3\text{PCl}]^+\text{Cl}^-$  precipitate. The ability of  $\text{PMe}_3$  to effect the dechlorination was also discussed by Protasiewicz et al. who showed the existence of an equilibrium in the chlorine atom exchange reaction involving the Wittig reagents  $\text{ArP}=\text{PR}_3$  ( $\text{ArP}=\text{PMe}_3 + \text{Ar}'\text{PCl}_2 \leftrightarrow \text{Ar}'\text{P}=\text{PMe}_3 + \text{ArPCl}_2$  (**eq 1**)).<sup>[226]</sup> Similarly, Sisler and co-workers previously reported the ability of tri-*n*-butylphosphine  $(\text{C}_4\text{H}_9)_3\text{P}$  to extract chlorine atoms from chlorides of trivalent phosphorus compound.<sup>[227]</sup> In particular, the reaction of phenyldichlorophosphine  $\text{C}_6\text{H}_5\text{PCl}_2$  with  $(\text{C}_4\text{H}_9)_3\text{P}$  resulted in the formation of  $(\text{C}_4\text{H}_9)_3\text{PCl}_2$  and a four-membered ring  $(\text{C}_6\text{H}_5\text{P})_4$ .

Next, we were curious about the role of the [OCO] ligand in **VI-16** for the success of reduction. Thus, we conducted an analogous reaction with PhPCl<sub>2</sub>. Like in the case of **VI-16**, the treatment of PhPCl<sub>2</sub> with PMe<sub>3</sub> gave a white precipitate after 5 mins. However, whereas the reaction proceeds rapidly, the <sup>31</sup>P{<sup>1</sup>H} NMR spectrum in DMSO showed a singlet at 30.0 ppm. No <sup>31</sup>P{<sup>1</sup>H} NMR signals of a cyclic product were observed, indicating that the bulky ligand might be indeed required to promote the reduction. Further, we also wanted to confirm the intermediacy of **VI-17** in such a reaction. Thus, the reduction of **VI-16** by PMe<sub>3</sub> was conducted in the presence of a trapping reagent 2,3-dimethyl-1,3-butadiene. However, there was no cycloaddition product regenerated as observed in the reduction by KC<sub>8</sub>. Such a difference between two routes can be rationalised in the following way: the reduction by PMe<sub>3</sub> occurs much faster than by KC<sub>8</sub>, so that there is a significant concentration of **VI-17** favouring the coupling of phosphinidene fragments. We reckon, albeit we have no experimental verification for this, that the rate of cyclization with butadiene is significantly slower than P-P coupling. In contrast, the reduction by KC<sub>8</sub> is slow, so that the coupling process is retarded by the low concentration of **VI-17** and the overall rate of cyclization with butadiene becomes faster than coupling.



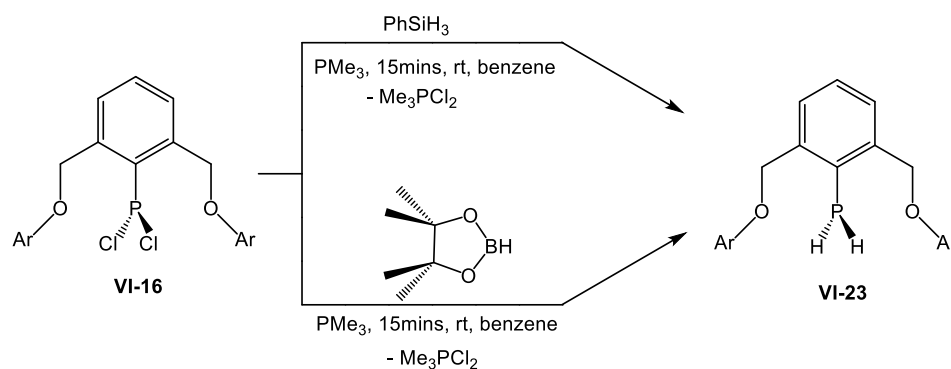
**Scheme VI-12.** The second path to cyclic product **VI-18**.

To understand the mechanism of the reduction by phosphine,  $\text{PMe}_3$  was added into an NMR tube containing solution of **VI-16** in toluene- $d_8$  cooled to  $-70^\circ\text{C}$ . Monitoring the reaction by VT- $^{31}\text{P}\{^1\text{H}\}$  NMR led to the observation of a reaction at  $-65^\circ\text{C}$  resulting in the appearance of two doublets at  $-28.5$  ppm and  $29.1$  ppm with a large coupling constant  $J_{\text{P-P}} = 474$  Hz, indicating a direct P-P bond. We tentatively assign this species the structure of Lewis acid-base adduct  $(\text{OCO})\text{Cl}_2\text{P}\leftarrow\text{PMe}_3$ . The reaction mixture was allowed to warm up slowly inside the NMR probe, which revealed two additional broad peaks at  $-2.0$  ppm and  $16.6$  ppm at  $-40^\circ\text{C}$ . These signals can be assigned to two P centres of the putative species  $(\text{OCO})\text{ClP-P}(\text{Cl})\text{Me}_3$ . Heating the reaction mixture up to  $-10^\circ\text{C}$  resulted in the disappearance of these four NMR peaks for two first products **VII-21** and **VII-22** and the build-up of a new singlet peak at  $67.1$  ppm. Such a signal was persistent upon heating the solution to  $10^\circ\text{C}$  and disappeared only when the solution reached the ambient temperature. Finally, at room temperature we observed signals corresponding to the cyclic three-membered compound **VI-18**. Taken together, these observations suggest that the reduction begins with the coordination of  $\text{PMe}_3$  to the P(III) centre of the precursor **VI-16**, affording the intermediate **VI-21**, which can be considered as a Lewis acid-base adduct. The next step involves chloride migration to  $\text{PMe}_3$  at  $-40^\circ\text{C}$  to give a phosphinyl phosphorane **VI-22**, which is in equilibrium with **VI-21**. The dissociation of  $\text{Me}_3\text{PCl}_2$  from **VI-22** proceeds by formal reductive elimination of the P-Cl bond from phosphorus and results in the formation of phosphindiene **VI-17**, which at room temperature undergoes cyclization to provide the final product **VI-18**.



**Scheme VI-13.**  $^{31}\text{P}\{^1\text{H}\}$  VT-NMR experiment (top) and possible mechanism of the reduction of **VI-16** by  $\text{PMe}_3$  (bottom).

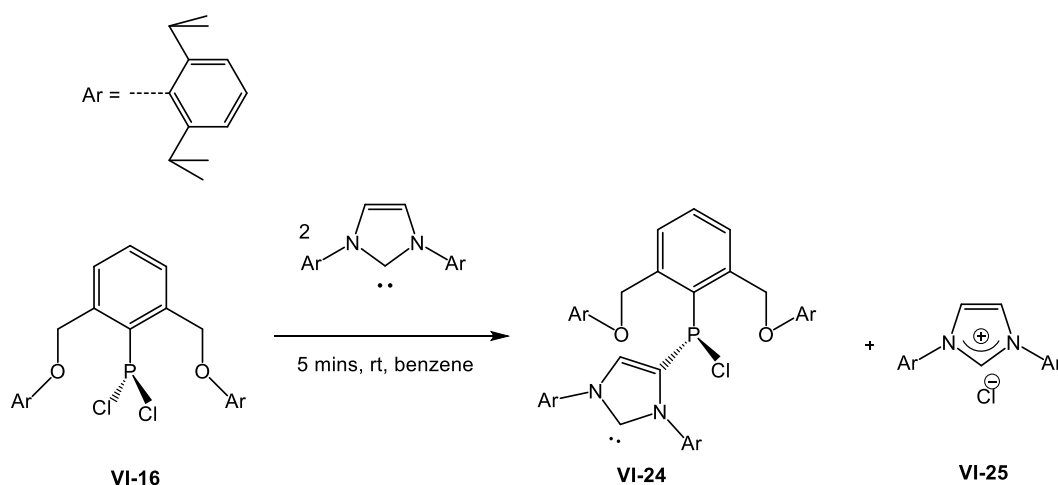
VT-NMR experiments described above suggest that the phosphinidene **VI-17** can be formed as an intermediate in the reduction of **VI-16** by  $\text{PMe}_3$ . We then turned our attention to study the reactivity of **VI-17** toward small molecules, such as silane, borane etc. The addition of  $\text{PMe}_3$  to a mixture of **VI-16** and  $\text{PhSiH}_3$  resulted in the formation of a novel phosphine **VI-23** after 15 minutes at room temperature. Compound **VI-23** was characterised by NMR spectroscopy, which showed a triplet peak at  $\delta = -162.0$  ppm in the proton-coupled  $^{31}\text{P}$  NMR spectrum, with a large coupling constant  $^1J_{\text{P-H}} = 205$  Hz indicating formation of  $\text{Ar-PH}_2$ .  $^1\text{H}$  NMR experiment revealed the  $\text{C}_{2v}$  symmetry of **VI-23** in the solution with one singlet peak at  $\delta = 4.96$  ppm for  $(-\text{CH}_2\text{O}-)$ , one septet peak at  $\delta = 3.49$  ppm for the methine groups, one doublet peak at  $\delta = 1.23$  ppm for the  $^i\text{Pr}$  groups, and a doublet at  $\delta = 3.50$  ppm for the  $\text{PH}_2$  unit. The combination of 1D and 2D NMR characterization indicated that  $\text{PhSiHCl}_2$  was generated as by-product in such reaction. The reaction was repeated by using 20% mole of  $\text{PMe}_3$ , resulting in the formation of **VI-23** after 1 day at room temperature. Interestingly, the same product **VI-23** was observed in an analogous reaction with HBpin. The mechanism of such reactions is still not clear at this point.



**Scheme VI-14** The reactivity of **VI-16**.



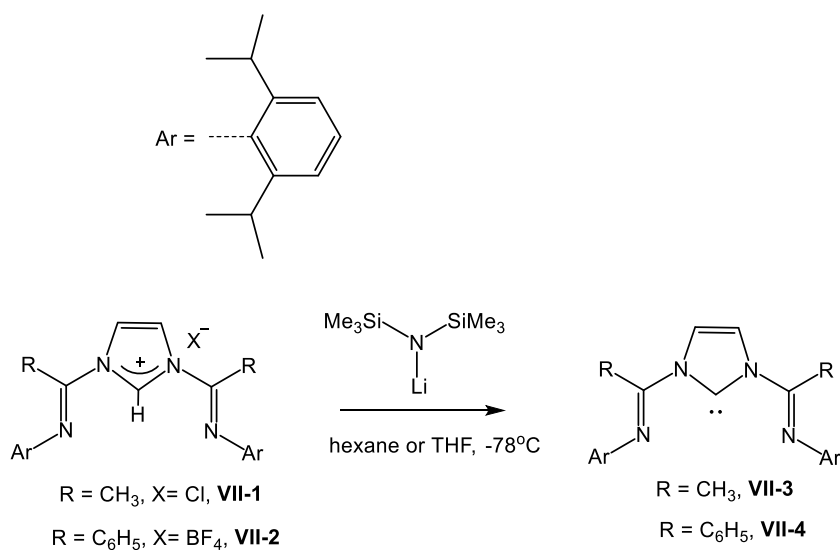
By applying Arduengo's protocol,<sup>[112]</sup> which prepared  $^{\text{Mes}}\text{NHC}=\text{PR}$  adducts ( $^{\text{Mes}}\text{NHC} = 1,3\text{-dimesitylimidazolin-2-ylidene}$ ) from  $^{\text{Mes}}\text{NHC}$  carbene and dichlorophosphines, we conducted the reaction of **VI-16** with 2 equivalents of  $^{\text{Dipp}}\text{NHC}$  carbene. The reaction resulted in the formation of unexpected product **VI-24** after 10 minutes at room temperature. The precipitate of the chloroimidazolium salt **VI-25** also formed and was easily filtered off from the solution. The  $^{31}\text{P}\{^1\text{H}\}$  NMR spectrum of **VI-24** displays only one single peak at  $\delta = 51.9$  ppm, which is upfield shifted relative to the putative phosphinidene **VI-17** (67.1 ppm). The structure of **VI-24** was confirmed by a combination of NMR spectra, X-ray diffraction. At the moment, the mechanism of this reaction remains unclear.



**Scheme VI-15.** The reactivity of **VI-16** toward NHC carbene.

## VII. Synthesis, Characterization, and Reactivity of Germanium Complexes in Low Oxidation State

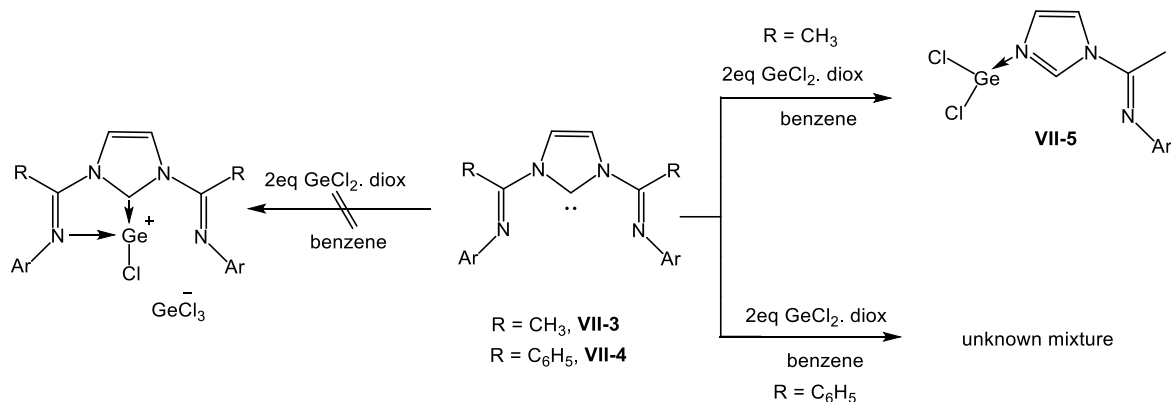
Our group has previously reported the formation of a germanium(0) complex stabilised by the dimpyr (bis(imino) pyridine) ligand.<sup>[53]</sup> Given this precedent and the work on reduced phosphorus compound stabilised by the dimph pincer described above, we became interested in the application of bis(imino) *N*-heterocyclic pincer pincers (dimNHC), isolobal with dimpyr and dimph, to the stabilization of Ge(0). Free ligands **VII-3** and **VII-4** were obtained via protonation of the corresponding imidazolium salts **VII-1** and **VII-2** by a silazide base at low temperature (Scheme VII-1). Thus, the reaction of 1,3-bis[1-(2,6-dimethylphenylimino)ethyl]imidazolium chloride with LiHMDS in hexane at -78°C afforded **VII-3**. However, the analogous reaction of 1,3-bis[(2,6-dimethylphenylimino)benzyl]imidazolium tetrafluoroborate with LiHMDS gave the target product **VII-4** in only very low yield (10%) presumably due to the low solubility of the imidazolium salt in hexane. Alternatively, changing the reaction media to THF improved the outcome of the reaction to 70% yield. NMR characterization of these products revealed different geometries for **VII-3** and **VII-4**. This, the <sup>1</sup>H NMR spectrum of **VII-3** shows the presence of a *C*<sub>2v</sub> compound displaying a singlet backbone (-NHC=CHN-) resonance at  $\delta$  = 8.06 ppm, while the spectrum of **VII-4** had two respective singlets, at 7.56 ppm and 7.26 ppm. The observed asymmetry of **VII-4** is likely brought about by conformational effects caused by the sterically congested ligand framework.



**Scheme VII-1.** Preparation free diimino carbene ligand <sup>Me</sup>dimNHC (**VII-3**) and <sup>Ph</sup>dimNHC (**VII-4**).

We attempted to synthesize the carbene supported germanium cations by adapting a procedure previously used for the dimpyr ligand.<sup>[66,175]</sup> Thus, when dimpyr reacted with two equivalents of  $\text{GeCl}_2 \cdot \text{dioxane}$  in aromatic solvents, the precipitate of cationic dimpyr compound  $[(\text{dimpyr})\text{Ge}][\text{GeCl}_3]$  formed. To this end, **VII-3** and **VII-4** was reacted with  $\text{GeCl}_2 \cdot \text{dioxane}$  in benzene. However, for the methyl-substituents precursor **VI-3** we observed the unexpected formation of deiminated compound **VII-5**. The  $^1\text{H}$  NMR spectrum of **VII-5** shows a downfield imidazole proton resonance at  $\delta = 8.07$  ppm and two distinguished singlet peaks for the backbone  $-\text{NHC}=\text{CHN}-$ protons, at 7.08 ppm and 7.13 ppm. The structure of **VII-5** was also confirmed by X-ray crystallography which confirmed that one iminyl moiety from replaced in the dimNHC ligand frame by coordinated  $\text{GeCl}_2$ . The Ge atom adapted a pyramidal geometry formed as a result of imidazole nitrogen donating lone pair to the empty 4p orbital of  $\text{GeCl}_2$ . The analogous reaction of **VII-4** with

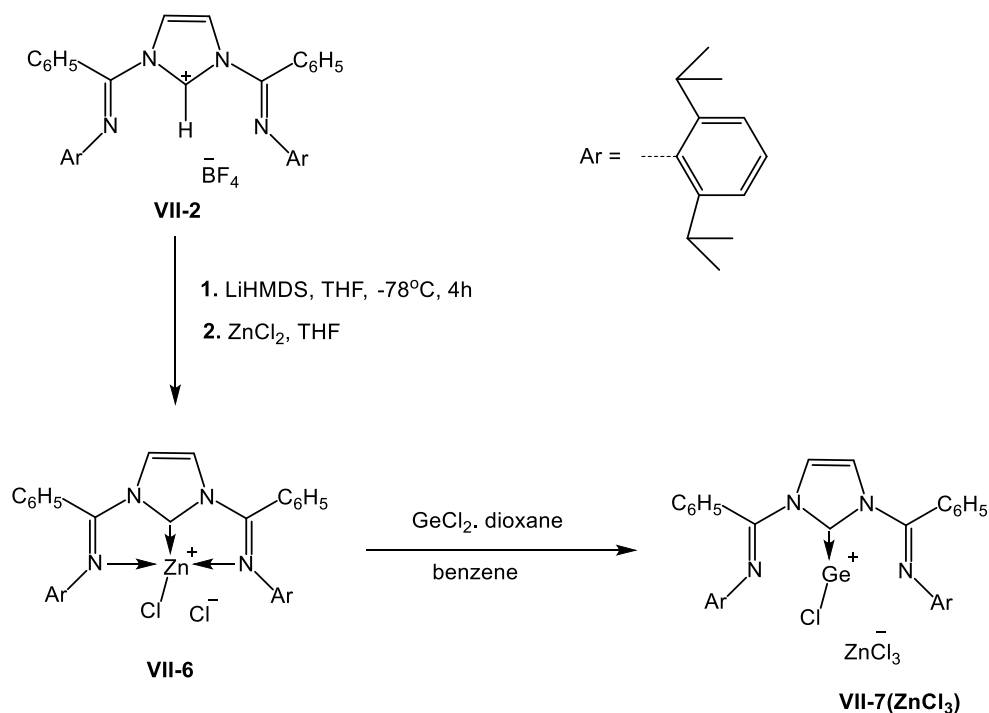
GeCl<sub>2</sub>\*dioxane in either benzene or DCM resulted in a mixture of an unknown composition.



**Scheme VII-2.** Attempts in preparation of germanium cation from dimNHC carbene ligands.

Many attempts to synthesize the target germanium cations by reacting GeCl<sub>2</sub> with *in-situ* deprotonated imidazolium salts also failed. Alternatively, a novel approach to the cation **VII-7**(ZnCl<sub>3</sub>) was found by using transmetalation from a novel zinc complex **VII-6**, which can be obtained by the treatment of imidazolium salt **VI-2** with lithium bis(trimethylsilyl)amide (LiHMDS) at -78°C, followed by addition of ZnCl<sub>2</sub> at the same temperature. The <sup>1</sup>H NMR spectrum of **VII-6** showed a C<sub>2v</sub> symmetrical species in solution, without an imidazolium proton signal. The signal at δ = 7.82 ppm was assigned for two equivalent backbone protons of the carbene (NCH=CHN). Two doublets at δ = 0.91 and 1.22 ppm were assigned to two <sup>i</sup>Pr groups, whereas a septet at δ = 3.04 ppm was assigned to four equivalent methine protons. The <sup>13</sup>C resonance of the carbene central carbon was observed at δ = 180.8 ppm, which is a higher field than the typical value for an NHC ligand.

To our delight, the treatment of  $\text{GeCl}_2 \cdot \text{dioxane}$  with a stoichiometric amount of the zinc compound **VII-6** in benzene afforded the desired germanium cation **VII-7**( $\text{ZnCl}_3$ ) via transmetalation. A yellow precipitate was formed after 1 hour at room temperature, which was filtered and washed by hexane to give a pure yellow solid of **VII-7**( $\text{ZnCl}_3$ ) in high yield. Crystals of **VII-7**( $\text{ZnCl}_3$ ) suitable for X-ray were grown from a concentrated acetonitrile solution at room temperature. The  $^1\text{H}$  NMR chemical shift of the backbone protons in **VII-7**( $\text{ZnCl}_3$ ) at  $\delta = 7.76$  ppm is in a slightly higher field than the corresponding signal of the zinc compound precursor **VII-6** ( $\delta = 7.82$  ppm). The  $^{13}\text{C}$  chemicals of the central carbene carbon also moved slightly upfield compared to **VII-6** (178.2 ppm vs. 180.8 ppm). Two septets at  $\delta = 2.94$  and 3.30 ppm were assigned to the methine protons of the isopropyl group, while the corresponding methyl protons appeared as three doublets integrated as 6: 6: 12.



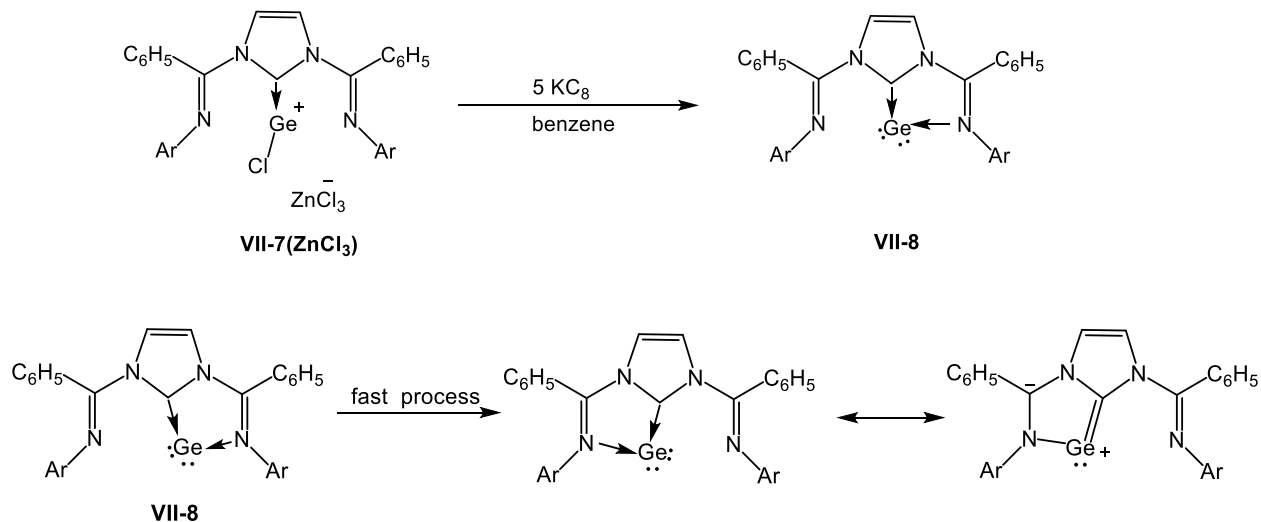
**Scheme VII-3.** A novel approach to germanium cation **VII-7**( $\text{ZnCl}_3$ )

In order to prepare the desired germylone, we conducted the reduction of compound **VII-7(ZnCl<sub>3</sub>)** by potassium graphite in benzene which afforded the dark red compound **VII-8**. The compound **VII-8** is extremely air and moisture sensitive. Its structure was confirmed by a combination of NMR spectra, X-ray diffraction, and elemental analysis. The NMR data of **VII-8** establish  $C_{2v}$  symmetric averaged geometry in solution. In the <sup>1</sup>H NMR spectrum, the <sup>i</sup>Pr methyl peaks appear as doublets at  $\delta = 1.01$  and  $1.40$  ppm while the methine signal comes as a septet at  $\delta = 3.21$  ppm, indicating the equivalent environment of the <sup>i</sup>Pr groups of the dimNHC ligand in this species. The olefine backbone protons were observed as a singlet at  $\delta = 6.84$  ppm, which is in a much higher field than the that of the germanium cation **VII-7(ZnCl<sub>3</sub>)** ( $7.76$  ppm). Likewise, the <sup>13</sup>C NMR spectrum of **VII-8** displayed a peak at  $176.1$  ppm for the central carbene carbon, which is slightly upfield in comparison to that of the precursor **VII-7(ZnCl<sub>3</sub>)** ( $178.2$  ppm). The NMR spectra of **VII-8** in toluene-d<sub>8</sub> in the temperature range  $-70 - +25^{\circ}\text{C}$  show consistently the averaged  $C_{2v}$  symmetry.

Crystals of **VII-8**, suitable for X-ray diffraction analysis, formed from a benzene solution at room temperature. The Ge atoms is two-coordinated, by the carbene and the imine nitrogen, forming the C1-Ge1-N3 angle of  $78.2^{\circ}$ . This angle is more acute than the corresponding angles reported by Kinjo et al. for carbene/imine-stabilised germylone **IV-29** ( $80.59(6)^{\circ}$ ).<sup>[179]</sup> Like in germylone dimpyrGe, the germanium position is disordered. In the main component, Ge is located much closer to one imine nitrogen atom (N3) than the other,  $2.004(1)$  vs  $2.908(1)$  Å. This Ge(1)-N(3) distance is slighter shorter than the dative bond  $\text{N} \rightarrow \text{Ge}$  ( $2.2722(15)$  Å and  $2.2746(15)$  in the related Stalke's compound dimphGeH (**II-7**),<sup>[31]</sup> despite the fact that the former is Ge(0) and is expected to be larger than the

Ge(II) atom of **II-7**. The Ge(1)-N(3) distance in **VII-8** is even shorter than the Ge-N bond in the dimpyrGe, 2.047(7) Å (where the other Ge-N distance is 2.306(7) Å). This asymmetric disposition of the germanium atom contradicts the observations made from NMR studies in solution that the average  $C_{2v}$  structure is persistent down to -60 °C. Taken together, these solution and solid state data suggest that the structure is fluxional and that the exchange takes place with a very low barrier. The situation is thus reminiscent of what was found for dimpyrGe and what we observed for the isoelectronic dimph phosphorus compound **VI-3**. Moreover, the Ge-C1 bond length of 1.881(1) Å is close to that of compound **IV-29** (1.8870(15) Å) reported by Kinjo et al.<sup>[179]</sup> and falls in between typical Ge-C bonds (1.9 - 2.0 Å) and Ge=C bonds (1.71- 1.81 Å).<sup>[145,228]</sup> However, it is comparable to the Ge-N distance in dimpyrGe (1.899(2) Å), and is even slightly longer, despite the fact that the atomic radius of carbon is larger than that of nitrogen. It thus becomes evident that the germanium atom interacts with the dimNHC ligand stronger than with related dimpyr. The asymmetric coordination of germanium is also manifested in the two very different C=N imino bonds. The imine, which coordinates to germanium, has a noticeably longer bond of 1.342(2) vs the normal 1.285(2) Å for the “free” imine, as a result back-donation from germanium to the former imine unit. For comparison, in dimpyrGe, C=N distances were 1.320(2) Å. However, the latter value was an average of two bonds, C=N and C-N, because of a crystallographic disorder. Therefore, the fact that in **VII-8** the C=N bond is only slightly longer, suggests a decreased extent of backdonation to the imine group. To verify that, the IR spectrum of **VII-8** displays a C=N imine stretch at 1562  $\text{cm}^{-1}$  which is red-shifted relative to the germanium cation **VII-7(ZnCl<sub>3</sub>)** (1643  $\text{cm}^{-1}$ ), suggesting a decrease in the C=N bond order in **VII-8**. Finally, the sum of the bond angles around the

carbene carbon atom is  $359.8^\circ$  while the five membered  $C_2N_2Ge$  ring is nearly planar, with the sum of internal pentagon angles of  $539.6^\circ$ .



**Scheme VII-4.** The synthesis to germylone **VII-8**, its fluxionary, and description in terms of resonance.

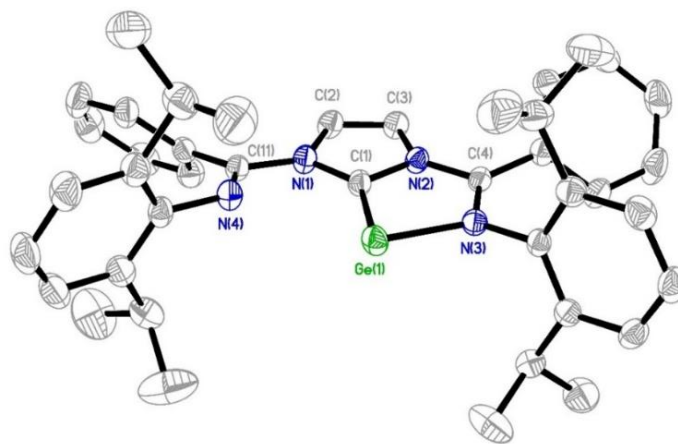


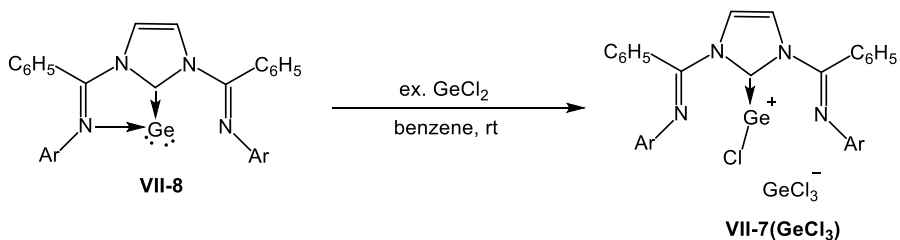
**Figure VII- 1.** Molecular structure of compound **VII-8** Thermal ellipsoids are shown at the 30% probability level. Hydrogen atoms are omitted for clarity.



**Table VII-1.** Selected bond lengths and angles for compound **VII-8**

Lengths, Å		Angles, °			
C1-Ge1	1.881(14)	C4-N2	1.359(18)	C1-Ge1-N3	78.2(5)
C1-N2	1.387(18)	C4-N3	1.342(18)	Ge1-C1-N2	116.8(10)
N3-Ge1	2.004(12)			C1-N2-C4	116.5(12)
				N2-C4-N3	110.6(12)
				C4-N3-Ge1	117.5(9)

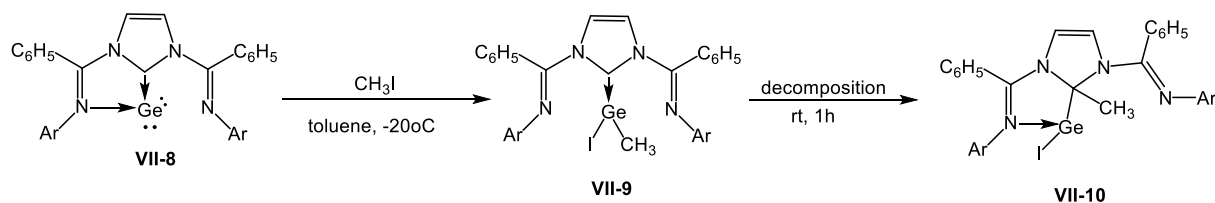
Further experiments were performed to study the reactivity of germylone **VII-8**. **VII-8** showed no reactivity toward PhSiH<sub>3</sub>, HBpin, 1,4-cyclohexadiene, (Ph)<sub>3</sub>P=S, and with CO gas. These reagents are typical for the chemistry metallenes, so that the lack of reactivity shows the absence of a carbenoid character in **VII-8**, which is consistent with the absence of an empty, germanium-centred orbital. Since germylone **VII-8** features two lone pairs of electrons, its reactivity towards Lewis acid was investigated next. The reaction of **VII-8** with excess amount of GeCl<sub>2</sub> in benzene, however, resulted in the formation of a new product which was isolated as a dark yellow solid. <sup>1</sup>H NMR spectrum of such compound in CDCl<sub>3</sub> revealed the same NMR signals as the cationic compound **VII-7(ZnCl<sub>3</sub>)**. The identity of this compound was established by a single-crystal X-ray diffraction analysis. Similar to the structure of **VII-7(ZnCl<sub>3</sub>)**, such germanium complex consists of [dimNHC]GeCl<sup>+</sup>/GeCl<sub>3</sub><sup>-</sup> as a cation/anion pair.



**Scheme VII-5.** The reaction of germylone **VII-8** with Lewis acid  $\text{GeCl}_3$ .

In addition to Lewis base properties of **VII-8**, we anticipated some nucleophilic properties. Indeed, addition of  $\text{CH}_3\text{I}$  to a red solution of **VII-8** in benzene furnished a new compound **VII-9** which gave rise to an orange solution after 15 minutes at room temperature. We could study this species by NMR spectroscopy, but unfortunately it quickly decomposed to an unknown product after 1 hour even stored in inner atmosphere. In order to characterise the intermediate **VII-9**, the reaction was conducted at low temperature ( $-25^\circ\text{C}$ ) in deuterated toluene and monitored by VT-NMR spectroscopy. **VII-9** was generated with full conversion after 4 hours at  $-22^\circ\text{C}$ . No further decomposition was observed in the course of 18 hours at  $-22^\circ\text{C}$ . The  $^1\text{H}$  NMR spectrum of **VII-9**, taken from a solution in toluene- $d_8$ , was recorded at  $-22^\circ\text{C}$  and showed a  $C_s$  symmetrical pattern. In particular, a distinct singlet at  $\delta = 1.16$  ppm integrated as three protons was assigned to the methyl group bound to the Ge atom. The methyl groups of the  $^i\text{Pr}$  substituents give rise to four doublets between 0.56 and 1.46 ppm, whereas two septets at 3.31 ppm and 3.55 ppm were assigned to the methine groups. The  $^{13}\text{C}$  NMR resonance of Ge- $\text{CH}_3$  at  $\delta = 6.2$  ppm is slightly downfield compared to that of the unreacted  $\text{CH}_3\text{I}$  ( $\delta = 1.4$  ppm). The  $^{13}\text{C}$  NMR spectrum also displayed a peak at  $\delta = 188.3$  ppm for the central carbene carbon, which was slightly downfield from the germylone **VII-8** ( $\delta = 176.1$  ppm), which may reflect the increase of the oxidation state of germanium from 0 to 2. The NMR data and the solubility

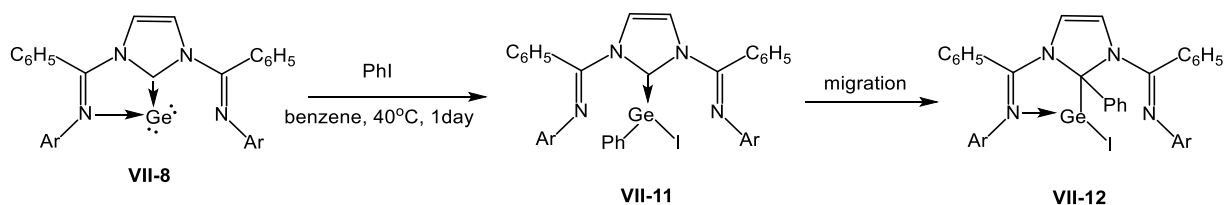
of **VII-9** in non-polar solvents, manifesting its neutrality, are consistent with the description of compound **VII-9** as the product of oxidative addition of  $\text{CH}_3\text{I}$  to the Ge centre of gerylone shown in Scheme VII-5. All attempts to identify unequivocally the product of decomposition of **VII-9** by 1D and 2D NMR experiments failed because of low resolution. However, some NMR data suggested that a migration of the methyl group from germanium to the carbene carbon could have occurred, resulting in the formation of **VII-10** after 1 hour at room temperature.



**Scheme VII-6.** The reactivity of gerylone **VII-8** towards several substrates.

The reactivity of gerylones towards carbon-based electrophiles is little studied, and in particular their reactivity towards  $\text{sp}^2$  C-X bonds has not been yet established. This prompted us to investigate the reaction of **VII-8** with  $\text{PhI}$ . An equimolar mixture of **VII-8** and  $\text{PhI}$  was stirred at  $40^\circ\text{C}$  for 1 day, resulting in the formation of **VII-12** confirmed by multinuclear NMR spectroscopy. A singlet at  $\delta = 6.00$  ppm in the  $^1\text{H}$  NMR spectrum was assigned to the backbone  $\text{CH}=\text{CH}$ , which also showed a correlation to the  $\text{C}_{\text{ipso}}$  of the phenyl moiety in the  $^{13}\text{C}$ - $^1\text{H}$  HMBC spectrum. We suggested that **VII-12** might be formed via a similar migration process from the intermediate **VII-11**. Two possible mechanisms for the formation of **VII-11** can be considered: either a concerted oxidative addition process or a stepwise, single electron transfer (SET). In order to get an insight into the mechanism of the reaction, a density functional theory (DFT) study was performed.<sup>[229]</sup> The conversion

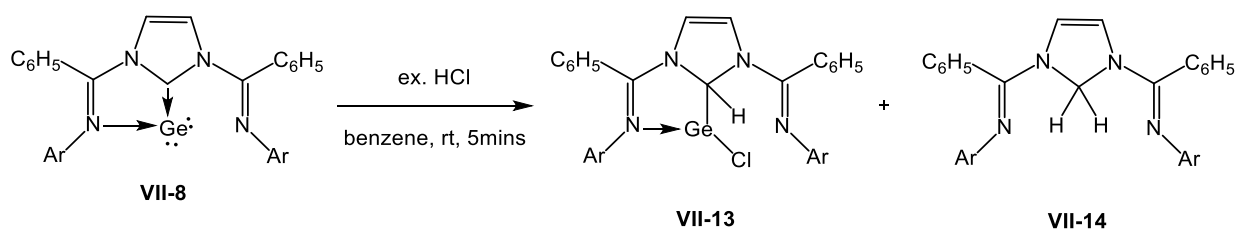
of **VII-8** to **VII-11** is an exergonic process by  $20 \text{ kcal mol}^{-1}$ , while the final product **VII-12** is found to be more stable than the intermediate **VII-11** by  $13 \text{ kcal mol}^{-1}$ . Unfortunately, the transition state  $\Delta G^\ddagger$  for the PhI addition could not be located, whereas the barrier for Ph group migration from **VII-11** to **VII-12** was found to be  $17.8 \text{ kcal mol}^{-1}$ . An intermediate corresponding to **VII-11** could not be detected by NMR, which is consistent with the lower barrier for the first step relative to migration. Given the ability of aryl iodides to participate in radical aromatic substitution,<sup>[230]</sup> a SET mechanism may be also operative. In attempt to verify this possibility, we tried to detect the possible *in situ*-generated radicals by using a radical trap reagent 2,3-dimethyl-1,3-butadiene. No C-C coupling product was observed upon heating the mixture in the presence of 2,3-dimethyl-1,3-butadiene. Direct observation of radicals by EPR heating the solution up to  $50^\circ\text{C}$  inside the EPR machine within 1 hour, returned no signal. A caution should be exercised in interpreting this negative result, as the radical can be short lived and formed in the vicinity of the germanium centre. However, they suggest a reasonable explanation that a radical process is not involved. At the moment, the mechanism of this reaction remains unclear.



**Scheme VII-7.** Reactivity of gerylone **VII-8** towards iodobenzene. The intermediate **VII-11** can be not observed in this reaction.

Similarly, treatment of **VII-8** in benzene with a strong acid, HCl, gave **VII-13** as the major product, precipitating from the solution. 1D and 2D NMR spectra were consistent with the structure of **VII-13** shown in Scheme VII-8. A singlet for the backbone  $\text{CH}=\text{CH}$

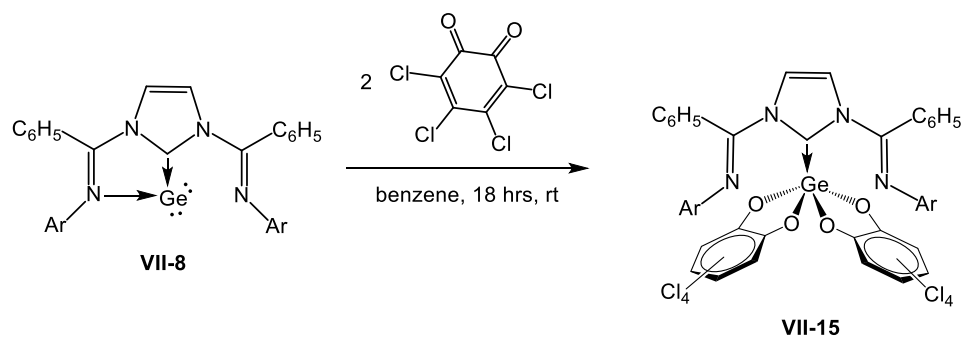
was observed at 6.04 ppm in the  $^1\text{H}$  NMR spectrum, along with a singlet at 6.21 ppm for the NCHN unit in the 2:1 integral ratio. Furthermore, the  $^{13}\text{C}$  NMR spectrum of **VII-13** displays signals at  $\delta = 88.0$  ppm and 117.8, corresponding to NC(H)N and NCH=CHN, respectively. A small amount of the protonated product **VII-14** was also observed in the reaction mixture and characterised by NMR spectroscopy. We observed two different crystals formed after 1 week at room temperature in the same Et<sub>2</sub>O solution. The light-yellow crystals of **VII-14** was collected for NMR characterization. The  $^1\text{H}$  NMR spectrum displayed two singlet peaks at  $\delta = 5.95$  and 6.59 ppm corresponding to the methylene bridge (-NCH<sub>2</sub>N-) and the backbone (-NCH=CHN-), respectively, and integrated as 2:2.



**Scheme VII-8.** The reaction of **VII-8** with strong acid HCl.

Given that **VII-8** is a compound of Ge(0), we expected it to be oxidizable. We also observed oxidation of **VII-8** with tetrachloro-*o*-benzoquinone to give a neutral cyclization product **VII-15**.  $^1\text{H}$  NMR spectrum of **VII-15** reveals a  $C_{2v}$  symmetrical species. The backbone olefin signal of **VII-15** at  $\delta = 7.20$  ppm is downfield, as compared to that of the precursor **VII-8**. The  $^{13}\text{C}$  NMR signal of the central carbon (-NCN-) was found at  $\delta = 158.1$  ppm and is shifted upfield relative to the precursor germylone (176.1 ppm). Elemental analysis and MS data suggested the presence of two tetrachloro-*o*-benzoquinone moieties in **VII-15**. The crystals of **VII-15** can be obtained from DCM/hexane mixture at room temperature. Unfortunately, the X-ray crystallographic data were compromised by the poor

quality of the crystal, which resulted in a relatively high R factor. Benzoquinones are well-known trapping reagents for carbenoids, so that the reactivity of a germylone toward tetrachloro-o-benzoquinone indicates some ambiphilic character of **VII-8**. Further investigation of the reactivity of **VII-8** is in progress.



**Scheme VII-9.** The oxidation of germylone **VII-8**.

## VIII. Conclusion and Future Work

In this thesis we investigated synthetic pathways to reduced main group element compounds stabilised by pincer ligands, related to our previously studied dimpyr platform, and studied their reactivity. Firstly, we performed the synthesis and isolation of novel zinc complexes  $2,6-(2,6\text{-}i\text{Pr}_2\text{C}_6\text{H}_3\text{N}=\text{CH})_2\text{C}_6\text{H}_3\text{ZnBu}$  (**V-2**) and  $2,6-(2,6\text{-}i\text{Pr}_2\text{C}_6\text{H}_3\text{N}=\text{CH})_2\text{C}_6\text{H}_3\text{ZnCl}_2\text{Li}(\text{THF})_3$  (**V-3**) stabilised by a bis(imino)phenyl NCN pincer. The former undergoes Cl/H exchange in the presence of Super Hydride ( $\text{LiHBEt}_3$ ), resulting in the formation of an unusual dimer **V-7** while complex **V-2** was converted to the hydrido zincate **V-9** by reacting with  $\text{KO}^t\text{Bu}$  and  $\text{PhSiH}_3$ . We also observed an unusual decomposition of the dimer **V-7** in the presence of THF and LiCl to afford the zincate **V-8** which was independently prepared by decomposition the butyl compound **V-2**.

Secondly, we prepared the compound  $(\text{dimph})\text{P}$  (**VI-2**) which can be rationalised either as a diiminophenyl-stabilised phosphinidene or a benzoazaphosphol (or a combination of both). Compound **IV-2** is remarkably robust and even regenerates in simple substitution reactions of P(III) derivatives by means of the less common deprotonation of the  $\text{CH}_2\text{N}$  moiety. This unexpected chemical stability of **IV-2** can be ascribed to the charge transfer from the P(I) centre to the non-innocent diiminophenyl platform. This result demonstrates the highly  $\pi$ -accepting ability of the imine moiety of dimpy ligand. A related compound  $(\text{dimH}_2\text{ph})\text{P}$  **VI-10** was obtained by an unusual N-H elimination reaction from a hydrogenated derivative of **IV-2**, the phosphine  $(\text{dimHph})\text{PH}$  **VI-9**, whereas the methyl and  $\text{PPh}_2$ -substituted analogues **VI-11** and **VI-12** do not enter into N-C and N-P elimination reactions, respectively. The remarkable chemical inertness of **VI-2** and its unusual

reactivity suggest that any strategy to design an isolable but reactive phosphinidene should decrease the  $\pi$ -accepting ability of the ligand.

To probe further the stability/reactivity dichotomy of phosphinidene, in our third project we investigated various routes to reduce dioxyphenyl-phosphorus dichloride **VI-16**. Compared to its imine analogue, the dioxyph ligand has minimal electron accepting ability, which was predicted to generate an electron-rich P(I) compound. However, it turns out that the dative capability of this ligand alone does not allow for the stabilisation of phosphinidene, resulting in the cyclization of the intermediate to generate a three membered-ring triphosphacyclopropane **VI-18**. The intermediacy of a phosphinidene in the reduction of **VI-16** by  $\text{KC}_8$  was confirmed by a trapping experiment with butadiene. On the other hand,  $\text{PMe}_3$  showed the ability to reduce phosphorus (III) dichloride to the triphosphacyclopropane **VI-18**. Unexpectedly, the reduction of phosphorus (III) compound by  $\text{PMe}_3$  in the presence of  $\text{PhSiH}_3$  or HBpin resulted in the formation of phosphine **VI-23**, the product of formal chloride substitution for hydride. The mechanism of the reduction by  $\text{PMe}_3$  was studied by a VT- $^{31}\text{P}$  NMR experiment, which showed that the intermediate phosphinidene can be involved in this reaction. Further investigation by DFT calculations is in progress.

Finally, we succeeded in the synthesis and characterisation of a germanium (0) compound **VII-8** stabilised by bis(imino)aryl N-heterocarbene ligand. Divalent germanium compounds were obtained via oxidative addition of  $\text{CH}_3\text{I}$ ,  $\text{PhI}$ , and  $\text{HCl}$  to the germylone **VII-8**. Interestingly, the final products of these additions were the products of C-C and C-H coupling with the central carbene carbon atom. The oxidative addition of  $\text{PhI}$  to germylone is the first example of such a reactivity for a  $\text{sp}^2$ -hybridised carbon electrophile.



In the case of CH<sub>3</sub>I, the oxidative addition product was formed by a nucleophilic attack of the Ge centre at the carbon of CH<sub>3</sub>I, which was studied by VT-NMR. Interestingly, **VII-8** also reacted with tetrachloro-*o*-benzoquinone to afford a cyclization product in a manner similar to that seen for carbenoids. These results indicate the ambiphilic nature of **VII-8**. Further, investigation on the reactivity of germylone **VII-8** with different substrates is in progress.

In the overview of this Thesis, we can state that the chemistry of highly reduced main group compounds starts to crystalize in a distinctive research area that shows reactivity patterns very different and, in some respect, complementary to what we usually observe for carbenoid species. The latter show ambiphilic properties that, depending on the nature of supporting ligand sets, can be either more electrophilic or more nucleophilic. Carbenoids are usually quite good bond splitters but their bond-activated products have so far shown rather limited ability to regenerate bonds, which limits their application in catalysis. On the other hand, carbenes and their heavy analogues largely demonstrate nucleophilic behaviour making them closer analogues of electron-rich phosphines. However, our work now reveals that this general feature can be changed by a judicious choice of the supporting ligand with a non-innocent character, so that a more pronounced charge delocalisation to the ligand “switches on” the ambiphilic properties to enable two-electron bond activations. The possibility to push electrons to the ligand, and hopefully back to the main group element, brings about an important question: Is it possible to combine the bond activation with bond formation to enable a catalytic process? Answering this question will be the next big leap in the study of reduced main group compounds.

## **Part C. Experimental Section**

## IX. Experimental

### IX.1 General Methods and Solvents

All manipulations were carried out using conventional inert atmosphere glove-box and Schlenk techniques. Solvents were pre-dried by using Grubbs-type purification columns and stored in ampoules equipped with Teflon valve. Deuterated solvents were dried over sodium, potassium, or CaH<sub>2</sub> as appropriate, distilled under reduced pressure and stored in Teflon valve ampoules.

### IX.2 Instrumentation and Analysis

NMR samples were prepared in New Era tubes equipped with J. Young type Teflon valves. NMR spectra were obtained at room temperature with a Bruker DPX-400 and Bruker DPX-600 instruments. NMR spectra at low temperature were obtained with Bruker DPX-600 instruments. <sup>1</sup>H and <sup>13</sup>C spectra were referenced internally to residual protio-solvent (<sup>1</sup>H) or solvent (<sup>13</sup>C) resonances and are reported relative to tetramethylsilane ( $\delta = 0$  ppm). Chemical shifts are quoted in ppm and coupling constants in Hertz. Then, NMR data were processed and analyzed with MestReNova software.

IR spectra were recorded on a Perkin-Elmer 1600 FT-IR spectrometer as Nujol mulls between NaCl windows. All data are quoted in wavenumbers (cm<sup>-1</sup>).

Elemental analyses were performed in the analytical laboratory of Université de Montreal and the ANALEST laboratory at the University of Toronto.

Mass spectrometry was performed on Bruker HCT Plus ion-trap mass spectrometer. The MS sample is introduced either through direct infusion or by coupling with one of LC systems (i.e. HP 1100 LC and Agilent 1100 capillary LC).

X-ray diffraction analysis were performed on suitable crystal which were grown from suitable solvents at either room temperature or -30°C. The crystals were mounted in a film of perfluoropolyether oil on a glass fibre and transferred to a diffractometer. Prior to data collection crystals were cooled to 120-238 K. Data were collected on a Bruker APEX II single crystal diffractometer equipped with a sealed Mo tube source (wavelength 0.71073 Å) and APEX II CCD detector. Raw data collection and processing were performed with APEX II software package from BRUKER AXS.<sup>37</sup> Full details can be found in individual tables for each crystal structure (Appendix).

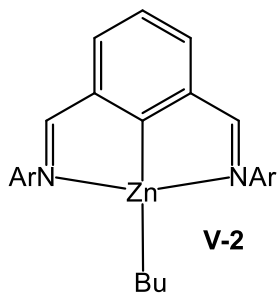
### IX.3 Starting Materials

1,3-bis(aldimino)-2-bromobenzene, n-butyllithium (1.6 M in hexane), Zinc Chloride, 2,6-diisopropylaniline, Lithium triethylborohydride, Potassium tert-butoxide, Methylphenylsilane, Potassium metal, Graphite, Lithium chloride, Phosphorus tribromide, Pyridine oxide, Methylmagnesium bromide (3 M in diethyl ether), Lithium diphenylphosphide, Ammonium formate, Lithium bis(trimethylsilyl)amide, Trimethylsilyl trifluoromethanesulfonate, Germanium(II) chloride dioxane complex (1:1), Bromine, Sulfur powder, Hydrogen chloride solution (2.0 M in diethyl ether), 2-Bromo-m-xylene, Azobisisobutyronitrile, N-bromosuccinimide, Potassium carbonate, 2,6-Diisopropylphenol, Phosphorus trichloride, Dichlorophenylphosphine, Trimethylphosphine, 2,3-dimethyl-1,3-butadiene, Catecholborane (HBcat), 4,4,5,5-Tetramethyl-1,3,2-dioxaborolane (HBpin), Methyl iodide, Iodobenzene, Trimethylsilyl iodide, Trimethylsilyl trifluoromethanesulfonate, 3,5-Di-tert-butyl-o-benzoquinone, tetrachloro-o-benzoquinone, Crotonaldehyde, Acetic anhydride, Phosphorus pentachloride, Thionyl chloride, Benzoyl chloride, Imidazole, Sodium hydride, 2-

Bromoisophthalaldehyde are commercial available chemicals which are purchased from either Sigma-Aldrich, or Pubchem, or Alfa Chemistry, ect.

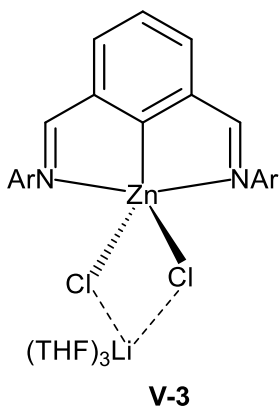
<sup>IPr</sup>NHC carbene<sup>[231]</sup>, Potassium graphite (KC<sub>8</sub>),<sup>[232]</sup> N,N'-bis(2,6-diisopropylphenyl)-2-bromo-isophthalaldimine,<sup>[233]</sup> 2,6-bis[(2,6-diisopropyl)phenoxy],<sup>[234]</sup> 1,3-bis[1-(2,6-dimethylphenylimino)ethyl]imidazolium chloride,<sup>[235]</sup> 1,3-bis[(2,6-dimethylphenylimino)benzyl]imidazolium tetrafluoroborate<sup>[235]</sup> were prepared according to the literatures.

IX.4 Experimental Procedures for Chapter V



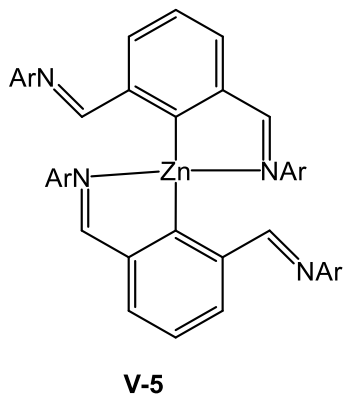
**(2,6-(2,6-<sup>i</sup>Pr<sub>2</sub>C<sub>6</sub>H<sub>3</sub>N=CH)<sub>2</sub>C<sub>6</sub>H<sub>3</sub>)ZnC<sub>4</sub>H<sub>9</sub> (V-2).** The

solution of 2,6-(2,6-<sup>i</sup>Pr<sub>2</sub>C<sub>6</sub>H<sub>3</sub>N=CH)<sub>2</sub>C<sub>6</sub>H<sub>3</sub>-1-Br (0.600 g, 1.13 mmol) in THF (20 mL) was cooled at -70°C. Then a solution of *n*BuLi in hexane (1.40 mL, 2.26 mmol) was added dropwise into this mixture at the same temperature. The addition of *n*BuLi caused solution to change color from light-yellow to deep-green. The reaction mixture was stirred at -70°C for 2 hours before adding of a solution of ZnCl<sub>2</sub> (0.153 g, 1.13 mmol) in THF (15 mL). The mixture was allowed to warm up gradually to room temperature and stirred overnight. The volatiles were removed under vacuum and the residue was dissolved in hexane to give a suspension. The precipitate was filtered off and the filtrate was dried to give a yellow-orange solid. The crystals were obtained from hexane solution at -30°C. Yield: 0.500 g, 0.87 mmol, 77%. <sup>1</sup>H NMR (400 MHz, C<sub>6</sub>D<sub>6</sub>, 22°C): δ (ppm) = 0.86 (m, 5H, Zn-CH<sub>2</sub>CH<sub>2</sub>CH<sub>2</sub>CH<sub>3</sub>), 1.15 (d, *J*<sub>H-H</sub> = 6.9 Hz, 24H, <sup>i</sup>Pr-CH<sub>3</sub>), 1.40 (sept, 2H, *J*<sub>H-H</sub> = 7.5 Hz, Zn-CH<sub>2</sub>CH<sub>2</sub>CH<sub>2</sub>CH<sub>3</sub>), 1.72 (quint, 2H, *J*<sub>H-H</sub> = 7.5 Hz, Zn-CH<sub>2</sub>CH<sub>2</sub>CH<sub>2</sub>CH<sub>3</sub>), 3.08 (sept, 4H, *J*<sub>H-H</sub> = 6.9 Hz, CH(CH<sub>3</sub>)<sub>2</sub>), 7.15-7.36 (m, 6H, Ph-N), 7.14 (t, 1H, *J*<sub>H-H</sub> = 4.6 Hz, p-H Ph-Zn), 7.38 (d, 2H, *J*<sub>H-H</sub> = 7.5 Hz, m-H Ph-Zn), 8.15 (s, 2H, CH=N). <sup>13</sup>C{<sup>1</sup>H} NMR (101 MHz, C<sub>6</sub>D<sub>6</sub>, 22°C): δ (ppm) = 11.9, 14.0, 29.6, 30.0 (Zn-CH<sub>2</sub>CH<sub>2</sub>CH<sub>2</sub>CH<sub>3</sub>), 23.4 (CH<sub>3</sub>), 28.3 (CH(CH<sub>3</sub>)), 123.1, 124.9, 133.2, 138.2, 144.0, 148.3 (aromatic ring), 167.8 (C=N-C). **Anal. Calcd** for C<sub>36</sub>H<sub>48</sub>N<sub>2</sub>Zn: C, 75.31; H, 8.43; N, 4.88. Found: C, 74.04; H, 8.71; N, 4.92%.



**(2,6(2,6-<sup>i</sup>Pr<sub>2</sub>C<sub>6</sub>H<sub>3</sub>N=CH)C<sub>6</sub>H<sub>3</sub>)ZnCl<sub>2</sub>LiCl\*THF<sub>x</sub> (V-3).**

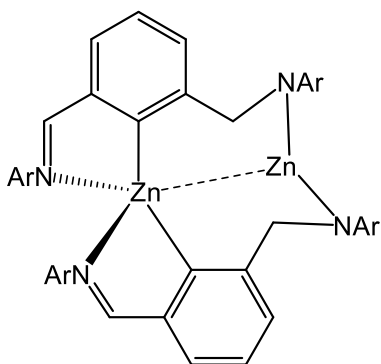
The solution of 2,6(2,6-<sup>i</sup>Pr<sub>2</sub>C<sub>6</sub>H<sub>3</sub>N=CH)C<sub>6</sub>H<sub>3</sub>-1-Br (0.600 g, 1.13 mmol) in THF (20 mL) was cooled at -70°C. Then, a solution of *n*BuLi in hexane (0.71 mL, 1.13 mmol) was added dropwise into the mixture at -70°C, which caused the solution to change color from light-yellow to deep-green. The reaction mixture was allowed to stir at the same temperature for 4 hours before a solution of ZnCl<sub>2</sub> (0.153 g, 1.13 mmol) in THF (15 mL) was added. The mixture was allowed to warm up gradually to room temperature and stirred overnight. The solution was concentrated to 2 mL. An amount of hexane (1 mL) was slowly added as a top layer into this solution. Crystals of **V-3** were obtained from this THF/hexane mixture at -30°C. Yield: 0.620 g, 0.76 mmol, 93%. <sup>1</sup>H NMR (400 MHz, C<sub>6</sub>D<sub>6</sub>, 22°C): δ (ppm) = 1.20 (d, 24H, *J*<sub>H-H</sub> = 6.9 Hz, <sup>i</sup>Pr-CH<sub>3</sub>), 1.29 (quint, 4H, *J*<sub>H-H</sub> = 3.2 Hz, THF), 3.43 (quint, 4H, *J*<sub>H-H</sub> = 3.2 Hz, THF), 3.48 (br, 4H, CH(CH<sub>3</sub>)<sub>2</sub>), 7.05-7.16 (m, 6H, Ph-N), 7.18 (t, 1H, *J*<sub>H-H</sub> = 7.5 Hz, *p*-H Ph-Zn), 7.43 (d, 2H, *J*<sub>H-H</sub> = 7.5 Hz, *m*-H Ph-Zn), 8.28 (s, 2H, *J*<sub>H-H</sub> = 7.5 Hz, CH=N). <sup>13</sup>C{<sup>1</sup>H} NMR (101 MHz, C<sub>6</sub>D<sub>6</sub>, 22°C): δ (ppm) = 24.0 (CH<sub>3</sub>), 25.7, 68.2 (THF), 27.7 (CH(CH<sub>3</sub>)<sub>2</sub>), 122.8, 124.3, 127.1, 132.9, 139.4, 142.4, 148.9 (aromatic ring), 167.8 (C=N-C). **Anal. Calcd** for



C<sub>44</sub>H<sub>63</sub>Cl<sub>2</sub>O<sub>3</sub>N<sub>2</sub>Li<sub>2</sub>Zn: C,65,15; H, 7.83; N, 3.45. Found: C, 63.49; H,7.29; N,3.91%.

**(2,6(2,6-<sup>i</sup>Pr<sub>2</sub>C<sub>6</sub>H<sub>3</sub>N=CH)<sub>2</sub>C<sub>6</sub>H<sub>3</sub>)<sub>2</sub>Zn (V-5).** 0.37 mmol (15mL) of **V-3** was dissolved into toluene. 0.099 g (0.74 mmol) of KC<sub>8</sub> was added into the solution. The suspension was stirring for 4 hours at room temperature. The precipitate

was filtered off. The solution was dried under vacuum to obtain a brown-red solid. Crystals were obtained from a hexane solution at  $-30^{\circ}\text{C}$ . Yield: 0.150 g, 0.16 mmol, 84%.  $^1\text{H NMR}$  (400 MHz,  $\text{C}_6\text{D}_6$ ,  $22^{\circ}\text{C}$ ):  $\delta$  (ppm) = 0.95 (d,  $J_{\text{H-H}} = 6.9$  Hz, 24H,  $^i\text{Pr-CH}_3$ ), 3.19 (sept, 4H,  $\text{CH}(\text{CH}_3)_2$ ), 6.98-7.02 (m, 6H, Ph-N), 7.18 (t, 1H,  $J_{\text{H-H}} = 7.5$  Hz, p-H Ph-Zn), 7.92 (d, 2H,  $J_{\text{H-H}} = 7.5$  Hz, m-H Ph-Zn), 8.17 (s, 2H,  $J_{\text{H-H}} = 7.5$  Hz, CH=N).  $^{13}\text{C}\{^1\text{H}\}$  NMR (101 MHz,  $\text{C}_6\text{D}_6$ ,  $22^{\circ}\text{C}$ ):  $\delta$  (ppm) = 23.8 ( $\text{CH}_3$ ), 28.0 ( $\text{CH}(\text{CH}_3)_2$ ), 123.4, 125.2, 127.0, 132.0, 139.2, 143.5, 147.7 (aromatic ring), 170.5 (C=N-C). **Anal. Calcd** for  $\text{C}_{64}\text{H}_{78}\text{N}_4\text{Zn}$ : C, 79.35; H, 8.12; N, 5.78. Found: C, 79.48; H, 8.60; N, 5.87%.



**V-7**

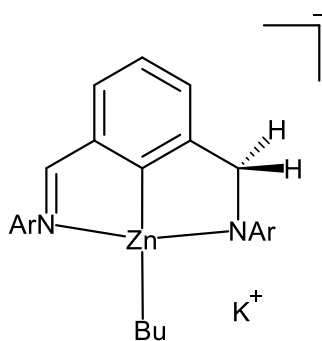
**Zinc dimer V-7.** 0.300 g (0.37 mmol) of **V-3** was

dissolved into toluene (15 mL). 0.35 mL (0.37 mmol) of  $\text{Li}[(\text{C}_2\text{H}_5)_3\text{BH}]$  (1M in THF) was added dropwise into the solution. The mixture was intermediately turned to orange color. The mixture was stirred for 4 hours. The precipitate was filtered off. The filtrate was treated under reduced pressure to obtained yellow solid. The crystals were

obtained from a toluene solution at  $-30^{\circ}\text{C}$ . Yield: 0.160 g, 0.15 mmol, 84%.  $^1\text{H NMR}$  (400 MHz,  $\text{C}_6\text{D}_6$ ,  $22^{\circ}\text{C}$ ):  $\delta$  (ppm) = 0.18 (d, 6H,  $J_{\text{H-H}} = 6.9$  Hz,  $^i\text{Pr-CH}_3$ ), 0.59 (t, 12H,  $J_{\text{H-H}} = 6.9$  Hz,  $^i\text{Pr-CH}_3$ ), 0.79 (d, 6H,  $J_{\text{H-H}} = 6.9$  Hz,  $^i\text{Pr-CH}_3$ ), 0.96 (d, 6H,  $J_{\text{H-H}} = 6.9$  Hz,  $^i\text{Pr-CH}_3$ ), 1.12 (d, 6H,  $J_{\text{H-H}} = 6.9$  Hz,  $^i\text{Pr-CH}_3$ ), 1.28 (d, 6H,  $J_{\text{H-H}} = 6.9$  Hz,  $^i\text{Pr-CH}_3$ ), 1.37 (d, 6H,  $J_{\text{H-H}} = 6.9$  Hz,  $^i\text{Pr-CH}_3$ ), 2.37 (quint, 2H,  $J_{\text{H-H}} = 6.9$  Hz,  $\text{CH}(\text{CH}_3)_2$ ), 3.50 (quint, 2H,  $J_{\text{H-H}} = 6.9$  Hz,  $\text{CH}(\text{CH}_3)_2$ ), 3.68 (m, 4H,  $\text{CH}(\text{CH}_3)_2$ ), 3.85 (d, 2H,  $J_{\text{H-H}} = 10.6$  Hz,  $\text{CH}_2\text{-N}$ ), 4.97 (d, 2H,  $J_{\text{H-H}} = 10.6$  Hz  $\text{CH}_2\text{-N}$ ), 6.90- 7.14 ( m, 12H, Ph-N), 7.02 (t, 2H,  $J_{\text{H-H}} = 7.5$  Hz, p-H Ph-Zn), 7.12 (d, 2H,  $J_{\text{H-H}} = 7.5$  Hz, m-H Ph-Zn), 7.47 (d, 2H,  $J_{\text{H-H}} = 7.5$  Hz, m-H Ph-



Zn), 8.03 (s, 2H,  $J_{\text{H-H}} = 7.5$  Hz, CH=N).  $^{13}\text{C}\{^1\text{H}\}$  NMR (101MHz,  $\text{C}_6\text{D}_6$ , 22°C):  $\delta$  (ppm) = 21.1 (toluene), 22.4 - 27.6 ( $\text{CH}_3$ ), 27.6 - 28.3 ( $\text{CH}(\text{CH}_3)$ ), 65.1 ( $-\text{CH}_2=\text{N-Ar}$ ), 122.7, 123.6, 123.8, 125.3, 126.3, , 130.5, 133.5, 141.6, 144.6, 146.1, 147.0 (aromatic ring), 124.7, 128.2, 129.0, 140.7 (toluene), 147.6, 150.1 (C-N-Zn), 155.8, 155.9 (C-N=C), 176.1 (C=N-C).  
**Anal. Calcd** for  $\text{C}_{64}\text{H}_{80}\text{N}_4\text{Zn}_2$ : C, 74.19; H, 7.78; N, 5.41. Found: C, 73.95; H, 7.55; N, 5.38%.



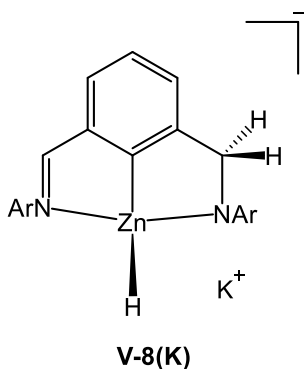
**v-9**

**[[2-(2,6- $i$ Pr $_2$ C $_6$ H $_3$ N=CH)-6-(2,6- $i$ Pr $_2$ C $_6$ H $_3$ N**

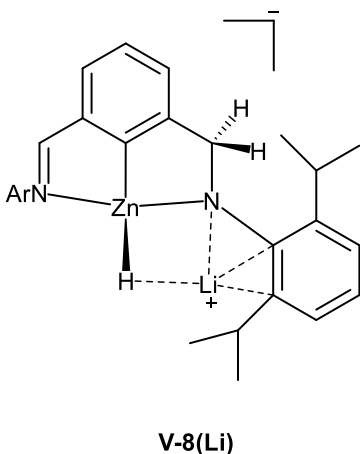
**CH $_2$ )C $_6$ H $_3$ ]ZnC $_4$ H $_9$ ]/[K] (V-9).** 0.300 g (0.52mmol) of **V-2** was dissolved into toluene (5 mL). 0.059 g (0.52 mmol) of KO $^t$ Bu in toluene (5 mL) was added once to the solution. The mixture changed color from light yellow to orange. The mixture was stirred for 10 minutes before adding of PhSiMeH $_2$

(0.52 mmol, 72  $\mu\text{L}$ ). The mixture was intermediately turned to red color. The whole solution was stirred for 1 hour. The solvent was removed under vacuum and the residual was washed by hexane. The crystal was obtained from a toluene solution at  $-30^\circ\text{C}$ . Yield: 0.249 g, 0.41 mmol, 78%.  $^1\text{H}$  NMR (400 MHz,  $\text{C}_6\text{D}_6$ , 22°C):  $\delta$  (ppm) = 0.13 (t, 2H,  $J_{\text{H-H}} = 7.5$  Hz, Zn-CH $_2$ CH $_2$ CH $_2$ CH $_3$ ), 0.93 (t, 2H,  $J_{\text{H-H}} = 7.5$  Hz, Zn-CH $_2$ CH $_2$ CH $_2$ CH $_3$ ), 1.20 (d,  $J_{\text{H-H}} = 6.9$  Hz, 12H,  $i$ Pr-CH $_3$ ), 1.29 (d,  $J_{\text{H-H}} = 6.9$  Hz, 12H,  $i$ Pr-CH $_3$ ), 1.46 (sept, 2H,  $J_{\text{H-H}} = 6.9$  Hz, Zn-CH $_2$ CH $_2$ CH $_2$ CH $_3$ ), 1.78 (quint, 2H,  $J_{\text{H-H}} = 7.5$  Hz, Zn-CH $_2$ CH $_2$ CH $_2$ CH $_3$ ), 3.35 (sept, 4H,  $J_{\text{H-H}} = 6.9$  Hz, CH(CH $_3$ ) $_2$ ), 3.51 (sept, 2H,  $J_{\text{H-H}} = 6.9$  Hz, CH(CH $_3$ ) $_2$ ), 4.72 (s, 2H, CH $_2$ -N), 7.01-7.30 (m, 6H, Ph-N), 7.28 (t, 1H,  $J_{\text{H-H}} = 7.5$  Hz, p-H Ph-Zn), 7.30 (d, 1H,  $J_{\text{H-H}} = 7.5$  Hz, m-H Ph-Zn), 7.35 (d, 1H,  $J_{\text{H-H}} = 7.5$  Hz, m-H Ph-Zn), 8.83 (s, 1H,  $J_{\text{H-H}} = 7.5$  Hz, CH=N).  $^{13}\text{C}\{^1\text{H}\}$  NMR (101MHz,  $\text{C}_6\text{D}_6$ , 22°C):  $\delta$  (ppm) = 11.5 (s, 1H, Zn-

CH<sub>2</sub>CH<sub>2</sub>CH<sub>2</sub>CH<sub>3</sub>), 14.4, 21.4, 24.5 (Zn-CH<sub>2</sub>CH<sub>2</sub>CH<sub>2</sub>CH<sub>3</sub>), 23.4, 28.0, 28.4, 30.4, 32.6 (CH<sub>3</sub>), 25.3 (CH<sub>3</sub>-toluene), 64.5 (CH(CH<sub>3</sub>)), 120.9, 123.4, 123.6, 124.1, 124.3, 125.6, 126.1, 126.6, 143.6, 146.5, 150.7, 157.2, 157.4 (aromatic ring), 125.6, 128.6, 129.3, 138.1 (toluene), 168.3(CH<sub>2</sub>-N-C), 171.8 (C=N-C).



**[[{2-(2,6-<sup>i</sup>Pr<sub>2</sub>C<sub>6</sub>H<sub>3</sub>N=CH)-6-(2,6-<sup>i</sup>Pr<sub>2</sub>C<sub>6</sub>H<sub>3</sub>NCH<sub>2</sub>)C<sub>6</sub>H<sub>3</sub>}ZnH]/[Li] V-8(Li)** 25mg of compound **V-7** was dissolved into C<sub>6</sub>D<sub>6</sub> to give a dark yellow solution and transfer into a sealed NMR tube. An equivalent amount of LiCl salt (1mg) and a few drops was added into this solution. The whole suspension was dried under vacuum for 1.5 h to give a light-yellow solid of **V-8(Li)**.

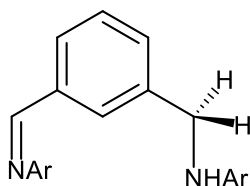


**[[{2-(2,6-<sup>i</sup>Pr<sub>2</sub>C<sub>6</sub>H<sub>3</sub>N=CH)-6-(2,6-<sup>i</sup>Pr<sub>2</sub>C<sub>6</sub>H<sub>3</sub>NCH<sub>2</sub>)C<sub>6</sub>H<sub>3</sub>}ZnH]/[K] V-8(K)**. 100mg of compound **V-9** was dissolved in toluene to give a red yellow solution. The volatiles were removed under vacuum and crude solid was re-dissolved in toluene. The whole mixture was kept at low temperature. The precipitate of **V-8(K)** was

crashed out of the cooled solution after 1 months. <sup>1</sup>H NMR (400 MHz, C<sub>6</sub>D<sub>6</sub>, 22°C): δ (ppm) = 0.62 (d, 6H, J<sub>H-H</sub> = 6.9 Hz, <sup>i</sup>Pr-CH<sub>3</sub>), 0.85 (d, 6H, J<sub>H-H</sub> = 6.9 Hz, <sup>i</sup>Pr-CH<sub>3</sub>), 1.09 (d, 6H, J<sub>H-H</sub> = 6.9 Hz, <sup>i</sup>Pr-CH<sub>3</sub>), 1.14 (d, 6H, J<sub>H-H</sub> = 6.9 Hz, <sup>i</sup>Pr-CH<sub>3</sub>), 3.12 (sept, 2H, J<sub>H-H</sub> = 6.9 Hz, (CH<sub>3</sub>)<sub>2</sub>), 3.52 (sept, 2H, J<sub>H-H</sub> = 6.9 Hz, CH(CH<sub>3</sub>)<sub>2</sub>), 3.56 (t, 1H, ZnH), 4.26 (d of d, 1H, CH<sub>2</sub>-N), 4.45 (d of d, 1H, CH<sub>2</sub>-N), 6.59- 7.08 (m, 6H, Ph-N), 7.17 (d, 1H, J<sub>H-H</sub> = 7.5 Hz, m-H Ph-Zn), 7.26 (t, 1H, J<sub>H-H</sub> = 7.5 Hz, p-H Ph-Zn), 7.95 (d, 1H, J<sub>H-H</sub>=7.5 Hz, m-H Ph-

Zn), 8.02 (s, 1H, CH=N).  $^{13}\text{C}\{^1\text{H}\}$  NMR (101 MHz,  $\text{C}_6\text{D}_6$ , 22°C):  $\delta$  (ppm) = 24.5, 24.9, 28.1, 28.4 ( $\text{CH}_3$ ), 62.2 ( $\text{CH}(\text{CH}_3)$ ), 123.9, 124.0, 124.6, 126.1, 127.5, 130.0, 132.9, 141.1, 143.1, 144.2, 143.8, 147.0, 149.6 (aromatic ring), 162.2, 174.9 ( $\text{C}=\text{N}-\text{C}$ ).

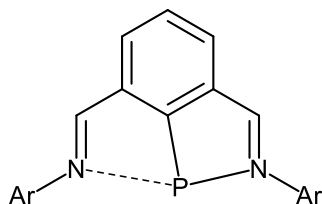
**2-(2,6- $^i\text{Pr}_2\text{C}_6\text{H}_3\text{N}-\text{CH}_2$ )-6-(2,6- $^i\text{Pr}_2\text{C}_6\text{H}_3\text{N}=\text{CH})\text{C}_6\text{H}_4$  V-10.** The complex **V-2**



**V-10**

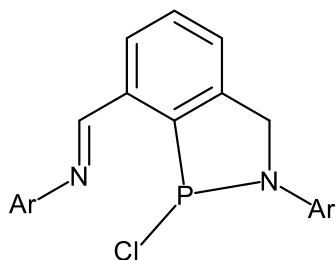
can be generated via two methods: either the composition of **V-9** in toluene solution over 2 weeks or the treatment of zinc dimer **V-7** under reduced pressure for 3h.  $^1\text{H}$  NMR (400 MHz,  $\text{C}_6\text{D}_6$ , 22°C):  $\delta$  (ppm) = 1.16 (d, 12H,  $J_{\text{H-H}} = 6.9$  Hz,  $^i\text{Pr}-\text{CH}_3$ ), 1.19 (d, 12H,  $J_{\text{H-H}} = 6.9$  Hz,  $^i\text{Pr}-\text{CH}_3$ ), 3.11(d, 12H,  $J_{\text{H-H}} = 7.8$  Hz,  $\text{CH}_2-\text{N}-\text{Ar}$ ), 3.17 (sept, 2H,  $\text{CH}(\text{CH}_3)_2$ ), 3.26 (sept, 2H,  $\text{CH}(\text{CH}_3)_2$ ), 4.01 (d, 2H,  $J_{\text{H-H}} = 7.5$  Hz,  $\text{CH}_2-\text{N}-\text{Ar}$ ), 7.11-7.16 (m, 6H, Ph-N), 7.18 (t, 1H,  $J_{\text{H-H}} = 7.5$  Hz, p-H Ph), 7.37(d, 1H,  $J_{\text{H-H}} = 7.5$  Hz, m-H Ph), 7.75(d, 1H,  $J_{\text{H-H}} = 7.5$  Hz, m-H Ph), 8.05 (s, 1H,  $J_{\text{H-H}} = 7.5$  Hz, CH=N), 8.06 (b, 1H, o-H Ph).

IX.5 Experimental Procedures for Chapter IV



**VI-2**

**[2,6-(2,6-<sup>i</sup>Pr<sub>2</sub>C<sub>6</sub>H<sub>3</sub>N=CH)<sub>2</sub>C<sub>6</sub>H<sub>3</sub>]P (VI-2).** 0.320 g (0.39 mmol) of **V-3** was dissolved into toluene (15 mL). 37  $\mu$ L (0.39 mmol) of PBr<sub>3</sub> was added into the solution. The solution was stirred for 4 hours at room temperature. The precipitate was filtered off and dried to obtain a crude yellow solid of compound **VI-2**. This solid was suspended in 15 mL of toluene. 0.107 g (0.78 mmol) of KC<sub>8</sub> was added into this suspension and the whole mixture was stirred for 4 hours at room temperature. The precipitate (graphite and KBr) was filtered off and dried to obtain an orange solid. Crystals of **3** were obtained from toluene solution at -30°C. Yield: 0.150 g (0.32 mmol, 80%). **<sup>1</sup>H NMR** (400 MHz, C<sub>6</sub>D<sub>6</sub>, 22°C):  $\delta$  = 1.14 (d,  $J_{\text{H-H}} = 6.9$  Hz, 24H, <sup>i</sup>Pr-CH<sub>3</sub>), 2.88 (sept, 4H,  $J_{\text{H-H}} = 6.9$  Hz, CH(CH<sub>3</sub>)<sub>2</sub>), 7.00 (t, 1H,  $J_{\text{H-H}} = 7.5$  Hz, p-H Ph-P), 7.10-7.20 (m, 6H, Ph-N), 7.45 (d, 2H,  $J_{\text{H-H}} = 7.5$  Hz, m-H Ph-C<sub>6</sub>H<sub>3</sub>), 8.09 (d, 2H,  $J_{\text{H-P}} = 8.0$  Hz, CH=N-Ar). **<sup>13</sup>C{<sup>1</sup>H} NMR** (101 MHz, C<sub>6</sub>D<sub>6</sub>, 22°C):  $\delta$  = 24.2 (CH<sub>3</sub>), 28.2 (CH(CH<sub>3</sub>)<sub>2</sub>), 121.7, 132.6, 143.72, 148.7 (Ph-P), 123.1, 126.6, 128.49, 141.7 (aromatic ring), 151.8 (C=N-Ar). **<sup>31</sup>P{<sup>1</sup>H} NMR** (162 MHz, C<sub>6</sub>D<sub>6</sub>, 22°C):  $\delta$  = 178.2 (s). **Anal. Calcd** for C<sub>32</sub>H<sub>39</sub>N<sub>2</sub>P: C, 79.63; H, 8.15; N, 5.80. Found: C, 78.90; H, 8.47; N, 5.61%.

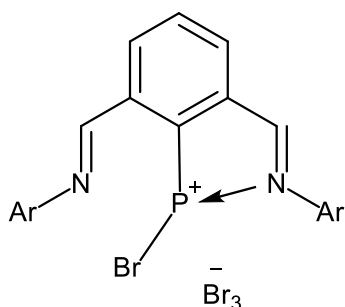


**VI-6**

**[2-(2,6-<sup>i</sup>Pr<sub>2</sub>C<sub>6</sub>H<sub>3</sub>N=CH)-6-(2,6-<sup>i</sup>Pr<sub>2</sub>C<sub>6</sub>H<sub>3</sub>N-CH<sub>2</sub>)]C<sub>6</sub>H<sub>3</sub>PCl (VI-6).** 0.500 g (1.03 mmol) of **VI-2** was dissolved into toluene (10 mL). Excess amount (1.5 mL, 3.09 mmol) of HCl (2M solution in Et<sub>2</sub>O) was added into the above solution and the mixture was stirred for 2 hours at room temperature.

Removing volatiles under reduced pressure produced a brown solid. This was washed by

cold hexane to afford pure solid **7**. Yield: 0.508 g (0.98 mmol, 95%).  $^1\text{H NMR}$  (400 MHz,  $\text{C}_6\text{D}_6$ ,  $22^\circ\text{C}$ ): 0.90 (d,  $J_{\text{H-H}} = 6.9$  Hz, 3H,  $^i\text{Pr-CH}_3$ ), 0.94-1.24 (m, 18H,  $^i\text{Pr-CH}_3$ ), 1.42 (d,  $J_{\text{H-H}} = 6.9$  Hz, 3H,  $^i\text{Pr-CH}_3$ ), 2.78 (sept, 1H,  $J_{\text{H-H}} = 6.9$  Hz,  $\text{CH}(\text{CH}_3)_2$ ), 3.37 (sept, 2H,  $J_{\text{H-H}} = 6.9$  Hz,  $\text{CH}(\text{CH}_3)_2$ ), 4.09 (t, 1H,  $J_{\text{P-H}} = 17.0$  Hz,  $J_{\text{H-H}} = 17.0$  Hz,  $\text{CH}_2\text{-N-Ar}$ ), 4.97 (t, 1H,  $J_{\text{P-H}} = 17.0$  Hz,  $J_{\text{H-H}} = 17.0$  Hz,  $\text{CH}_2\text{-N-Ar}$ ), 6.95 (d, 1H,  $J_{\text{H-H}} = 7.5$  Hz, m-H Ph-P), 7.01 (t, 1H,  $J_{\text{H-H}} = 6.9$  Hz, p-H Ph-P), 7.10-7.20 (m, 6H, Ph-N), 7.28 (m, 1H,  $J_{\text{P-H}} \sim J_{\text{H-H}} = 7.3$  Hz, m-H Ph-P), 8.23 (s, 1H,  $\text{CH}=\text{N}$ ).  $^{13}\text{C}\{^1\text{H}\}$  NMR (101 MHz,  $\text{C}_6\text{D}_6$ ,  $22^\circ\text{C}$ ): 23.8 ( $\text{CH}_3$ ), 28.1, 28.6 ( $\text{CH}(\text{CH}_3)_2$ ), 62.4, 62.5 ( $\text{CH}_2\text{-N-Ar}$ ), 123.2, 123.6, 124.7, 130.0, 146.1, 128.3, 130.3, 137.7, 137.8, 148.7 (aromatic ring), 160.2 ( $\text{CH}=\text{N-Ar}$ ).  $^{31}\text{P}\{^1\text{H}\}$  NMR (162 MHz,  $\text{C}_6\text{D}_6$ ,  $22^\circ\text{C}$ ): 134.1 (s). **Anal. Calcd** for  $\text{C}_{32}\text{H}_{40}\text{ClN}_2\text{P}$ : C, 74.04; H, 7.77; N, 5.40. Found: C, 74.05; H, 8.04; N, 5.39%.

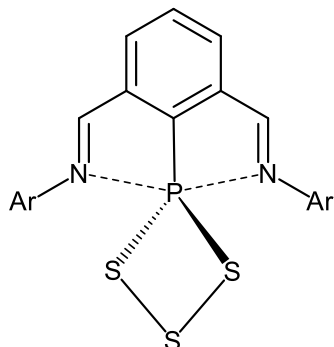


**VI-7**

**[[2,6-(2,6- $^i\text{Pr}_2\text{C}_6\text{H}_3\text{N}=\text{CH}$ ) $_2\text{C}_6\text{H}_3$ ] $_2\text{PBr}$ ][ $\text{Br}_3$ ]** (VI-7).

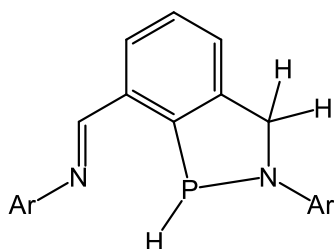
0.050 g (0.10 mmol) of **VI-2** was dissolved in 5 mL of toluene). Excess amount (6  $\mu\text{L}$ , 0.23 mmol) of  $\text{Br}_2$  was added into the above solution and the whole mixture was stirred for 30 mins at room temperature to give a suspension. The precipitate was filtered and dried to give a yellow solid as the final product. Yield: 0.072 g (0.09 mmol, 90%).  $^1\text{H NMR}$  (600 MHz,  $\text{CD}_2\text{Cl}_2$ ,  $22^\circ\text{C}$ ): 1.23-1.24 (d,  $J_{\text{H-H}} = 6.9$  Hz, 24H,  $^i\text{Pr-CH}_3$ ), 2.90 (sept, 4H,  $J_{\text{H-H}} = 6.9$  Hz,  $\text{CH}(\text{CH}_3)_2$ ), 7.32 (d,  $J_{\text{H-H}} = 7.8$  Hz, 4H, m-H Ph-N), 7.42 (t,  $J_{\text{H-H}} = 7.6$  Hz, 2H, p-H Ph-N), 8.27 (br, 1H, p-H Ph-P), 8.69 (br, 2H, m-H Ph-P), 9.04 (br, 2H,  $\text{CH}=\text{N-Ar}$ ).  $^{13}\text{C}\{^1\text{H}\}$  NMR (151 MHz,  $\text{CD}_2\text{Cl}_2$ ,  $22^\circ\text{C}$ ): 24.7 ( $\text{CH}_3$ ), 29.2 ( $\text{CH}(\text{CH}_3)_2$ ), 124.6, 127.8, 129.3, 135.6 (aromatic rings), 142.3 ( $\text{C}=\text{N-Ar}$ ).  $^{31}\text{P}\{^1\text{H}\}$  NMR (243 MHz,  $\text{CD}_2\text{Cl}_2$ ,  $22^\circ\text{C}$ ): 67.3 (br). **Anal. Calcd** for

0.945\* $C_{32}H_{39}Br_4N_2P$ /0.055\* $C_{32}H_{39}Br_2N_2P$ : C, 51.20; N, 5.24; N, 3.73. Found: C, 51.68; H, 5.55; N, 3.30 %.



**VI-8**

**[2,6-(2,6-<sup>i</sup>Pr<sub>2</sub>C<sub>6</sub>H<sub>3</sub>N=CH)<sub>2</sub>C<sub>6</sub>H<sub>3</sub>]PS<sub>3</sub> (VI-8).** 0.200 g (0.41 mmol) of **VI-2** was dissolved into toluene (10 mL). 0.013 g of ground sulphur was added to the above solution and the whole mixture was stirred at 80°C for 1 day. The precipitate was filtered, dried under vacuum, and dissolved in 1 mL of THF. A few drops of DCM were added into the THF solution. The mixture was kept at -30°C for a week to furnish the precipitate of pure **VI-8**. Yield: 0.123 g (0.12 mmol, 60%). <sup>1</sup>H NMR (400 MHz, CD<sub>2</sub>Cl<sub>2</sub>, 22°C): 1.20 (d, *J*<sub>H-H</sub> = 6.9 Hz, 24H, <sup>i</sup>Pr-CH<sub>3</sub>), 3.23 (sept, 4H, *J*<sub>H-H</sub> = 6.9 Hz, CH(CH<sub>3</sub>)<sub>2</sub>), 7.27-7.34 (m, 6H, Ph-N), 7.83 (t, 1H, *J*<sub>H-H</sub> = 7.5 Hz, p-H Ph-P), 8.46 (d, 2H, *J*<sub>H-H</sub> = 7.5 Hz, m-H Ph-P), 8.95 (d, 2H, *J*<sub>P-H</sub> = 1.7 Hz, CH=N-Ar). <sup>13</sup>C{<sup>1</sup>H} NMR (101 MHz, CD<sub>2</sub>Cl<sub>2</sub>, 22°C): 22.6, 24.7, 29.3 (CH<sub>3</sub>), 54.3 (CH(CH<sub>3</sub>)<sub>2</sub>), 122.9, 124.4, 128.0, 131.8, 134.1, 141.9 (aromatic ring), 160.8 (C=N-Ar). <sup>31</sup>P{<sup>1</sup>H} NMR (162 MHz, CD<sub>2</sub>Cl<sub>2</sub>, 22°C): 120.7 (s). **Anal. Calcd for C<sub>32</sub>H<sub>39</sub>N<sub>2</sub>PS<sub>3</sub>:** C, 66.40; H, 6.79; N, 4.84 Found: C, 67.46; H, 6.77; N, 4.46%.

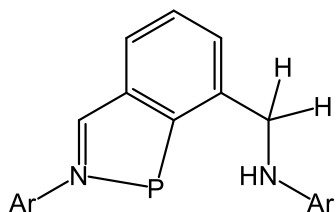


**VI-9**

**[2-(2,6-<sup>i</sup>Pr<sub>2</sub>C<sub>6</sub>H<sub>3</sub>N=CH)-6-(2,6-<sup>i</sup>Pr<sub>2</sub>C<sub>6</sub>H<sub>3</sub>N-CH<sub>2</sub>)]C<sub>6</sub>H<sub>3</sub>PH (VI-9).** 0.200 g (0.39 mmol) of **VI-2** was dissolved in 10 mL of toluene). 0.39 mL (0.39 mmol) of LiHBEt<sub>3</sub> (1M in THF) was added to the above solution and the whole mixture was stirred for 1 hour at room temperature. The precipitate was filtered off and the filtrate was dried under reduced pressure to obtain a yellow/brown solid. Yield: 0.170 g (0.35 mmol, 89%). <sup>1</sup>H NMR (400 MHz, C<sub>6</sub>D<sub>6</sub>, 22°C):

1.11 (d,  $J_{\text{H-H}} = 6.9$  Hz, 3H,  $^i\text{Pr-CH}_3$ ), 1.16 (t,  $J_{\text{H-H}} = 6.9$  Hz, 12H,  $\text{CH}_3$ ), 1.23 (t,  $J_{\text{H-H}} = 6.9$  Hz, 6H,  $^i\text{Pr-CH}_3$ ), 1.27 (d,  $J_{\text{H-H}} = 6.9$  Hz, 3H,  $^i\text{Pr-CH}_3$ ), 3.18 (m, 3H,  $\text{CH}(\text{CH}_3)_2$ ), 3.48 (sept, 1H,  $J_{\text{H-H}} = 6.9$  Hz,  $\text{CH}(\text{CH}_3)_2$ ), 4.41 (m, 1H,  $\text{CH}_2\text{-N-Ar}$ ), 4.84 (d of d, 1H,  $J_{\text{H-H}} = 7.8$  Hz,  $^2J_{\text{H-H}} = 14.2$  Hz,  $\text{CH}_2\text{-N-Ar}$ ), 6.80 (d of t, 1H,  $^1J_{\text{P-H}} = 164.9$  Hz,  $J_{\text{P-H}} = 7.4$  Hz, H-P), 6.98 (d, 1H,  $J_{\text{H-H}} = 7.5$  Hz, m-H Ph-P), 7.09 (t, 1H,  $J_{\text{H-H}} = 7.5$  Hz, p-H Ph-P), 7.10-7.20 (m, 6H, Ph-N), 7.21 (t, 1H,  $J_{\text{H-H}} = 7.5$  Hz, m-H Ph-P), 8.07 (s, 1H,  $\text{CH}=\text{N}$ ).  $^{13}\text{C}\{^1\text{H}\}$  NMR (101 MHz,  $\text{C}_6\text{D}_6$ , 22°C): 24.3, 24.7, 24.8, 25.5, 25.6 ( $\text{CH}_3$ ), 28.7, 29.1, 29.3 ( $\text{CH}(\text{CH}_3)_2$ ), 63.5, 63.6 ( $\text{CH}_2\text{-N-Ar}$ ), 123.7, 124.4, 125.0, 125.4, 127.9, 129.8, 136.6, 141.3, 141.7, 141.9, 146.9, 149.0, 149.3, 151.7 (aromatic ring), 162.1 ( $\text{C}=\text{N-Ar}$ ).  $^{31}\text{P}\{^1\text{H}\}$  NMR (400 MHz;  $\text{C}_6\text{D}_6$ ; 22°C): 19.9 (s).  $^{31}\text{P}$  NMR (162 MHz,  $\text{C}_6\text{D}_6$ , 22°C): 19.9 (d of d,  $^1J_{\text{P-H}} = 164.9$  Hz,  $^3J_{\text{P-H}} = 8.9$  Hz, P-H).

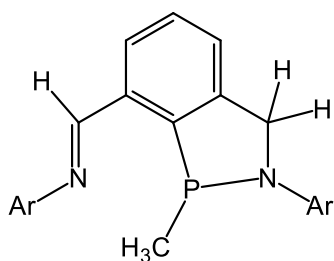
[2-(2,6- $^i\text{Pr}_2\text{C}_6\text{H}_3\text{N}=\text{CH}$ )-6-(2,6- $^i\text{Pr}_2\text{C}_6\text{H}_3\text{N}(\text{H})\text{CH}_2$ )] $\text{C}_6\text{H}_3\text{P}$  (VI-10). Compound



VI-10

VI-10 can be generated in quantitative yields by two methods: either heating phosphine VI-9 at 80°C overnight or by mixing a toluene solution of VI-9 with THF. Crystals of VI-9 were obtained from a toluene solution at -30°C.  $^1\text{H}$  NMR (400 MHz,  $\text{C}_6\text{D}_6$ , 22°C): 1.02 (d,  $J_{\text{H-H}} = 6.9$  Hz, 6H,  $^i\text{Pr-CH}_3$ ), 1.17-1.9 (d,  $J_{\text{H-H}} = 6.9$  Hz, 18 H,  $^i\text{Pr-CH}_3$ ), 2.50 (m, 2H,  $J_{\text{H-H}} = 6.9$  Hz,  $\text{CH}(\text{CH}_3)_2$ ), 3.54 (sept, 2H,  $J_{\text{H-H}} = 6.9$  Hz,  $\text{CH}(\text{CH}_3)_2$ ), 3.63 (t, 1H,  $J_{\text{H-H}} = 7.9$  Hz,  $\text{NH-Ar}$ ), 4.53 (d, 2H,  $J_{\text{H-H}} = 7.9$  Hz,  $\text{CH}_2\text{-NAr}$ ), 7.05-7.13 (m, 7H, m-H Ph-P & Ph-N), 7.23 (d, 1H,  $J_{\text{H-H}} = 7.5$  Hz, p-H Ph-P), 7.69 (d, 1H,  $J_{\text{H-H}} = 7.5$  Hz, m-H Ph-P), 7.72 (s, 1H,  $\text{CH}=\text{N}$ ).  $^{13}\text{C}\{^1\text{H}\}$  NMR (101 MHz,  $\text{C}_6\text{D}_6$ , 22°C): 24.5, 24.9, 25.5 ( $\text{CH}_3$ ), 28.2, 28.3 ( $\text{CH}(\text{CH}_3)_2$ ), 57.2 ( $\text{CH}_2\text{-N-Ar}$ ), 120.1, 123.3, 123.6, 124.1, 124.7, 127.8, 129.3, 132.2, 136.2, 137.7, 138.8, 138.9, 143.2 (aromatic ring),

157.8 (C=N-Ar).  $^{31}\text{P}\{^1\text{H}\}$  NMR (162 MHz,  $\text{C}_6\text{D}_6$ , 22°C): 174.7 (s). **Anal. Calcd** for  $\text{C}_{32}\text{H}_{41}\text{N}_2\text{P}$ : C, 79.30; H, 8.53; N, 5.78. Found: C, 78.27; H, 8.42; N, 5.49 %.



**VI-11**

**[2-(2,6- $^i\text{Pr}_2\text{C}_6\text{H}_3\text{N}=\text{CH}$ )-6-(2,6-**

**$^i\text{Pr}_2\text{C}_6\text{H}_3\text{N}(\text{H})\text{CH}_2$ )] $\text{C}_6\text{H}_3\text{PCH}_3$  (**VI-11**). 0.050 g (0.10**

mmol) of **VI-6** was dissolved into toluene (5 mL). 30  $\mu\text{L}$  (0.10

mmol) of MeMgBr (3M in EtO<sub>2</sub>) was added into above

solution and the whole mixture was stirred at room

temperature for 30 mins. The precipitate was filtered and the filtrate was dried under

vacuum to obtain a brown solid. The crude solid was washed by hexane to obtain the pure

solid of **VI-11**. Yield: 0.044 g (0.09 mmol, 90%).  $^1\text{H}$  NMR (600 MHz,  $\text{C}_6\text{D}_6$ , 22°C): 1.03

(d, 3H,  $J_{\text{H-H}} = 6.9$  Hz,  $^i\text{Pr-CH}_3$ ), 1.10 (t, Et<sub>2</sub>O), 1.17 (d, 6H,  $J_{\text{H-H}} = 6.9$  Hz,  $^i\text{Pr-CH}_3$ ), 1.23

(d, 9H,  $J_{\text{H-H}} = 6.9$  Hz,  $^i\text{Pr-CH}_3$ ), 1.30 (d, 3H,  $J_{\text{H-H}} = 6.9$  Hz,  $^i\text{Pr-CH}_3$ ), 1.37 (d, 3H,  $J_{\text{H-H}} =$

6.9 Hz,  $^i\text{Pr-CH}_3$ ), 1.50 (d, 3H,  $J_{\text{H-H}} = 5.0$  Hz,  $\text{CH}_3\text{-P}$ ), 3.03 (sept, 1H,  $J_{\text{H-H}} = 6.9$  Hz,

$\text{CH}(\text{CH}_3)_2$ ), 3.27 (m,  $\text{CH}(\text{CH}_3)_2$  overlapped with Et<sub>2</sub>O), 3.71 (sept, 1H,  $J_{\text{H-H}} = 6.9$  Hz,

$\text{CH}(\text{CH}_3)_2$ ), 4.24 (dd, 1 H,  $J_{\text{H-H}} = 7.9$  Hz,  $^2J_{\text{H-H}} = 15.0$  Hz,  $\text{CH}_2\text{-N-Ar}$ ), 5.03 (d, 1H,  $J_{\text{H-H}} =$

7.9 Hz  $\text{CH}_2\text{-N-Ar}$ ), 7.02 (d, 1H,  $J_{\text{H-H}} = 7.5$  Hz, m-H Ph-P), 7.08 (t, 1H,  $J_{\text{H-H}} = 7.5$  Hz, p-H

Ph-P), 7.10-7.25 (m, 6H, Ph-N & 1H, m-H Ph-P)), 8.18 (s, 1H,  $\text{CH}=\text{N-Ar}$ ).  $^{13}\text{C}\{^1\text{H}\}$  NMR

(151 MHz,  $\text{C}_6\text{D}_6$ , 22°C): 17.9, 18.3 ( $\text{CH}_3\text{-P}$ ), 23.8, 23.9, 24.6, 24.7, 24.9 ( $\text{CH}_3$ ), 28.6, 28.0,

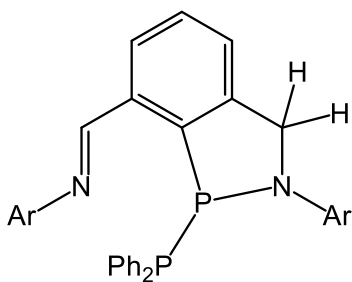
28.3 ( $\text{CH}(\text{CH}_3)_2$ ), 62.1( $\text{CH}_2\text{-N-Ar}$ ), 123.1, 123.3, 124.7, 129.8, 135.3, 137.6, 142.9, 146.0,

148.5, 149.1, 150.0 (aromatic ring), 161.9 (C=N-Ar).  $^{31}\text{P}\{^1\text{H}\}$  NMR (243 MHz,  $\text{C}_6\text{D}_6$ ,

22°C): 61.0 (s). **Anal. Calcd** for  $\text{C}_{33}\text{H}_{42}\text{N}_2\text{P}$ : C, 79.48; H, 8.69; N, 5.62. Found: C, 78.32;

H, 8.49; N, 5.32%.



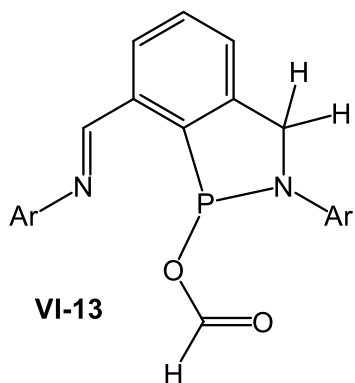


**VI-12**

**[2-(2,6-<sup>i</sup>Pr<sub>2</sub>C<sub>6</sub>H<sub>3</sub>N=CH)-6-(2,6-**

**<sup>i</sup>Pr<sub>2</sub>C<sub>6</sub>H<sub>3</sub>N(H)CH<sub>2</sub>)]C<sub>6</sub>H<sub>3</sub>P-PPh<sub>2</sub> (VI-12). 0.050g (0.10 mmol) of **VI-6** was dissolved into toluene (5 mL). 0.027 g (0.10 mmol) of Ph<sub>2</sub>PLi\*OEt<sub>2</sub> was added to the above solution and the whole mixture was stirred at room temperature for 30**

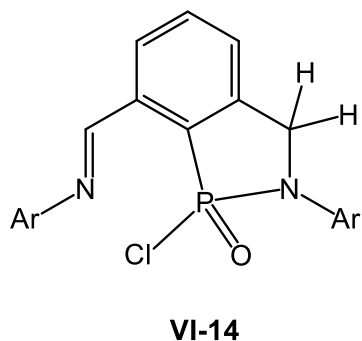
mins. The precipitate was filtered and the filtrate was dried under vacuum to obtain a brown solid. The crude solid was washed by hexane to obtain pure solid **VI-12**. Yield: 0.057 g (0.09 mmol, 86%). <sup>1</sup>H NMR (600 MHz, C<sub>6</sub>D<sub>6</sub>, 22°C): 0.89 (d, 3H, *J*<sub>H-H</sub> = 6.9 Hz, <sup>i</sup>Pr-CH<sub>3</sub>), 1.03 (d, 3H, *J*<sub>H-H</sub> = 6.9 Hz, <sup>i</sup>Pr-CH<sub>3</sub>), 1.07 (d, 3H, *J*<sub>H-H</sub> = 6.9 Hz, <sup>i</sup>Pr-CH<sub>3</sub>), 1.20 (d, 6H, *J*<sub>H-H</sub> = 6.9 Hz, <sup>i</sup>Pr-CH<sub>3</sub>), 1.28 (d, 6H, *J*<sub>H-H</sub> = 6.9 Hz, <sup>i</sup>Pr-CH<sub>3</sub>), 1.37 (d, 3H, *J*<sub>H-H</sub> = 6.9 Hz, <sup>i</sup>Pr-CH<sub>3</sub>), 2.98 (sept, 1H, *J*<sub>H-H</sub> = 6.9 Hz, CH(CH<sub>3</sub>)<sub>2</sub>), 3.47 (sept, 2H, *J*<sub>H-H</sub> = 6.9 Hz, CH(CH<sub>3</sub>)<sub>2</sub>), 3.81 (sept, 1H, *J*<sub>H-H</sub> = 6.9 Hz, CH(CH<sub>3</sub>)<sub>2</sub>), 3.87 (m, 1 H, CH<sub>2</sub>-NAr), 4.25 (dd, 1 H, *J*<sub>H-H</sub> = 14.9 Hz, *J*<sub>P-H</sub> = 11.5 Hz, CH<sub>2</sub>-N-Ar), 6.81-7.22 (m, 6H, Ph-N & 10H, PPh<sub>2</sub>), 7.37 (m, 1H, *J*<sub>H-H</sub> = 7.5 Hz, m-H Ph-P), 7.51 (t, 1H, *J*<sub>H-H</sub> = 7.5 Hz, p-H Ph-P), 7.73 (m, 1H, *J*<sub>H-H</sub> = 7.5 Hz, m-H Ph-P), 8.32 (s, 1H, CH=N). <sup>13</sup>C{<sup>1</sup>H} NMR (151 MHz, C<sub>6</sub>D<sub>6</sub>, 22°C): <sup>13</sup>C{<sup>1</sup>H} NMR (600 MHz; C<sub>6</sub>D<sub>6</sub>; 22°C): 23.1, 24.4, 24.5, 25.3, 26.4 (CH<sub>3</sub>), 28.4, 29.3, 29.4 (CH(CH<sub>3</sub>)<sub>2</sub>), 64.0, 64.1(CH<sub>2</sub>-N-Ar), 123.6, 124.0, 124.6, 125.0, 125.4, 134.1, 138.5, 143.9, 147.8, 148.4, 149.5, 149.9 (aromatic ring), 161.6 (C=N-Ar). <sup>31</sup>P{<sup>1</sup>H} NMR (243 MHz, C<sub>6</sub>D<sub>6</sub>, 22°C): 82.8 (d, <sup>1</sup>*J*<sub>P-P</sub> = 324.3 Hz, P-PPh<sub>2</sub>), 11.4 (d, <sup>1</sup>*J*<sub>P-P</sub> = 324.3 Hz, PPh<sub>2</sub>-P).



**[[2-(2,6-<sup>i</sup>Pr<sub>2</sub>C<sub>6</sub>H<sub>3</sub>N=CH)-6-(2,6-**

**<sup>i</sup>Pr<sub>2</sub>C<sub>6</sub>H<sub>3</sub>N(H)CH<sub>2</sub>)]C<sub>6</sub>H<sub>3</sub>P-OC(O)H (VI-13).** 0.100 g (0.20 mmol) of **VI-6** was dissolved into THF (5 mL). 0.013 g (0.20 mmol) of ammonium formate (NH<sub>4</sub>O<sub>2</sub>CH) was added to the above solution and the whole mixture was stirred at room temperature for 1 day. The volatiles were removed under

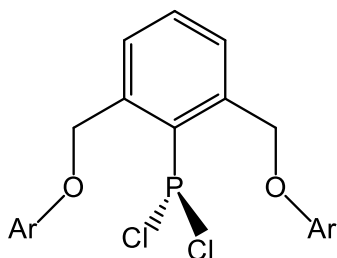
vacuum to obtain a brown solid. Crystals were obtained from a toluene solution at room temperature after 2 weeks. Yield: 0.095 g (0.18 mmol, 90%) **<sup>1</sup>H NMR** (400 MHz, C<sub>6</sub>D<sub>6</sub>, 22°C): 0.99 (d, 3H, *J*<sub>H-H</sub> = 6.9 Hz, CH<sub>3</sub>), 1.16-1.18 (t, 9H, *J*<sub>H-H</sub> = 6.9 Hz, CH<sub>3</sub>), 1.22-1.27 (t, 12H, *J*<sub>H-H</sub> = 6.9 Hz, CH<sub>3</sub>), 2.12 (CH<sub>3</sub>, toluene), 2.83 (sept, 1H, CH(CH<sub>3</sub>)<sub>2</sub>), 3.17 (sept, 2H, CH(CH<sub>3</sub>)<sub>2</sub>), 3.67 (sept, 1H, CH(CH<sub>3</sub>)<sub>2</sub>), 4.07 (m, 1H, CH<sub>2</sub>-N-Ar), 4.90 (m, 1H, CH<sub>2</sub>-N-Ar), 6.95 – 7.21 (m, 6H, Ph-N & 3H Ph-P), 8.10 (d, 1H, *J*<sub>H-H</sub> = 1.5 Hz, CH=N), 8.48 (d, 1H, *J*<sub>H-H</sub> = 1.5 Hz, C(O)H). **<sup>13</sup>C{<sup>1</sup>H} NMR** (101 MHz, C<sub>6</sub>D<sub>6</sub>, 22°C): 23.4, 24.1, 24.2, 24.7, 24.8, 25.0 (CH<sub>3</sub>), 28.0, 28.1, 28.5, 28.6 (CH(CH<sub>3</sub>)<sub>2</sub>), 62.3, 62.4 (CH<sub>2</sub>-N-Ar), 123.3, 124.1, 124.8, 125.0, 127.4, 127.6, 127.8, 127.9, 136.3, 137.8, 147.0, 148.4, 149.5 (aromatic rings), 160.7, 161.0 (C=N-Ar), 161.4 (O<sub>2</sub>CH). **<sup>31</sup>P{<sup>1</sup>H} NMR** (162 MHz, C<sub>6</sub>D<sub>6</sub>, 22°C): 124.6 (s). **Anal. Calcd** for C<sub>33</sub>H<sub>41</sub>N<sub>2</sub>O<sub>2</sub>P: C, 74.97; H, 7.82; N, 5.30. Found: C, 74.10; H, 9.78; N, 5.33 %.



**(2,6(2,6-<sup>i</sup>Pr<sub>2</sub>C<sub>6</sub>H<sub>3</sub>N=CH)<sub>2</sub>C<sub>6</sub>H<sub>3</sub>)<sub>2</sub>P=O(Cl) (VI-14).**

0.500 g (1.00 mmol) of was dissolved into toluene (10 mL). An equal amount (0.019 g, 0.40 mmol) of pyridine oxide was added into above solution and the whole mixture was stirred at room temperature for 1 day. The volatiles were removed

from the solution to obtain a light yellow solid with full conversion. Crystals were obtained from a toluene solution at  $-30^{\circ}\text{C}$ . Yield: 0.198 g (0.37 mmol, 93%).  $^1\text{H NMR}$  (400 MHz,  $\text{C}_6\text{D}_6$ ,  $22^{\circ}\text{C}$ ): 1.02 (d, 3H,  $J_{\text{H-H}} = 6.9$  Hz,  $^i\text{Pr-CH}_3$ ), 1.14 (d, 3H,  $J_{\text{H-H}} = 6.9$  Hz,  $^i\text{Pr-CH}_3$ ), 1.24 (d, 15H,  $J_{\text{H-H}} = 6.9$  Hz,  $^i\text{Pr-CH}_3$ ), 1.46 (d, 3H,  $J_{\text{H-H}} = 6.9$  Hz,  $^i\text{Pr-CH}_3$ ), 3.32 (sept, 3H,  $J_{\text{H-H}} = 6.9$  Hz,  $\text{CH}(\text{CH}_3)_2$ ), 3.45 (sept, 3H,  $J_{\text{H-H}} = 6.9$  Hz,  $\text{CH}(\text{CH}_3)_2$ ), 4.13 (t, 1H,  $J_{\text{H-H}} = 14.2$  Hz,  $J_{\text{P-H}} = 13.3$  Hz,  $\text{CH}_2\text{-N-Ar}$ ), 4.38 (dd, 1H,  $J_{\text{H-H}} = 14.2$  Hz,  $J_{\text{P-H}} = 3.6$  Hz,  $\text{CH}_2\text{-N-Ar}$ ), 6.62 (1H,  $J_{\text{H-H}} = 7.5$  Hz, m-H Ph-P), 7.06-7.18 (m, 6H, Ph-N & 1H, p-H Ph-P), 8.48 (1H,  $J_{\text{H-H}} = 7.5$  Hz, m-H Ph-P), 9.42 (d, 1H,  $\text{CH}=\text{N}$ ).  $^{13}\text{C}\{^1\text{H}\}$  NMR (101 MHz,  $\text{C}_6\text{D}_6$ ,  $22^{\circ}\text{C}$ ): 24.2, 24.3, 24.9, 25.1, 26.1 ( $\text{CH}_3$ ), 28.9, 29.2, 29.5 ( $\text{CH}(\text{CH}_3)_2$ ), 55.9, 56.2 ( $\text{CH}_2\text{-N-Ar}$ ), 124.1, 125.3, 125.7, 126.5, 127.4, 130.0, 130.4, 131.4, 131.9, 133.5, 137.3, 137.4, 138.1, 140.5, 140.7, 149.5, 149.7, 150.4 (aromatic ring), 158.3, 158.4 ( $\text{C}=\text{N-Ar}$ ).  $^{31}\text{P}\{^1\text{H}\}$  NMR (162 MHz,  $\text{C}_6\text{D}_6$ ,  $22^{\circ}\text{C}$ ): 29.1 (s,  $\text{P}=\text{O}(\text{Cl})$ ). **Anal. Calcd** for  $\text{C}_{32}\text{H}_{40}\text{ClN}_2\text{OP}$ : C, 71.83; H, 7.53; N, 5.24. Found: C, 72.10; H, 7.63; N, 5.12%.



**VI-16**

**Synthesis of (2,6-(2,6- $^i\text{Pr}_2\text{C}_6\text{H}_3\text{OCH}_2$ ) $_2\text{C}_6\text{H}_3$ ) $\text{PCl}_2$  (VI-16).**

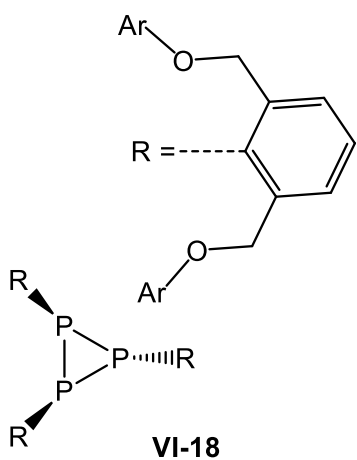
The solution of 2,6-(2,6- $^i\text{Pr}_2\text{C}_6\text{H}_3\text{OCH}_2$ ) $\text{C}_6\text{H}_3$ -1-Br (0.955 g, 1.78 mmol) was suspended in hexane solvent (20 mL).

Then, a solution of *n*BuLi (1.6 M in hexane) (1.20 mL, 1.90

mmol) was added dropwise into the suspension at room

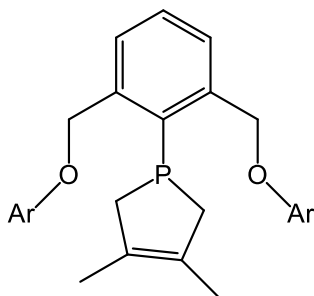
temperature. The white precipitate was formed after 10 mins. The whole mixture was stirred for 1 day at room temperature. The white precipitate was filtered and dissolved in toluene (10 mL). This solution was added dropwise into  $\text{PCl}_3$  solution (0.16 mL, 1.78) in hexane (5 mL) at  $0^{\circ}\text{C}$ . The solution was stirred for 1 day at room temperature. LiCl salt was filtered off and the volatiles were removed under vacuum to give a white oil. The pure

solid of VI-16 was obtained from crystallization from toluene/hexane mixture at  $-30^{\circ}\text{C}$ . Yield: 0.750 g, 1.40 mmol, 80%.  $^1\text{H NMR}$  (600 MHz,  $\text{C}_6\text{D}_6$ ,  $22^{\circ}\text{C}$ ):  $\delta$  (ppm) = 1.22 (d, 24H,  $J_{\text{H-H}} = 6.9$  Hz,  $^i\text{Pr-CH}_3$ ), 3.48 (sept, 4H,  $J_{\text{H-H}} = 6.9$  Hz,  $\text{CH}(\text{CH}_3)_2$ ), 5.39 (s, 4H,  $\text{CH}_2\text{-O}$ ) 7.10-7.11 (m, 6H, Ph-O), 7.23 (t, 1H,  $J_{\text{H-H}} = 7.5$  Hz, p-H Ph-P), 7.78 (m, 2H, m-H Ph-P).  $^{13}\text{C}\{^1\text{H}\}$  NMR (151 MHz,  $\text{C}_6\text{D}_6$ ,  $25^{\circ}\text{C}$ ):  $\delta$  (ppm) = 24.3 ( $^i\text{Pr-CH}_3$ ), 27.2 ( $-\text{CH}(\text{CH}_3)_2$ ), 74.1 ( $\text{CH}_2\text{-O-}$ ), 124.3 - 148.9 (aromatic ring), 153.8 ( $\text{C-O}(\text{CH}_2)$ ).  $^{31}\text{P}\{^1\text{H}\}$  NMR (243 MHz,  $\text{C}_6\text{D}_6$ ,  $22^{\circ}\text{C}$ ): 158.5 (s). **Anal. Calcd** for  $\text{C}_{32}\text{H}_{41}\text{Cl}_2\text{O}_2\text{P}$ : C, 68.69; H, 7.39. Found: C, 68.91; H, 7.42 %.



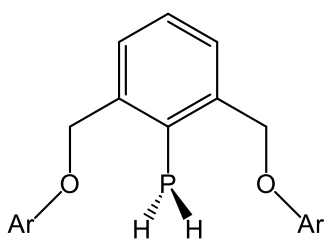
**(2,6-(2,6- $^i\text{Pr}_2\text{C}_6\text{H}_3\text{OCH}_2$ ) $\text{C}_6\text{H}_3$ ) $_2\text{P}_2\text{R}_4$  (VI-18)** was prepared via two different methods: **The method 1:** 0.100 g (0.18 mmol) of **VI-16** was dissolved into benzene. 0.050 g (0.37 mmol) of  $\text{KC}_8$  was added into above solution. The whole mixture was stirred for 18 hours at room temperature. The precipitate was filtered off and dried to give a crude solid of **VI-18**. **The method 2:** 0.100 g (0.18 mmol) of **VI-16** was dissolved into benzene. 22  $\mu\text{L}$  (0.22 mmol) of  $\text{PMe}_3$  was added into solution of **VI-16**. The white precipitate was formed within 5 mins and was filtered off. The volatiles were removed under vacuum and the obtained solid was dissolved into 2 mL of  $\text{Et}_2\text{O}$  for the purification. The pure solid of **VI-18** was formed from  $\text{Et}_2\text{O}$  solution after 2 days at  $-30^{\circ}\text{C}$ .  $^1\text{H NMR}$  (600 MHz,  $\text{C}_6\text{D}_6$ ,  $22^{\circ}\text{C}$ ):  $\delta$  (ppm) = 1.09 (d, 24H,  $J_{\text{H-H}} = 6.9$  Hz,  $^i\text{Pr-CH}_3$ ), 1.12 (d, 48H,  $J_{\text{H-H}} = 6.9$  Hz,  $^i\text{Pr-CH}_3$ ), 3.24 (sept, 8H,  $J_{\text{H-H}} = 6.9$  Hz,  $\text{CH}(\text{CH}_3)_2$ ), 3.34 (sept, 4H,  $J_{\text{H-H}} = 6.9$  Hz,  $\text{CH}(\text{CH}_3)_2$ ), 4.97(s, 4H,  $\text{CH}_2\text{-O}$ ), 5.70 (s, 4H,  $\text{CH}_2\text{-O}$ ), 5.75 (s, 4H,  $\text{CH}_2\text{-O}$ ) 6.99 (m, 6H, Ph-O), 7.00 (m, 12H, Ph-O), 7.14 (t, 2H,  $J_{\text{H-H}} = 7.5$  Hz, p-H Ph-P), 7.24 (t,

1H,  $J_{H-H} = 7.5$  Hz, p-H Ph-P), 7.55 (d, 4H,  $J_{H-H} = 7.5$  Hz, m-H Ph-P) 8.00 (d, 2H,  $J_{H-H} = 7.5$  Hz, m-H Ph-P).  $^{13}\text{C}\{^1\text{H}\}$  NMR (151 MHz,  $\text{C}_6\text{D}_6$ , 22°C):  $\delta$  (ppm) = 24.2, 24.3 ( $^i\text{Pr-CH}_3$ ), 27.1, 27.2 ( $\text{CH}(\text{CH}_3)_2$ ), 74.9, 75.6 ( $\text{CH}_2\text{-O}$ ), 124.4 – 142.1 (aromatic ring), 153.6 ( $\text{C-O-CH}_2$ ).  $^{31}\text{P}\{^1\text{H}\}$  NMR (243 MHz,  $\text{C}_6\text{D}_6$ , 22°C): -113.9 (d,  $J_{\text{P-P}} = 192.7$  Hz), -150.2 (t,  $J_{\text{P-P}} = 192.7$  Hz). **Anal. Calcd** for  $\text{C}_9\text{H}_{123}\text{O}_6\text{P}_3$ : C, 78.66; H, 8.46. Found: C, 77.96; H, 8.92%.



**VI-19**

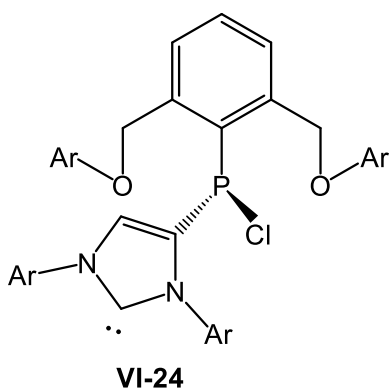
**(2,6-(2,6- $^i\text{Pr}_2\text{C}_6\text{H}_3\text{OCH}_2$ ) $_2\text{C}_6\text{H}_3$ )P( $\eta^2\text{-C,C}$ ) (VI-19).** 0.100 g (0.18 mmol) of **VI-16** was dissolved into benzene. 20  $\mu\text{L}$  g (0.18 mmol) of 2,3-dimethyl-1,3-butadiene was added into solution of **VI-16**. The whole solution was stirred for 10mins before adding 0.050 g (0.36 mmol) of  $\text{KC}_8$  into the mixture. The whole suspension was stirred for 3 days. The precipitate was filtered off and the solution was dried to give a crude solid of **VI-19**.  $^1\text{H}$  NMR (600 MHz,  $\text{C}_6\text{D}_6$ , 22°C):  $\delta$  (ppm) = 1.22 (d, 24H,  $J_{H-H} = 6.9$  Hz,  $^i\text{Pr-CH}_3$ ), 1.31 (s, 6H,  $\text{CH}_3\text{-butadiene}$ ), 2.70 (m, 4H,  $\text{CH}_2\text{-butadiene}$ ), 3.49 (sept, 4H,  $J_{H-H} = 6.9$  Hz,  $\text{CH}(\text{CH}_3)_2$ ), 5.29 (s, 4H,  $\text{CH}_2\text{-O}$ ) 6.95-7.12 (m, 6H, Ph-O), 7.36 (t, 1H,  $J_{H-H} = 7.5$  Hz, p-H Ph-P), 7.95 (d, 2H,  $J_{H-H} = 7.5$  Hz, m-H Ph-P).  $^{31}\text{P}\{^1\text{H}\}$  NMR (243 MHz,  $\text{C}_6\text{D}_6$ , 22°C): 50.0 (s).



**VI-23**

**(2,6-(2,6- $^i\text{Pr}_2\text{C}_6\text{H}_3\text{OCH}_2$ ) $_2\text{C}_6\text{H}_3$ )PH $_2$  (VI-23)** was obtained via two different methods either using  $\text{PhSiH}_3$  or  $\text{HBpin}$ : 0.050 g (0.09 mmol) of **VI-16** was dissolved into benzene. Either 11  $\mu\text{L}$  g (0.09 mmol) of  $\text{PhSiH}_3$  or 13  $\mu\text{L}$  g (0.09 mmol) of  $\text{HBpin}$  was added into solution of **VI-16**. The whole solution was stirred for 10mins before adding 0.14  $\mu\text{L}$  (0.14 mmol) of  $\text{PMe}_3$  into the mixture. The precipitate was formed after 20 mins and the whole mixture was stirred for another 1 hour.

The precipitate was filtered off and the solution was dried to give a white solid of **VI-23**.  $^1\text{H NMR}$  (600 MHz,  $\text{C}_6\text{D}_6$ ,  $22^\circ\text{C}$ ):  $\delta$  (ppm) = 1.22 (d, 24H,  $J_{\text{H-H}} = 6.9$  Hz,  $^i\text{Pr-CH}_3$ ), 3.34, 3.68 (d, 2H,  $J_{\text{P-H}} = 203.4$  Hz,  $\text{PH}_2$ ), 3.49 (sept, 4H,  $J_{\text{H-H}} = 6.9$  Hz,  $\text{CH}(\text{CH}_3)_2$ ), 4.95 (s, 4H,  $\text{CH}_2\text{-O}$ ) 7.07-7.12 (m, 6H, Ph-O), 7.29 (t, 1H,  $J_{\text{H-H}} = 7.5$  Hz, p-H Ph-P), 7.78 (d, 2H,  $J_{\text{H-H}} = 7.5$  Hz, m-H Ph-P).  $^{13}\text{C}\{^1\text{H}\}$  NMR (151 MHz,  $\text{C}_6\text{D}_6$ ,  $22^\circ\text{C}$ ):  $\delta$  (ppm) = 24.3 ( $^i\text{Pr-CH}_3$ ), 27.2 ( $\text{CH}(\text{CH}_3)_2$ ), 76.1 ( $\text{CH}_2\text{-O}$ ), 124.6 – 142.2 (aromatic ring), 154.1 (C-O- $\text{CH}_2$ ).  $^{31}\text{P}\{^1\text{H}\}$  NMR (243 MHz,  $\text{C}_6\text{D}_6$ ,  $22^\circ\text{C}$ ): -162.1 (s).  $^{31}\text{P}$  NMR (243 MHz,  $\text{C}_6\text{D}_6$ ,  $22^\circ\text{C}$ ): -162.1 (t,  $J_{\text{P-H}} = 211.4$  Hz).

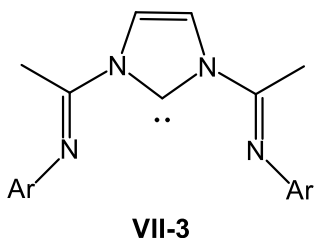


**Synthesis of (2,6-(2,6-**  
 **$^i\text{Pr}_2\text{C}_6\text{H}_3\text{OCH}_2)_2\text{C}_6\text{H}_3\text{P}(\text{Cl})\text{NHC}$  (VI-24).** 0.100 g (0.18  
 mmol) of **VI-16** was dissolved into benzene. 0.140 g (0.36  
 mmol) of NHC carbene was added into above solution.  
 The whole mixture was stirred for 1 hour at room  
 temperature. The white precipitate was formed and was

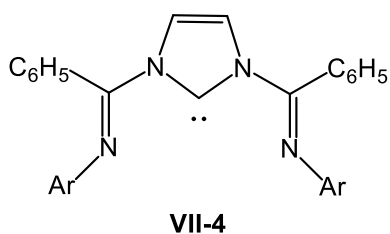
filtered off. The volatiles were removed under vacuum and the obtained solid was dissolved into 2 mL of hexane for the purification. The pure solid of **VI-24** was formed from hexane solution after a week at  $-30^\circ\text{C}$ .  $^1\text{H NMR}$  (600 MHz,  $\text{C}_6\text{D}_6$ ,  $22^\circ\text{C}$ ):  $\delta$  (ppm) = 0.69 (d, 3H,  $J_{\text{H-H}} = 6.9$  Hz,  $^i\text{Pr-CH}_3$ ), 0.72 (d, 3H,  $J_{\text{H-H}} = 6.9$  Hz,  $^i\text{Pr-CH}_3$ ), 1.07 (d, 3H,  $J_{\text{H-H}} = 6.9$  Hz,  $^i\text{Pr-CH}_3$ ), 1.15 (d, 3H,  $J_{\text{H-H}} = 6.9$  Hz,  $^i\text{Pr-CH}_3$ ), 1.22 - 1.27 (m, 36H,  $^i\text{Pr-CH}_3$ ), 2.49 (sept, 1H,  $J_{\text{H-H}} = 6.9$  Hz,  $\text{CH}(\text{CH}_3)_2$  of [NHC]), 2.73 (sept, 1H,  $J_{\text{H-H}} = 6.9$  Hz,  $\text{CH}(\text{CH}_3)_2$  of [NHC]), 2.84 (sept, 1H,  $J_{\text{H-H}} = 6.9$  Hz,  $\text{CH}(\text{CH}_3)_2$  of [NHC]), 3.00 (sept, 1H,  $J_{\text{H-H}} = 6.9$  Hz,  $\text{CH}(\text{CH}_3)_2$  of [NHC]), 3.46 (br, 4H,  $\text{CH}(\text{CH}_3)_2$  of [OCO]), 5.27 (s, 2H,  $\text{CH}_2\text{-O}$ ) 7.20, (s, 2H,  $\text{CH}_2\text{-O}$ ), 6.92 - 7.29 (m, 13H, Ph & 1H,  $\text{NC}(\text{H}=\text{C})$ ), 8.01 (br, 2H, Ph-O).  $^{13}\text{C}\{^1\text{H}\}$

**NMR** (151 MHz, C<sub>6</sub>D<sub>6</sub>, 22°C):  $\delta$  (ppm) = 21.2, 22.1, 23.4, 24.0, 24.2, 24.4, 24.6, 26.1 (<sup>i</sup>Pr-CH<sub>3</sub>), 27.2, 28.7, 28.8, 29.7 (CH(CH<sub>3</sub>)<sub>2</sub>), 73.5 (CH<sub>2</sub>-O), 123.4 – 147.3 (aromatic ring & N-C(H)=C(P)-N), 153.0 (-NCN-). **<sup>31</sup>P{<sup>1</sup>H} NMR** (243 MHz, C<sub>6</sub>D<sub>6</sub>, 22°C):  $\delta$  (ppm) = 51.9 (s).

IX.6 Experimental Procedures for Chapter VII



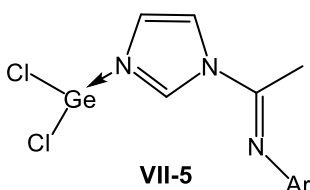
**[(2,6-<sup>i</sup>Pr<sub>2</sub>C<sub>6</sub>H<sub>3</sub>N=C(CH<sub>3</sub>))<sub>2</sub>NHC (VII-3).** 0.167 g (1.00 mmol) of lithium bis(trimethylsilyl)amide was dissolved in hexane (5mL) and dropwise add into a hexane (15mL) suspension of 1,3-bis[1-(2,6-dimethylphenylimino)ethyl]imidazolium chloride ( 0.508 g, 1.00 mmol) at -78°C. The mixture was stirred for 4 hours at -78°C and brought to room temperature in 12 hours. The precipitate was filtered off and dried to obtain a crude yellow solid. This solid was washed by cooled hexane (2ml) to give a pure solid of compound **VII-3**. Yield: 0.250 g (0.53 mmol, 53%). <sup>1</sup>H NMR (600 MHz, C<sub>6</sub>D<sub>6</sub>, 22°C): δ = 1.12 (d, 12H, *J*<sub>H-H</sub> = 6.9 Hz, <sup>i</sup>Pr-CH<sub>3</sub>), 1.18 (d, 12H, *J*<sub>H-H</sub> = 6.9 Hz, <sup>i</sup>Pr-CH<sub>3</sub>), 2.47 (s, 6H, CH<sub>3</sub>-C=N), 2.93 (sept, 4H, *J*<sub>H-H</sub> = 6.9 Hz, CH(CH<sub>3</sub>)<sub>2</sub>), 7.13-7.18 (m, 4H, Ph-N), 7.18 (d, 2H, *J*<sub>H-H</sub> = 3.40 Hz, Ph-N), 8.06 (s, 2H, NC(H)=C(H)N).



**[(2,6-<sup>i</sup>Pr<sub>2</sub>C<sub>6</sub>H<sub>3</sub>N=C(C<sub>6</sub>H<sub>5</sub>))<sub>2</sub>NHC]<sub>2</sub> (VII-4).** 0.171 g (1.03 mmol) of lithium bis(trimethylsilyl)amide was dissolved in THF (5mL) and dropwise add into a THF (15mL) solution of 1,3-bis[(2,6-dimethylphenylimino)benzyl]imidazolium tetrafluoroborate ( 0.700 g, 1.02 mmol) at -78°C. The mixture was stirred for 4 hours at -78°C and brought to room temperature in 12 hours. The solution was dried under vacuum to obtain a crude yellow solid. This solid was washed by cooled hexane (2ml) to give a pure solid of compound **VII-4**. Yield: 0.420 g (0.70 mmol, 70%). <sup>1</sup>H NMR (600 MHz, C<sub>6</sub>D<sub>6</sub>, 22°C): δ = 0.61 (d, 6H, *J*<sub>H-H</sub> = 6.9 Hz, <sup>i</sup>Pr-CH<sub>3</sub>), 0.79 (d, 6H, *J*<sub>H-H</sub> = 6.9 Hz, <sup>i</sup>Pr-CH<sub>3</sub>), 0.99 (d, 6H, *J*<sub>H-H</sub> = 6.9 Hz, <sup>i</sup>Pr-CH<sub>3</sub>), 1.17 (d,

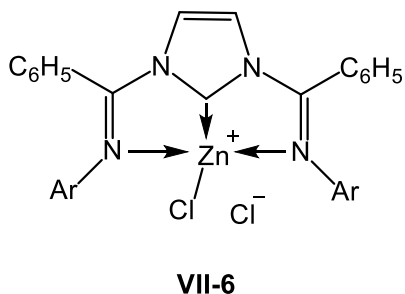


6H,  $J_{H-H} = 6.9$  Hz,  $^i\text{Pr-CH}_3$ ), 2.50 (br, 2H,  $\text{CH}(\text{CH}_3)_2$ ), 3.08 (br, 2H,  $\text{CH}(\text{CH}_3)_2$ ), 6.71-7.19 (m, 16H, Ph), 7.51 (s, 1H,  $\text{NC}(\text{H})=\text{C}(\text{H})\text{N}$ ), 7.26 (s, 1H,  $\text{NC}(\text{H})=\text{C}(\text{H})\text{N}$ ).  $^{13}\text{C}\{^1\text{H}\}$  NMR (151 MHz,  $\text{C}_6\text{D}_6$ ,  $22^\circ\text{C}$ ): 22.5, 23.0, 24.1, 24.9 ( $\text{CH}_3$ ), 28.2, 28.7 ( $\text{CH}(\text{CH}_3)_2$ ), 124.2, 129.4 ( $\text{NC}(\text{H})=\text{C}(\text{H})\text{N}$ ), 123.5 – 148.2 (aromatic ring), 151.2, ( $\text{C}=\text{N-Ar}$ ), 158.3 (NCN).



**[1-(2,6- $^i\text{Pr}_2\text{C}_6\text{H}_3\text{N}=\text{C}(\text{CH}_3))\text{NC}(\text{H})\text{NGeCl}_2$  (VII-5). 0.400**

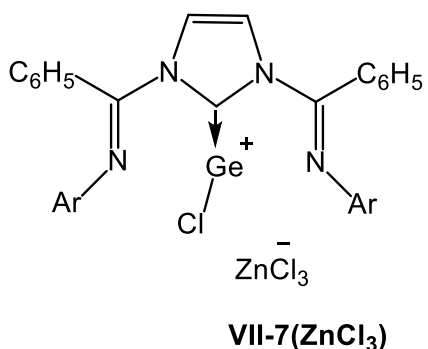
g (0.85 mmol) of **VII-3** was dissolved into benzene (5 mL). A benzene solution of  $\text{GeCl}_2$ .dioxane (0.330 g, 1.70 mmol) was added into the above solution. The mixture was stirred for 4 hours at room temperature. The precipitate was filtered off and dried to obtain a crude yellow/brown solid. This solid was dissolved in 3ml of ACN. Crystals of **VII-5** were obtained from ACN solution at  $-30^\circ\text{C}$ . Yield: 0.250 g (0.61 mmol, 72%).  $^1\text{H}$  NMR (400 MHz,  $\text{C}_6\text{D}_6$ ,  $22^\circ\text{C}$ ):  $\delta = 0.99$  (d, 6H,  $J_{H-H} = 6.9$  Hz,  $^i\text{Pr-CH}_3$ ), 1.03 (s, 3H,  $\text{H}_3\text{C-C}=\text{N}$ ), 1.03 (d, 6H,  $J_{H-H} = 6.9$  Hz,  $^i\text{Pr-CH}_3$ ), 2.41 (sept, 2H,  $J_{H-H} = 6.9$  Hz,  $\text{CH}(\text{CH}_3)_2$ ), 6.79 (br, 1H,  $\text{NC}(\text{H})=\text{C}(\text{H})\text{N}$ ), 7.08 (m, 3H, Ph-N), 7.13 (br, 1H,  $\text{NC}(\text{H})=\text{C}(\text{H})\text{N}$ ), 8.07 (br, 1H,  $\text{NC}(\text{H})\text{N}$ ).



**[(2,6- $^i\text{Pr}_2\text{C}_6\text{H}_3\text{N}=\text{C}(\text{C}_6\text{H}_5))_2\text{NHC}]\text{ZnCl}/\text{Cl}$  (VII-6). 0.247 g (1.48 mmol) of lithium bis(trimethylsilyl)amide was dissolved in THF (10 mL) and added dropwise into a THF (5 mL) solution of  $\text{ZnCl}_2$  (0.200g, 1.46 mmol) at  $-78^\circ\text{C}$ . The solution was stirred**

for 2 hours at  $-78^\circ\text{C}$ . A THF (10 mL) solution of 1,3-bis[(2,6 dimethylphenylimino)benzyl]imidazolium tetrafluoroborate (1.000g, 1.46 mmol) was added into above mixture at  $-78^\circ\text{C}$ . The solution was stirred for 2 hours at  $-78^\circ\text{C}$  and allowed to warm up to room temperature overnight. The volatiles were removed under

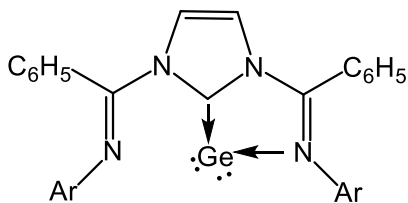
vacuum to obtain a crude yellow solid. This solid was washed by toluene and hexane to give solid of **VII-6** containing LiCl. Crystals of pure **VII-6** were obtained from DCM/hexane mixture at room temperature. Yield: 0.882g = 0.820 g of **VII-6** (1.18 mmol, 78%) + 0.062 g LiCl (estimated amount from the calculation: 42.39 g/mole x 1.48 mmol). **<sup>1</sup>H NMR** (600 MHz, CDCl<sub>3</sub>, 22°C): δ = 0.91 (d, 12H, *J*<sub>H-H</sub> = 6.9 Hz, <sup>i</sup>Pr-CH<sub>3</sub>), 1.22 (d, 12H, *J*<sub>H-H</sub> = 6.9 Hz, <sup>i</sup>Pr-CH<sub>3</sub>), 3.04 (sept, 4H, *J*<sub>H-H</sub> = 6.9 Hz, CH(CH<sub>3</sub>)<sub>2</sub>), 5.32 (s, DCM residue), 7.04 (d, 4H, *J*<sub>H-H</sub> = 7.5 Hz, m-H Ph-N), 7.11 (t, 2H, *J*<sub>H-H</sub> = 7.5 Hz, p-H Ph-N), 7.39-7.47 (m, 10H, Ph-C=N), 7.82 (s, 2H, NC(H)=C(H)N). **<sup>13</sup>C{<sup>1</sup>H} NMR** (151 MHz, CDCl<sub>3</sub>, 22°C): 22.9, 25.2 (CH<sub>3</sub>), 28.6 (CH(CH<sub>3</sub>)<sub>2</sub>), 53.6 (DCM residue), 121.0 (NC(H)=C(H)N), 123.8, 126.2, 127.3 (Ph-N), 129.5, 129.7, 132.3, 138.4, 139.7 (Ph-C=N), 153.1, (C=N-Ar), 180.8, (NCN). **Anal. Calcd** for C<sub>41</sub>H<sub>48</sub>Cl<sub>2</sub>N<sub>4</sub>Zn: C, 67.14; H, 6.60; N, 7.64. Found: C, 67.38; H, 6.19; N, 7.56 %.



**[(2,6-<sup>i</sup>Pr<sub>2</sub>C<sub>6</sub>H<sub>3</sub>N=C(C<sub>6</sub>H<sub>5</sub>))<sub>2</sub>NHC]GeCl/ZnCl<sub>3</sub>**  
**(VII-7(ZnCl<sub>3</sub>))**. 0.370 g (0.51 mmol) of **VII-6** was suspended into benzene (15 mL). 0.150 g (0.65 mmol) of GeCl<sub>2</sub>.dioxane was added into this suspension. The mixture was stirred for 1 day at room temperature. The precipitate was filtered and dried to obtain a yellow solid of compound **VII-7(ZnCl<sub>3</sub>)**.

Yield: 0.424 g (0.48 mmol, 96%). **<sup>1</sup>H NMR** (600 MHz, CDCl<sub>3</sub>, 22°C): δ = 0.71 (br, 6H, CH<sub>3</sub>), 1.04 (br, 6H, <sup>i</sup>Pr-CH<sub>3</sub>), 1.20 (br, 12H, <sup>i</sup>Pr-CH<sub>3</sub>), 2.94 (br, 2H, CH(CH<sub>3</sub>)<sub>2</sub>), 3.30 (br, 2H, CH(CH<sub>3</sub>)<sub>2</sub>), 7.09 (br, 4H, m-H Ph-N), 7.20 (t, 2H, *J*<sub>H-H</sub> = 7.5 Hz, p-H Ph-N), 7.44-7.54 (m, 10H, Ph-C=N), 7.76 (s, 2H, NC(H)=C(H)N). **<sup>13</sup>C{<sup>1</sup>H} NMR** (151 MHz, CDCl<sub>3</sub>, 22°C): 23.2, 25.7, 26.2 (CH<sub>3</sub>), 28.6, 28.7 (CH(CH<sub>3</sub>)<sub>2</sub>), 123.4 (NC(H)=C(H)N), 124.4, 125.0, 127.6

(Ph-N), 129.5, 130.3, 133.3, 137.5, 139.8, 140.6 (Ph-C=N), 153.8, (C=N-Ar), 178.2, (NCN).

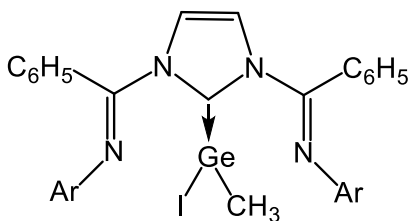


**VII-8**

**[(2,6-<sup>i</sup>Pr<sub>2</sub>C<sub>6</sub>H<sub>3</sub>N=C(C<sub>6</sub>H<sub>5</sub>))<sub>2</sub>NHC]Ge (VII-8).**

0.400 g (0.45 mmol) of **VII-7**(ZnCl<sub>3</sub>) was suspended into benzene (15 mL). 0.305 g (2.25 mmol) of KC<sub>8</sub> was added into this suspension. The solution was stirred for 4 hours at room temperature. The precipitate was filtered

off and dried to obtain a red solid of compound **VII-8**. Crystals of **VII-8** were obtained from benzene solution at room temperature. Yield: 0.228 g (0.34 mmol, 76%). <sup>1</sup>H NMR (600 MHz, C<sub>6</sub>D<sub>6</sub>, 22°C): δ = 1.01 (d, 12H, J<sub>H-H</sub> = 6.9 Hz, <sup>i</sup>Pr-CH<sub>3</sub>), 1.40 (d, 12H, J<sub>H-H</sub> = 6.9 Hz, <sup>i</sup>Pr-CH<sub>3</sub>), 3.21 (sept, 4H, J<sub>H-H</sub> = 6.9 Hz, CH(CH<sub>3</sub>)<sub>2</sub>), 6.81 (s, 2H, NC(H)=C(H)N), 6.84 (t, 2H, J<sub>H-H</sub> = 7.5 Hz, p-H Ph-C=N), 6.92 (t, 4H, J<sub>H-H</sub> = 7.5 Hz, m-H Ph-C=N), 7.01 (m, 6H, Ph-N), 7.19 (d, J<sub>H-H</sub> = 7.5 Hz, o-H Ph-C=N) <sup>13</sup>C{<sup>1</sup>H} NMR (151 MHz, C<sub>6</sub>D<sub>6</sub>, 22°C): 22.6, 26.5 (CH<sub>3</sub>), 28.5 (CH(CH<sub>3</sub>)<sub>2</sub>), 116.4 (NC(H)=C(H)N), 123.2 (Ph-N), 127.9, 128.1, 128.2, 128.6, 128.9 (Ph-C=N), 141.2, 143.0 (C=N-Ar), 176.1 (NCN).



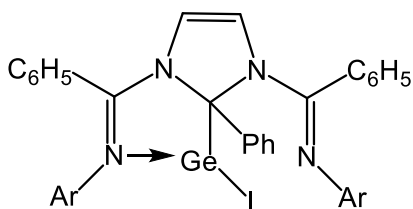
**VII-9**

**[(2,6-<sup>i</sup>Pr<sub>2</sub>C<sub>6</sub>H<sub>3</sub>N=C(C<sub>6</sub>H<sub>5</sub>))<sub>2</sub>NHC]Ge(CH<sub>3</sub>)I (VII-9).**

0.010 g (0.015 mmol) of **VII-8** was dissolved into deuterated toluene (0.2 mL) in NMR tube. 1.5 μL (0.021 mmol) of CH<sub>3</sub>I was added into the solution at -30°C. The

sample was kept at -30°C and run for NMR at -22°C. The reaction was completed with full conversion after 4 hours, confirmed by NMR data. NMR characterization was carried out at -22°C overnight. <sup>1</sup>H NMR (600 MHz, C<sub>6</sub>D<sub>5</sub>CD<sub>3</sub>, -22°C): δ = 0.56 (d, 6H, J<sub>H-H</sub> = 6.9 Hz, <sup>i</sup>Pr-CH<sub>3</sub>), 1.16 (s, 3H, CH<sub>3</sub>-Ge), 1.21 (d, 6H, J<sub>H-H</sub> = 6.9 Hz, <sup>i</sup>Pr-CH<sub>3</sub>), 1.24 (d, 6H, J<sub>H-H</sub> =

6.9 Hz,  $^1\text{Pr-CH}_3$ ), 1.37 (s,  $\text{CH}_3\text{I}$  residue), 1.46 (d, 6H,  $J_{\text{H-H}} = 6.9$  Hz,  $^1\text{Pr-CH}_3$ ), 3.31 (br, 2H,  $\text{CH}(\text{CH}_3)_2$ ), 3.55 (br, 2H,  $\text{CH}(\text{CH}_3)_2$ ) 7.04 (s, 2H,  $\text{NC}(\text{H})=\text{C}(\text{H})\text{N}$ ), 6.81-7.91 (m, 16H, aromatic ring).  $^{13}\text{C}\{^1\text{H}\}$  NMR (151 MHz,  $\text{C}_6\text{D}_5\text{CD}_3$ ,  $-22^\circ\text{C}$ ): 1.4 ( $\text{CH}_3\text{I}$  residue), 6.2 ( $\text{CH}_3\text{-Ge}$ ) 20.4 ( $\text{CH}_3\text{-toluene}$ ), 23.3, 23.7, 25.6, 26.7 ( $\text{CH}_3$ ), 27.8, 28.6 ( $\text{CH}(\text{CH}_3)_2$ ), 122.2 ( $\text{NC}(\text{H})=\text{C}(\text{H})\text{N}$ ), 123.8 - 140.3 (aromatic ring), 152.2 ( $\text{C}=\text{N-Ar}$ ), 188.3 ( $\text{NCN}$ ).

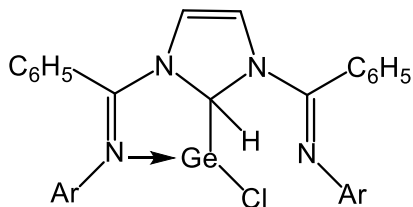


**VII-12**

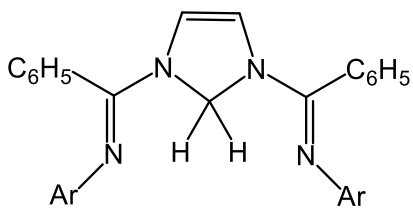
**[(2,6- $^i\text{Pr}_2\text{C}_6\text{H}_3\text{N}=\text{C}(\text{C}_6\text{H}_5)_2\text{NC}(\text{C}_6\text{H}_5)\text{N}] \text{GeI}$**  (**VII-**

**12**). 0.100 g (0.15 mmol) of **VII-8** was dissolved into 5 mL benzene. 17  $\mu\text{L}$  (0.15 mmol) of iodobenzene was added into benzene solution at room temperature. The whole solution was stirred at  $40^\circ\text{C}$  for 1 day. The color

of solution changes from red to orange. The volatiles were removed under vacuum to obtain an orange solid. The pure solid was obtained from  $\text{Et}_2\text{O}$ /hexane mixture at room temperature. The crystals of **VII-12** was grown from the mixture benzene/hexane at room temperature.  $^1\text{H}$  NMR (600 MHz,  $\text{C}_6\text{D}_6$ ,  $22^\circ\text{C}$ ):  $\delta = 0.63$  (d, 6H,  $J_{\text{H-H}} = 6.9$  Hz,  $^i\text{Pr-CH}_3$ ), 0.80 (d, 6H,  $J_{\text{H-H}} = 6.9$  Hz,  $^i\text{Pr-CH}_3$ ), 1.35 (d, 6H,  $J_{\text{H-H}} = 6.9$  Hz,  $^i\text{Pr-CH}_3$ ), 1.62 (d, 6H,  $J_{\text{H-H}} = 6.9$  Hz,  $^i\text{Pr-CH}_3$ ), 2.41 (sept, 2H,  $J_{\text{H-H}} = 6.9$  Hz,  $\text{CH}(\text{CH}_3)_2$ ), 4.55 (sept, 2H,  $J_{\text{H-H}} = 6.9$  Hz,  $\text{CH}(\text{CH}_3)_2$ ), 6.00 (s, 2H,  $-\text{NC}(\text{H})=\text{C}(\text{H})\text{N}$ ), 6.77-8.30 (m, 16H, aromatic ring).  $^{13}\text{C}\{^1\text{H}\}$  NMR (151 MHz,  $\text{C}_6\text{D}_6$ ,  $22^\circ\text{C}$ ): 23.0, 23.3, 26.8, 27.0 ( $\text{CH}_3$ ), 27.8, 29.3 ( $\text{CH}(\text{CH}_3)_2$ ), 90.5 ( $\text{NC}(\text{Ph})\text{N}$ ), 118.7 ( $\text{NC}(\text{H})=\text{C}(\text{H})\text{N}$ ), 128.1 – 143.2 (aromatic ring), 157.0 ( $\text{C}=\text{N-Ar}$ ).



**VII-13**



**VII-14**

**[(2,6-<sup>i</sup>Pr<sub>2</sub>C<sub>6</sub>H<sub>3</sub>N=C(C<sub>6</sub>H<sub>5</sub>))<sub>2</sub>NC(H)N]GeCl (VII-**

**13)** 0.100 g (0.15 mmol) of **VII-8** was dissolved into 5 mL benzene. 80 μL (0.16 mmol) of HCl (2M in Et<sub>2</sub>O) was added into benzene solution at room temperature.

The color of solution changes immediately from red to dark yellow. The volatiles were removed under vacuum to obtain an orange solid. This solid was dissolved in Et<sub>2</sub>O to give suspension. The precipitate was filtered off. The solution was dried to give a dark yellow solid. This

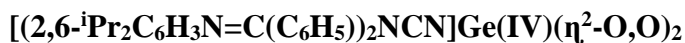
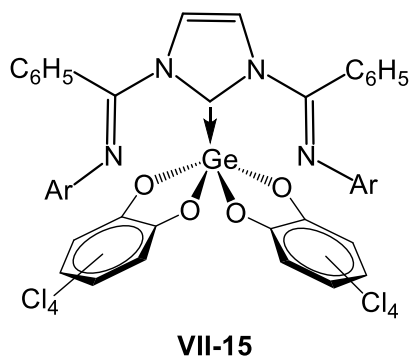
solid was re-dissolved in Et<sub>2</sub>O (2 mL) for the

crystallization. The orange crystals of **VII-13** and light yellow crystals of **VII-14** were

formed after 1 week at room temperature in the same vial. **NMR characterization of VII-**

**13:** <sup>1</sup>H NMR (600 MHz, C<sub>6</sub>D<sub>6</sub>, 22°C): δ = 1.25 (d, 6H, *J*<sub>H-H</sub> = 6.9 Hz, <sup>i</sup>Pr-CH<sub>3</sub>), 1.27 (d, 6H, *J*<sub>H-H</sub> = 6.9 Hz, <sup>i</sup>Pr-CH<sub>3</sub>), 1.46 (d, 6H, *J*<sub>H-H</sub> = 6.9 Hz, <sup>i</sup>Pr-CH<sub>3</sub>), 1.64 (d, 6H, *J*<sub>H-H</sub> = 6.9 Hz, <sup>i</sup>Pr-CH<sub>3</sub>), 3.31 (sept, 2H, *J*<sub>H-H</sub> = 6.9 Hz, CH(CH<sub>3</sub>)<sub>2</sub>), 4.05 (sept, 2H, *J*<sub>H-H</sub> = 6.9 Hz, CH(CH<sub>3</sub>)<sub>2</sub>), 6.04 (s, 2H, NC(H)=C(H)N), 6.21 (s, 1H, NC(H)-N), 6.94-7.39 (m, 16H, aromatic ring). <sup>13</sup>C{<sup>1</sup>H} NMR (151 MHz, C<sub>6</sub>D<sub>6</sub>, 22°C): 22.0, 22.9, 25.2, 26.8 (CH<sub>3</sub>), 28.4, 29.3 (CH(CH<sub>3</sub>)<sub>2</sub>), 88.0 (NC(H)N), 117.8 (NC(H)=C(H)N), 122.7 – 142.0 (aromatic ring), 154.8 (C=N-Ar).

**NMR characterization of VII-14:** <sup>1</sup>H NMR (600 MHz, C<sub>6</sub>D<sub>6</sub>, 22°C): δ = 1.20 (d, 12H, *J*<sub>H-H</sub> = 6.9 Hz, <sup>i</sup>Pr-CH<sub>3</sub>), 1.41 (d, 12H, *J*<sub>H-H</sub> = 6.9 Hz, <sup>i</sup>Pr-CH<sub>3</sub>), 3.37 (m, 4H, CH(CH<sub>3</sub>)<sub>2</sub>), 5.95 (s, 2H, NC(H)=C(H)N), 6.59 (s, 2H, NCH<sub>2</sub>N) 6.94-7.39 (m, 16H, aromatic ring). <sup>13</sup>C{<sup>1</sup>H} NMR (151 MHz, C<sub>6</sub>D<sub>6</sub>, 22°C): 22.3, 24.5 (CH<sub>3</sub>), 29.8 (CH(CH<sub>3</sub>)<sub>2</sub>), 65.9 (NC(H)=C(H)N), 67.4 (NCH<sub>2</sub>N), 114.0 – 145.0 (aromatic ring), 150.1 (C=N-Ar).

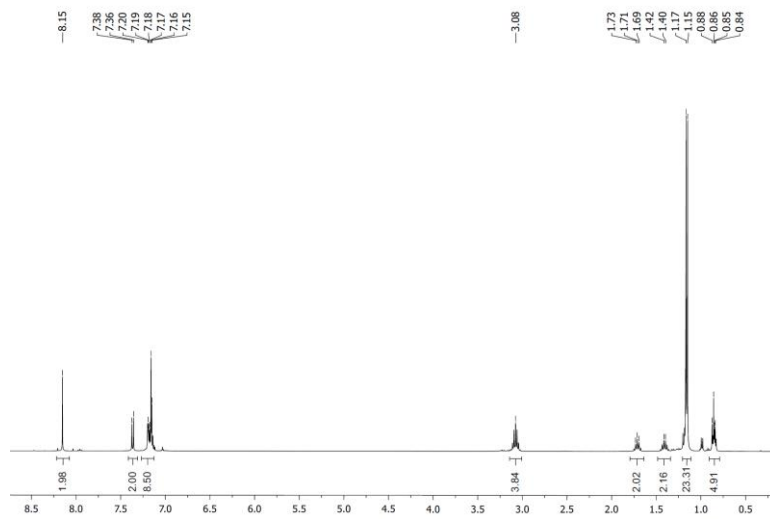


**(VII-15)**. 0.100 g (0.15 mmol) of **VII-8** was dissolved into 5 mL benzene. 0.074 g (0.30 mmol) of tetrachloro-*o*-benzoquinone was added into benzene solution. The mixture was stirred at room temperature for 1 day. The precipitate was filtered and dried to a yellow solid of **VII-**

**15**. The crystals were grown from DCM at room temperature.  $^1\text{H NMR}$  (600 MHz,  $\text{CDCl}_3$ ,  $22^\circ\text{C}$ ):  $\delta$  = 0.62 (br, 12H,  $^i\text{Pr-CH}_3$ ), 0.91 (d, 12H,  $J_{\text{H-H}} = 6.9$  Hz,  $^i\text{Pr-CH}_3$ ), 2.88 (br, 4H,  $\text{CH}(\text{CH}_3)_2$ ), 6.95 (d, 4H,  $J_{\text{H-H}} = 7.5$  Hz, m-H Ph-N), 7.06 (t, 4H,  $J_{\text{H-H}} = 7.5$  Hz, p-H Ph-N), 7.14 (m, 4H, o-H Ph-C=N), 7.20 (s, 2H,  $\text{NC}(\text{H})=\text{C}(\text{H})\text{N}$ ), 7.24 (t, 4H,  $J_{\text{H-H}} = 7.5$  Hz, m-H Ph-C=N), 7.34 (t, 2H,  $J_{\text{H-H}} = 7.5$  Hz, p-H Ph-C=N).  $^{13}\text{C}\{^1\text{H}\}$  NMR (151 MHz,  $\text{CDCl}_3$ ,  $22^\circ\text{C}$ ): 23.5, 23.8 ( $\text{CH}_3$ ), 28.6 ( $\text{CH}(\text{CH}_3)_2$ ), 120.8 ( $\text{NC}(\text{H})=\text{C}(\text{H})\text{N}$ ), 116.1 – 146.2 (aromatic ring), 149.8 (C=N-Ar), 158.1 (NCN). **Anal. Calcd** for  $\text{C}_{55}\text{H}_{52}\text{Cl}_8\text{GeN}_4\text{O}_4$ : C, 55.55; H, 4.41; N, 4.71. Found: C, 55.03; H, 4.01; N, 4.79 %.

## X. Appendix

### $^1\text{H}$ NMR spectrum



### $^{13}\text{C}\{^1\text{H}\}$ NMR spectrum

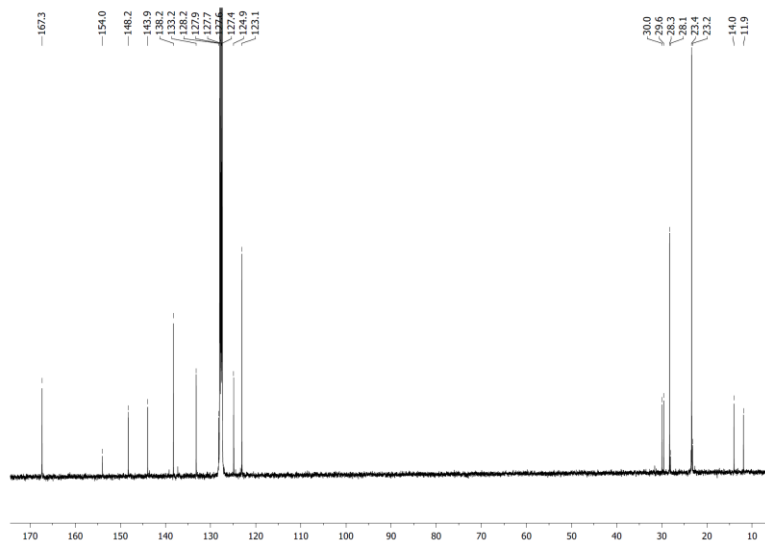
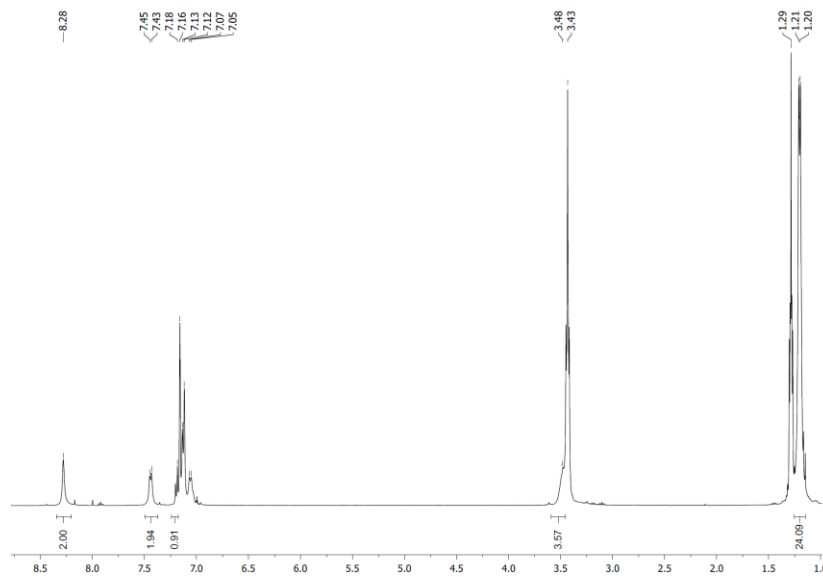


**Figure X-1.**  $^1\text{H}$  and  $^{13}\text{C}\{^1\text{H}\}$  NMR spectra of V-2

$^1\text{H}$  NMR spectrum



$^{13}\text{C}\{^1\text{H}\}$  NMR spectrum

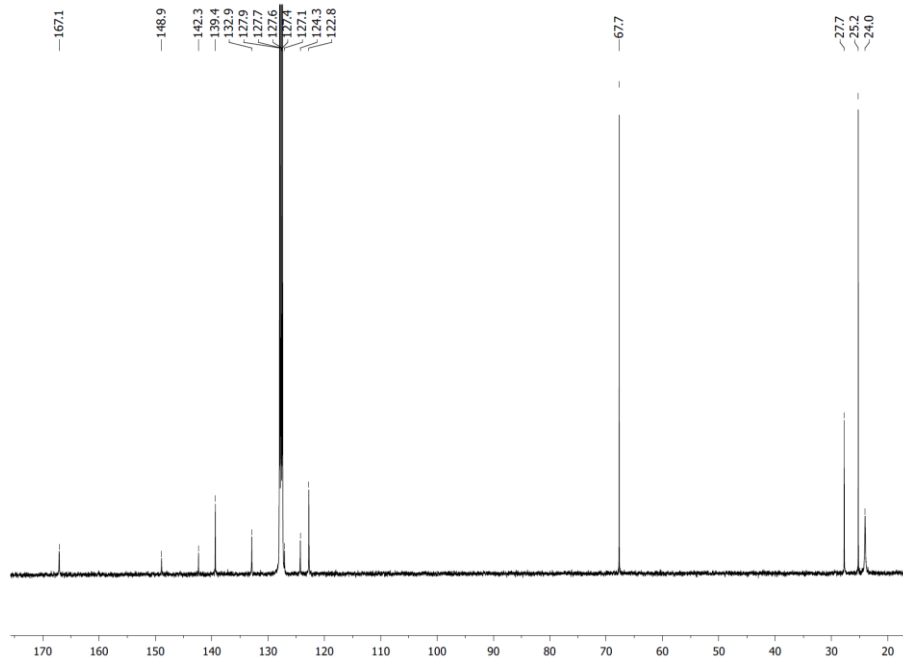
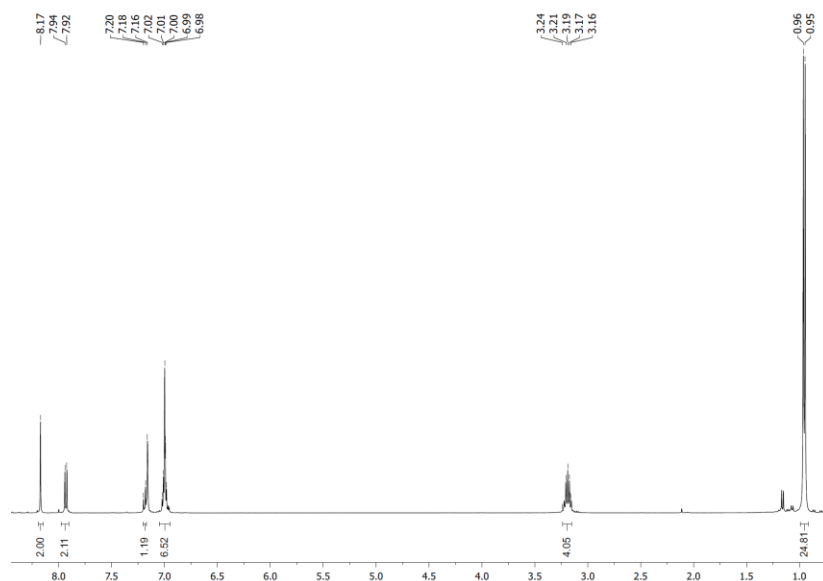


Figure X-2.  $^1\text{H}$  and  $^{13}\text{C}\{^1\text{H}\}$  NMR spectra of V-3



$^1\text{H}$  NMR spectrum



$^{13}\text{C}\{^1\text{H}\}$  NMR spectrum

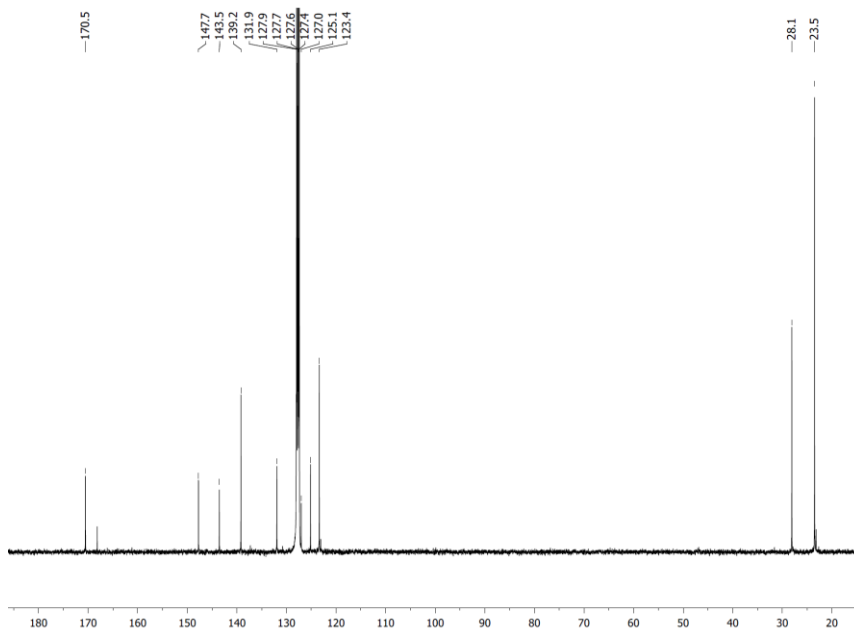
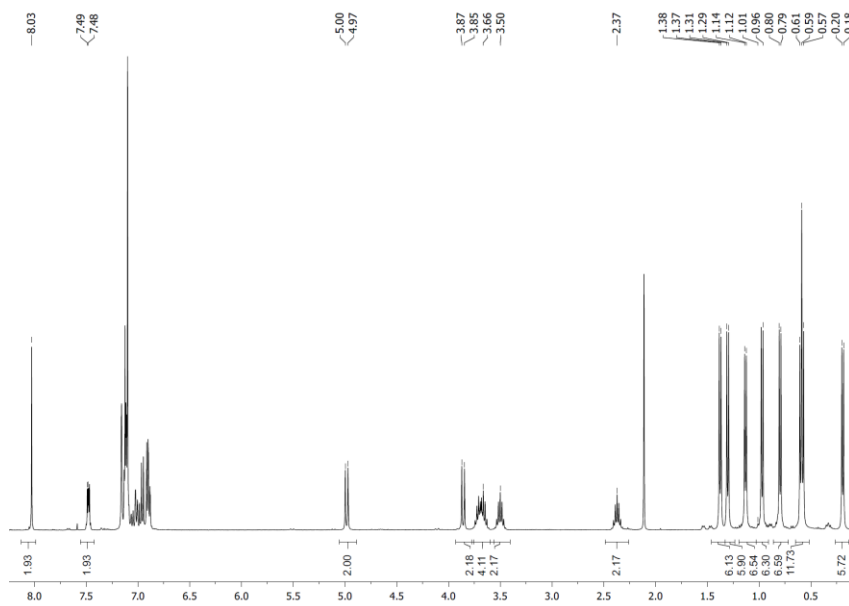


**Figure X-3.**  $^1\text{H}$  and  $^{13}\text{C}\{^1\text{H}\}$  NMR spectra of **V-5**

$^1\text{H}$  NMR spectrum



$^{13}\text{C}\{^1\text{H}\}$  NMR spectrum

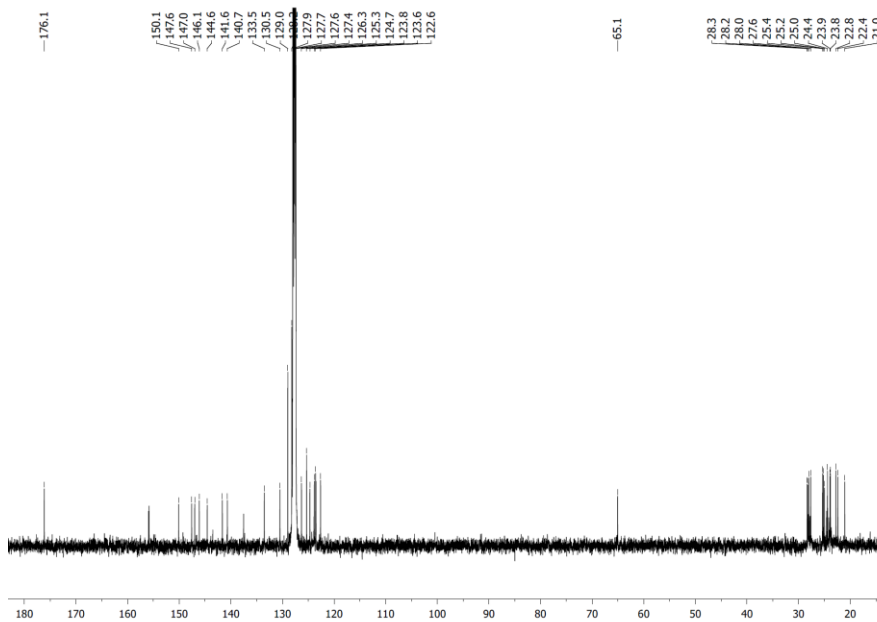
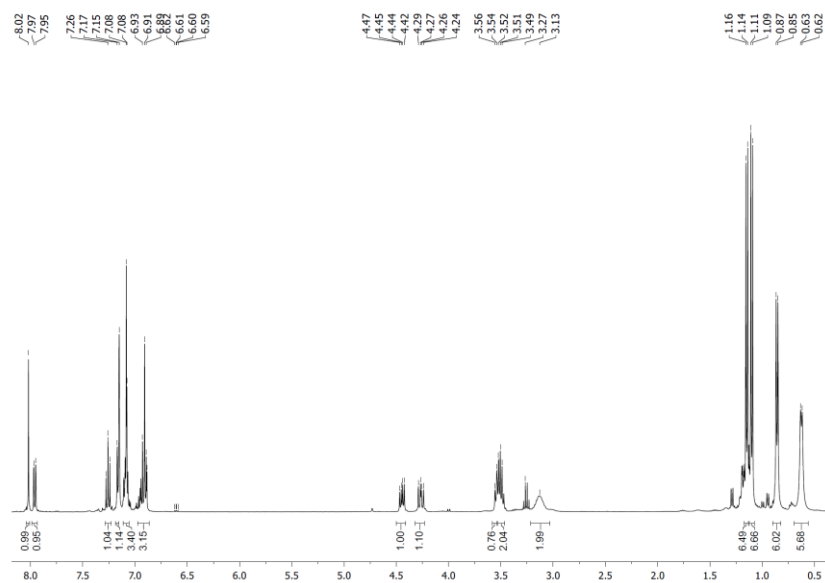


Figure X-4.  $^1\text{H}$  and  $^{13}\text{C}\{^1\text{H}\}$  NMR spectra of V-7

$^1\text{H}$  NMR spectrum



$^{13}\text{C}\{^1\text{H}\}$  NMR spectrum

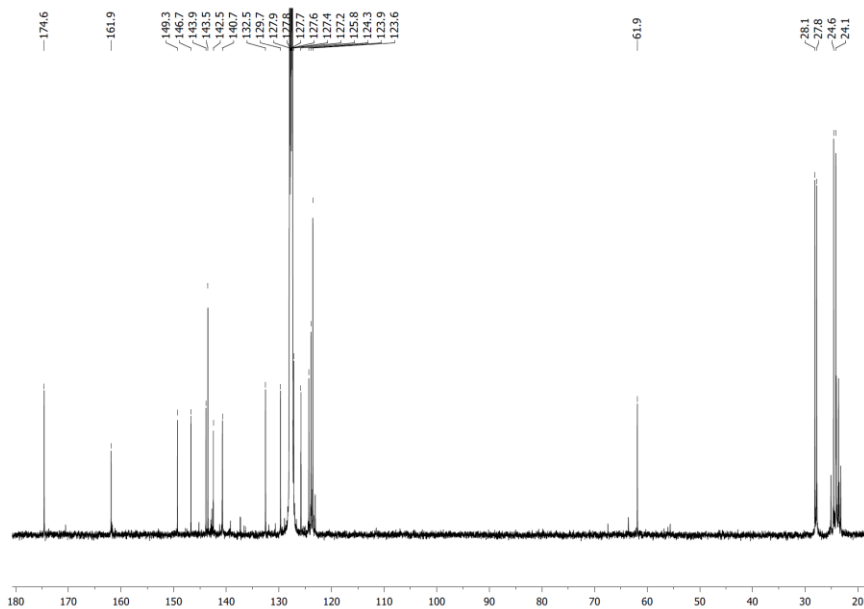
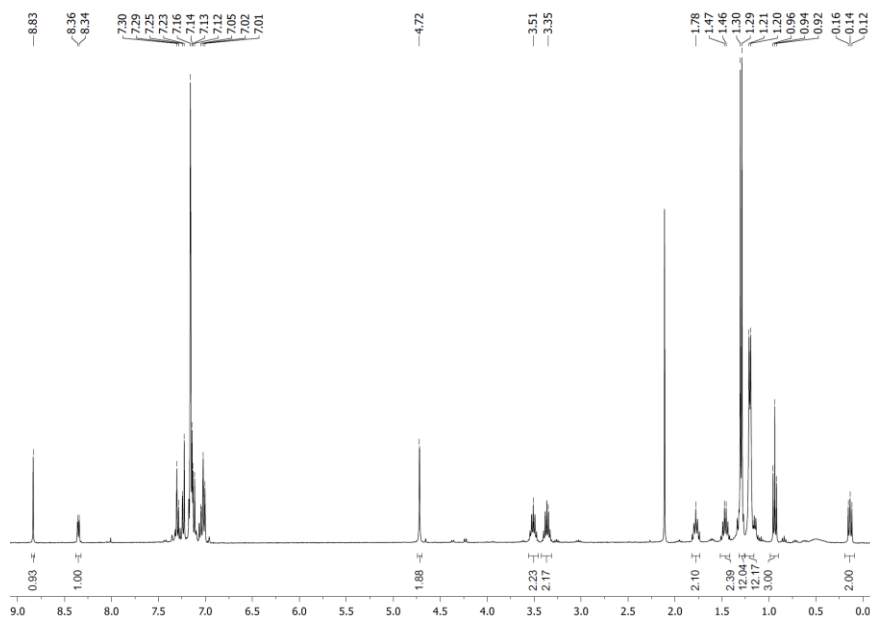


Figure X-5.  $^1\text{H}$  and  $^{13}\text{C}\{^1\text{H}\}$  NMR spectra of V-8(Li) or V-8(K)

$^1\text{H}$  NMR spectrum



$^{13}\text{C}\{^1\text{H}\}$  NMR spectrum

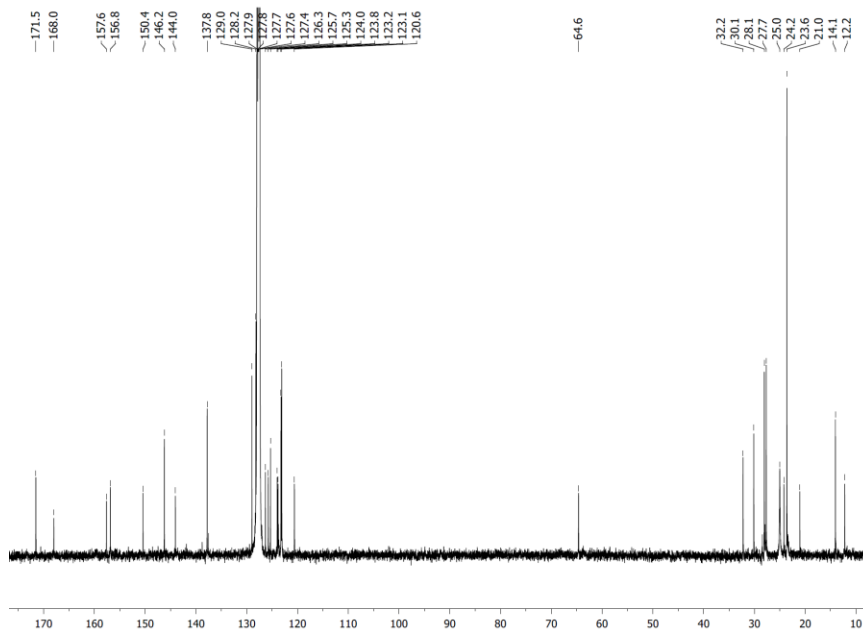


Figure X-6.  $^1\text{H}$  and  $^{13}\text{C}\{^1\text{H}\}$  NMR spectra of V-9

$^1\text{H}$  NMR spectrum

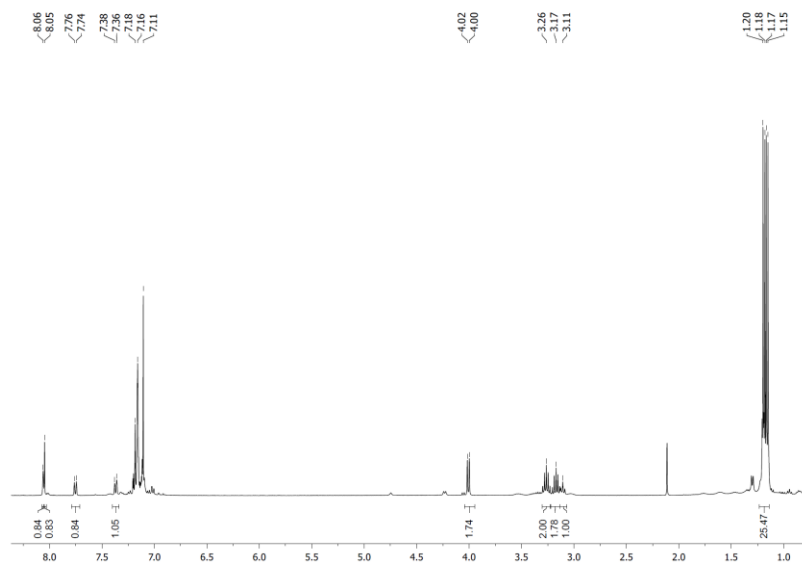


Figure X-7.  $^1\text{H}$  spectrum of V-10

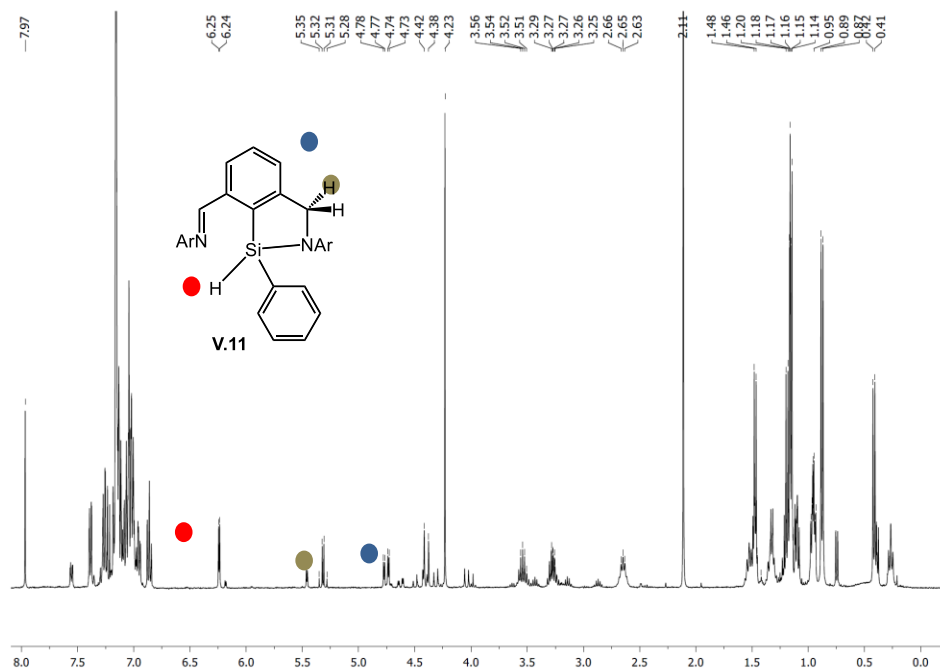
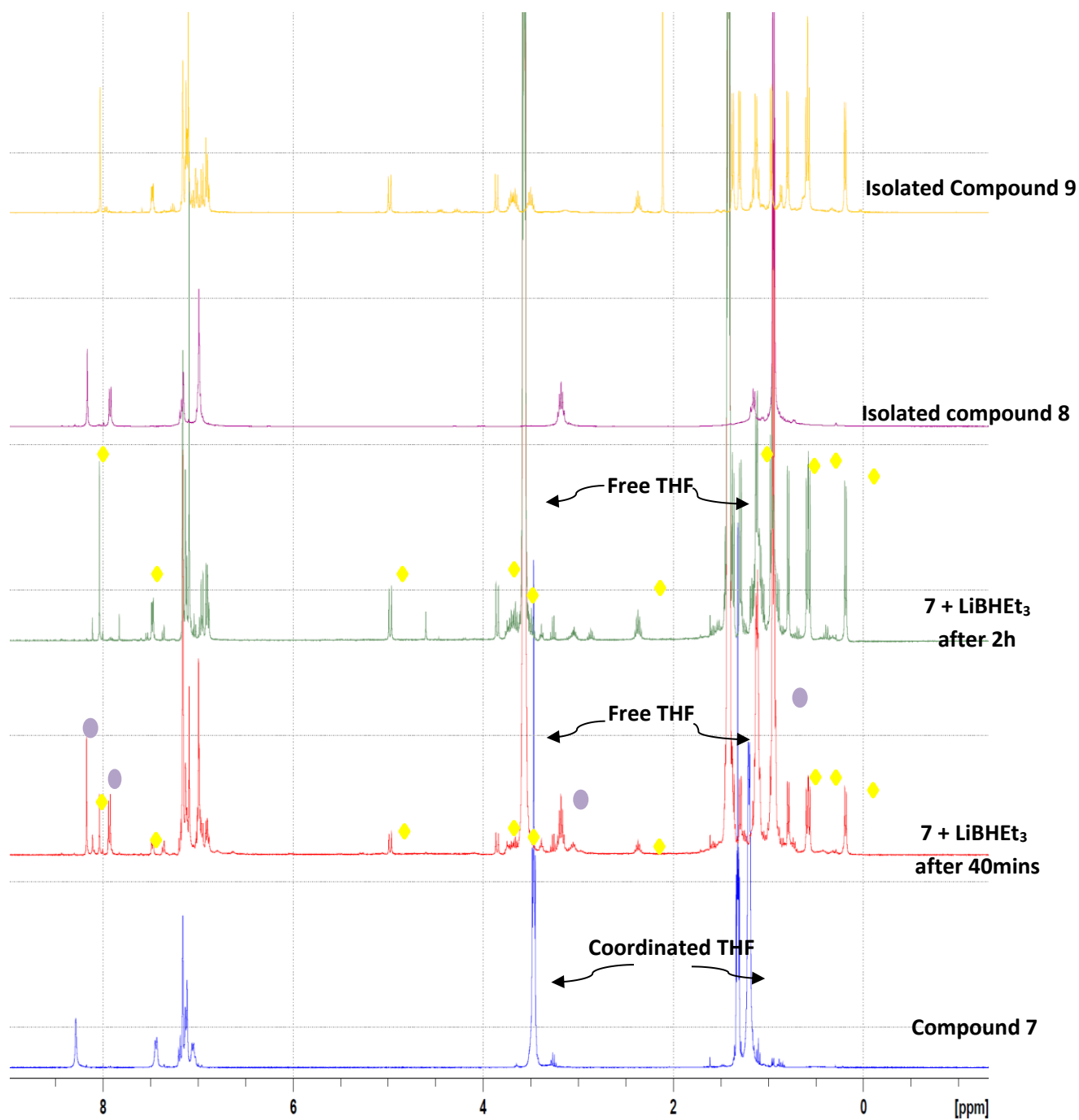
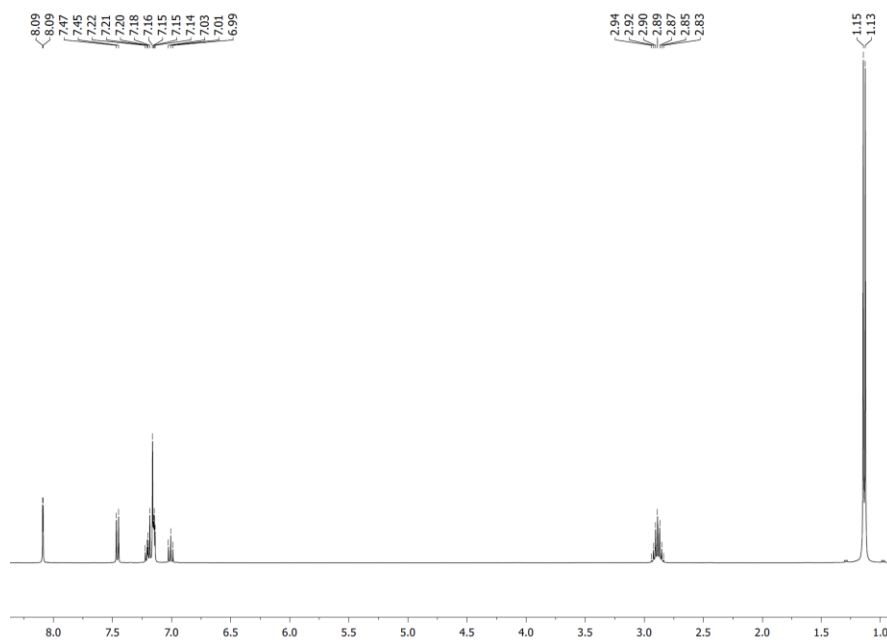


Figure X-8.  $^1\text{H}$  and  $^{13}\text{C}\{^1\text{H}\}$  NMR spectra of V-9 +  $\text{PhSiH}_3$

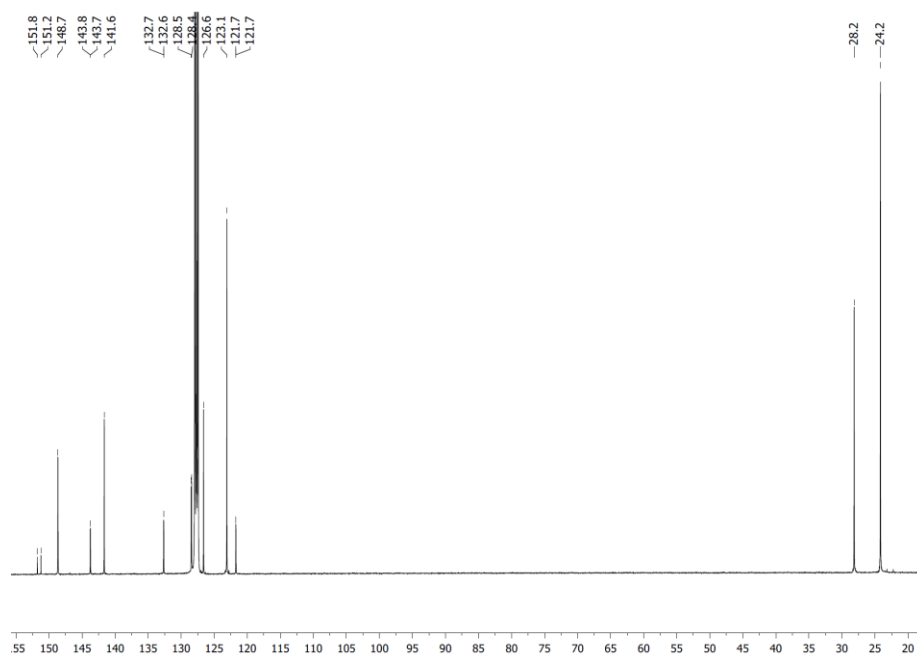


**Figure X-9.**  $^1\text{H}$  NMR spectrum of the reaction between **V-3** + (superhydride)  $\text{LiBHET}_3$  at various time (yellow diamond corresponding to compound **V-7**, purple circle corresponding to compound **V-5**).

$^1\text{H}$  NMR spectrum



$^{13}\text{C}\{^1\text{H}\}$  NMR spectrum



$^{31}\text{P}\{^1\text{H}\}$  NMR spectrum

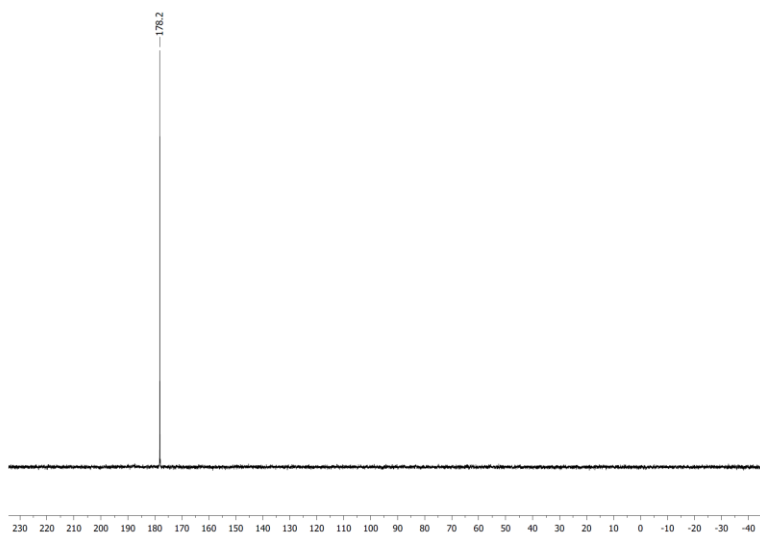
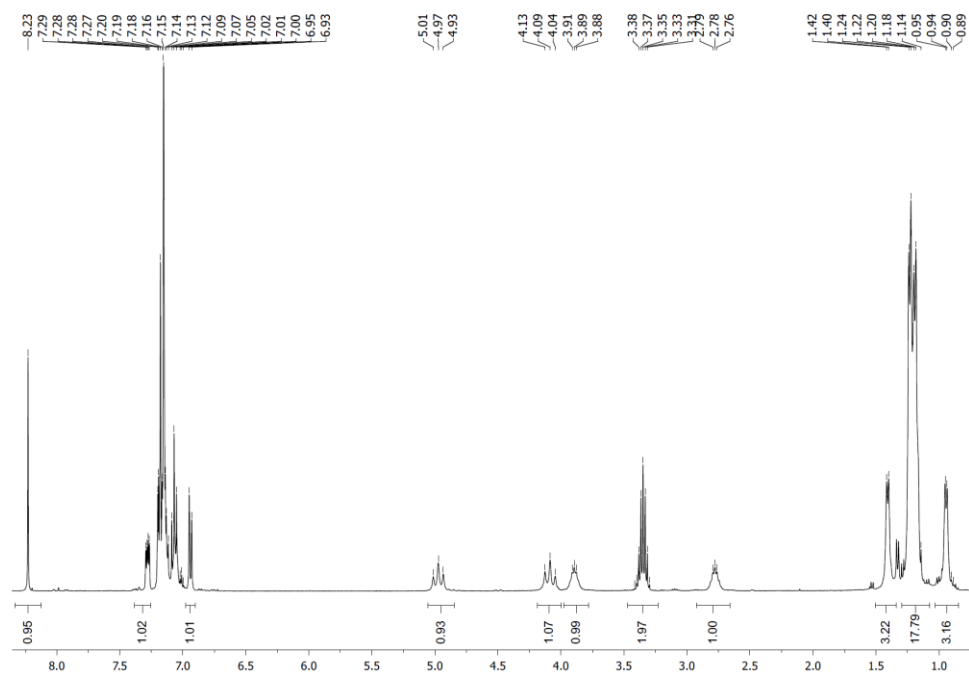


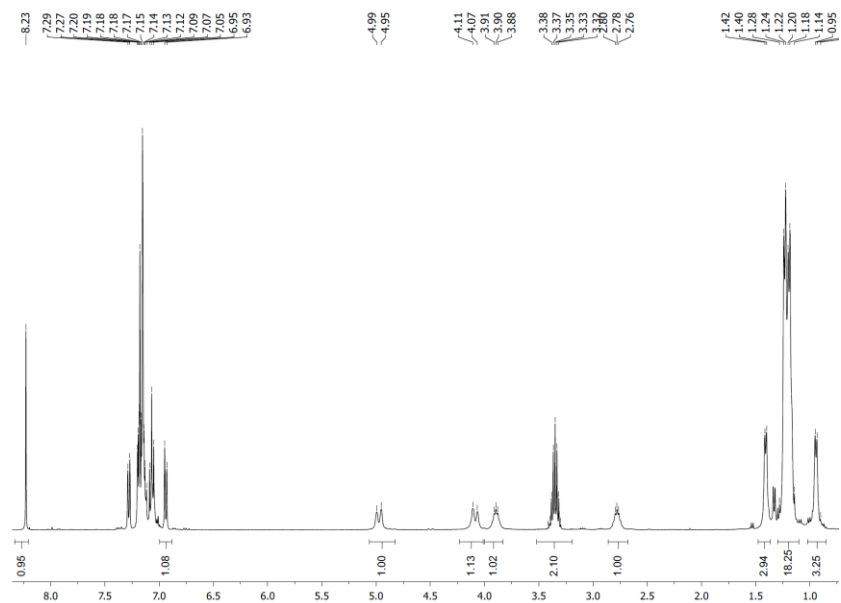
**Figure X-10.**  $^1\text{H}$ ,  $^{13}\text{C}\{^1\text{H}\}$ , and  $^{31}\text{P}\{^1\text{H}\}$  NMR spectra of **VI-2** in  $\text{C}_6\text{D}_6$

$^1\text{H}$  NMR spectrum

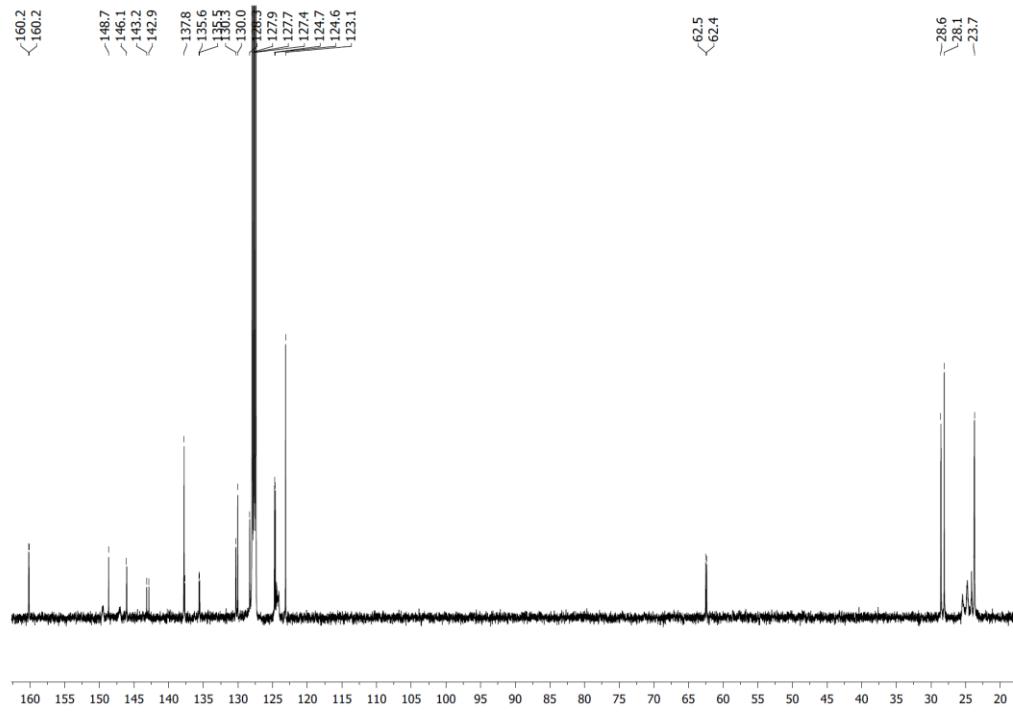




$^1\text{H}\{^3\text{P}\}$  NMR spectrum



$^{13}\text{C}\{^1\text{H}\}$  NMR spectrum



$^{31}\text{P}\{^1\text{H}\}$  NMR spectrum

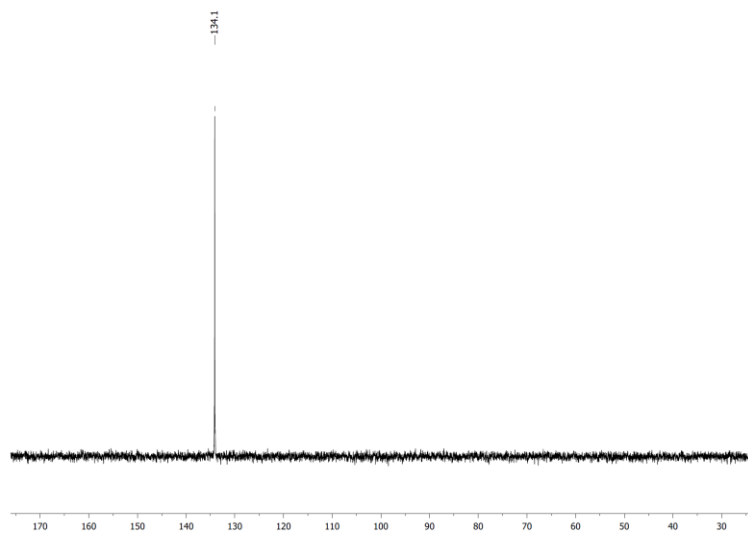
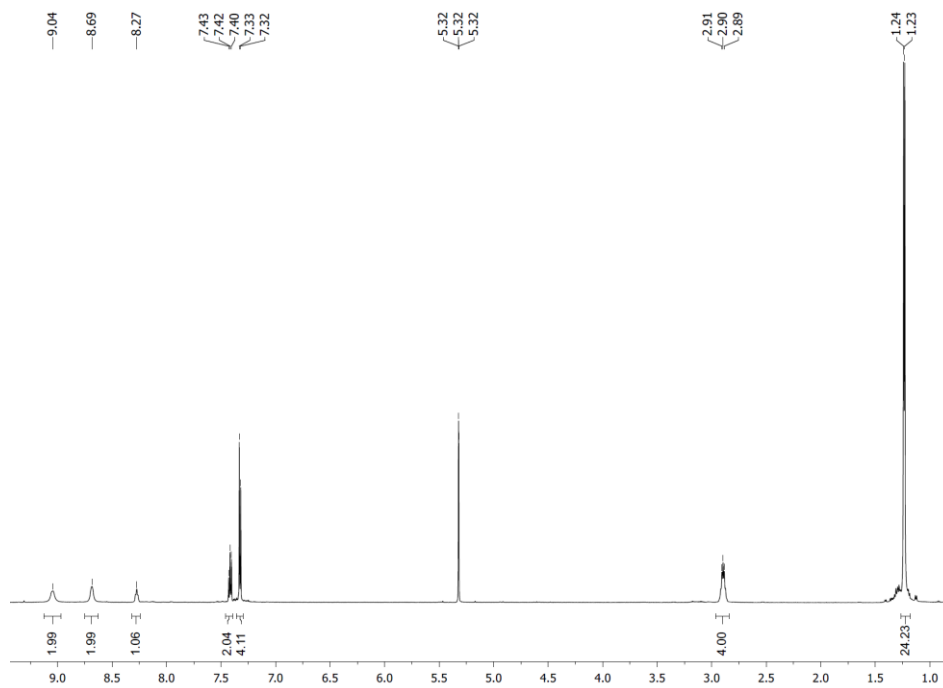
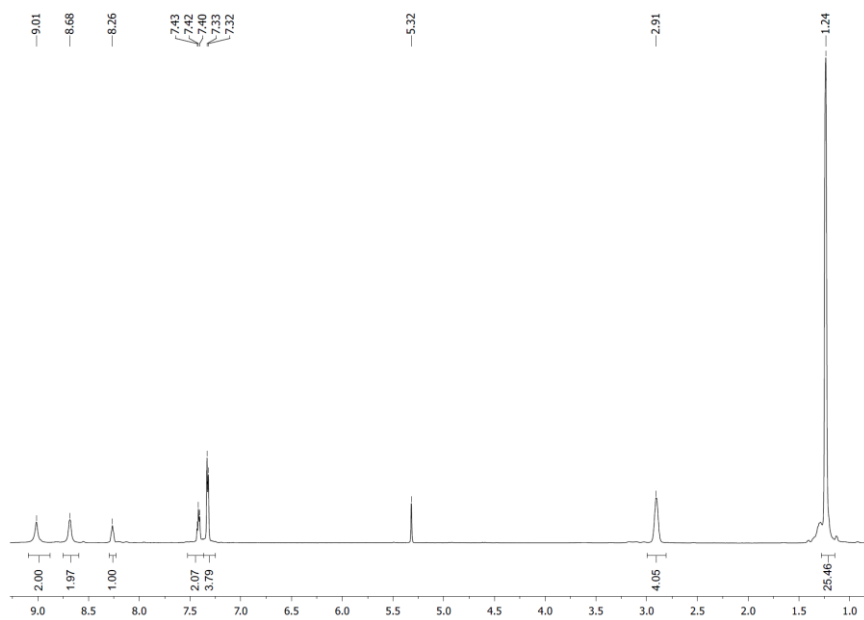


**Figure X-11.**  $^1\text{H}$ ,  $^1\text{H}\{^{31}\text{P}\}$ ,  $^{13}\text{C}\{^1\text{H}\}$ , and  $^{31}\text{P}\{^1\text{H}\}$  NMR spectra of VI-6 in  $\text{C}_6\text{D}_6$

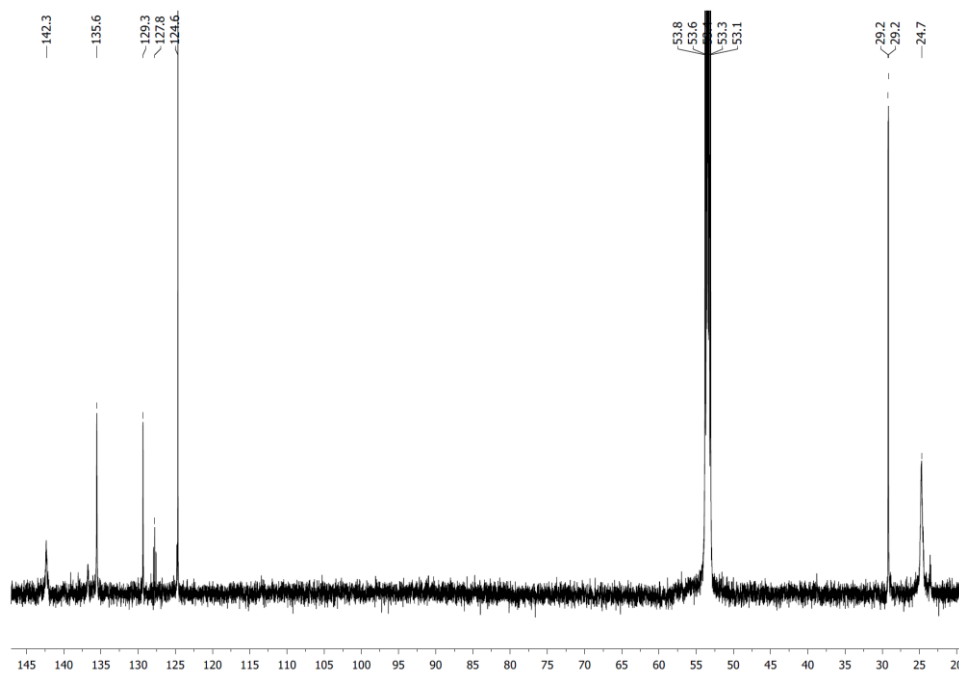
$^1\text{H}$  NMR spectrum



$^1\text{H}\{^3\text{P}\}$  NMR spectrum



$^{13}\text{C}\{^1\text{H}\}$  NMR spectrum



$^{31}\text{P}\{^1\text{H}\}$  NMR spectrum

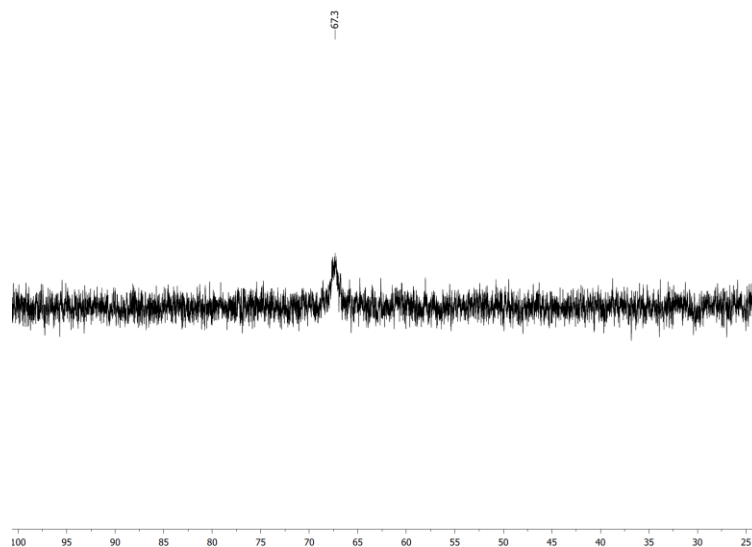
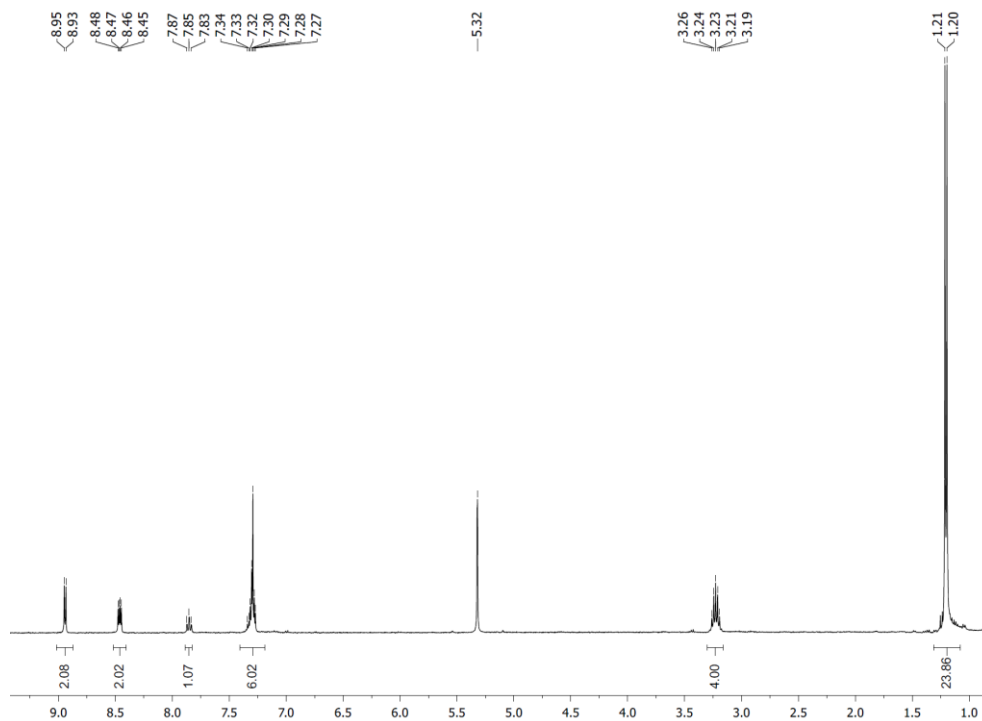
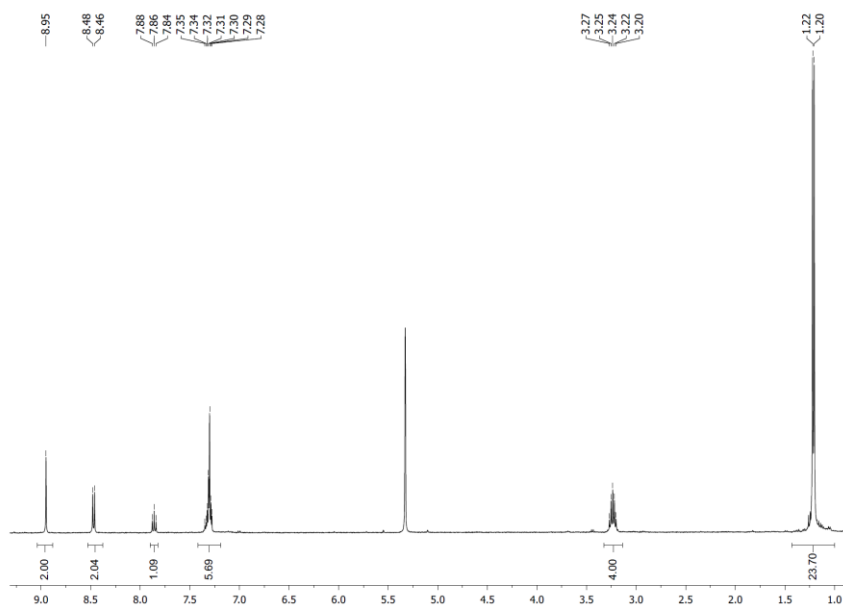


**Figure X-12.**  $^1\text{H}$ ,  $^1\text{H}\{^{31}\text{P}\}$ ,  $^{13}\text{C}\{^1\text{H}\}$ , and  $^{31}\text{P}\{^1\text{H}\}$  NMR spectra of **V-7** in  $\text{CD}_2\text{Cl}_2$

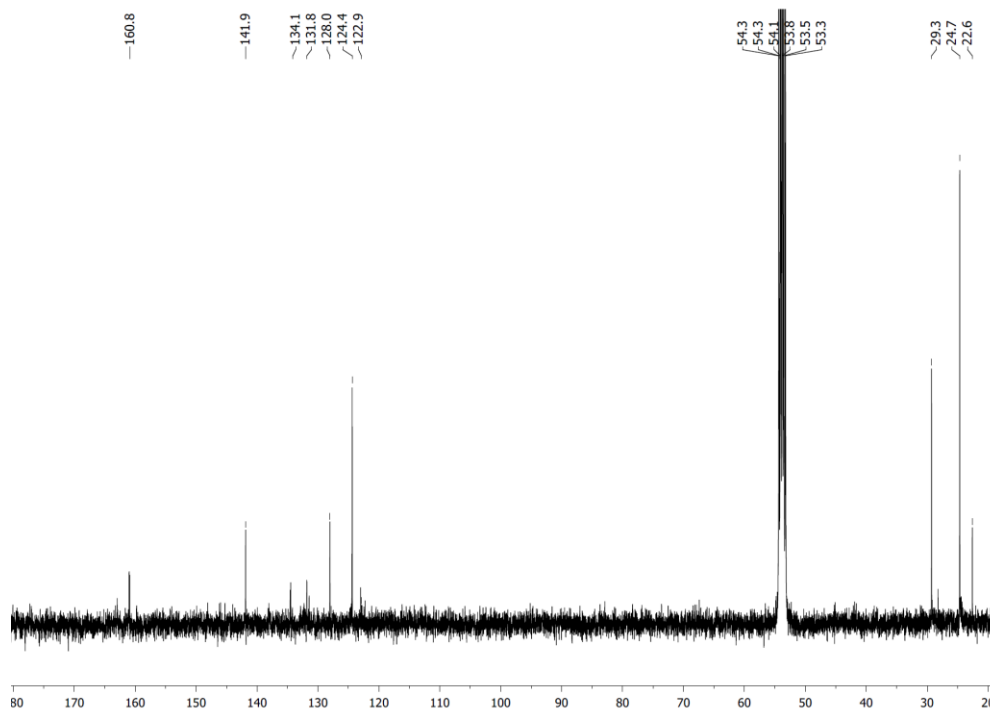
$^1\text{H}$  NMR spectrum



$^1\text{H}\{^3\text{P}\}$  NMR spectrum



$^{13}\text{C}\{^1\text{H}\}$  NMR spectrum



$^{31}\text{P}\{^1\text{H}\}$  NMR spectrum

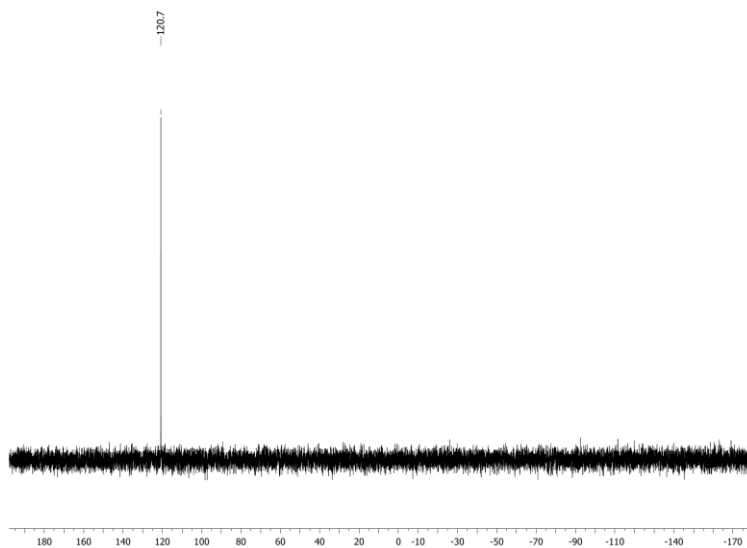
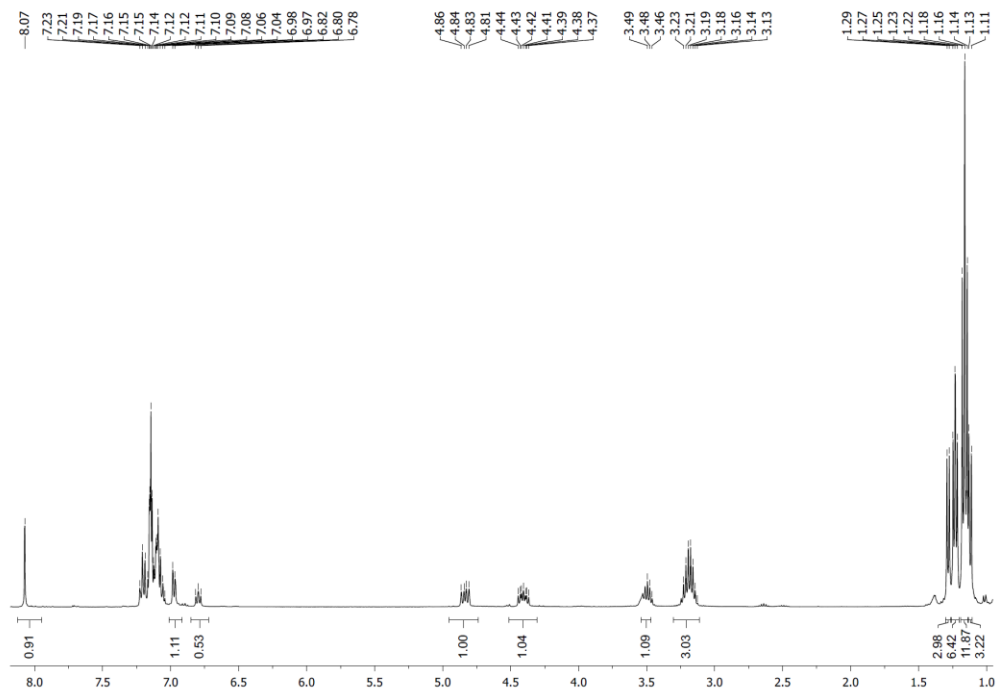
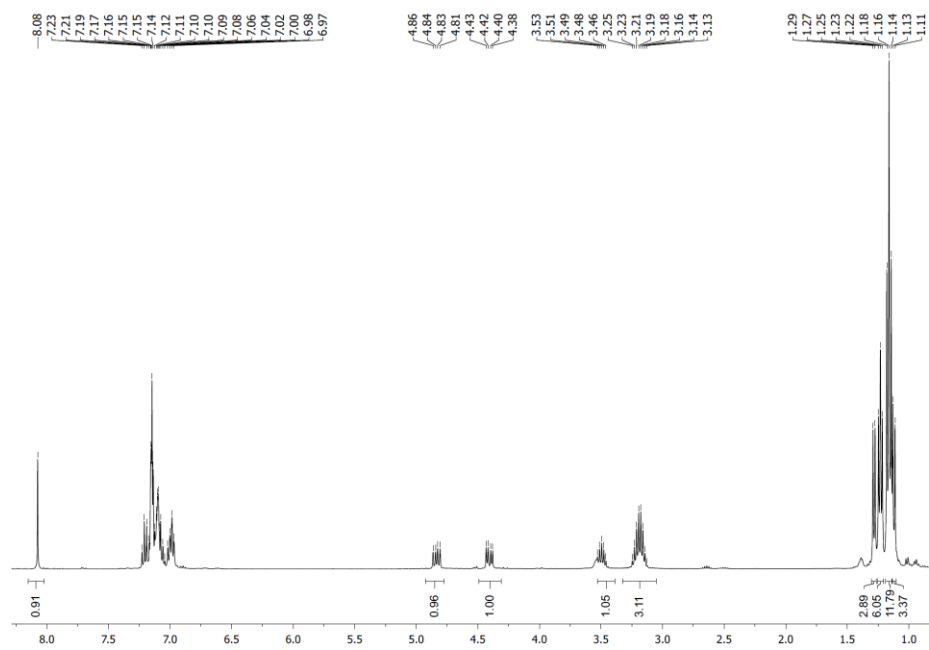


**Figure X-13.**  $^1\text{H}$ ,  $^1\text{H}\{^{31}\text{P}\}$ ,  $^{13}\text{C}\{^1\text{H}\}$ , and  $^{31}\text{P}\{^1\text{H}\}$  NMR spectra of **VI-8** in  $\text{CD}_2\text{Cl}_2$

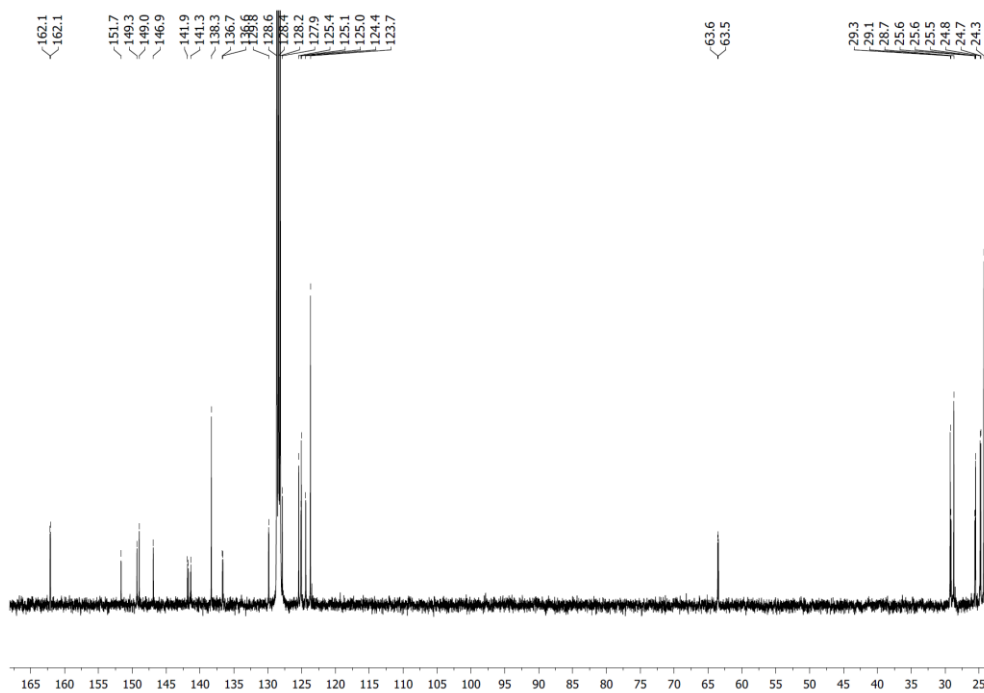
$^1\text{H}$  NMR spectrum



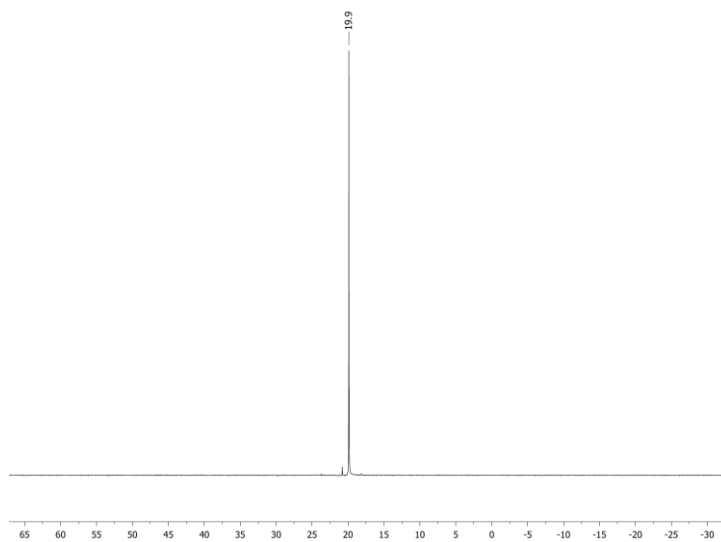
$^1\text{H}\{^3\text{P}\}$  NMR spectrum



$^{13}\text{C}\{^1\text{H}\}$  NMR spectrum



$^{31}\text{P}\{^1\text{H}\}$  NMR spectrum



$^{31}\text{P}$  NMR spectrum

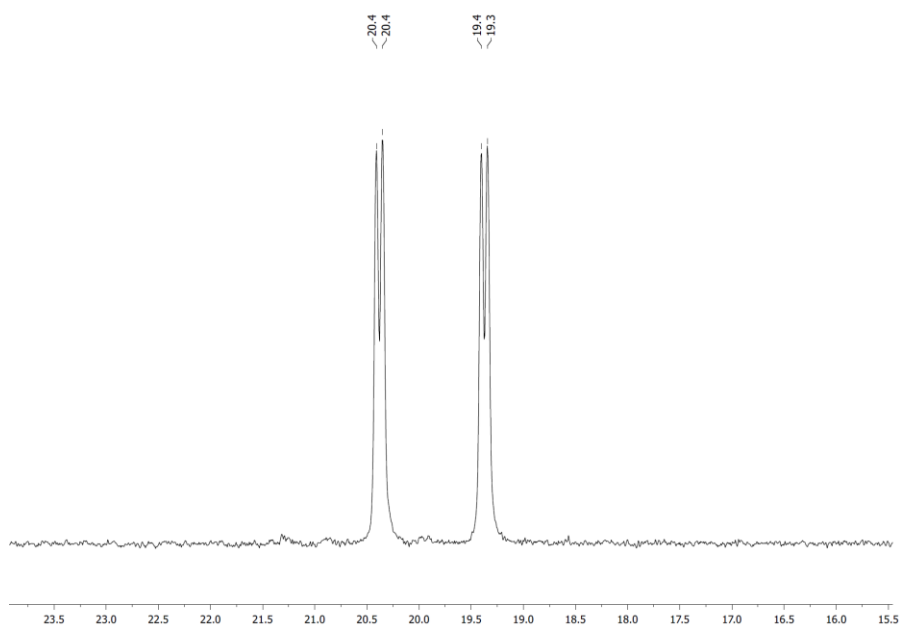
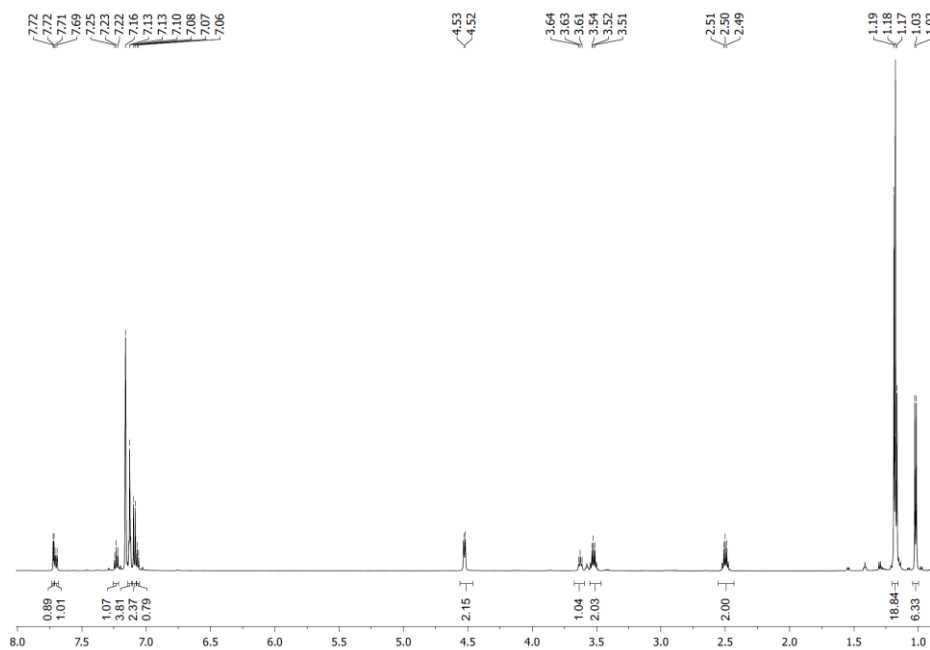


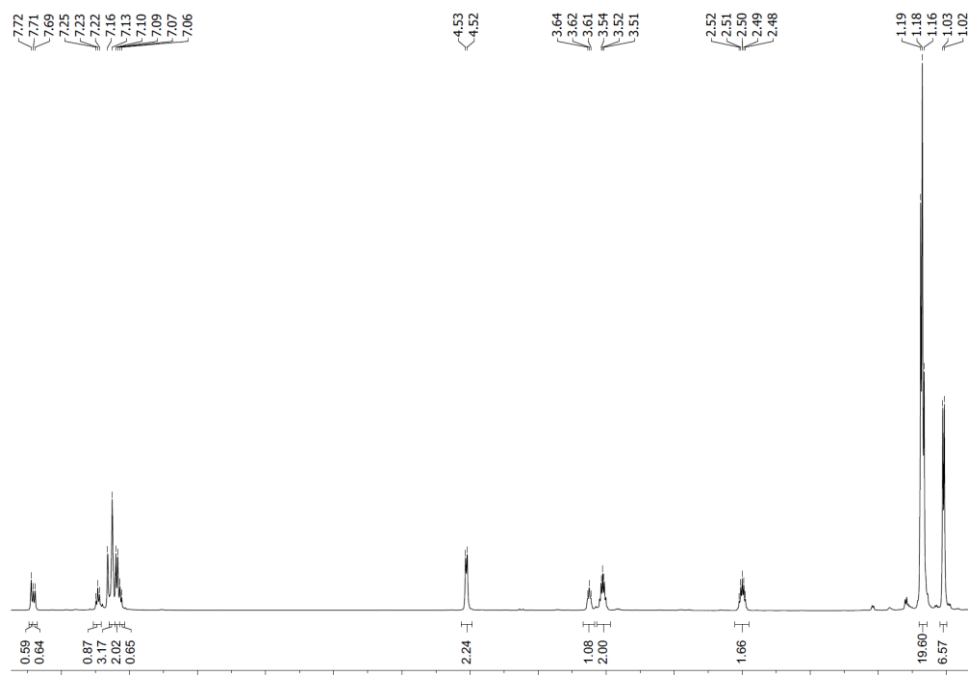
**Figure X-14.**  $^1\text{H}$ ,  $^1\text{H}\{^{31}\text{P}\}$ ,  $^{13}\text{C}\{^1\text{H}\}$ ,  $^{31}\text{P}\{^1\text{H}\}$ , and  $^{31}\text{P}$  NMR spectra of **VI-9** in  $\text{C}_6\text{D}_6$



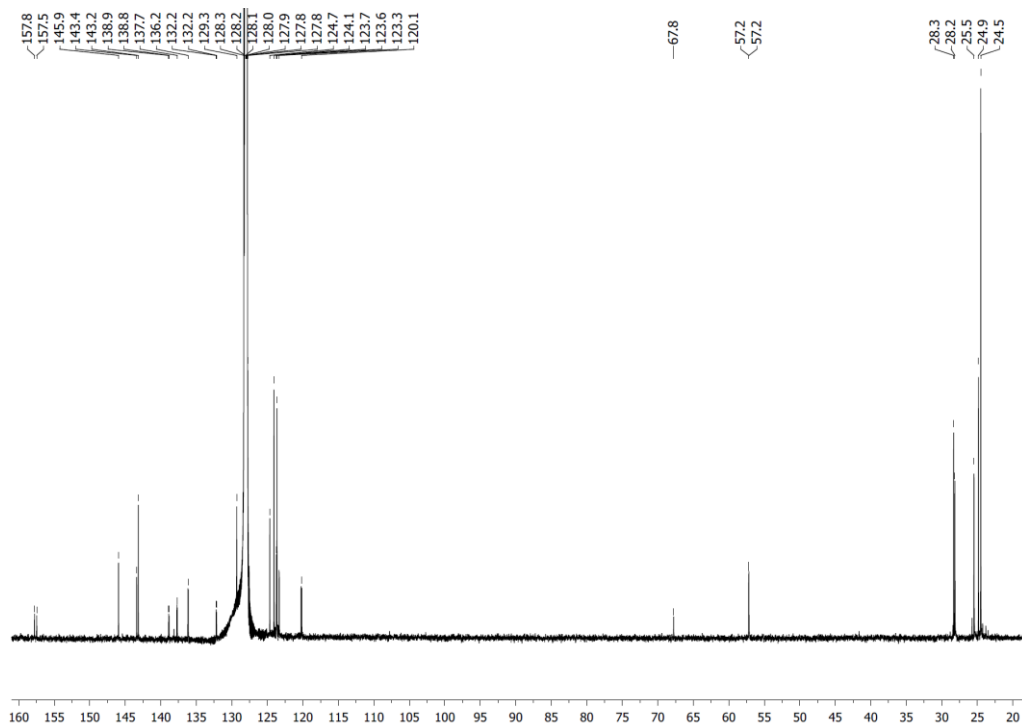
$^1\text{H}$  NMR spectrum



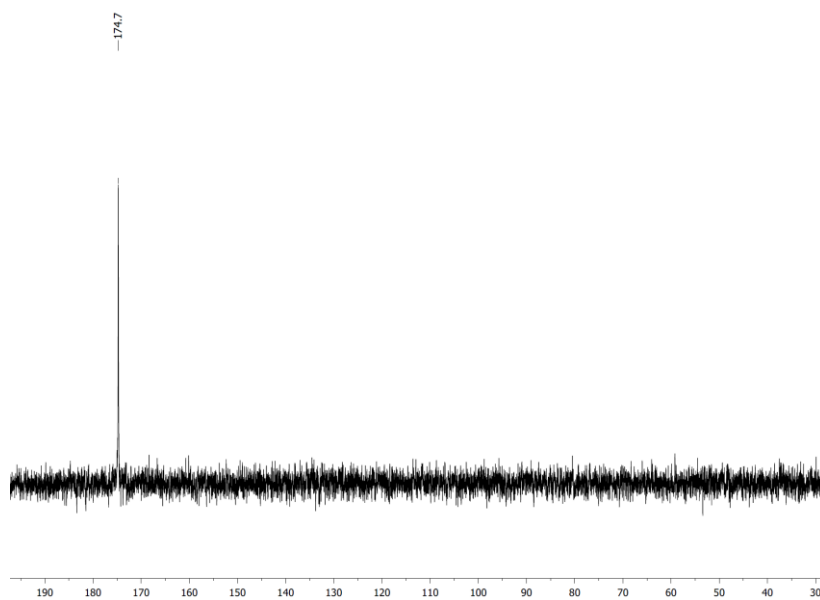
$^1\text{H}\{^3\text{P}\}$  NMR spectrum



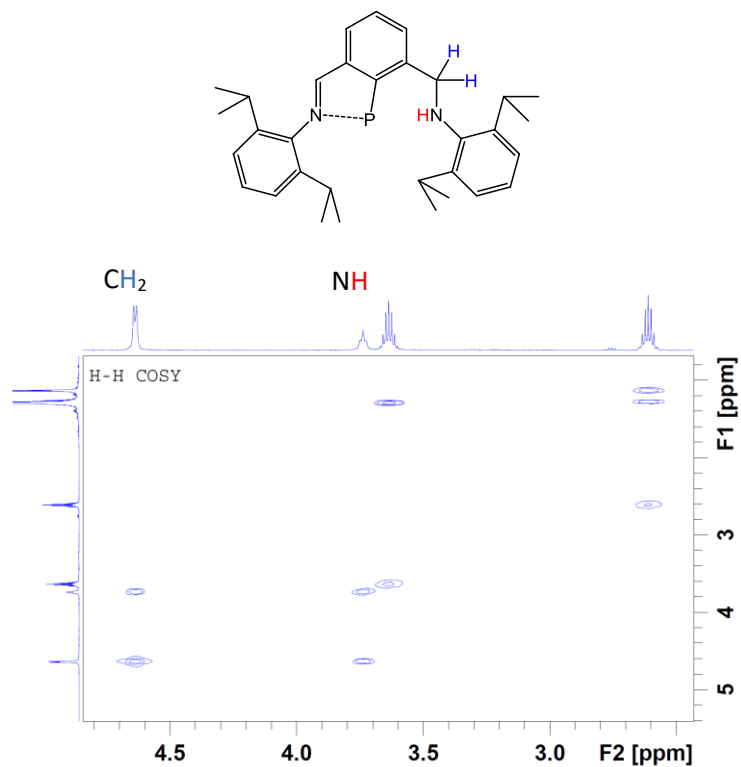
$^{13}\text{C}\{^1\text{H}\}$  NMR spectrum



$^{31}\text{P}\{^1\text{H}\}$  NMR spectrum



$^1\text{H}$ - $^1\text{H}$  COSY spectrum



$^1\text{H}$ - $^{13}\text{C}$  HSQC spectrum

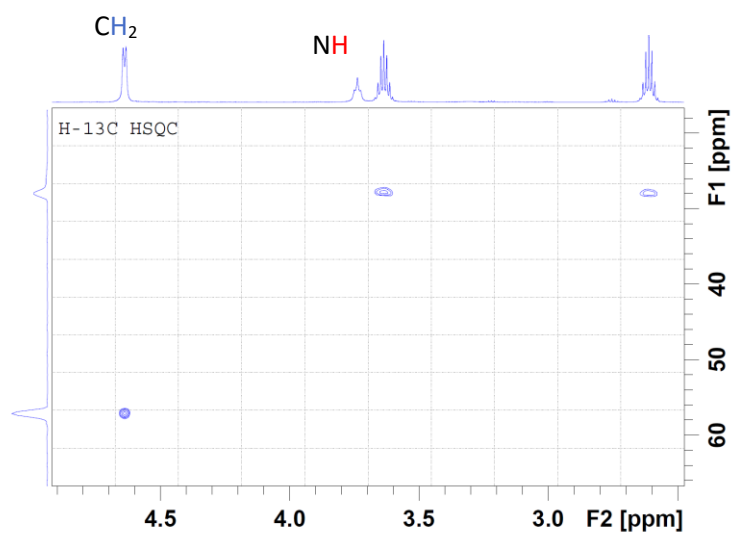
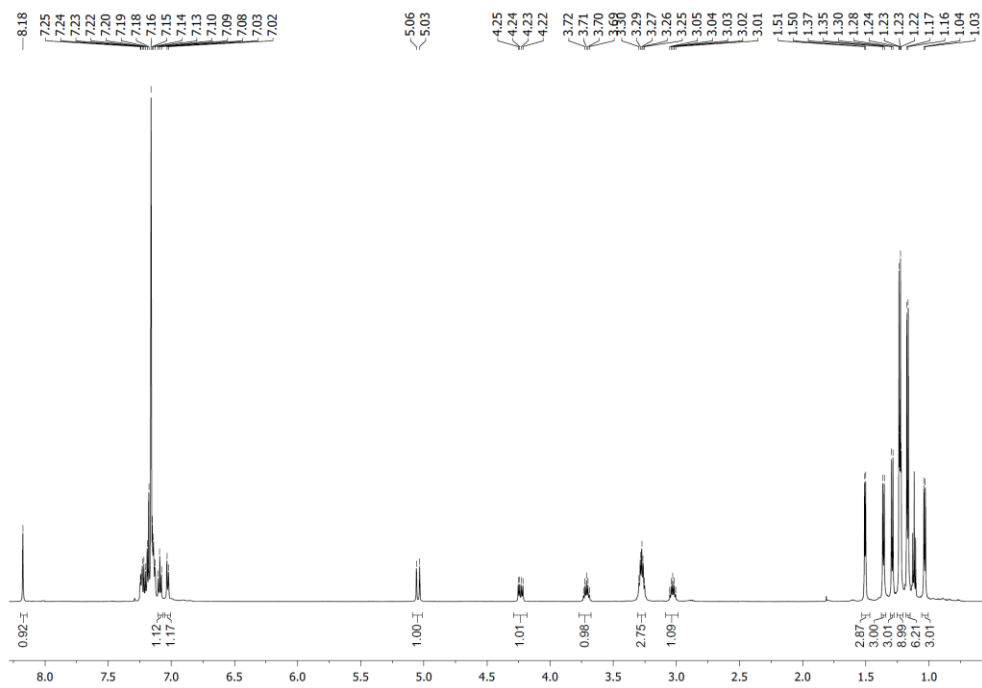
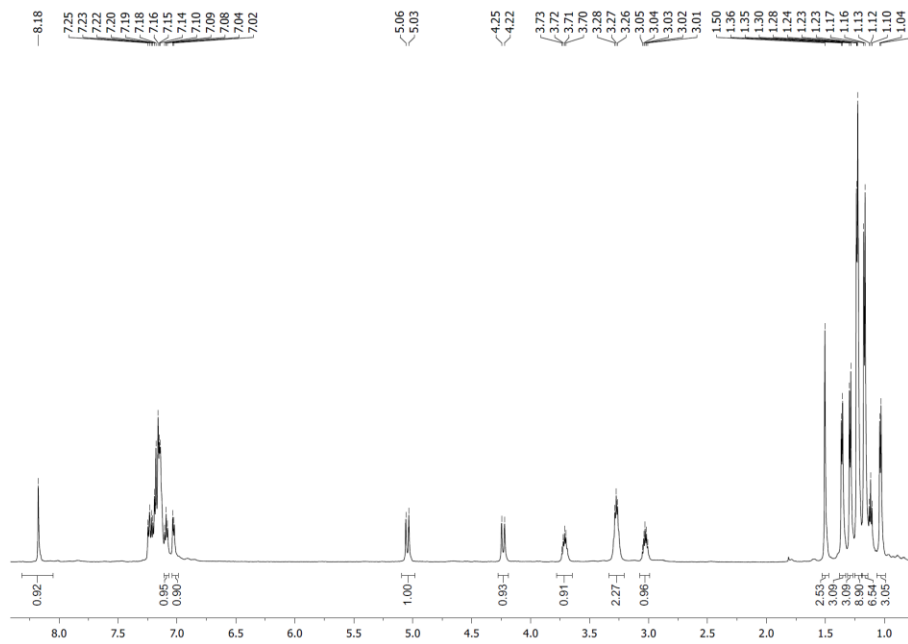


**Figure X-15.**  $^1\text{H}$ ,  $^1\text{H}\{^{31}\text{P}\}$ ,  $^{13}\text{C}\{^1\text{H}\}$ , and  $^{31}\text{P}\{^1\text{H}\}$ ,  $^1\text{H}$ - $^1\text{H}$  COSY NMR spectra of **VI-10** in  $\text{C}_6\text{D}_6$

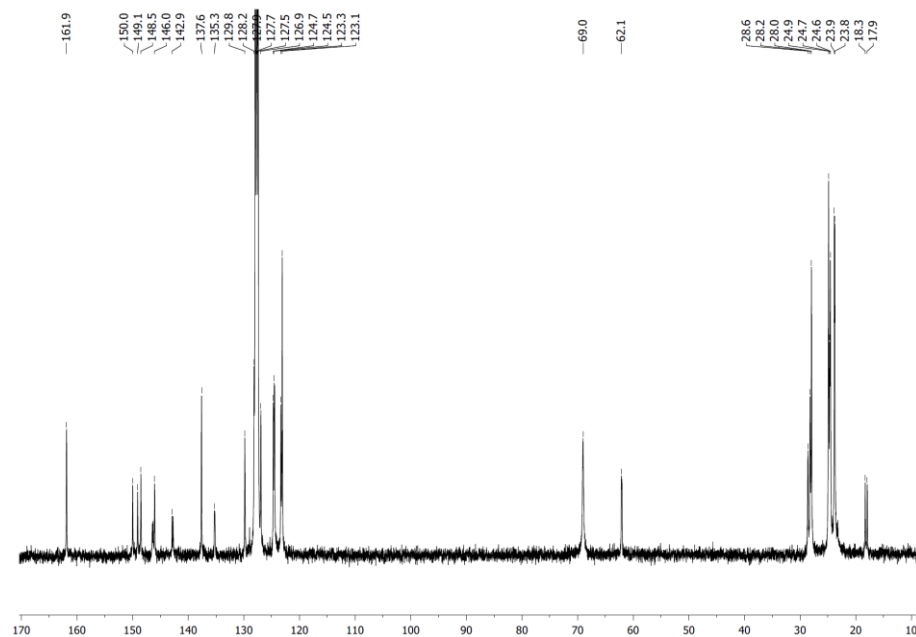
$^1\text{H}$  NMR spectrum



$^1\text{H}\{^3\text{P}\}$  NMR spectrum



$^{13}\text{C}\{^1\text{H}\}$  NMR spectrum



$^{31}\text{P}\{^1\text{H}\}$  NMR spectrum

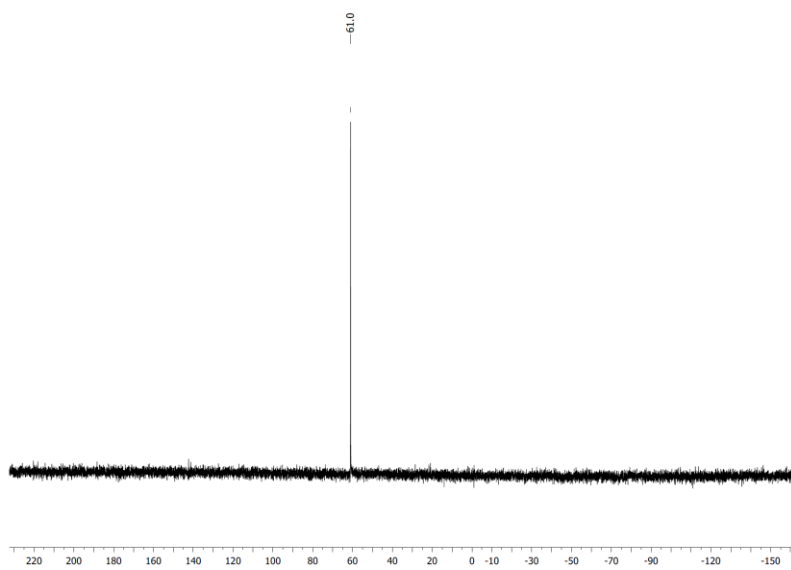
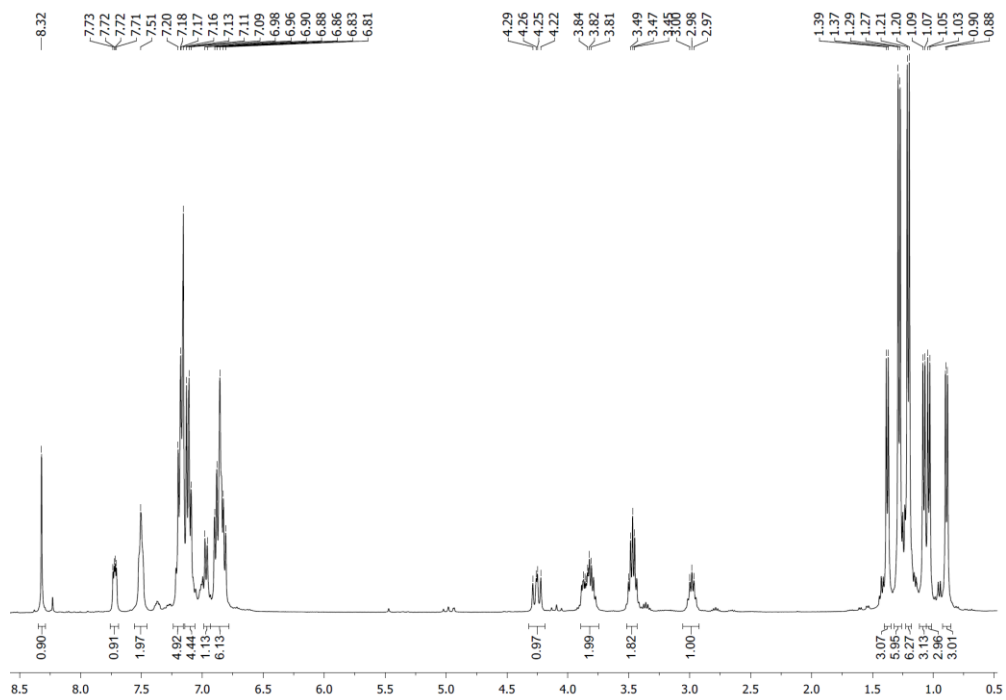
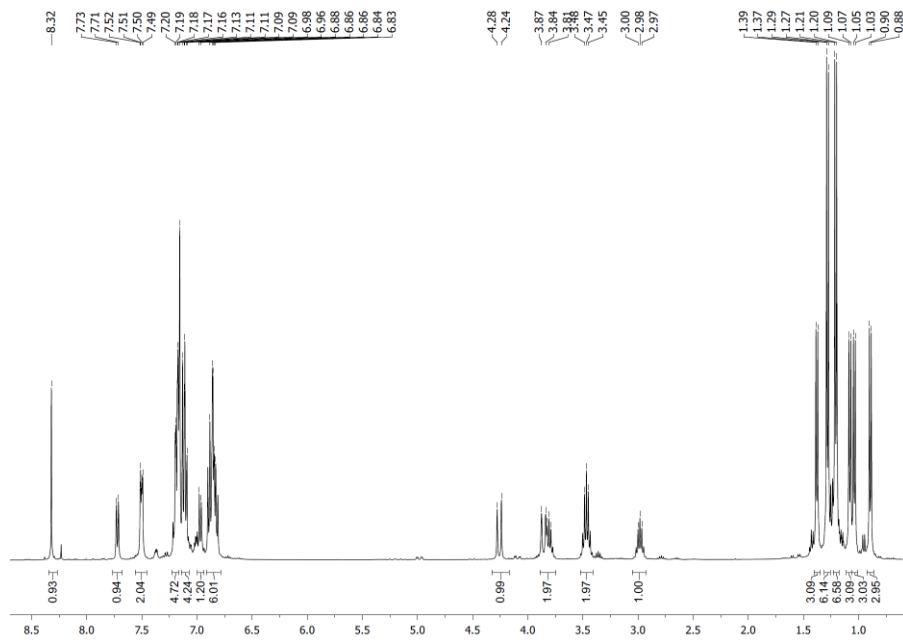


**Figure X-16.**  $^1\text{H}$ ,  $^1\text{H}\{^{31}\text{P}\}$ ,  $^{13}\text{C}\{^1\text{H}\}$ , and  $^{31}\text{P}\{^1\text{H}\}$  NMR spectra of V-11 in  $\text{C}_6\text{D}_6$

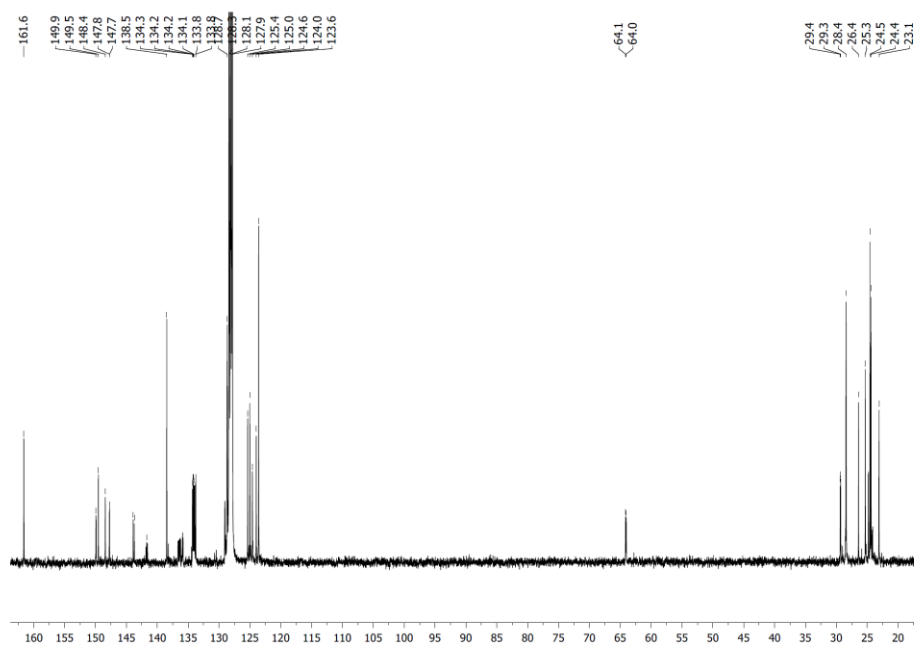
$^1\text{H}$  NMR spectrum



$^1\text{H}\{^{31}\text{P}\}$  NMR spectrum



$^{13}\text{C}\{^1\text{H}\}$  NMR spectrum



$^{31}\text{P}\{^1\text{H}\}$  NMR spectrum

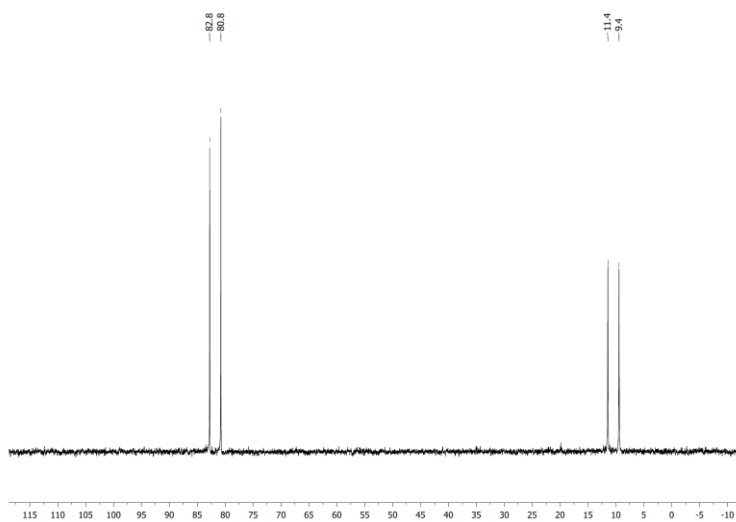
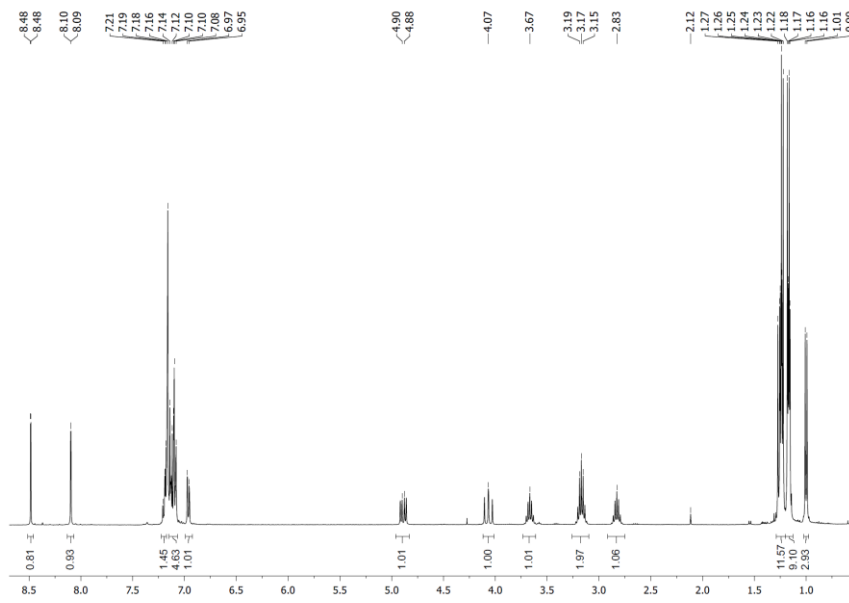
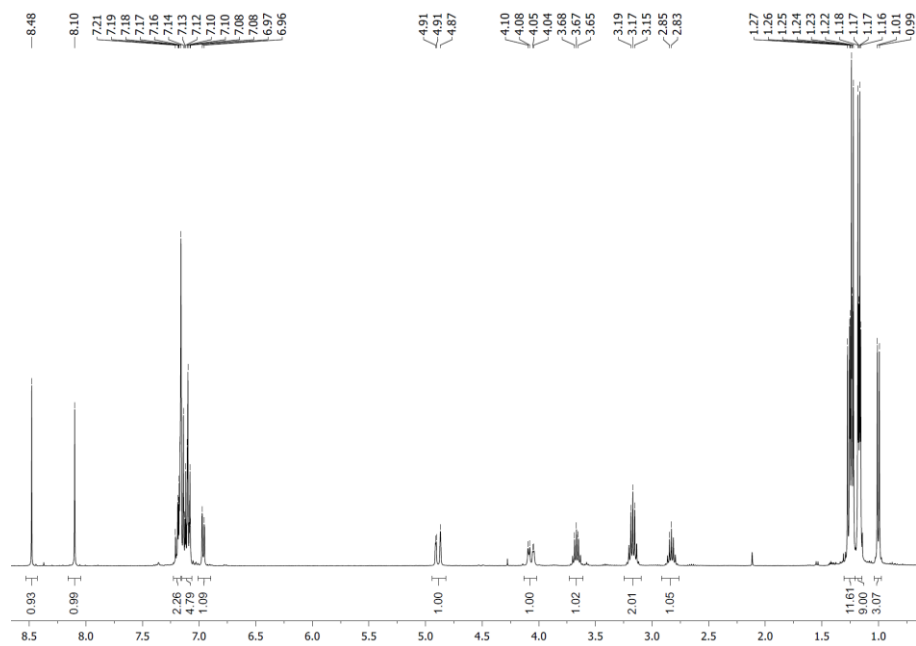


**Figure X-17.**  $^1\text{H}$ ,  $^1\text{H}\{^{31}\text{P}\}$ ,  $^{13}\text{C}\{^1\text{H}\}$ , and  $^{31}\text{P}\{^1\text{H}\}$  NMR spectra of VI-12 in  $\text{C}_6\text{D}_6$

$^1\text{H}$  NMR spectrum

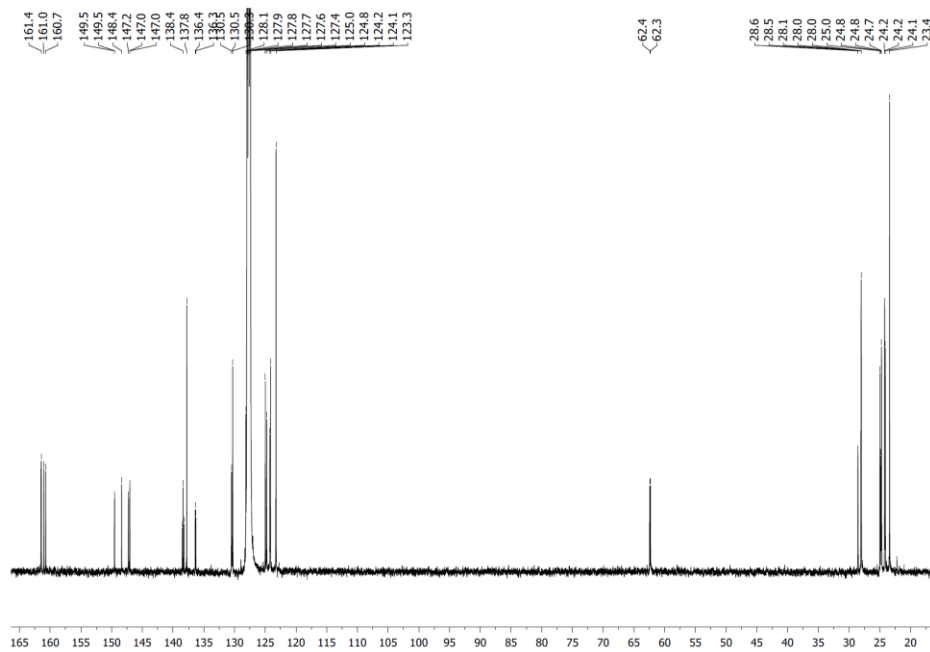


$^1\text{H}\{^3\text{P}\}$  NMR spectrum





$^{13}\text{C}\{^1\text{H}\}$  NMR spectrum



$^{31}\text{P}\{^1\text{H}\}$  NMR spectrum

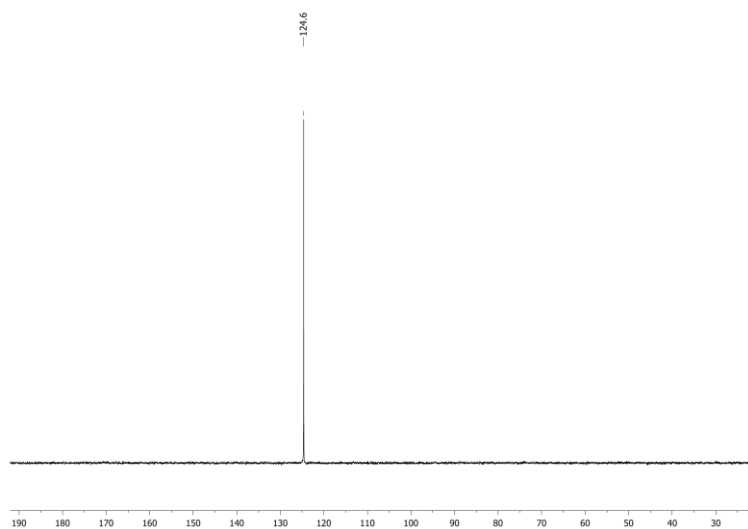
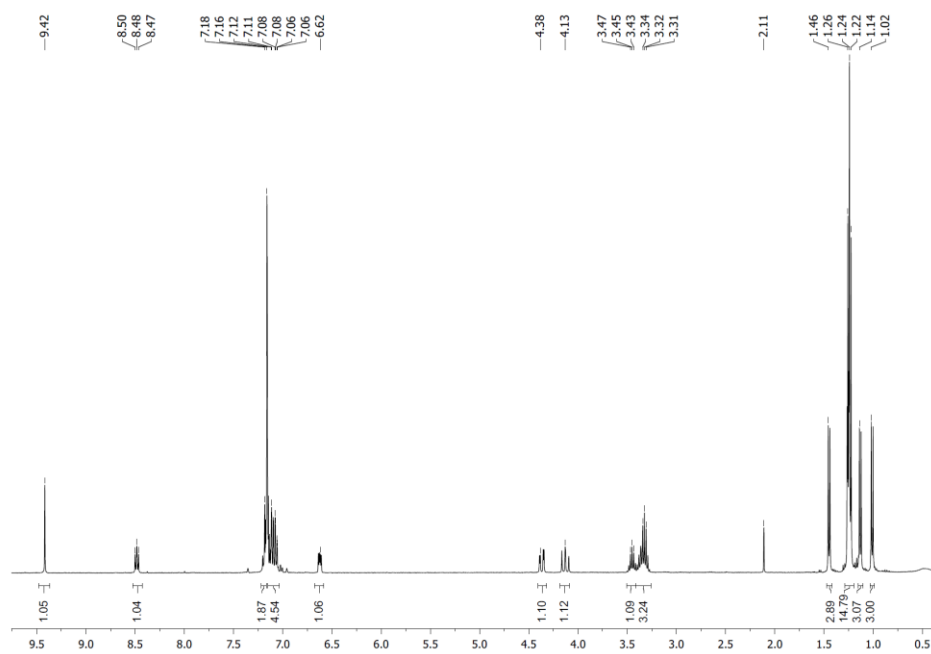
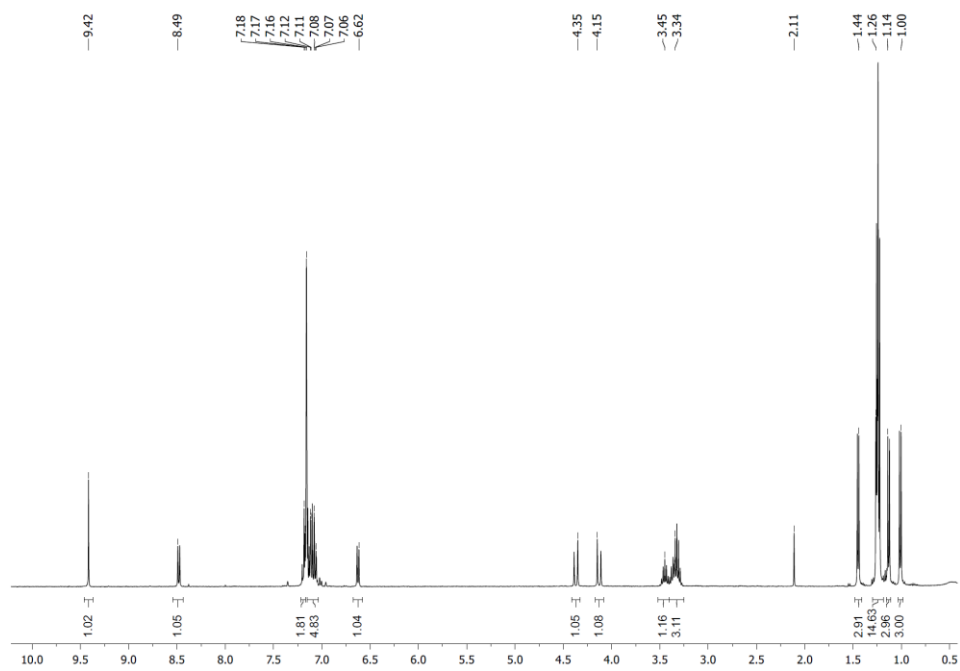


**Figure X-18.**  $^1\text{H}$ ,  $^1\text{H}\{^{31}\text{P}\}$ ,  $^{13}\text{C}\{^1\text{H}\}$ , and  $^{31}\text{P}\{^1\text{H}\}$  NMR spectra of **VI-13** in  $\text{C}_6\text{D}_6$

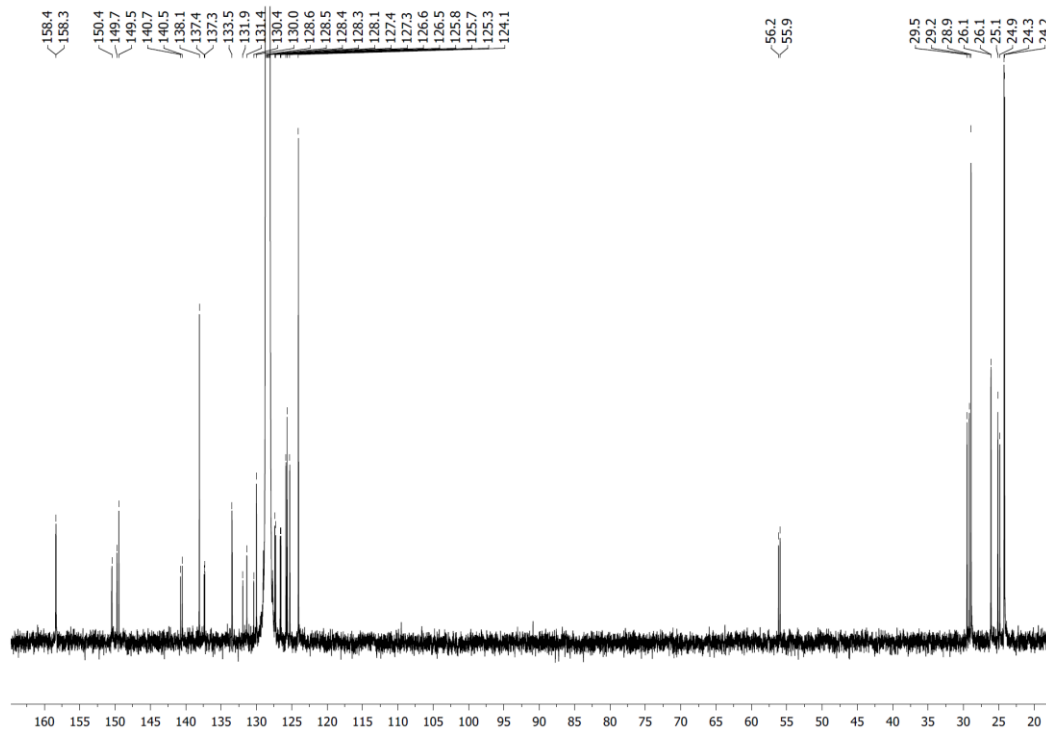
$^1\text{H}$  NMR spectrum



$^1\text{H}\{^{31}\text{P}\}$  NMR spectrum



$^{13}\text{C}\{^1\text{H}\}$  NMR spectrum



$^{31}\text{P}\{^1\text{H}\}$  NMR spectrum

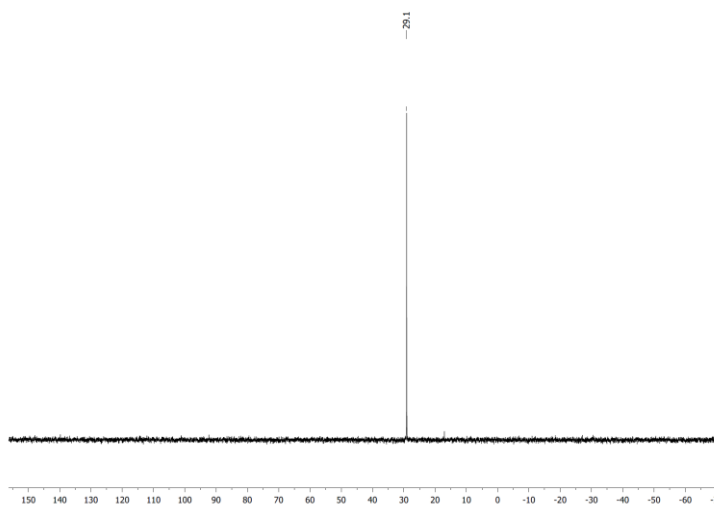
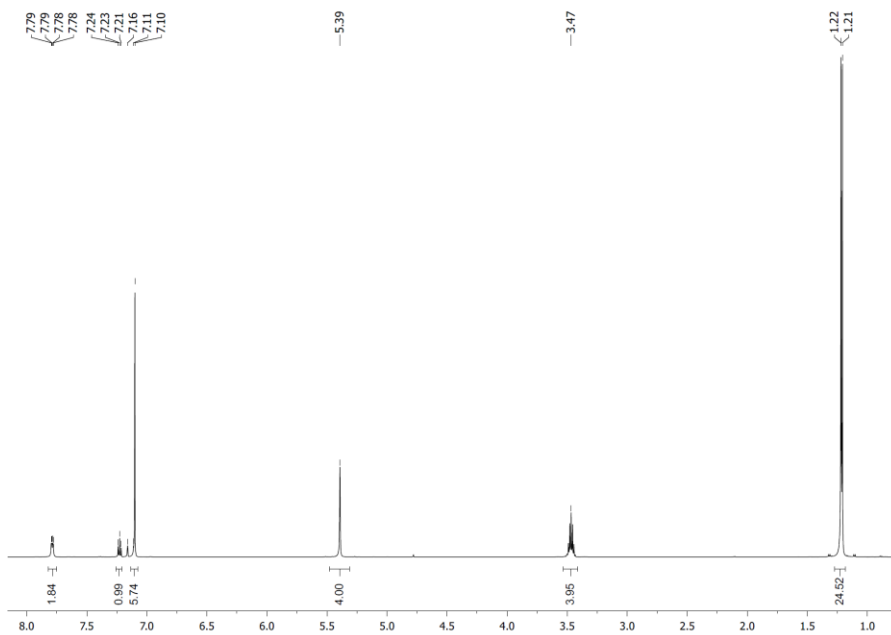
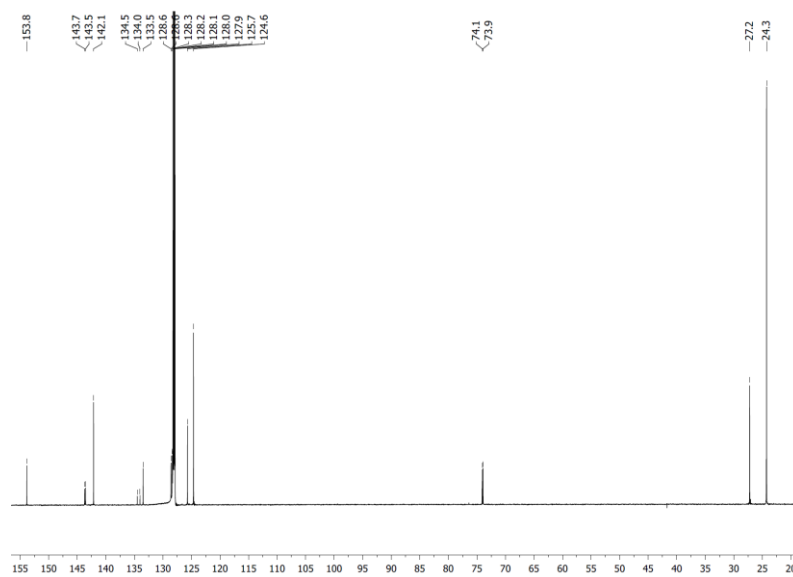


**Figure X-19.**  $^1\text{H}$ ,  $^1\text{H}\{^{31}\text{P}\}$ ,  $^{13}\text{C}\{^1\text{H}\}$ , and  $^{31}\text{P}\{^1\text{H}\}$  NMR spectra of **VI-14** in  $\text{C}_6\text{D}_6$

$^1\text{H}$  NMR spectrum



$^{13}\text{C}\{^1\text{H}\}$  NMR spectrum



$^{31}\text{P}\{^1\text{H}\}$  NMR spectrum

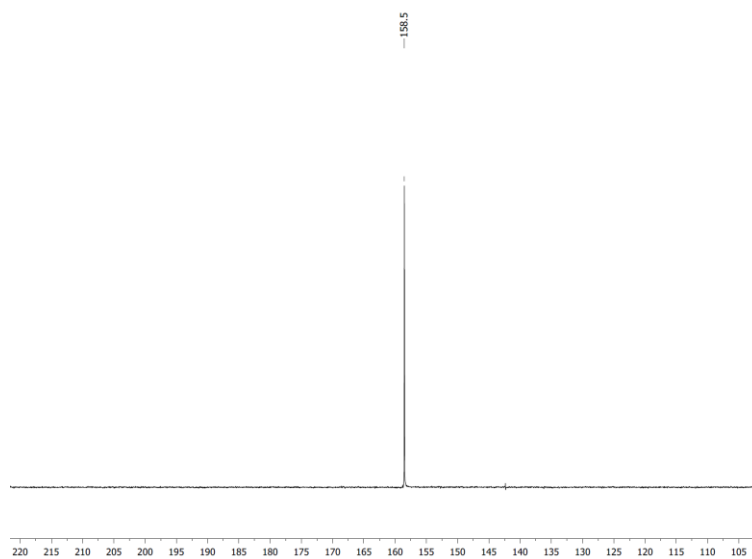
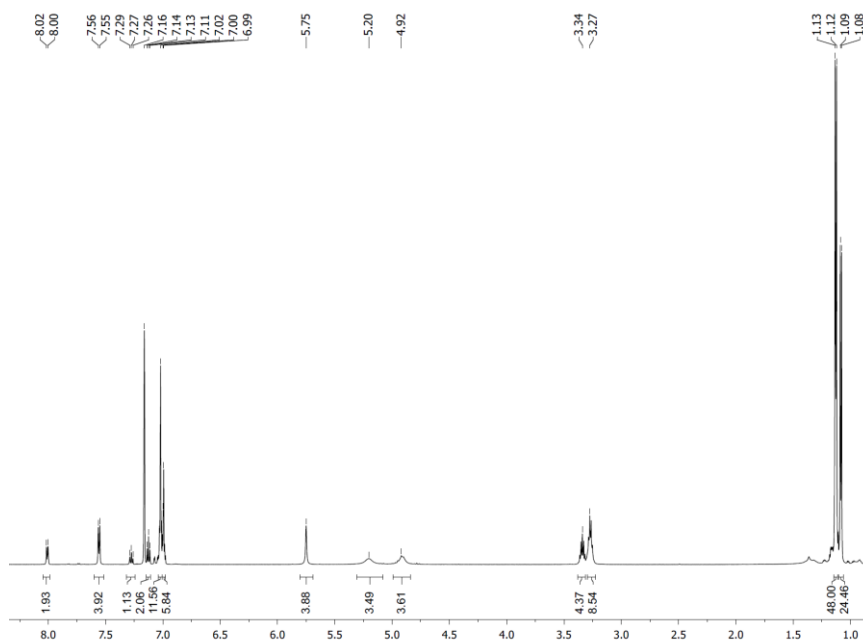
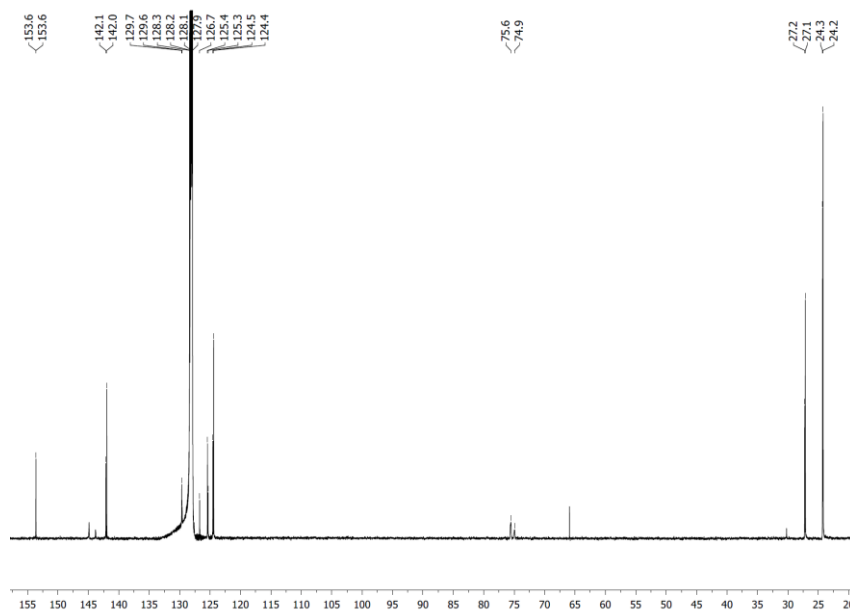


**Figure X-20.**  $^1\text{H}$ ,  $^{13}\text{C}\{^1\text{H}\}$ ,  $^{31}\text{P}\{^1\text{H}\}$  NMR spectra of **VI-16** in  $\text{C}_6\text{D}_6$

$^1\text{H}$  NMR spectrum



$^{13}\text{C}\{^1\text{H}\}$  NMR spectrum



$^{31}\text{P}\{^1\text{H}\}$  NMR spectrum

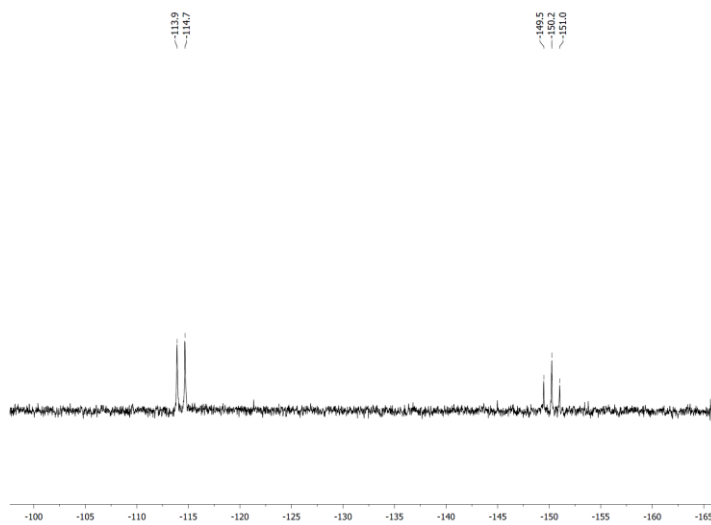
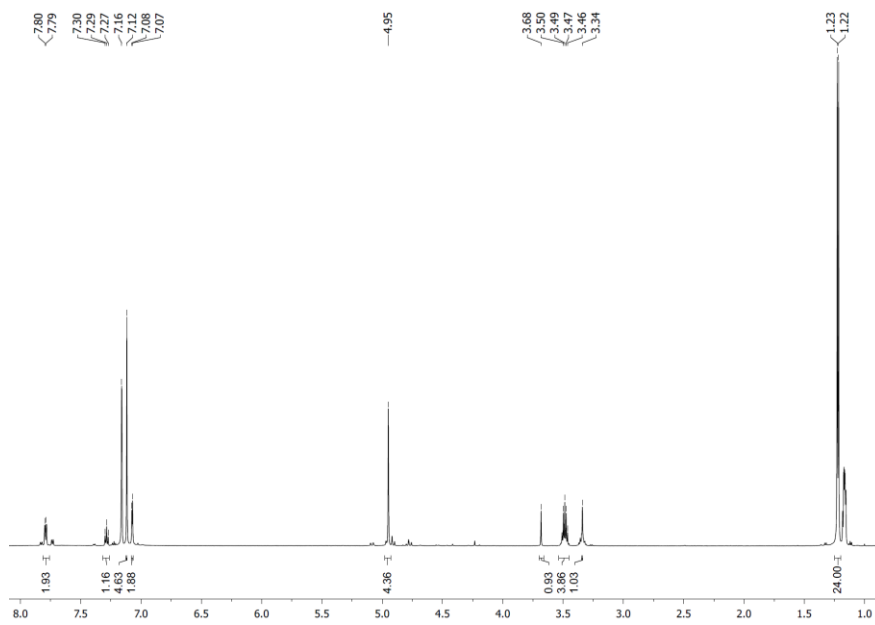
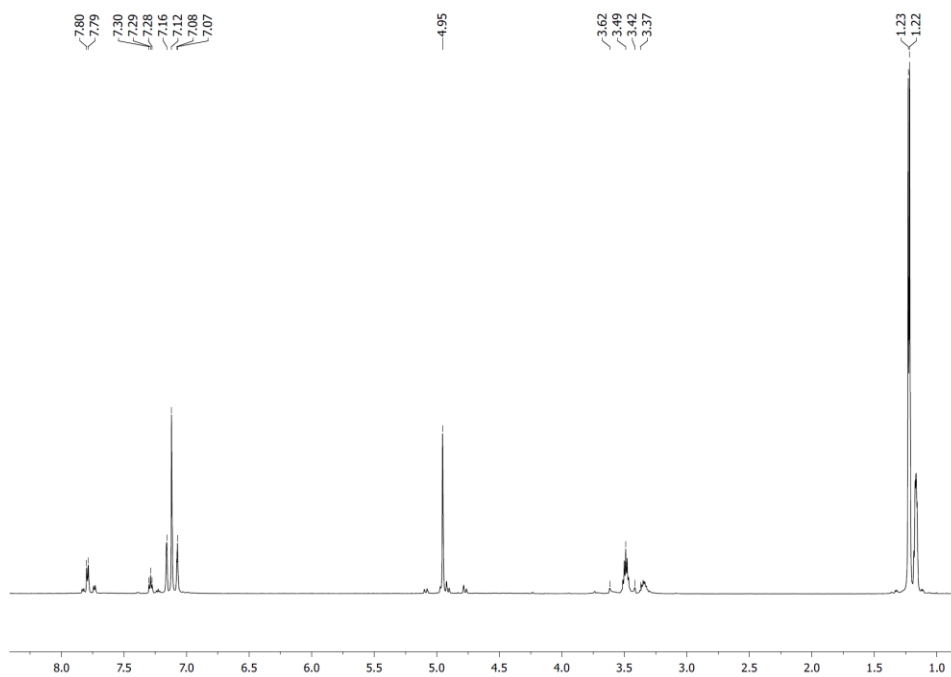


**Figure X-21.**  $^1\text{H}$ ,  $^{13}\text{C}\{^1\text{H}\}$ ,  $^{31}\text{P}\{^1\text{H}\}$  NMR spectra of **VI-18** in  $\text{C}_6\text{D}_6$

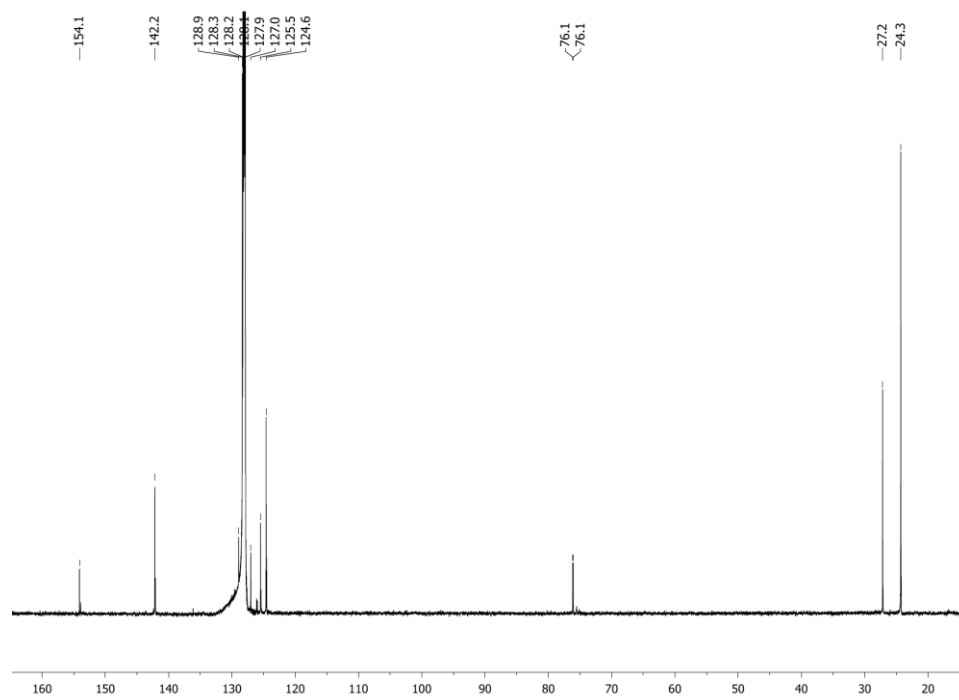
$^1\text{H}$  NMR spectrum



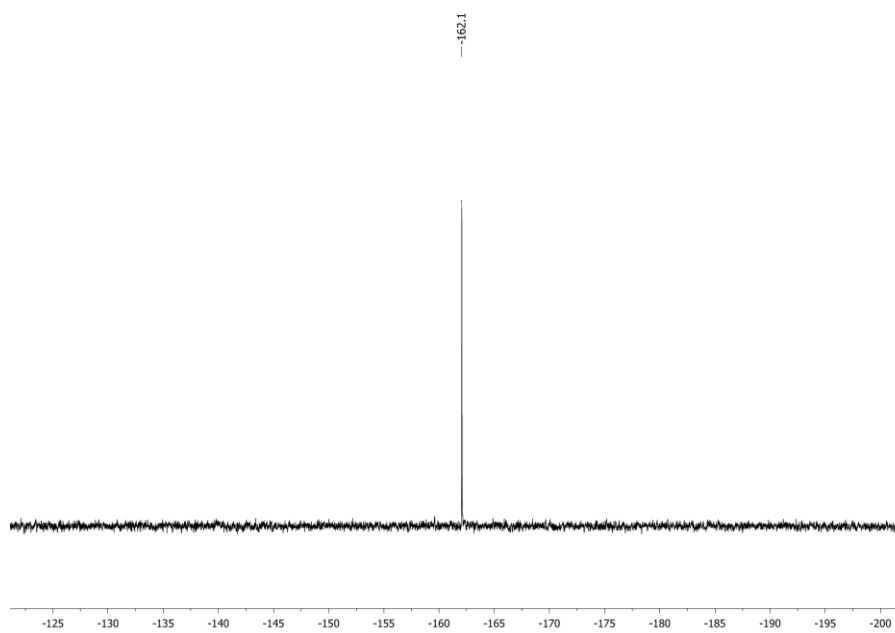
$^1\text{H}\{^3\text{P}\}$  NMR spectrum



$^{13}\text{C}\{^1\text{H}\}$  NMR spectrum



$^{31}\text{P}\{^1\text{H}\}$  NMR spectrum





$^{31}\text{P}$  NMR spectrum

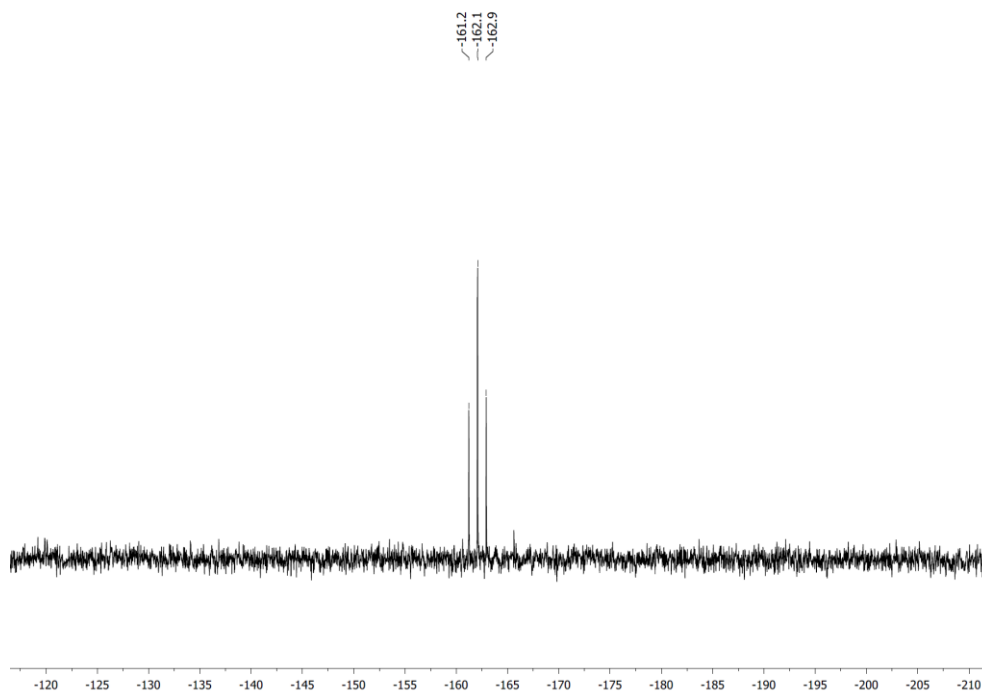
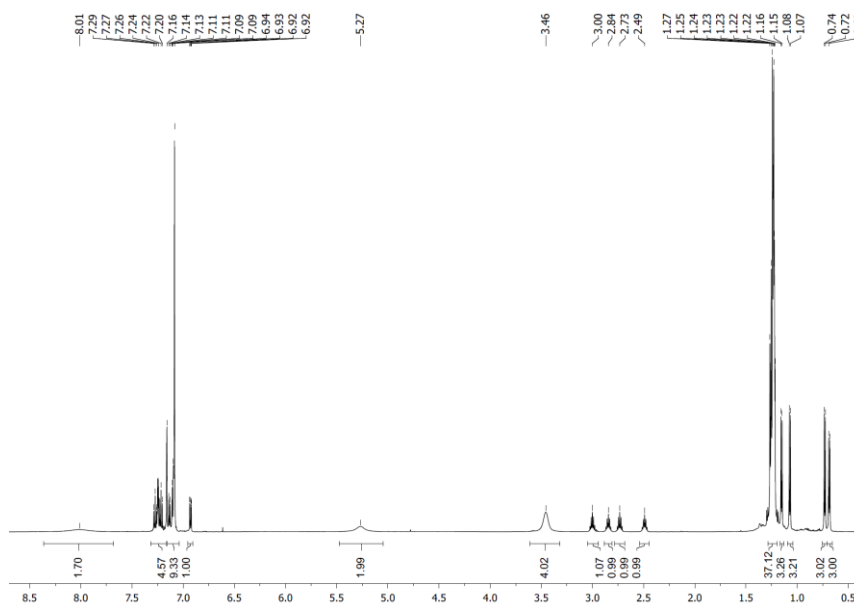
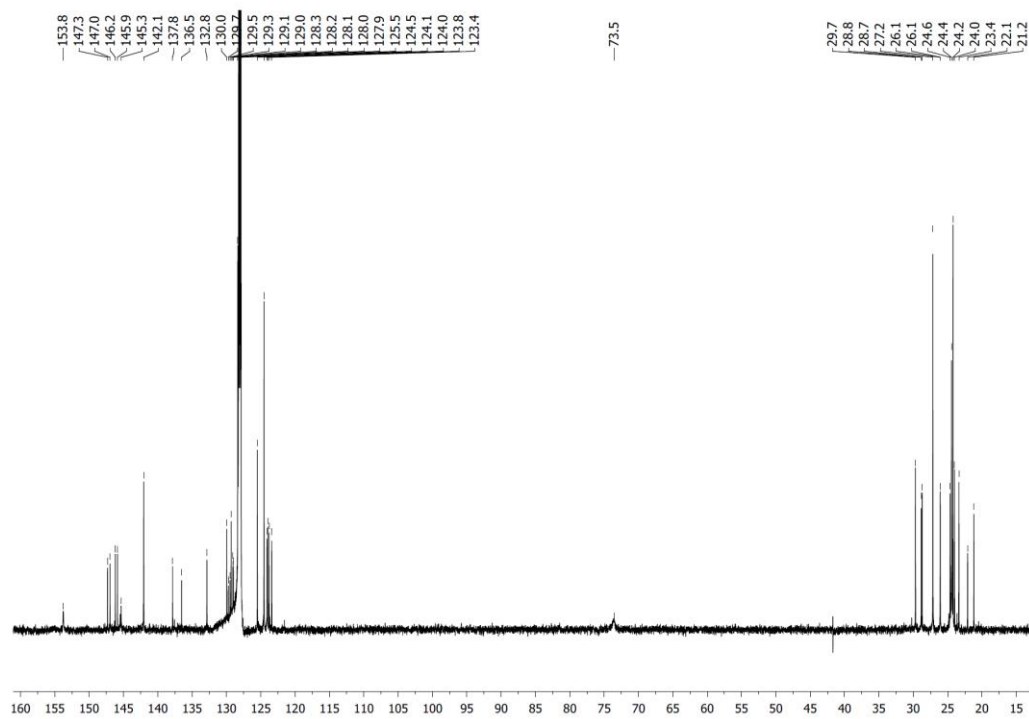


**Figure X-22.**  $^1\text{H}$ ,  $^1\text{H}\{^{31}\text{P}\}$ ,  $^{13}\text{C}\{^1\text{H}\}$ ,  $^{31}\text{P}\{^1\text{H}\}$ ,  $^{31}\text{P}$  NMR spectra of **VI-23** in  $\text{C}_6\text{D}_6$

$^1\text{H}$  NMR spectrum



$^{13}\text{C}\{^1\text{H}\}$  NMR spectrum



$^{31}\text{P}\{^1\text{H}\}$  NMR spectrum

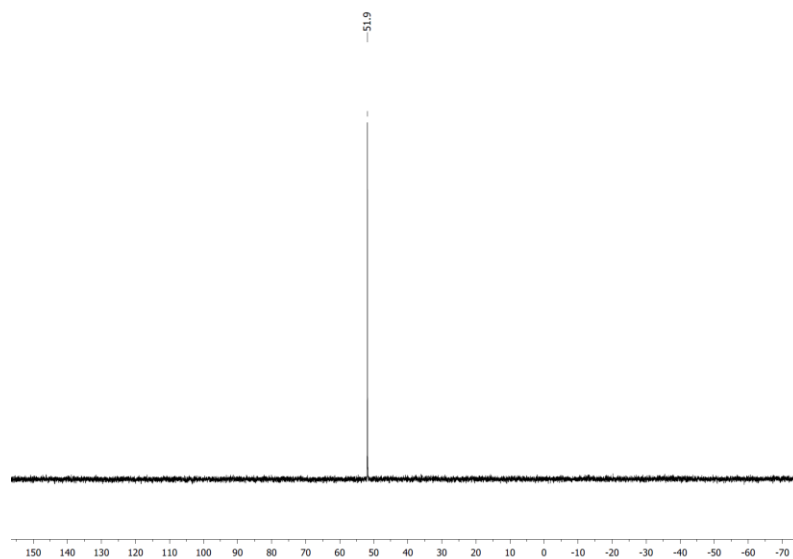
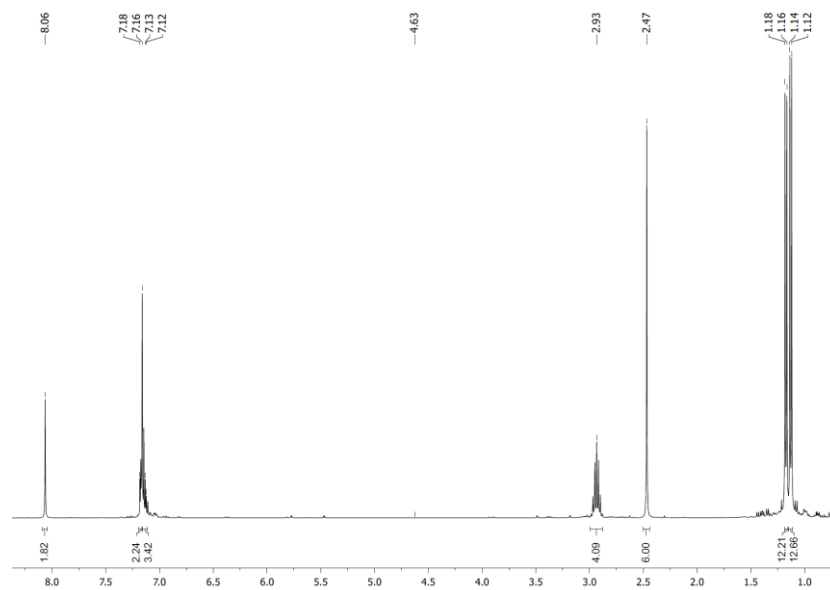


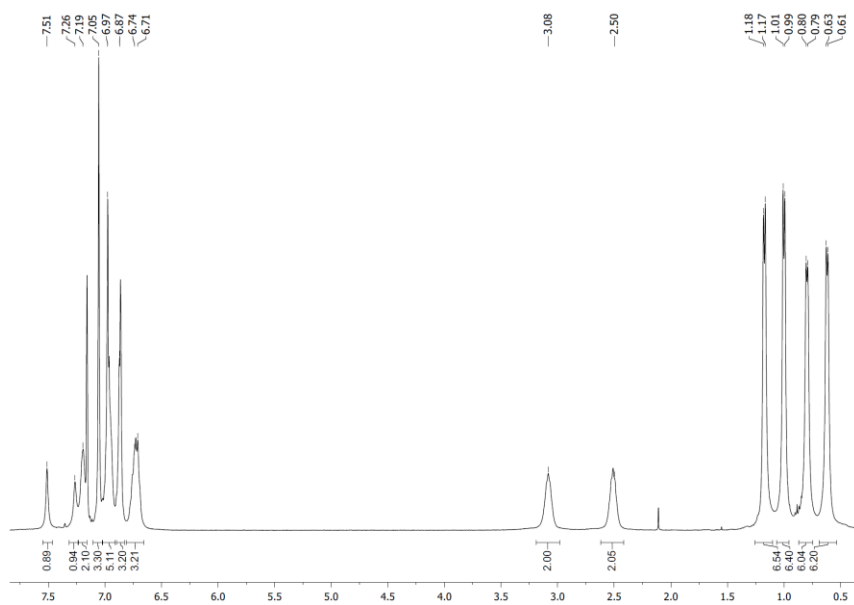
Figure X-23.  $^1\text{H}$ ,  $^{13}\text{C}\{^1\text{H}\}$ ,  $^{31}\text{P}\{^1\text{H}\}$  NMR spectra of **VI-24** in  $\text{C}_6\text{D}_6$

$^1\text{H}$  NMR spectrum



**Figure X-24.**  $^1\text{H}$  NMR spectrum of  $\text{Me dimNHC}$  ligand **VII-3** in  $\text{C}_6\text{D}_6$

$^1\text{H}$  NMR spectrum



$^{13}\text{C}\{^1\text{H}\}$  NMR spectrum

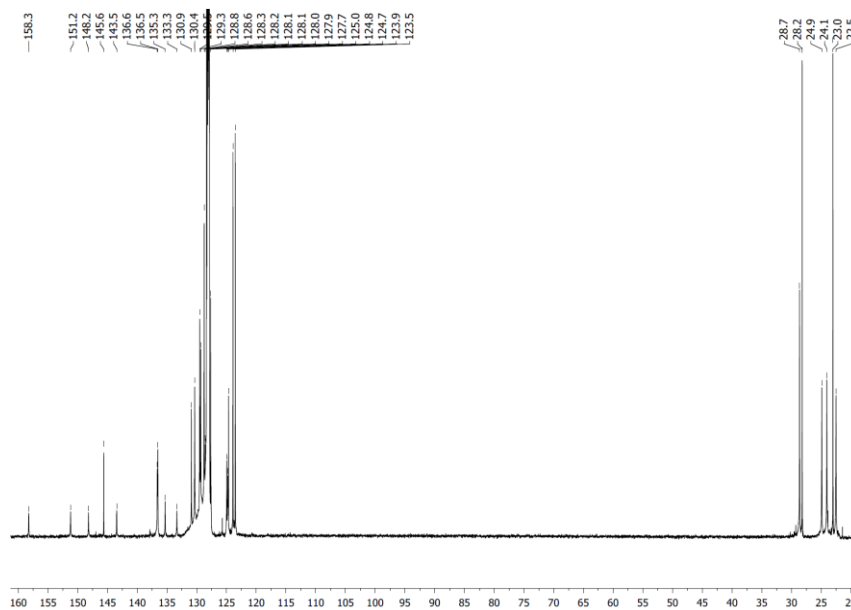


**Figure X-25.**  $^1\text{H}$ ,  $^{13}\text{C}\{^1\text{H}\}$  NMR spectrum of **VII-4** in  $\text{C}_6\text{D}_6$

$^1\text{H}$  NMR spectrum

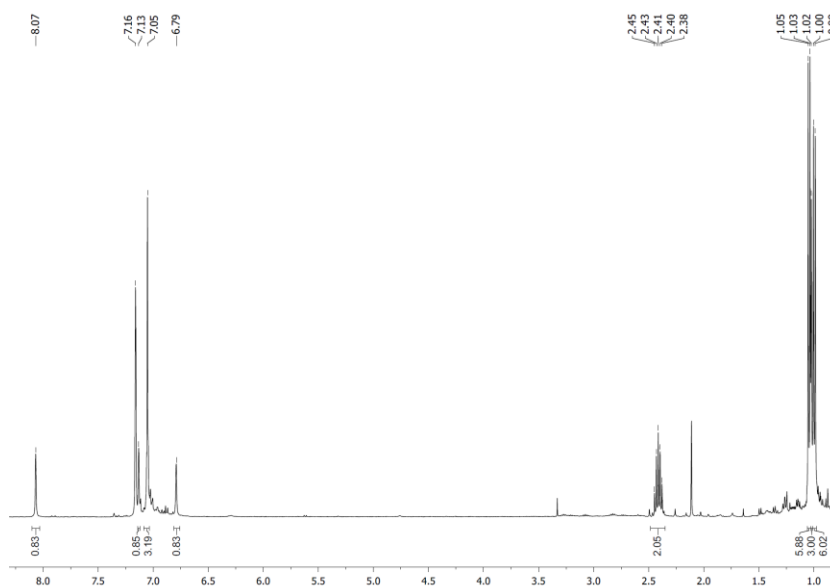
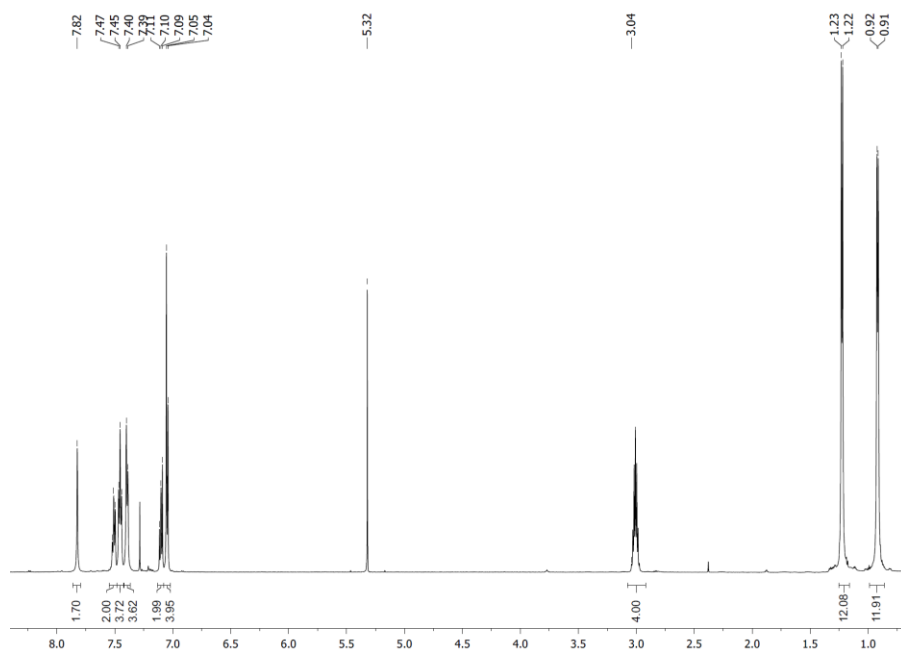


**Figure X-26.**  $^1\text{H}$  NMR spectrum of **VII-5** in  $\text{C}_6\text{D}_6$

$^1\text{H}$  NMR spectrum



$^{13}\text{C}\{^1\text{H}\}$  NMR spectrum

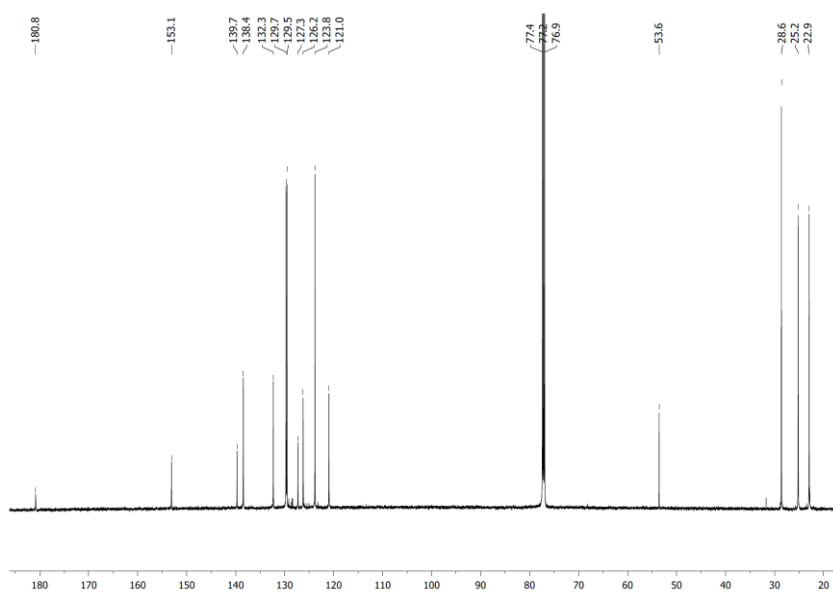
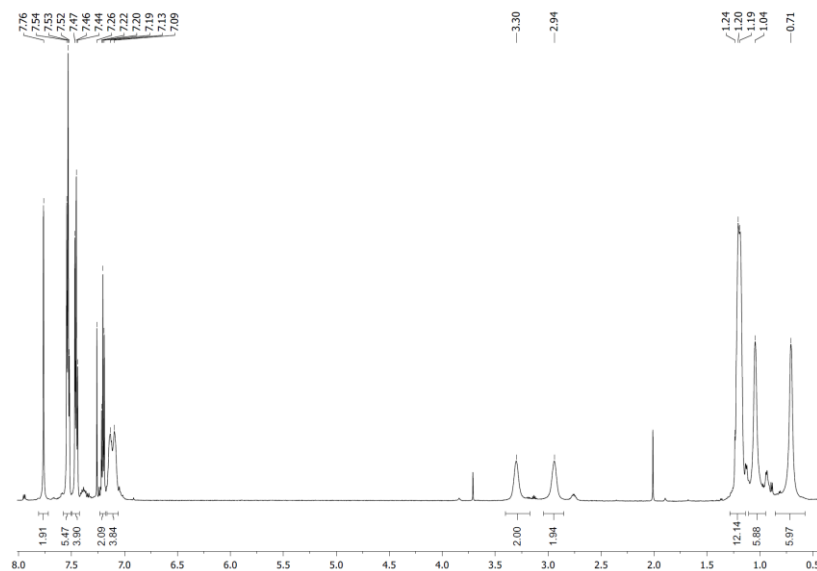


Figure X-27.  $^1\text{H}$ ,  $^{13}\text{C}\{^1\text{H}\}$  NMR spectra of zinc compound VII-6 in  $\text{CDCl}_3$ .

$^1\text{H}$  NMR spectrum



$^{13}\text{C}\{^1\text{H}\}$  NMR spectrum

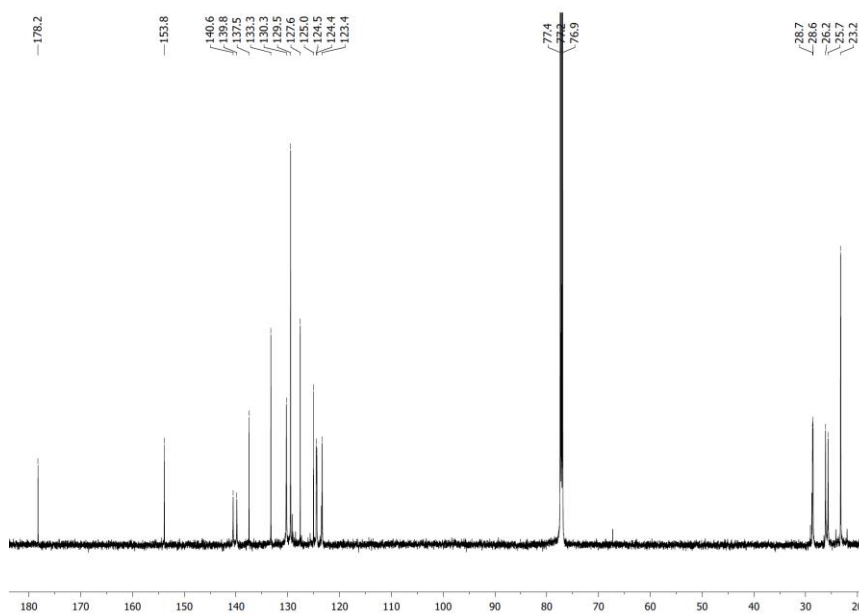
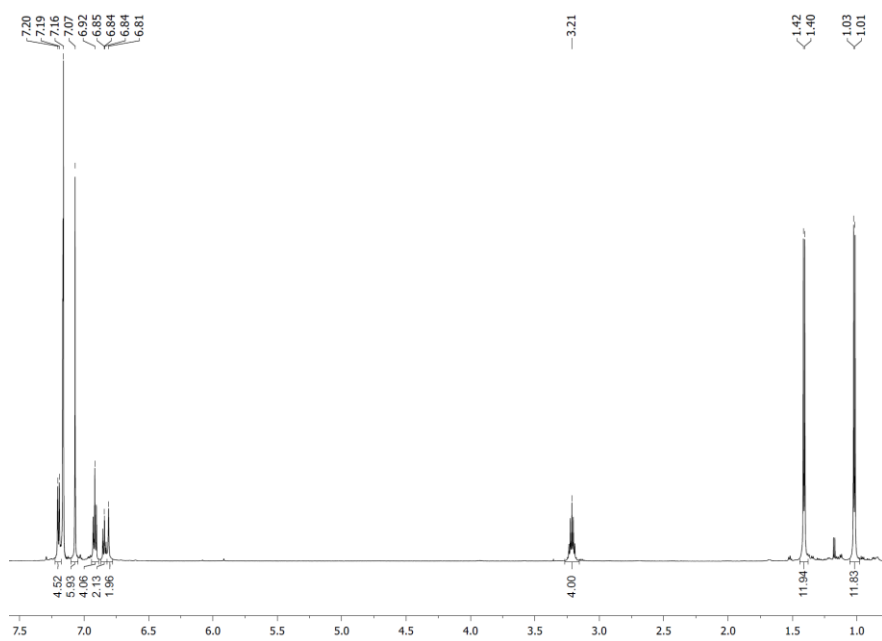
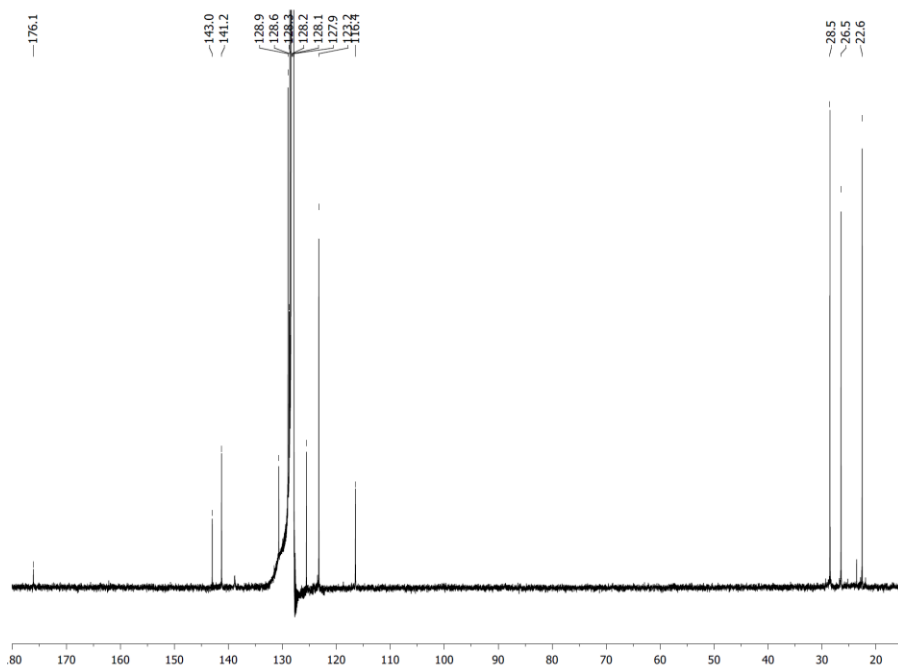


Figure X-28.  $^1\text{H}$ ,  $^{13}\text{C}\{^1\text{H}\}$  NMR spectra of germanium cation VII-7( $\text{ZnCl}_3$ ) in  $\text{CDCl}_3$ .

$^1\text{H}$  NMR spectrum



$^{13}\text{C}\{^1\text{H}\}$  NMR spectrum



*<sup>1</sup>H NMR spectra at various temperature*

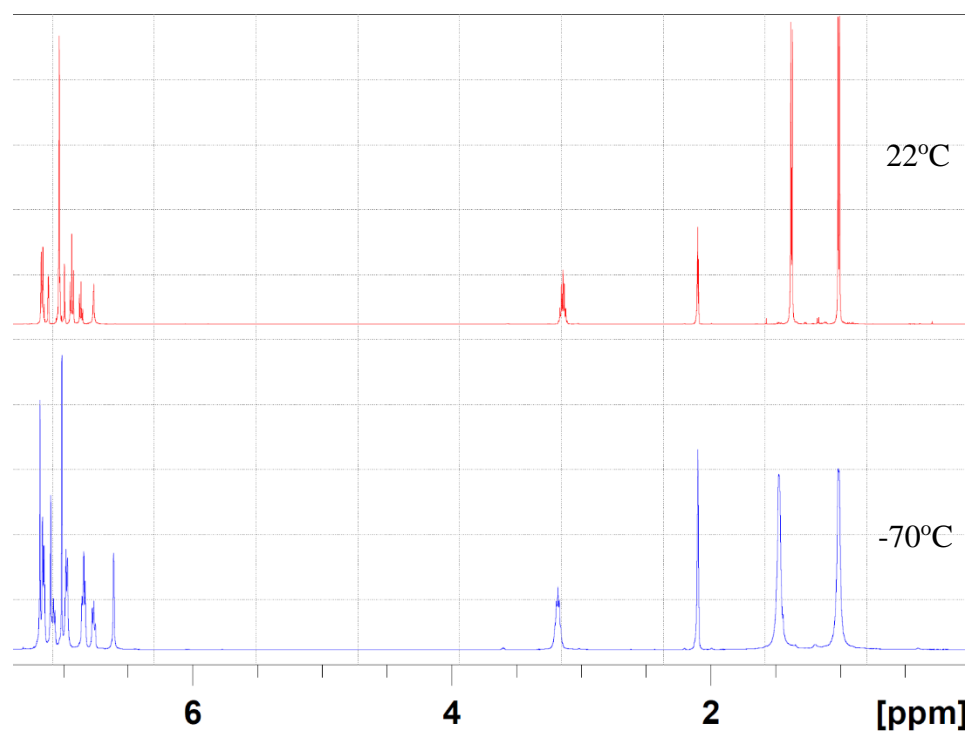
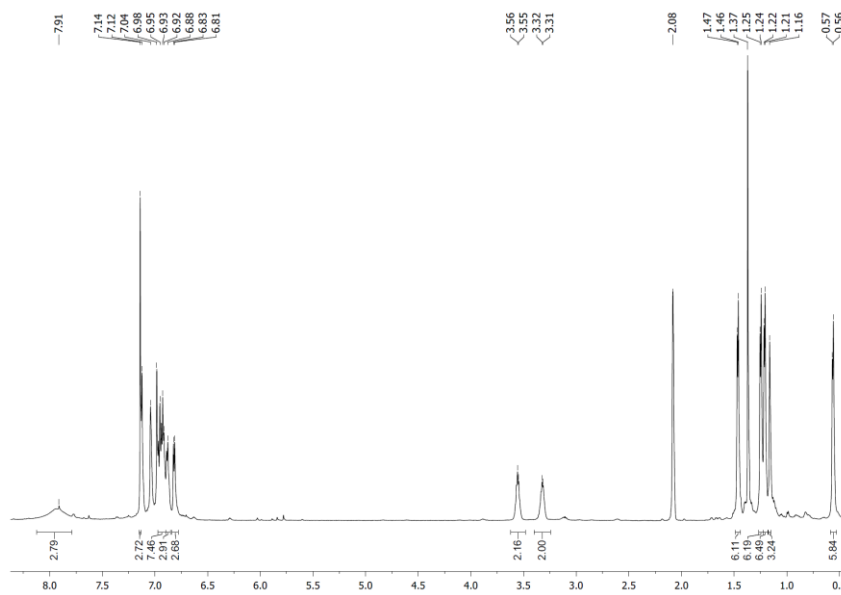


**Figure X-29.**  $^1\text{H}$ ,  $^{13}\text{C}\{^1\text{H}\}$  NMR spectra of germylone **VII-8** in  $\text{C}_6\text{D}_6$  and  $^1\text{H}$  NMR spectra of **VII-8** at various temperature (22°C (red), -70°C (blue)) in toluene- $d_8$ .



$^1\text{H}$  NMR spectrum



$^{13}\text{C}\{^1\text{H}\}$  NMR spectrum

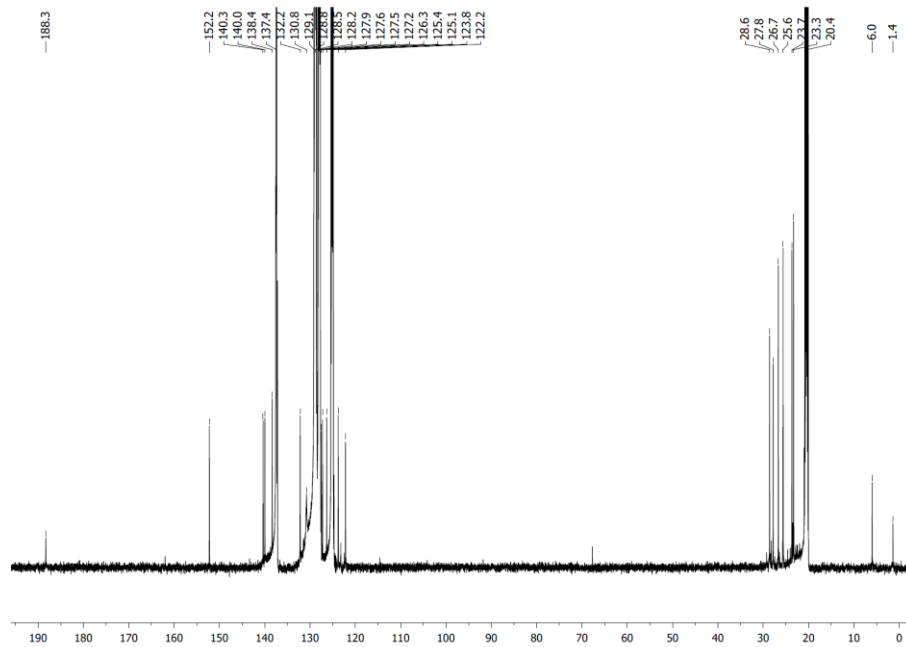
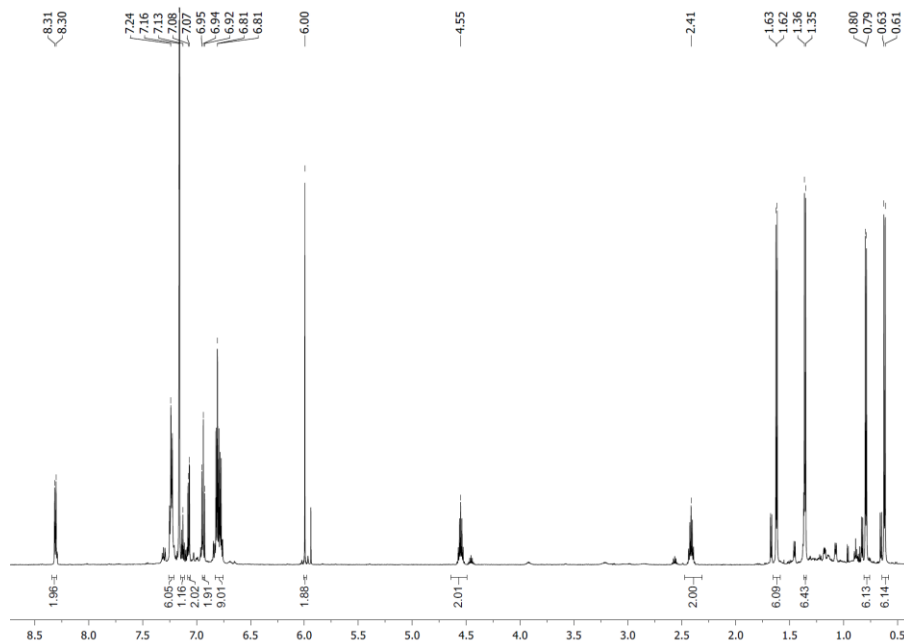
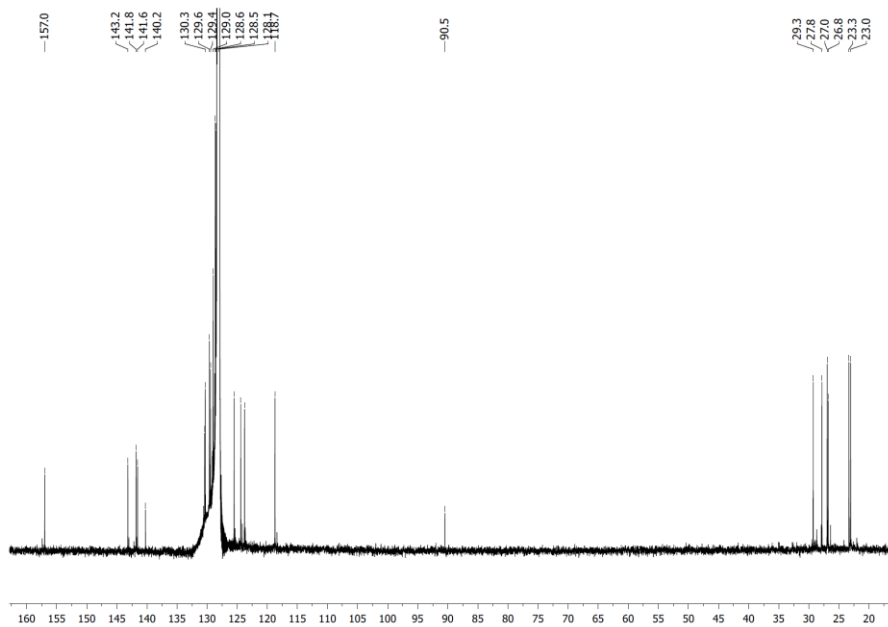


Figure X-30.  $^1\text{H}$ ,  $^{13}\text{C}\{^1\text{H}\}$  NMR spectra of VII-9 in  $\text{C}_6\text{D}_5\text{CD}_3$ .

$^1\text{H}$  NMR spectrum



$^{13}\text{C}\{^1\text{H}\}$  NMR spectrum



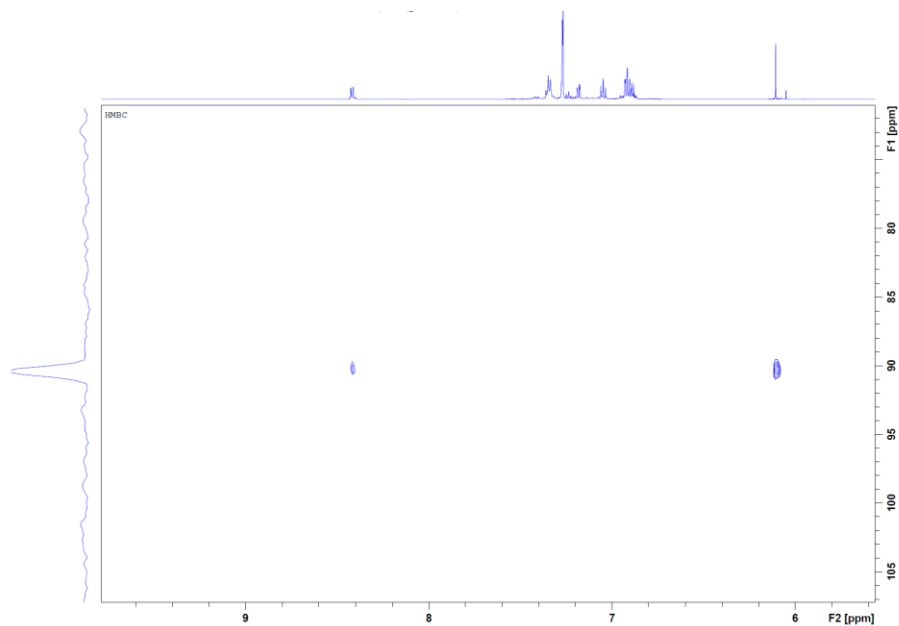
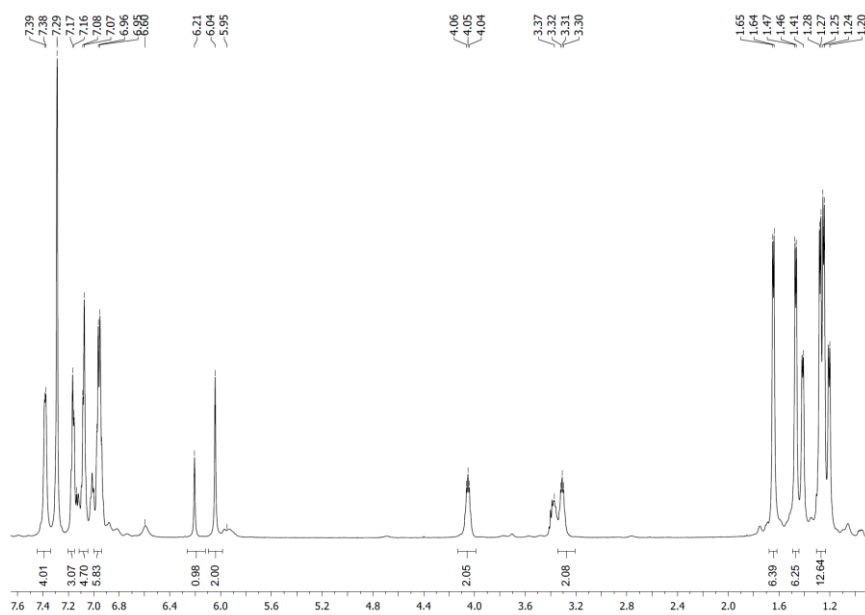


**Figure X-31.**  $^1\text{H}$ ,  $^{13}\text{C}\{^1\text{H}\}$ , 2D-HMBC NMR spectra of **VII-12** in  $\text{C}_6\text{D}_6$ .

*$^1\text{H}$  NMR spectrum*



$^{13}\text{C}\{^1\text{H}\}$  NMR spectrum

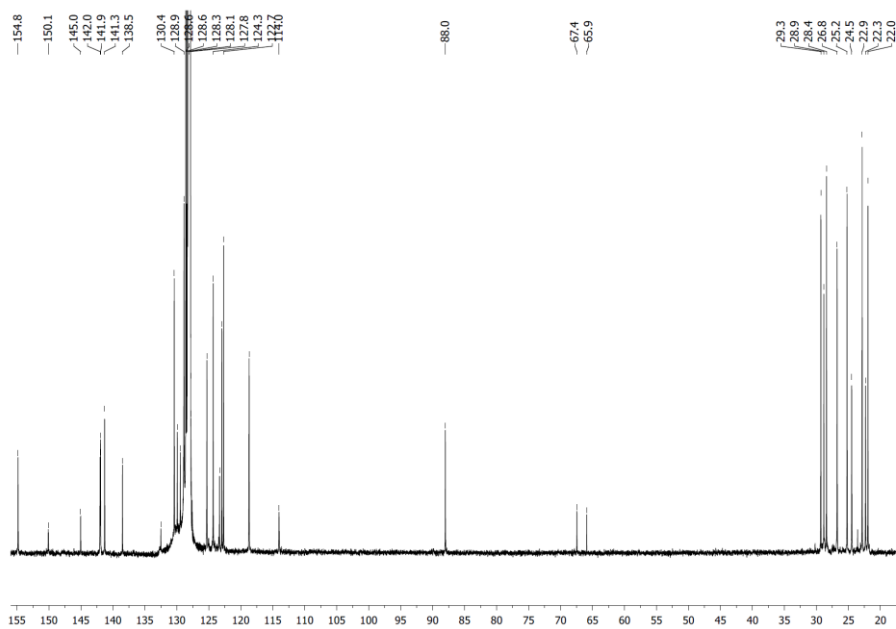
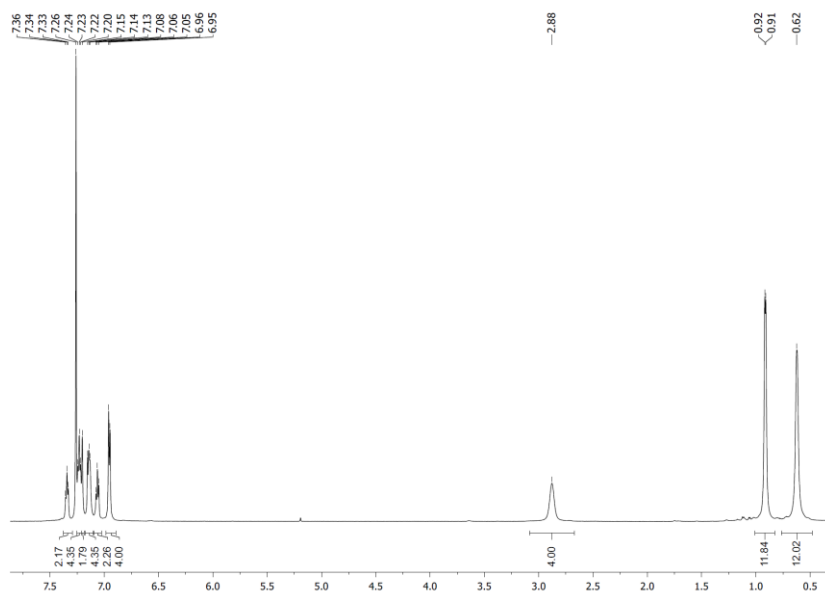
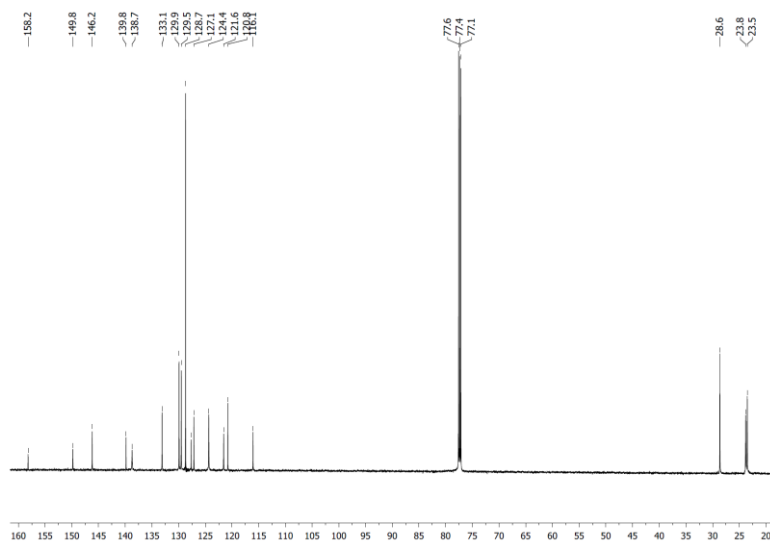


Figure X-32.  $^1\text{H}$ ,  $^{13}\text{C}\{^1\text{H}\}$  NMR spectra of mixture VII-13 + VII-14 in  $\text{C}_6\text{D}_6$ .

$^1\text{H}$  NMR spectrum



$^{13}\text{C}\{^1\text{H}\}$  NMR spectrum



**Figure X-33.**  $^1\text{H}$ ,  $^{13}\text{C}\{^1\text{H}\}$  NMR spectra of **VII-15** in  $\text{CDCl}_3$ .

## Mass spectroscopy

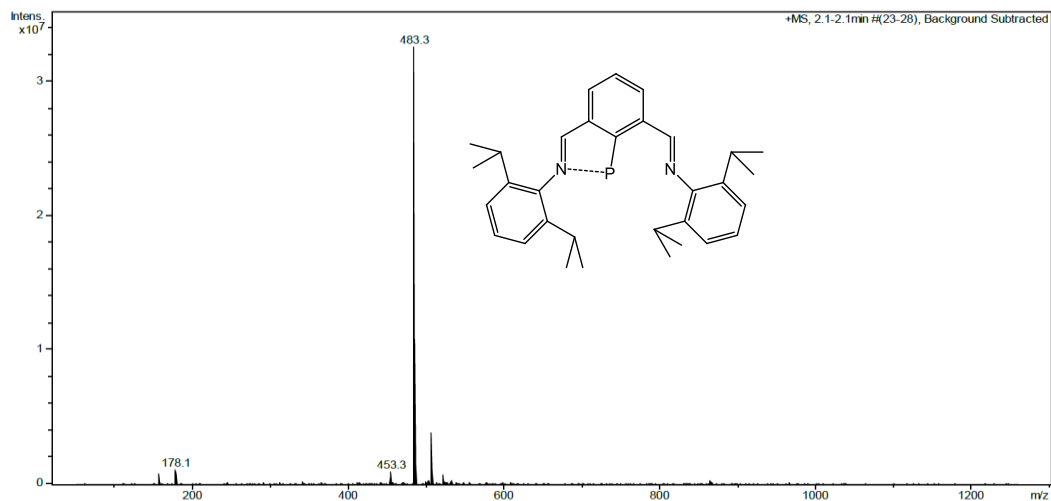


**Figure X-34.** ESI<sup>+</sup> mass spectrum (MeOH/DCM) of VI-2

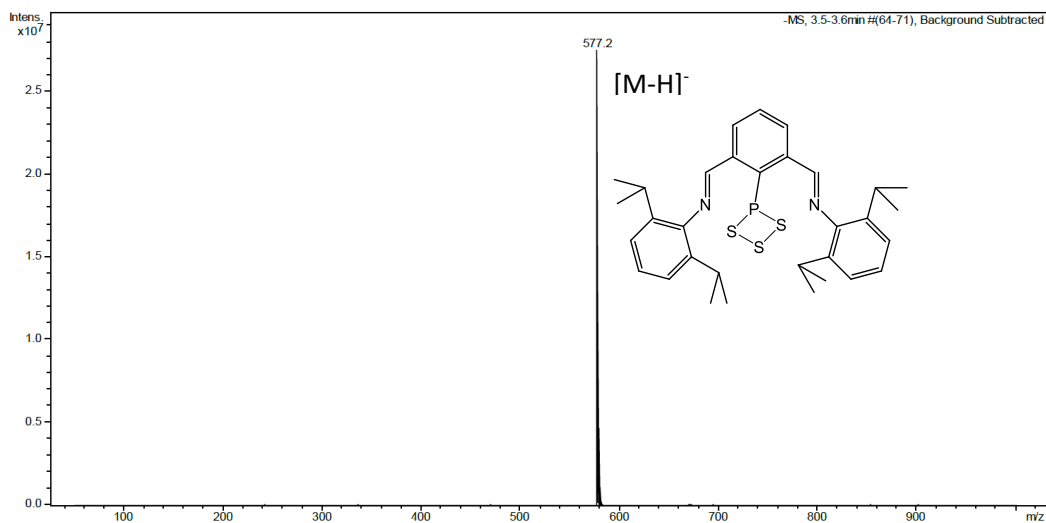
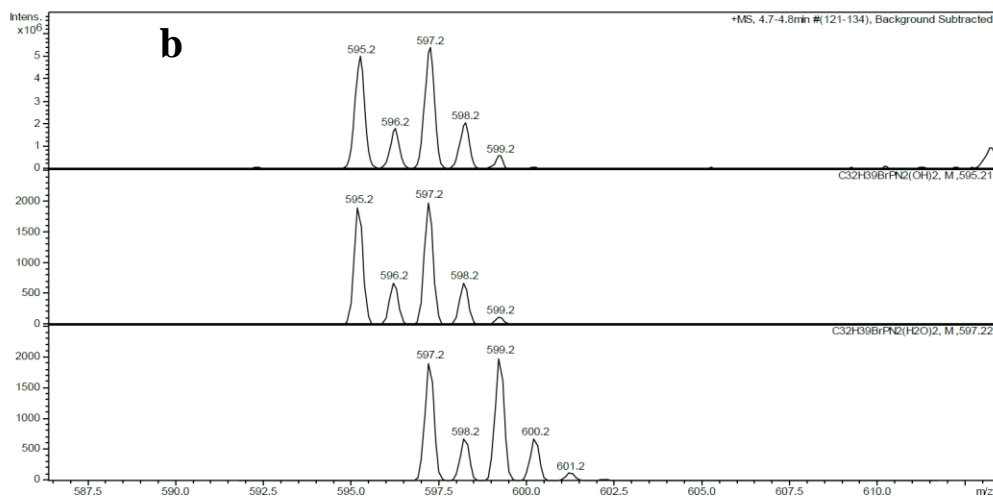
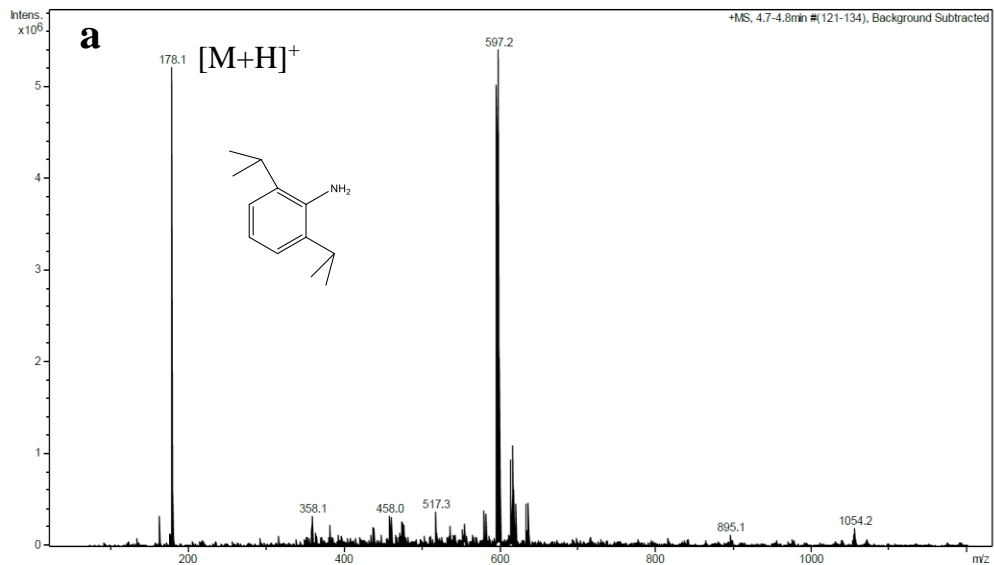


**Figure X-35.** ESI<sup>-</sup> mass spectrum (MeOH/DCM) of VI-8



The middle and bottom spectra are theoretical isotope models of C<sub>32</sub>H<sub>39</sub>BrPN<sub>2</sub>(OH)<sub>2</sub> and C<sub>32</sub>H<sub>39</sub>BrPN<sub>2</sub>(H<sub>2</sub>O)<sub>2</sub>, respectively.

**Figure X-36.** ESI<sup>+</sup> mass spectrum (MeOH/DCM) of **VI-7** (a and b, top) and theoretical modes with OH<sup>-</sup> (b, middle) and H<sub>2</sub>O (b, bottom). The MS data is consistent with theoretical modes of [(dimph)PBr]<sup>+</sup> cation with two [OH]<sup>-</sup> moiety. It's approximately 1.5 mins from when sample vial was open to when sample got into the MS analyzer. Two

[OH]<sup>-</sup> moiety are presented due to exposing the sample to air during the process of preparation.

ESI-

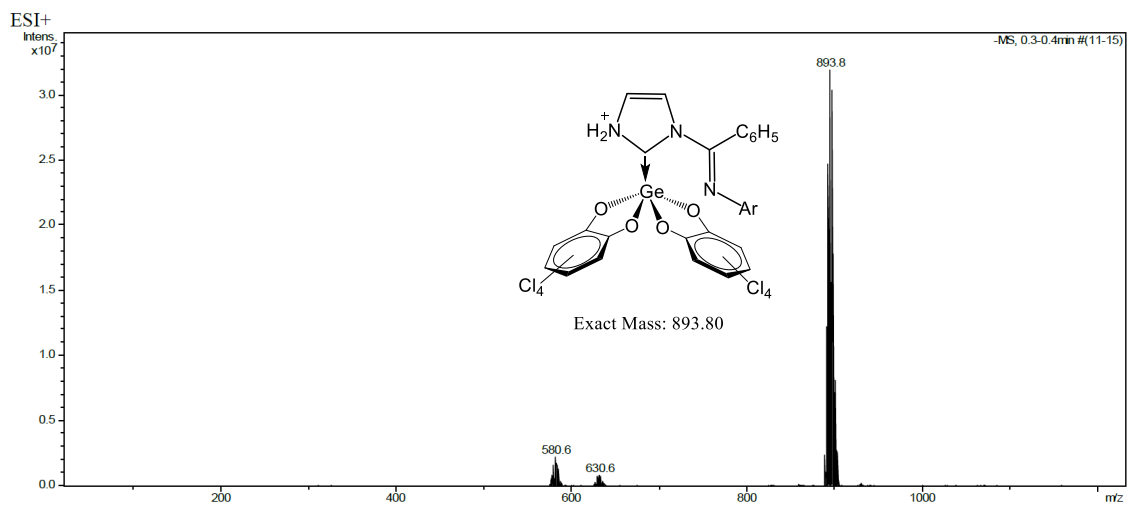
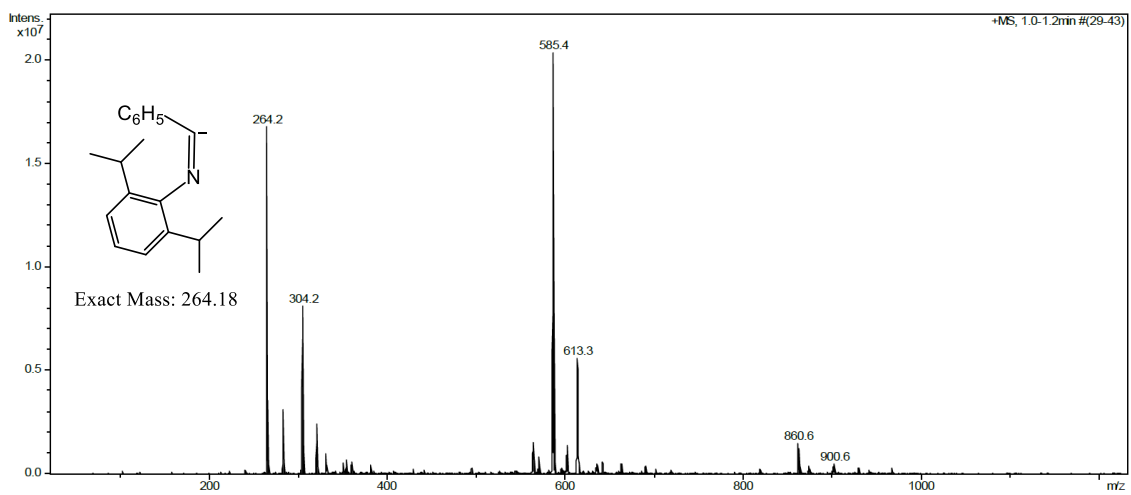


**Figure X-37.** ESI mass spectrum (DCM/ACN) of **VII-15**



## IR spectroscopy

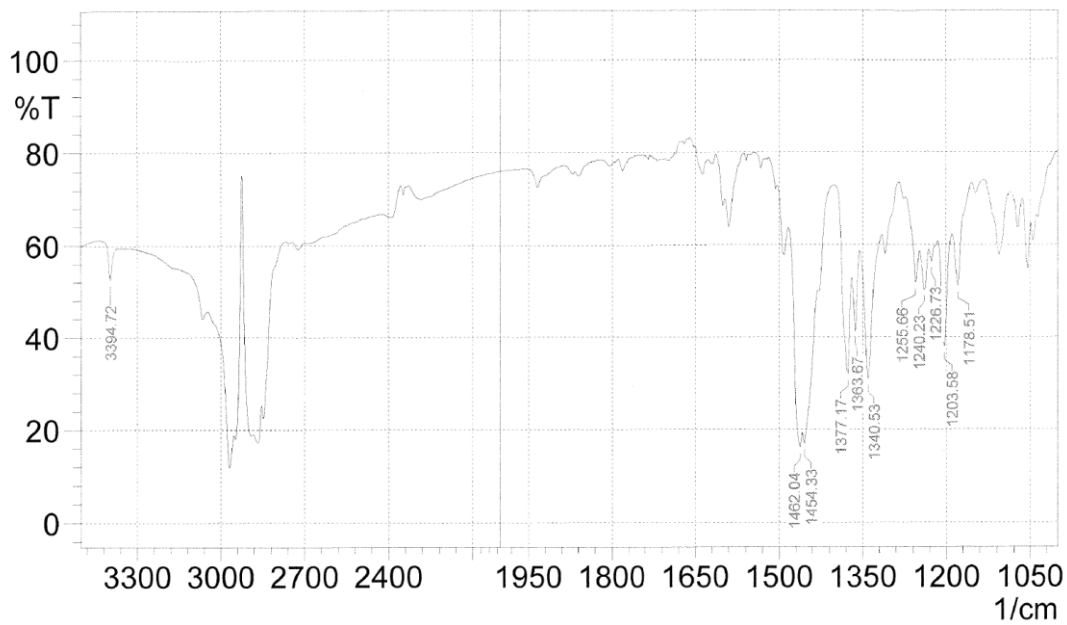


Figure X-38. IR spectrum of VI-10

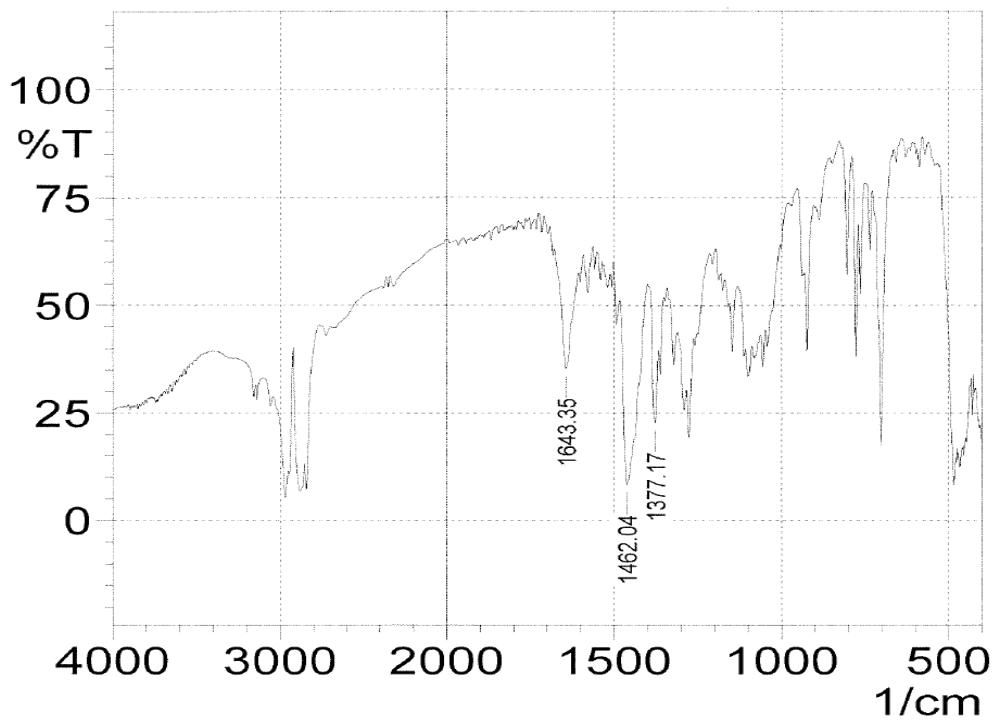
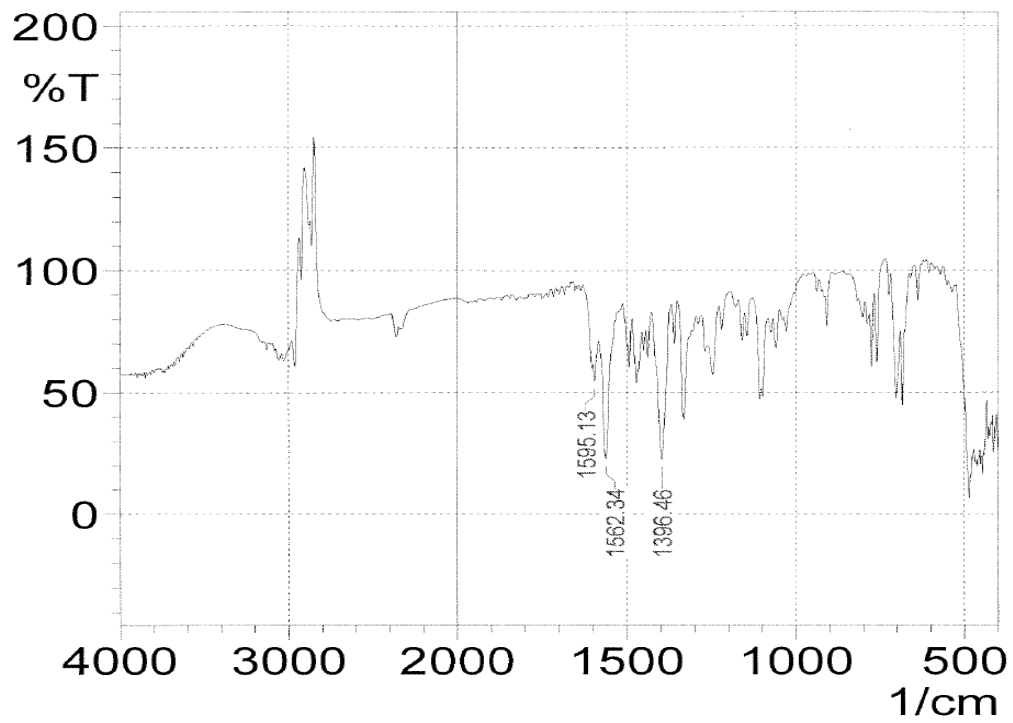


Figure X-39. IR spectrum of VII-7(ZnCl<sub>3</sub>)



**Figure X-40.** IR spectrum of **VII-8**

**X-ray diffraction analyses.****Table X-1.** Crystal and structure refinement data for compound **V-2, V-5, V-7**

	<b>V-2</b>	<b>V-5</b>	<b>V-7</b>
Empirical formula	C <sub>26</sub> H <sub>48</sub> N <sub>4</sub> Zn	C <sub>64</sub> H <sub>78</sub> N <sub>4</sub> Zn	C <sub>64</sub> H <sub>80</sub> N <sub>4</sub> Zn <sub>2</sub>
Formula weight	574.1	968.67	1036.06
colour, habit	colorless, block		orange, block
Crystal size, mm <sup>3</sup>	0.16x0.31x0.84	0.21x 0.25x0.27	0.08 x0.34x0.43
Crystal system	monoclinic	triclinic	monoclinic
Space group	P2 <sub>1</sub> /n	P-1	P2(1)/c
Unit cell dimensions:			
a, Å	9.555(3)	13.522(4)	21.465(2)
b, Å	23.515(9)	14.632(4)	15.5065(14)
c, Å	15.776(6)	15.856(5)	19.1466(18)
α, °	90	77.163(4)	90
β, °	106.742(4)	86.790(4)	114.8170(10)
γ, °	90	67.573(4)	90
Volume, Å <sup>3</sup>	3394(2)	2826.0(15)	5784.3(9)
Z	4	2	4
Density (calcd), g/cm <sup>3</sup>	1.123	1.138	1.190
Absorption coefficient, mm <sup>-1</sup>	0.747	0.476	0.870
F(000)	1232	1040	2208

Temperature, K	200(2)	238(2)	123(2)
2 $\theta$ range for data collection, °	2.19 to 28.28	1.77 to 27.00	1.68 to 28.32
Reflections collected	8256	12177	14211
Independent reflections	4899 [R(int) = 0.0590]	6607 [R(int) = 0.0600]	7845 [R(int) = 0.0594]
Data / restraints / parameters	8256/0/ 352	12177/0/622	14211/ 0/631
Goodness-of-fit on F <sup>2</sup>	1.010	0.947	1.009
Final R indices [I>2 $\sigma$ (I)]	R <sub>1</sub> = 0.0639 wR <sub>2</sub> = 0.1189	R <sub>1</sub> = 0.0592 wR <sub>2</sub> = 0.1243	R <sub>1</sub> = 0.0508 wR <sub>2</sub> = 0.1191
R indices (all data)	R <sub>1</sub> = 0.1418 wR <sub>2</sub> = 0.1651	R <sub>1</sub> = 0.1198 wR <sub>2</sub> = 0.1461	R <sub>1</sub> = 0.1325 wR <sub>2</sub> = 0.1825
Largest diff. peak and hole, e.Å <sup>-3</sup>	0.576 and -0.700	0.280 and -0.463	1.594 and -1.282

**Table X-2.** Crystal and structure refinement data for **VI-2, VI-10, VI-13, VI-14**

	<b>VI-2</b>	<b>VI-10</b>	<b>VI-13</b>	<b>VI-14</b>
empirical formula	C <sub>32</sub> H <sub>39</sub> N <sub>2</sub> P	C <sub>32</sub> H <sub>41</sub> N <sub>2</sub> P	C <sub>33</sub> H <sub>41</sub> N <sub>2</sub> O <sub>2</sub> P	C <sub>32</sub> H <sub>40</sub> N <sub>2</sub> OCIP
formula weight	482.62	484.64	528.65	535.08
crystal habit	block	block	block	prism
crystal color	orange	red	yellow	white
temperature, K	200(2)	200(2)	200(2)	200(2)
wavelength, Å	0.71073	0.71073	0.71073	0.71073
crystal system	Orthorhombic	Monoclinic	Monoclinic	Orthorhombic
space group	Pbcn	Cc	P2(1)/n	Cmc2(1)
unit cell dimensions:				
a, Å	21.2829(7)	8.277(5)	10.6711(6)	30.90(4)
b, Å	8.2036(3)	43.32(3)	20.7210(12)	11.407(14)
c, Å	16.1186(6)	8.716(5)	13.5816(7)	17.67(2)
a, °	90	90	90	90
b, °	90	112.867(8)	91.933(3)	90

g, °	90	90	90	90
volume, Å <sup>3</sup>	2814.25(17)	2880(3)	3001.4(3)	6228(13)
Z	4	4	4	8
density (calc), Mg/m <sup>3</sup>	1.139	1.118	1.170	1.141
absorption coeff., mm <sup>-1</sup>	0.120	0.117	0.123	0.199
<i>F</i> (000)	1040	1048	1136	2288
crystal size, mm <sup>3</sup>	0.14 x 0.23 x 0.47	0.19 x 0.11 x 0.08	0.34 x 0.27 x 0.13	0.40 x 0.50 x 0.90
θ range for data collection	1.91 to 27.91	2.00 to 28.37	1.79 to 30.03	1.90 to 25.25
index ranges	-28 ≤ h ≤ 26, - 10 ≤ k ≤ 10, -21 ≤ l ≤ 21	-10 ≤ h ≤ 10, - 57 ≤ k ≤ 56, - 10 ≤ l ≤ 11	-14 ≤ h ≤ 14, - 21 ≤ k ≤ 27, - 18 ≤ l ≤ 18	-36 ≤ h ≤ 36, - 13 ≤ k ≤ 13, - 21 ≤ l ≤ 21
reflections collected	30233	14188	32015	25625
independent reflections	3370 [R <sub>int</sub> = 0.0508]	6151 [R <sub>int</sub> = 0.0585]	8168 [R <sub>int</sub> = 0.0584]	5582 [R(int) = 0.0883]

absorption correction	SADABS	SADABS	SADABS	SADABS
max- and min. transmission	0.9458 and 0.9837	0.9779 and 0.9902	0.9595 and 0.9842	0.8409 and 0.9245
refinement method	full-matrix least-squares on $F^2$	full-matrix least-squares on $F^2$	full-matrix least-squares on $F^2$	full-matrix least-squares on $F^2$
data / restraints / parameters	3370 / 0 / 164	6151 / 23 / 342	8168 / 0 / 343	5582 / 768 / 533
goodness-of-fit on $F^2$	1.022	0.950	1.015	1.236
final $R$ indices [ $I > 2\sigma(I)$ ]	$R1 = 0.0479$ , $wR2 = 0.1119$	$R1 = 0.0513$ , $wR2 = 0.1092$	$R1 = 0.0607$ $wR2 = 0.1485$	$R1 = 0.1249$ $wR2 = 0.2974$
$R$ indices (all data)	$R1 = 0.0873$ , $wR2 = 0.1341$	$R1 = 0.1050$ , $wR2 = 0.1315$	$R1 = 0.1065$ , $wR2 = 0.1816$	$R1 = 0.1858$ , $wR2 = 0.3508$
largest diff. peak and hole, e. $\text{\AA}^{-3}$	0.197 and -0.196	0.217 and -0.227	0.678 and -0.544	0.337 and -1.869
absolute structure parameter	-	0.13(16)	-	0.4(4)

## XI. References

- [1] J. V. Obligacion, P. J. Chirik, *Nat. Rev. Chem.* **2018**, *2*, 15–34.
- [2] A. K. Smith, J. M. Basset, *J. Mol. Catal.* **1977**, *2*, 229–241.
- [3] M. V. Twigg, in *Mech. Inorg. Organomet. React.*, Springer, Boston, MA, **1994**, pp. 363–396.
- [4] M. R. DuBois, *Chem. Rev.* **1989**, *89*, 1–9.
- [5] P. P. Power, *Nature* **2010**, *463*, 171–177.
- [6] G. Bertrand, *Chem. Rev.* **2010**, *110*, 3851–3851.
- [7] L. C. Wilkins, R. L. Melen, *Coord. Chem. Rev.* **2016**, *324*, 123–139.
- [8] E. M. Leitao, T. Jurca, I. Manners, *Nat. Chem.* **2013**, *5*, 817–829.
- [9] C. L. B. Macdonald, B. D. Ellis, A. Swidan, in *Encycl. Inorg. Bioinorg. Chem.*, American Cancer Society, **2012**.
- [10] G. van Koten, D. Milstein, Eds., *Organometallic Pincer Chemistry*, Springer, Berlin ; New York, **2013**.
- [11] N. Selander, K. J. Szabó, *Chem. Rev.* **2011**, *111*, 2048–2076.
- [12] E. Peris, R. H. Crabtree, *Chem. Soc. Rev.* **2018**, *47*, 1959–1968.
- [13] S. Wanniarachchi, **n.d.**, 332.
- [14] M. A. W. Lawrence, K.-A. Green, P. N. Nelson, S. C. Lorraine, *Polyhedron* **2018**, *143*, 11–27.
- [15] E. Peris, R. H. Crabtree, *Chem. Soc. Rev.* **2018**, *47*, 1959–1968.
- [16] C. J. Moulton, B. L. Shaw, *J. Chem. Soc. Dalton Trans.* **1976**, *0*, 1020–1024.
- [17] L. Dostál, R. Jambor, in *Pincer Compd.* (Ed.: D. Morales-Morales), Elsevier, **2018**, pp. 47–65.
- [18] G. van Koten, J. T. B. H. Jastrzebski, J. G. Noltes, A. L. Spek, J. C. Schoone, *J. Organomet. Chem.* **1978**, *148*, 233–245.
- [19] M. Mehring, I. Vrasidas, D. Horn, M. Schürmann, K. Jurkschat, *Organometallics* **2001**, *20*, 4647–4653.
- [20] K. Takenaka, M. Minakawa, Y. Uozumi, *J. Am. Chem. Soc.* **2005**, *127*, 12273–12281.
- [21] M. Albrecht, G. van Koten, *Angew. Chem. Int. Ed.* **n.d.**, *40*, 3750–3781.
- [22] M. E. van der Boom, D. Milstein, *Chem. Rev.* **2003**, *103*, 1759–1792.
- [23] N. Selander, K. Szabo, *Chem. Rev.* **2011**, *111*, 2048–2076.



- [24] M. Q. Slagt, D. A. P. van Zwieten, A. J. C. M. Moerkerk, R. J. M. K. Gebbink, G. van Koten, *Coord. Chem. Rev.* **2004**, *248*, 2275–2282.
- [25] Z. Liu, W. Gao, X. Liu, X. Luo, D. Cui, Y. Mu, *Organometallics* **2011**, *30*, 752–759.
- [26] O. A. Blackburn, B. J. Coe, M. Helliwell, J. Raftery, *Organometallics* **2012**, *31*, 5307–5320.
- [27] W. J. Hoogervorst, C. J. Elsevier, M. Lutz, A. L. Spek, *Organometallics* **2001**, *20*, 4437–4440.
- [28] W. J. Hoogervorst, A. L. Koster, M. Lutz, A. L. Spek, C. J. Elsevier, *Organometallics* **2004**, *23*, 1161–1164.
- [29] Z. Liu, W. Gao, J. Zhang, D. Cui, Q. Wu, Y. Mu, *Organometallics* **2010**, *29*, 5783–5790.
- [30] S. Khan, R. Michel, J. M. Dieterich, R. A. Mata, H. W. Roesky, J.-P. Demers, A. Lange, D. Stalke, *J. Am. Chem. Soc.* **2011**, *133*, 17889–17894.
- [31] S. Khan, P. P. Samuel, R. Michel, J. M. Dieterich, R. A. Mata, J.-P. Demers, A. Lange, H. W. Roesky, D. Stalke, *Chem. Commun.* **2012**, *48*, 4890–4892.
- [32] S.-P. Chia, H.-X. Yeong, C.-W. So, *Inorg. Chem.* **2012**, *51*, 1002–1010.
- [33] C. Seow, H.-W. Xi, Y. Li, C.-W. So, *Organometallics* **2016**, *35*, 1060–1063.
- [34] C. Seow, M. L. B. Ismail, H.-W. Xi, Y. Li, K. H. Lim, C.-W. So, *Organometallics* **2018**, *37*, 1368–1372.
- [35] S.-P. Chia, H.-W. Xi, Y. Li, K. H. Lim, C.-W. So, *Angew. Chem. Int. Ed.* **n.d.**, *52*, 6298–6301.
- [36] P. Šimon, R. Jambor, A. Růžička, A. Lyčka, F. D. Proft, L. Dostál, *Dalton Trans.* **2012**, *41*, 5140–5143.
- [37] I. Vránová, R. Jambor, A. Růžička, R. Jirásko, L. Dostál, *Organometallics* **2015**, *34*, 534–541.
- [38] I. Vránová, M. Alonso, R. Jambor, A. Růžička, J. Turek, L. Dostál, *Chem. – Eur. J.* **n.d.**, *23*, 2340–2349.
- [39] J. Hyvl, W. Y. Yoshida, A. L. Rheingold, R. P. Hughes, M. F. Cain, *Chem. – Eur. J.* **n.d.**, *22*, 17562–17565.
- [40] V. C. Gibson, C. Redshaw, G. A. Solan, *Chem. Rev.* **2007**, *107*, 1745–1776.
- [41] W. Li, Y. Lyu, H. Zhang, M. Zhu, H. Tang, *Dalton Trans.* **2016**, *46*, 106–115.

- [42] Z. Flisak, W.-H. Sun, *ACS Catal.* **2015**, *5*, 4713–4724.
- [43] B. L. Small, M. Brookhart, A. M. A. Bennett, *J. Am. Chem. Soc.* **1998**, *120*, 4049–4050.
- [44] V. C. Gibson, K. P. Tellmann, M. J. Humphries, D. F. Wass, *Chem. Commun.* **2002**, *0*, 2316–2317.
- [45] C. C. Hojilla Atienza, A. M. Tondreau, K. J. Weller, K. M. Lewis, R. W. Cruse, S. A. Nye, J. L. Boyer, J. G. P. Delis, P. J. Chirik, *ACS Catal.* **2012**, *2*, 2169–2172.
- [46] M. W. Bouwkamp, A. C. Bowman, E. Lobkovsky, P. J. Chirik, *J. Am. Chem. Soc.* **2006**, *128*, 13340–13341.
- [47] P. Liu, M. Yan, R. He, *Appl. Organomet. Chem.* **2010**, *24*, 131–134.
- [48] D. A. Edwards, M. F. Mahon, W. R. Martin, K. C. Molloy, P. E. Fanwick, R. A. Walton, *J. Chem. Soc. Dalton Trans.* **1990**, *0*, 3161–3168.
- [49] T. M. Smit, A. K. Tomov, V. C. Gibson, A. J. P. White, D. J. Williams, *Inorg. Chem.* **2004**, *43*, 6511–6512.
- [50] J. E. Steves, M. D. Kennedy, K. P. Chiang, W. S. Kassel, W. G. Dougherty, T. J. Dudley, D. L. Zubris, *Dalton Trans.* **2009**, *0*, 1214–1222.
- [51] T. W. Myers, T. J. Sherbow, J. C. Fettinger, L. A. Berben, *Dalton Trans.* **2016**, *45*, 5989–5998.
- [52] Q. Knijnenburg, J. M. M. Smits, P. H. M. Budzelaar, *Organometallics* **2006**, *25*, 1036–1046.
- [53] T. Chu, L. Belding, A. van der Est, T. Dudding, I. Korobkov, G. I. Nikonov, *Angew. Chem. Int. Ed.* **n.d.**, *53*, 2711–2715.
- [54] J. Flock, A. Suljanovic, A. Torvisco, W. Schoefberger, B. Gerke, R. Pöttgen, R. C. Fischer, M. Flock, *Chem. – Eur. J.* **n.d.**, *19*, 15504–15517.
- [55] D. Enright, S. Gambarotta, G. P. A. Yap, P. H. M. Budzelaar, *Angew. Chem.* **n.d.**, *114*, 4029–4032.
- [56] M. Arrowsmith, M. S. Hill, G. Kociok-Köhn, *Organometallics* **2010**, *29*, 4203–4206.
- [57] J. J. Sandoval, P. Palma, E. Álvarez, J. Cámpora, A. Rodríguez-Delgado, *Organometallics* **2016**, *35*, 3197–3204.
- [58] J. Scott, S. Gambarotta, I. Korobkov, Q. Knijnenburg, B. de Bruin, P. H. M. Budzelaar, *J. Am. Chem. Soc.* **2005**, *127*, 17204–17206.

- [59] T. W. Myers, L. A. Berben, *J. Am. Chem. Soc.* **2013**, *135*, 9988–9990.
- [60] T. J. Sherbow, C. R. Carr, T. Saisu, J. C. Fettinger, L. A. Berben, *Organometallics* **2016**, *35*, 9–14.
- [61] T. W. Myers, L. A. Berben, *Chem. Sci.* **2014**, *5*, 2771–2777.
- [62] Q.-Q. Lu, H.-Z. Yu, Y. Fu, *Chem. – Eur. J.* **n.d.**, *22*, 4584–4591.
- [63] T. Jurca, K. Dawson, I. Mallov, T. Burchell, G. P. A. Yap, D. S. Richeson, *Dalton Trans.* **2010**, *39*, 1266–1272.
- [64] T. Jurca, J. Lummiss, T. J. Burchell, S. I. Gorelsky, D. S. Richeson, *J. Am. Chem. Soc.* **2009**, *131*, 4608–4609.
- [65] M. S. Hill, P. B. Hitchcock, *Chem. Commun.* **2004**, *0*, 1818–1819.
- [66] A. P. Singh, H. W. Roesky, E. Carl, D. Stalke, J.-P. Demers, A. Lange, *J. Am. Chem. Soc.* **2012**, *134*, 4998–5003.
- [67] G. Reeske, A. H. Cowley, *Chem. Commun.* **2006**, *0*, 1784–1786.
- [68] C. D. Martin, P. J. Ragogna, *Dalton Trans.* **2011**, *40*, 11976–11980.
- [69] C. D. Martin, C. M. Le, P. J. Ragogna, *J. Am. Chem. Soc.* **2009**, *131*, 15126–15127.
- [70] A. J. Arduengo, R. L. Harlow, M. Kline, *J. Am. Chem. Soc.* **1991**, *113*, 361–363.
- [71] W. D. Jones, *J. Am. Chem. Soc.* **2009**, *131*, 15075–15077.
- [72] D. An, J. Wang, T. Dong, Y. Yang, T. Wen, H. Zhu, X. Lu, Y. Wang, *Eur. J. Inorg. Chem.* **2010**, *2010*, 4506–4512.
- [73] D. M. Flanigan, F. Romanov-Michailidis, N. A. White, T. Rovis, *Chem. Rev.* **2015**, *115*, 9307–9387.
- [74] E. Peris, *Chem. Rev.* **2017**, DOI 10.1021/acs.chemrev.6b00695.
- [75] M. N. Hopkinson, C. Richter, M. Schedler, F. Glorius, *Nature* **2014**, *510*, 485–496.
- [76] W. A. Herrmann, J. Schütz, G. D. Frey, E. Herdtweck, *Organometallics* **2006**, *25*, 2437–2448.
- [77] H. V. Huynh, *Chem. Rev.* **2018**, DOI 10.1021/acs.chemrev.8b00067.
- [78] J. C. Y. Lin, R. T. W. Huang, C. S. Lee, A. Bhattacharyya, W. S. Hwang, I. J. B. Lin, *Chem. Rev.* **2009**, *109*, 3561–3598.
- [79] N. Marion, S. Díez-González, S. P. Nolan, *Angew. Chem. Int. Ed.* **2007**, *46*, 2988–3000.
- [80] D. Enders, O. Niemeier, A. Henseler, *Chem. Rev.* **2007**, *107*, 5606–5655.

- [81] J. Al Thagfi, S. Dastgir, A. J. Lough, G. G. Lavoie, *Organometallics* **2010**, *29*, 3133–3138.
- [82] J. Al Thagfi, G. G. Lavoie, *Can. J. Chem.* **2014**, *92*, 925–931.
- [83] H. Z. Kaplan, B. Li, J. A. Byers, *Organometallics* **2012**, *31*, 7343–7350.
- [84] F. Mathey, *Multiple Bonds and Low Coordination in Phosphorus Chemistry*, **1990**.
- [85] R. C. Smith, S. Shah, J. D. Protasiewicz, *J. Organomet. Chem.* **2002**, *646*, 255–261.
- [86] S. Shah, M. C. Simpson, R. C. Smith, J. D. Protasiewicz, *J. Am. Chem. Soc.* **2001**, *123*, 6925–6926.
- [87] A. H. Cowley, F. Gabbai, R. Schluter, D. Atwood, *J. Am. Chem. Soc.* **1992**, *114*, 3142–3144.
- [88] M. Yoshifuji, I. Shima, N. Inamoto, K. Hirotsu, T. Higuchi, *J. Am. Chem. Soc.* **1981**, *103*, 4587–4589.
- [89] A. W. Ehlers, E. J. Baerends, K. Lammertsma, *J. Am. Chem. Soc.* **2002**, *124*, 2831–2838.
- [90] H. Aktaş, J. C. Slootweg, K. Lammertsma, *Angew. Chem. Int. Ed.* **2010**, *49*, 2102–2113.
- [91] F. Mathey, N. H. T. Huy, A. Marinetti, *Helv. Chim. Acta* **2001**, *84*, 2938–2957.
- [92] F. Mathey, *Dalton Trans.* **2007**, *0*, 1861–1868.
- [93] H. Aktaş, J. C. Slootweg, K. Lammertsma, *Angew. Chem. Int. Ed.* **2010**, *49*, 2102–2113.
- [94] P. L. Floch, *Coord. Chem. Rev.* **2006**, *250*, 627–681.
- [95] B. T. Sterenberg, K. A. Udachin, A. J. Carty, *Organometallics* **2003**, *22*, 3927–3932.
- [96] T. W. Graham, R. P.-Y. Cariou, J. Sánchez-Nieves, A. E. Allen, K. A. Udachin, R. Regragui, A. J. Carty, *Organometallics* **2005**, *24*, 2023–2026.
- [97] B. T. Sterenberg, K. A. Udachin, A. J. Carty, *Organometallics* **2001**, *20*, 2657–2659.
- [98] J. Sánchez-Nieves, B. T. Sterenberg, K. A. Udachin, A. J. Carty, *J. Am. Chem. Soc.* **2003**, *125*, 2404–2405.
- [99] A. Marinetti, F. Mathey, *Organometallics* **1984**, *3*, 456–461.
- [100] C. C. Cummins, R. R. Schrock, W. M. Davis, *Angew. Chem. Int. Ed. Engl.* **1993**, *32*, 756–759.
- [101] T. L. Breen, D. W. Stephan, *J. Am. Chem. Soc.* **1995**, *117*, 11914–11921.

- [102] U. Schmidt, *Angew. Chem. Int. Ed. Engl.* **1975**, *14*, 523–528.
- [103] M.-A. Courtemanche, W. J. Transue, C. C. Cummins, *J. Am. Chem. Soc.* **2016**, *138*, 16220–16223.
- [104] X. Li, D. Lei, M. Y. Chiang, P. P. Gaspar, *J. Am. Chem. Soc.* **1992**, *114*, 8526–8531.
- [105] A. H. Cowley, F. Gabbai, R. Schluter, D. Atwood, *J. Am. Chem. Soc.* **1992**, *114*, 3142–3144.
- [106] X. Li, D. Lei, M. Y. Chiang, P. P. Gaspar, *J. Am. Chem. Soc.* **1992**, *114*, 8526–8531.
- [107] X. Li, S. I. Weissman, T.-S. Lin, P. P. Gaspar, A. H. Cowley, A. I. Smirnov, *J. Am. Chem. Soc.* **1994**, *116*, 7899–7900.
- [108] S. Shah, M. C. Simpson, R. C. Smith, J. D. Protasiewicz, *J. Am. Chem. Soc.* **2001**, *123*, 6925–6926.
- [109] R. C. Smith, S. Shah, J. D. Protasiewicz, *J. Organomet. Chem.* **2002**, *646*, 255–261.
- [110] B. Twamley, C. D. Sofield, M. M. Olmstead, P. P. Power, *J. Am. Chem. Soc.* **1999**, *121*, 3357–3367.
- [111] G. Frison, A. Sevin, *J. Phys. Chem. A* **1999**, *103*, 10998–11003.
- [112] A. J. Arduengo, J. C. Calabrese, A. H. Cowley, H. V. R. Dias, J. R. Goerlich, W. J. Marshall, B. Riegel, *Inorg. Chem.* **1997**, *36*, 2151–2158.
- [113] A. Jouaiti, M. Geoffroy, G. Terron, G. Bernardinelli, *J. Am. Chem. Soc.* **1995**, *117*, 2251–2258.
- [114] A. H. Cowley, R. A. Jones, J. G. Lasch, N. C. Norman, C. A. Stewart, A. L. Stuart, J. L. Atwood, W. E. Hunter, H. M. Zhang, *J. Am. Chem. Soc.* **1984**, *106*, 7015–7020.
- [115] G. Frison, A. Sevin, *J. Organomet. Chem.* **2002**, *643–644*, 105–111.
- [116] M. T. Nguyen, A. Van Keer, L. G. Vanquickenborne, *J. Org. Chem.* **1996**, *61*, 7077–7084.
- [117] D. Bourissou, Y. Canac, H. Gornitzka, C. J. Marsden, A. Baceiredo, G. Bertrand, *Eur. J. Inorg. Chem.* **1999**, *1999*, 1479–1488.
- [118] A. Doddi, D. Bockfeld, T. Bannenberg, P. G. Jones, M. Tamm, *Angew. Chem. Int. Ed.* **2014**, *53*, 13568–13572.

- [119] Y. Wang, Y. Xie, M. Y. Abraham, R. J. Gilliard, P. Wei, H. F. Schaefer, P. v. R. Schleyer, G. H. Robinson, *Organometallics* **2010**, *29*, 4778–4780.
- [120] A. M. Tondreau, Z. Benkő, J. R. Harmer, H. Grützmacher, *Chem. Sci.* **2014**, *5*, 1545–1554.
- [121] M. Cicač-Hudi, J. Bender, S. H. Schlindwein, M. Bispinghoff, M. Nieger, H. Grützmacher, D. Gudat, *Eur. J. Inorg. Chem.* **2016**, *2016*, 649–658.
- [122] M. Bispinghoff, A. M. Tondreau, H. Grützmacher, C. A. Faradji, P. G. Pringle, *Dalton Trans.* **2016**, *45*, 5999–6003.
- [123] O. Back, M. Henry-Ellinger, C. D. Martin, D. Martin, G. Bertrand, *Angew. Chem. Int. Ed.* **2013**, *52*, 2939–2943.
- [124] R. R. Rodrigues, C. L. Dorsey, C. A. Arceneaux, T. W. Hudnall, *Chem. Commun.* **2013**, *50*, 162–164.
- [125] P. K. Majhi, G. Schnakenburg, Z. Kelemen, L. Nyulaszi, D. P. Gates, R. Streubel, *Angew. Chem. Int. Ed.* **2013**, *52*, 10080–10083.
- [126] N. Hayakawa, K. Sadamori, S. Tsujimoto, M. Hatanaka, T. Wakabayashi, T. Matsuo, *Angew. Chem. Int. Ed.* **2017**, *56*, 5765–5769.
- [127] B. D. Ellis, C. A. Dyker, A. Decken, C. L. B. Macdonald, *Chem. Commun.* **2005**, *0*, 1965–1967.
- [128] J. F. Binder, A. Swidan, M. Tang, J. H. Nguyen, C. L. B. Macdonald, *Chem. Commun.* **2015**, *51*, 7741–7744.
- [129] K. Schwedtmann, M. H. Holthausen, K.-O. Feldmann, J. J. Weigand, *Angew. Chem. Int. Ed.* **2013**, *52*, 14204–14208.
- [130] R. Armbrust, M. Sanchez, R. Reau, U. Bergstraesser, M. Regitz, G. Bertrand, *J. Am. Chem. Soc.* **1995**, *117*, 10785–10786.
- [131] M. Sanchez, R. Réau, H. Gornitzka, F. Dahan, M. Regitz, G. Bertrand, *J. Am. Chem. Soc.* **1997**, *119*, 9720–9728.
- [132] B. A. Surgenor, M. Bühl, A. M. Z. Slawin, J. D. Woollins, P. Kilian, *Angew. Chem. Int. Ed.* **2012**, *51*, 10150–10153.
- [133] J. W. Dube, C. L. B. Macdonald, P. J. Ragona, *Angew. Chem. Int. Ed.* **2012**, *51*, 13026–13030.

- [134] J. Henn, K. Meindl, A. Oechsner, G. Schwab, T. Koritsanszky, D. Stalke, *Angew. Chem. Int. Ed.* **2010**, *49*, 2422–2426.
- [135] T. Stey, J. Henn, D. Stalke, *Chem. Commun.* **2007**, *0*, 413–415.
- [136] T. L. Chan, Z. Xie, *Chem. Commun.* **2016**, *52*, 7280–7283.
- [137] L. Liu, D. A. Ruiz, D. Munz, G. Bertrand, *Chem* **2016**, *1*, 147–153.
- [138] M. M. Hansmann, R. Jazzar, G. Bertrand, *J. Am. Chem. Soc.* **2016**, *138*, 8356–8359.
- [139] M. M. Hansmann, G. Bertrand, *J. Am. Chem. Soc.* **2016**, *138*, 15885–15888.
- [140] O. Lemp, M. Balmer, K. Reiter, F. Weigend, C. von Hänisch, *Chem. Commun.* **2017**, *53*, 7620–7623.
- [141] S. Khan, S. S. Sen, H. W. Roesky, *Chem. Commun.* **2012**, *48*, 2169–2179.
- [142] P. P. Power, *Nature* **2010**, *463*, 171–177.
- [143] Y. Wang, G. H. Robinson, *Inorg. Chem.* **2014**, *53*, 11815–11832.
- [144] H. Braunschweig, R. D. Dewhurst, V. H. Gessner, *Chem. Soc. Rev.* **2013**, *42*, 3197–3208.
- [145] R. C. Fischer, P. P. Power, *Chem. Rev.* **2010**, *110*, 3877–3923.
- [146] P. K. Majhi, T. Sasamori, *Chem. – Eur. J.* **2018**, *24*, 9441–9455.
- [147] J. Turek, B. Braïda, F. De Proft, *Chem. – Eur. J.* **2017**, *23*, 14604–14613.
- [148] F. Ramirez, N. B. Desai, B. Hansen, N. McKelvie, *J. Am. Chem. Soc.* **1961**, *83*, 3539–3540.
- [149] G. E. Hardy, J. I. Zink, W. C. Kaska, J. C. Baldwin, *J. Am. Chem. Soc.* **1978**, *100*, 8001–8002.
- [150] R. Tonner, F. Öxler, B. Neumüller, W. Petz, G. Frenking, *Angew. Chem. Int. Ed.* **2006**, *45*, 8038–8042.
- [151] N. Wiberg, H.-W. Lerner, S.-K. Vasisht, S. Wagner, K. Karaghiosoff, H. Nöth, W. Ponikwar, *Eur. J. Inorg. Chem.* **1999**, *1999*, 1211–1218.
- [152] S. Masamune, L. R. Sita, *J. Am. Chem. Soc.* **1985**, *107*, 6390–6391.
- [153] M. Kira, R. Yauchibara, R. Hirano, C. Kabuto, H. Sakurai, *J. Am. Chem. Soc.* **1991**, *113*, 7785–7787.
- [154] K. W. Zilm, G. A. Lawless, R. M. Merrill, J. M. Millar, G. G. Webb, *J. Am. Chem. Soc.* **1987**, *109*, 7236–7238.
- [155] S. Ishida, T. Iwamoto, C. Kabuto, M. Kira, *Nature* **2003**, *421*, 725–727.

- [156] N. Takagi, T. Shimizu, G. Frenking, *Chem. – Eur. J.* **2009**, *15*, 3448–3456.
- [157] T. Iwamoto, T. Abe, C. Kabuto, M. Kira, *Chem. Commun.* **2005**, *0*, 5190–5192.
- [158] T. Iwamoto, H. Masuda, C. Kabuto, M. Kira, *Organometallics* **2005**, *24*, 197–199.
- [159] Y. Wang, Y. Xie, P. Wei, R. B. King, H. F. Schaefer, P. von R. Schleyer, G. H. Robinson, *Science* **2008**, *321*, 1069–1071.
- [160] P. P. Power, *Organometallics* **2007**, *26*, 4362–4372.
- [161] M. KIRA, *Proc. Jpn. Acad. Ser. B Phys. Biol. Sci.* **2012**, *88*, 167–191.
- [162] A. Sidiropoulos, C. Jones, A. Stasch, S. Klein, G. Frenking, *Angew. Chem. Int. Ed.* **2009**, *48*, 9701–9704.
- [163] C. Jones, A. Sidiropoulos, N. Holzmann, G. Frenking, A. Stasch, *Chem. Commun.* **2012**, *48*, 9855–9857.
- [164] A. J. Boutland, D. Dange, A. Stasch, L. Maron, C. Jones, *Angew. Chem. Int. Ed.* **2016**, *55*, 9239–9243.
- [165] K. C. Mondal, H. W. Roesky, M. C. Schwarzer, G. Frenking, B. Niepötter, H. Wolf, R. Herbst-Irmer, D. Stalke, *Angew. Chem. Int. Ed.* **2013**, *52*, 2963–2967.
- [166] V. Lavallo, Y. Canac, A. DeHope, B. Donnadiou, G. Bertrand, *Angew. Chem. Int. Ed.* **2005**, *44*, 7236–7239.
- [167] V. Lavallo, Y. Canac, C. Präsang, B. Donnadiou, G. Bertrand, *Angew. Chem. Int. Ed.* **2005**, *44*, 5705–5709.
- [168] D. Martin, M. Melaimi, M. Soleilhavoup, G. Bertrand, *Organometallics* **2011**, *30*, 5304–5313.
- [169] P. F. Hudrlik, *J. Chem. Educ.* **2000**, *77*, 313.
- [170] V. Y. Lee, A. Sekiguchi, *Organometallic Compounds of Low-Coordinate Si, Ge, Sn and Pb: From Phantom Species to Stable Compounds*, **2010**.
- [171] Y. Xiong, S. Yao, S. Inoue, J. D. Epping, M. Driess, *Angew. Chem. Int. Ed.* **2013**, *52*, 7147–7150.
- [172] Y. Xiong, S. Yao, G. Tan, S. Inoue, M. Driess, *J. Am. Chem. Soc.* **2013**, *135*, 5004–5007.
- [173] Y. Li, K. C. Mondal, H. W. Roesky, H. Zhu, P. Stollberg, R. Herbst-Irmer, D. Stalke, D. M. Andrada, *J. Am. Chem. Soc.* **2013**, *135*, 12422–12428.
- [174] T. Sugahara, T. Sasamori, N. Tokitoh, *Angew. Chem. Int. Ed.* **2017**, *56*, 9920–9923.



- [175] M. G. Chegerev, A. V. Piskunov, A. A. Starikova, *Russ. J. Gen. Chem.* **2017**, *87*, 2582–2588.
- [176] T. Kuwabara, M. Nakada, J. Hamada, J. D. Guo, S. Nagase, M. Saito, *J. Am. Chem. Soc.* **2016**, *138*, 11378–11382.
- [177] V. Ya. Lee, Y. Ito, A. Sekiguchi, H. Gornitzka, O. A. Gapurenko, V. I. Minkin, R. M. Minyaev, *J. Am. Chem. Soc.* **2013**, *135*, 8794–8797.
- [178] K. M. Krebs, J. Wiederkehr, J. Schneider, H. Schubert, K. Eichele, L. Wesemann, *Angew. Chem. Int. Ed.* **2015**, *54*, 5502–5506.
- [179] B. Su, R. Ganguly, Y. Li, R. Kinjo, *Angew. Chem. Int. Ed.* **2014**, *53*, 13106–13109.
- [180] R. C. Fischer, P. P. Power, *Chem. Rev.* **2010**, *110*, 3877–3923.
- [181] Y. Xiong, S. Yao, R. Müller, M. Kaupp, M. Driess, *Angew. Chem. Int. Ed.* **2015**, *54*, 10254–10257.
- [182] S. Yao, Y. Xiong, M. Driess, *Acc. Chem. Res.* **2017**, *50*, 2026–2037.
- [183] A. Burchert, R. Müller, S. Yao, C. Schattenberg, Y. Xiong, M. Kaupp, M. Driess, *Angew. Chem. Int. Ed.* **2017**, *56*, 6298–6301.
- [184] A. Burchert, S. Yao, R. Müller, C. Schattenberg, Y. Xiong, M. Kaupp, M. Driess, *Angew. Chem. Int. Ed.* **2017**, *56*, 1894–1897.
- [185] Y. Xiong, S. Yao, M. Karni, A. Kostenko, A. Burchert, Y. Apeloig, M. Driess, *Chem. Sci.* **2016**, *7*, 5462–5469.
- [186] B. Su, R. Ganguly, Y. Li, R. Kinjo, *Chem. Commun.* **2015**, *52*, 613–616.
- [187] Y.-P. Zhou, M. Karni, S. Yao, Y. Apeloig, M. Driess, *Angew. Chem. Int. Ed.* **2016**, *55*, 15096–15099.
- [188] L.-C. Liang, J.-M. Lin, C.-H. Hung, *Organometallics* **2003**, *22*, 3007–3009.
- [189] M. Albrecht, G. van Koten, *Angew. Chem. Int. Ed.* **2001**, *40*, 3750–3781.
- [190] H. Nishiyama, *Chem. Soc. Rev.* **2007**, *36*, 1133–1141.
- [191] K. Kubo, N. D. Jones, M. J. Ferguson, R. McDonald, R. G. Cavell, *J. Am. Chem. Soc.* **2005**, *127*, 5314–5315.
- [192] M. E. van der Boom, D. Milstein, *Chem. Rev.* **2003**, *103*, 1759–1792.
- [193] P. P. Power, *Acc. Chem. Res.* **2011**, *44*, 627–637.
- [194] M. Asay, C. Jones, M. Driess, *Chem. Rev.* **2011**, *111*, 354–396.
- [195] P. P. Power, *Nature* **2010**, *463*, 171–177.

- [196] P. P. Power, *Chem. Rec.* **2012**, *12*, 238–255.
- [197] S. Harder, *Chem. Rev.* **2010**, *110*, 3852–3876.
- [198] W. E. Piers, A. J. V. Marwitz, L. G. Mercier, *Inorg. Chem.* **2011**, *50*, 12252–12262.
- [199] G. Parkin, *Chem. Rev.* **2004**, *104*, 699–768.
- [200] K. Revunova, G. I. Nikonov, *Dalton Trans.* **2014**, *44*, 840–866.
- [201] J. Lortie, B. Gabidullin, T. Dudding, G. I. Nikonov, submitted., **n.d.**
- [202] W. Sattler, G. Parkin, *J. Am. Chem. Soc.* **2012**, *134*, 17462–17465.
- [203] M. Tüchler, L. Gärtner, S. Fischer, A. D. Boese, F. Belaj, N. C. Mösch-Zanetti, *Angew. Chem. Int. Ed.* **2018**, *57*, 6906–6909.
- [204] W. Sattler, G. Parkin, *J. Am. Chem. Soc.* **2011**, *133*, 9708–9711.
- [205] W. Sattler, G. Parkin, *J. Am. Chem. Soc.* **2012**, *134*, 17462–17465.
- [206] M. Kahnes, H. Görls, L. González, M. Westerhausen, *Organometallics* **2010**, *29*, 3098–3108.
- [207] T. Chu, L. Belding, P. K. Poddutoori, A. van der Est, T. Dudding, I. Korobkov, G. I. Nikonov, *Dalton Trans.* **2016**, *45*, 13440–13448.
- [208] T. W. Myers, T. J. Sherbow, J. C. Fettinger, L. A. Berben, *Dalton Trans.* **2016**, *45*, 5989–5998.
- [209] Based on a search in the Cambridge Crystallographic Data Centre, **n.d.**
- [210] L. Yang, D. R. Powell, R. P. Houser, *Dalton Trans.* **2007**, *0*, 955–964.
- [211] H. Schmidbaur, A. Schier, *Chem. Soc. Rev.* **2011**, *41*, 370–412.
- [212] H. Schmidbaur, A. Schier, *Organometallics* **2015**, *34*, 2048–2066.
- [213] M. T. Nguyen, B. Gabidullin, G. I. Nikonov, *Dalton Trans.* **2018**, *47*, 4607–4612.
- [214] O. Puntigam, D. Förster, N. A. Giffin, S. Burck, J. Bender, F. Ehret, A. D. Hendsbee, M. Nieger, J. D. Masuda, D. Gudat, *Eur. J. Inorg. Chem.* **2013**, *2013*, 2041–2050.
- [215] T. Svoboda, R. Jambor, A. Růžička, Z. Padělková, M. Erben, L. Dostál, *Eur. J. Inorg. Chem.* **n.d.**, *2010*, 5222–5230.
- [216] K. Karaghiosoff, H. Klehr, A. Schmidpeter, *Chem. Ber.* **1986**, *119*, 410–419.
- [217] K. Angermund, A. Eckerle, J. Monkiewicz, C. Krüger, G. Wilke, *Inorganica Chim. Acta* **1998**, *270*, 273–278.

- [218] C. Peters, F. Tabellion, M. Schröder, U. Bergsträßer, F. Preuss, M. Regitz, *Synthesis* **2000**, 2000, 417–428.
- [219] Norihiro Tokitoh, Teruyuki Matsumoto, Takahiro Sasamori, *Heterocycles* **2008**, 76, 981–987.
- [220] Prof. L. Dostal reported during the recent IRIS-15 conference (Kyoto, June 28, 2018) a "mono-arm" version of compound **VI-2** which like **VI-5** was rationalised as benzoazaphosphole. We thank Prof. Dostal for bringing the azaphosphole interpretation to our attention.
- [221] B. Cordero, V. Gómez, A. E. Platero-Prats, M. Revés, J. Echeverría, E. Cremades, F. Barragán, S. Alvarez, *Dalton Trans.* **2008**, 0, 2832–2838.
- [222] F. H. Allen, O. Kennard, D. G. Watson, L. Brammer, A. G. Orpen, R. Taylor, *J. Chem. Soc. Perkin Trans. 2* **1987**, 0, S1–S19.
- [223] J. Hyvl, W. Y. Yoshida, C. E. Moore, A. L. Rheingold, M. F. Cain, *Polyhedron* **2018**, 143, 99–104.
- [224] S. Burck, D. Gudat, K. Nättinen, M. Nieger, M. Niemeyer, D. Schmid, *Eur. J. Inorg. Chem.* **2007**, 2007, 5112–5119.
- [225] T. Řezníček, L. Dostál, A. Růžička, R. Jirásko, R. Jambor, *Inorganica Chim. Acta* **2010**, 363, 3302–3307.
- [226] R. C. Smith, S. Shah, E. Urnezis, J. D. Protasiewicz, *J. Am. Chem. Soc.* **2003**, 125, 40–41.
- [227] S. E. Frazier, R. P. Nielsen, H. H. Sisler, *Inorg. Chem.* **1964**, 3, 292–294.
- [228] T. L. Windus, M. S. Gordon, *J. Am. Chem. Soc.* **1992**, 114, 9559–9568.
- [229] We thank Prof. Dmitri G. Goussev (Gusev) from Wilfrid Laurier University for helping us with DFT study.
- [230] M. B. Smith, J. March, *March's Advanced Organic Chemistry*, **2013**.
- [231] L. Jafarpour, E. D. Stevens, S. P. Nolan, *J. Organomet. Chem.* **2000**, 606, 49–54.
- [232] Y. Ohki, K. Tanifuji, N. Yamada, M. Imada, T. Tajima, K. Tatsumi, *Proc. Natl. Acad. Sci.* **2011**, 108, 12635–12640.
- [233] W. J. Hoogervorst, C. J. Elsevier, M. Lutz, A. L. Spek, *Organometallics* **2001**, 20, 4437–4440.

- [234] T. Řezníček, L. Dostál, A. Růžička, R. Jirásko, R. Jambor, *Inorganica Chim. Acta* **2010**, *363*, 3302–3307.
- [235] J. Al Thagfi, S. Dastgir, A. J. Lough, G. G. Lavoie, *Organometallics* **2010**, *29*, 3133–3138.